The Role of *Bacillus subtilis* Clp/Hsp100 Proteases in the Regulation of Swimming Motility and Stress Response

Dissertation zur Erlangung des akademischen Grades des

Doktors der Naturwissenschaften (Dr. rer. nat.)

eingereicht im Fachbereich Biologie, Chemie, Pharmazie

der Freien Universität Berlin

vorgelegt von

Pascal Noël Molière

aus Berlin

2012

Diese Arbeit wurde im Zeitraum vom 1. Juni 2007 bis zum 30. September 2011 am Institut für Pflanzenphysiologie, Pflanzenbiochemie und Mikrobiologie der FU Berlin unter der Anleitung von Prof. Dr. Kürşad Turgay durchgeführt.

1. Gutachter: Prof. Dr. Kürşad Turgay
2. Gutachterin: Prof. Dr. Regine Hengge

Disputation am 7. August 2012

Für Gesa und meine Eltern

Zusammenfassung

Die ATP-abhängigen Proteasen ClpCP und ClpXP sind an der generellen und regulatorischen Proteolyse in dem grampositiven Bakterium *Bacillus subtilis* beteiligt. Im Rahmen der generellen Proteolyse bauen sie unter Stress falsch gefaltete und aggregierte Proteine ab und tragen gemeinsam mit Chaperonen zur Proteinqualitätskontrolle, zum Überleben bei hohen Temperaturen und zur Thermotoleranz bei. Die gleichen Proteasekomplexe beeinflussen die zelluläre Regulation durch kontrollierten Abbau von Regulatorproteinen. Regulatorische Proteolyse spielt eine wichtige Rolle bei der Genregulation, Signaltransduktion und bei der Differenzierung in spezialisierte Zelltypen wie Endosporen und kompetente Zellen.

ClpCP und ClpXP sind essentiell für die Motilität von *B. subtilis*. Die hier gezeigten Daten sprechen dafür, dass eine Funktion von ClpCP während der Motilitätsentwicklung darin besteht, durch Proteolyse die Konzentration des Regulators DegU zu vermindern, der als Repressor von Motilitätsgenen wirkt. ClpXP reguliert die Motilitätsentwicklung durch Abbau des Redoxstressregulators Spx. Zusätzlich konnte gezeigt werden, dass Spx die Motilitätsgene transient herunter reguliert, wenn der Regulator durch oxidativen Stress stabilisiert wird. Erste Ergebnisse zum Mechanismus der Spx-vermittelten Motilitätsregulation sprechen dafür, dass Spx indirekt durch Transkriptionsaktivierung eines unbekannten negativen Motilitätsregulators wirkt.

Im zweiten Teil dieser Arbeit wurde die Proteolyse von Hag, der Hauptstruktureinheit des Flagellums, untersucht. Hag wurde *in vitro* von ClpCP mit Hilfe des Adapterproteins YpbH abgebaut und von FliW vor der Proteolyse geschützt. *In vivo* wurde Hag jedoch nur in Abwesenheit des Exportchaperons FliS unabhängig von ClpP abgebaut. Diese Ergebnisse sprechen für die Existenz von zwei unterschiedlichen Wegen der Hag-Proteolyse. Einer dieser Wege könnte dazu dienen, die Aggregation oder verfrühte Assemblierung von Hag zu verhindern, wenn seine Sekretion gestört ist.

Es konnte ebenfalls gezeigt werden, dass Spx für die Ausprägung der Thermotoleranz benötigt wird, wahrscheinlich durch Aktivierung unbekannter schützender Zielgene. Außerdem wurde gezeigt, dass *gsiB*, *mcsB* und *ywlE* wichtig für die Thermotoleranzentwicklung sind. Schließlich wurden Hinweise auf eine ClpP-unabhängige Funktion von ClpC in der Thermotoleranz gefunden. Möglicherweise wirkt ClpC als Proteindisaggregase, ähnlich wie ClpB und Hsp104.

Abstract

The ATP–dependent proteases ClpCP and ClpXP are involved in general and regulatory proteolysis in the Gram–positive bacterium *Bacillus subtilis*. In general proteolysis, they degrade misfolded and aggregated proteins during stress and contribute to protein quality control, survival at high temperatures and thermotolerance together with chaperones. The same protease complexes act as key players in cellular regulation by controlled proteolysis of regulators. Regulatory proteolysis is important for gene regulation, signal transduction and differentiation into specialized cell types, such as endospores and competent cells.

ClpCP and ClpXP are required for swimming motility in *B. subtilis*. The results presented in this work suggest that one function of ClpCP in motility regulation is to reduce the levels of the response regulator DegU, which acts as a repressor of motility genes. ClpXP positively regulates swimming motility by proteolysis of the oxidative stress regulator Spx. Furthermore, it could be demonstrated that Spx transiently downregulates motility genes when the regulator is stabilized during oxidative stress. Initial studies of the mechanism, by which Spx regulates motility genes imply that Spx acts indirectly by transcriptional activation of an unknown negative regulator of motility.

In the second part of this study, the degradation of Hag, the structural component of the flagellum, was investigated. Hag was degraded *in vitro* by ClpCP assisted by the adaptor protein YpbH and protected from proteolysis by FliW. However, Hag was only degraded in the absence of the export chaperone FliS *in vivo*, which was independent of ClpP. These results suggest that two distinct pathways of Hag proteolysis exist, one of which may be important to prevent Hag aggregation or premature assembly, when its secretion is compromised.

Spx was also shown to be required for thermotolerance, probably through the activation of unknown protective target genes. Furthermore, it was demonstrated that *gsiB*, *mcsB* and *ywlE* are important for thermotolerance development. Finally, evidence for a ClpP–independent function of ClpC in thermotolerance was acquired. Possibly, ClpC acts as a protein disaggregase, similar to ClpB and Hsp104.

Contents

1 Abbreviations

A   adenosine

AAA+   ATPases associated with various activities

AB-3   3x acryl amide-bis acryl amide

AP   alkaline phosphatase

APS   ammonium persulfate

ATP   adenosine triphosphate

BCIP   5-bromo-4-chloro-3-indoyl-phosphate

BSA   bovine serum albumine

C   cytosine

CCD   charge coupled device

CDP   cytidine diphosphate

CFU   colony forming units

CHAPS   3-[(3-cholamidopropyl)-dimethylammonio]-1-propanesulfonate

CI   chloroform isoamyl alcohol

CM   competence medium

CTD   carboxy(C)-terminal domain

Da   Dalton

DEPC   diethylpyrocarbonate

DIG   digoxigenin

DNA   desoxy ribonucleic acid

dNTP   desoxy nucleotide triphosphate

DTT   dithiothreitol

DYT   double yeast tryptone

ECF   enhanced chemofluorescence

EDTA   ethylene diamine tetra acetic acid

FPLC   fast protein liquid chromatography

FR   flanking region

G   guanosin

GFP   green fluorescent protein

HAP   hook associated protein

IPTG	isopropyl β-D thiogalactoside
KI	Koimmunopräzipitation
LB	Luria Bertani
kb	kilobases
kDa	kilo Dalton
MDH	malate dehydrogenase
MOPS	3-(N-morpholino)propanesulfonic acid
NBT	nitro blue tetrazolium chloride
Ni-NTA	nickel nitrilotriacetic acid
NTD	amino(N)-terminal domain
OD	optical density (absorbance)
OD_{600}	optical density (absorbance) at 600 nm
ONPG	ortho-nitrophenyl-β-galactoside
PAGE	poly acryl amide gel electrophoresis
PCI	phenol chloroform isoamyl alcohol
PCR	polymerase chain reaction
PEP	phosphoenol pyruvate
PK	pyruvate kinase
PQC	protein quality control
PVDF	polyvinylidene fluoride
RNA	ribonucleic acid
rpm	rotations per minute
SDS	sodium dodecyl sulfate
SSC	standard saline citrate
STM	sucrose tris magnesium
T	tymidine
TAE	Tris acetate EDTA
TBS	Tris buffered saline
TBS-M	Tris buffered saline-milk
TBS-T	Tris buffered saline-tween
TCA	trichloro acetic acid

TE	Tris EDTA
TEMED	N, N, N', N'- tetra methyl ethylen diamine
TES	Tris EDTA salt
TM	Tris magnesium
Tris	tris-(hydroxymethyl)-aminomethane
TTSS	Type III secretion system
U	uracil
UV	ultra violet
v/v	volume per volume
w/v	weight per volume
X-Gal	5-bromo-4-chloro-indolyl-β-D-galactopyranoside

2 Introduction

Proteolysis is a crucial process in all living cells. The proteome is in a dynamic equilibrium of constant protein synthesis and degradation. This equilibrium is frequently perturbed by changing environmental conditions such as starvation and stress. Stress can be defined as external physical or chemical conditions, which interfere with vital cellular functions, such as protein folding and membrane integrity.

For example, during heat stress, proteases can remove unfolded and aggregated proteins, which would otherwise become toxic to the cell. Molecular chaperones can protect unfolded proteins from aggregation, actively induce protein folding or remove aggregates by disaggregation. By their combined function, chaperones and proteases contribute to protein quality control[241, 25]. Proteases are also intricately involved in gene regulation and signaling by controlled degradation of key transcription factors and other regulator proteins[170].

In this work, protein degradation was studied in the Gram–positive model organism *Bacillus subtilis*. This bacterium is ideally suited for these experiments because it is easy to manipulate, highly stress tolerant and able to differentiate into a number of different cell types, which requires complex signaling and regulation. Furthermore, *B. subtilis* is the best characterized Gram–positive bacterium and serves as a model organism for this taxonomic group, which includes pathogens, such as *Bacillus anthracis* and *Staphylococcus aureus*.

Recently, the protease ClpP was identified as the target of the novel antibiotic ADEP, which triggers non-selective degradation of nascent polypeptide chains emerging from the ribosome as well as the essential cell division protein FtsZ[24, 115, 205]. This example demonstrates the vital importance of controlled proteolysis for the bacterial cell and suggests that proteases can serve as drug targets.

In the following sections, the current knowledge about chaperones and proteases in *B. subtilis* will be presented as scientific background of this study. In addition, the regulatory pathways and stress response mechanisms, which are influenced by chaperones and proteases will be discussed.

2.1   Proteolysis

Proteolysis is defined as the cleavage of peptide bonds within a protein by hydrolytic enzymes termed proteases. The first enzymes with such an activity to be discovered were extracellular proteases from the mammalian digestive tract, namely pepsin, trypsin and chymotrypsin. These enzymes degrade proteins from food into small peptides, which are then further broken down into amino acids. They are synthesized as inactive preproteins, which are secreted and later cleaved resulting in their active form. Bacteria also secrete extracellular proteases into the culture medium in order to scavenge nutrients[197]. An example from *B. subtilis* is subtilisin (AprE)[102].

In contrast to nutrient proteins, cellular proteins were viewed as stable structures up to the mid-20th century. This changed with the groundbreaking studies of Schoenheimer who used isotope labeled amino acids to show that proteins are in a dynamic equilibrium of synthesis and turnover in living organisms[211]. Later, it was discovered that in contrast to extracellular proteolysis during digestion, intracellular protein breakdown requires metabolic energy[217]. With the discovery of the lysosome[45] it became clear that intracellular proteolysis takes place in membrane embedded organelles in eukaryotes and it was assumed that metabolic energy is required for the transport of substrates into the lysosomes.

However, protein degradation activity could still be demonstrated in a cell free system lacking lysosomes[40, 63] and subsequently, a totally different class of proteases was identified in the cytosol of bacteria[34, 39, 77, 101, 106] and eukaryotes[52]. In contrast to the extracellular proteases, these enzymes hydrolyze ATP to fuel protein degradation. At first glance, the consumption of energy to permanently destroy proteins may seem like a wasteful process. However, proteins frequently unfold, form toxic aggregates or become chemically modified, interfering with normal cellular function[25]. These non-native proteins can either be protected or repaired by chaperones or degraded by energy dependent proteases (general proteolysis)[25]. This becomes especially important when cells are confronted with stressful environmental conditions.

Furthermore, many important regulatory proteins are tightly controlled by proteolysis at times when their accumulation is unwanted or even damaging to the cell (regulatory proteolysis)[116, 170]. In addition, proteolysis might benefit cell metabolism by

generation of peptides, which can be further broken down into amino acids.

In the eukaryotic cytosol, energy–dependent protein degradation is mediated by the 26S proteasome[89], whereas in Bacteria this task is shared between several protease complexes, such as Clp, Lon, HslUV and FtsH[170].

2.2 Structural and biochemical properties of protein degradation machines

The most critical requirement of proteases in the cytosol is the ability to discriminate between substrates and non-substrate proteins. Without this pre-selection, intact cellular proteins could be destroyed, while aggregated and damaged substrates might be retained in the cell. As a solution to this problem, evolution has led to cellular protein destruction machines of a very elaborate compartmentalized architecture.

These proteases form large cylindrical complexes with a central pore. The active site residues line the inner surface of this cavity, thus preventing interaction of these residues with protein substrates. Access of substrates to the active sites is regulated by a ring-shaped complex of ATPases of the AAA+ (*A*TPases *a*ssociated with various *a*ctivities) family that binds and unfolds cognate substrates and translocates the unfolded protein chains into the central chamber of the protease component, where they are cleaved into small peptides (Figure 1)[125, 206].

2.2.1 Structure and function of bacterial protein degradation machines

Clp proteases   Prokaryotes have several different compartmentalized protease complexes. ClpP is a double heptameric serine protease that interacts with the AAA+ ATPases ClpA and ClpX in *E. coli* or ClpC, ClpE and ClpX in *B. subtilis*. The Clp/Hsp100 ATPases are composed of one or two AAA+ Walker type ATPase domains with relatively high sequence conservation, a more diverse N–terminal domain (NTD) and in some cases (ClpB and ClpC) an additional domain inserted near the junction of the two AAA+ domains[125, 206]. Whereas monomeric Clp/Hsp100 proteins display very low ATPase activity, ATP hydrolysis is stimulated by assembly into a donut-shaped hexameric complex. Most Clp proteins spontaneously oligomerize into this active hexamer, but *B. subtilis* ClpC requires an adaptor protein such as MecA

for hexamerization[117]. Conserved loops near the C–termini of the monomers bind to ClpP, leading to formation of a large ATPase/protease complex[157].

ClpYP, Lon and FtsH   The hexameric ClpQ (HslV) serine protease associates with the AAA+ ATPase ClpY (HslU). In the hexameric Lon and FtsH proteases, AAA+ ATPase and protease domains are fused together on a single polypeptide chain. Whereas Lon is a cytosolic serine protease, FtsH is a zinc metalloprotease with a transmembrane domain.

Functions of *B. subtilis* proteases   The protease complexes described in the previous section contribute to the degradation of misfolded, aggregated proteins during stress (general proteolysis), but also influence important regulatory pathways by proteolysis of transcription factors and other regulators (regulatory proteolysis)[170]. Specifically, ClpCP is involved in competence development, motility, sporulation, regulation of the heat shock response and protein quality control[227, 226, 198, 147, 189, 114, 128, 103, 209]. ClpXP regulates the oxidative stress response[179] and is involved in the degradation of ssrA-tagged proteins[242] and in protein quality control[128, 103]. ClpEP is thought to modulate the heat shock response and may influence protein quality control[160].

The ClpYQ protease complex is localized in foci close to the cytoplasmic membrane[216]. However, the function of this protease is elusive at the moment. *B. subtilis* encodes two *lon* genes. Whereas *lonA* is induced by stress[202], *lonB* is expressed in the forespore during sporulation[214]. Both genes are involved in sporulation[210, 146], and *lonA* plays only a minor role in general proteolysis[128]. FtsH is involved in heat and salt tolerance, secretion of exoenzymes and sporulation, but not in heat shock regulation[48, 47].

2.2.2   Substrate targeting mechanism of bacterial Clp proteases

Degradation tags   In contrast to the eukaryotic proteasome, which binds substrate proteins by a covalently attached ubiquitin tag (see section 2.2.3), bacterial protease complexes can directly recognize short peptide sequences in their substrates. These recognition sequences are termed degrons or degradation tags[206]. For example, ClpX
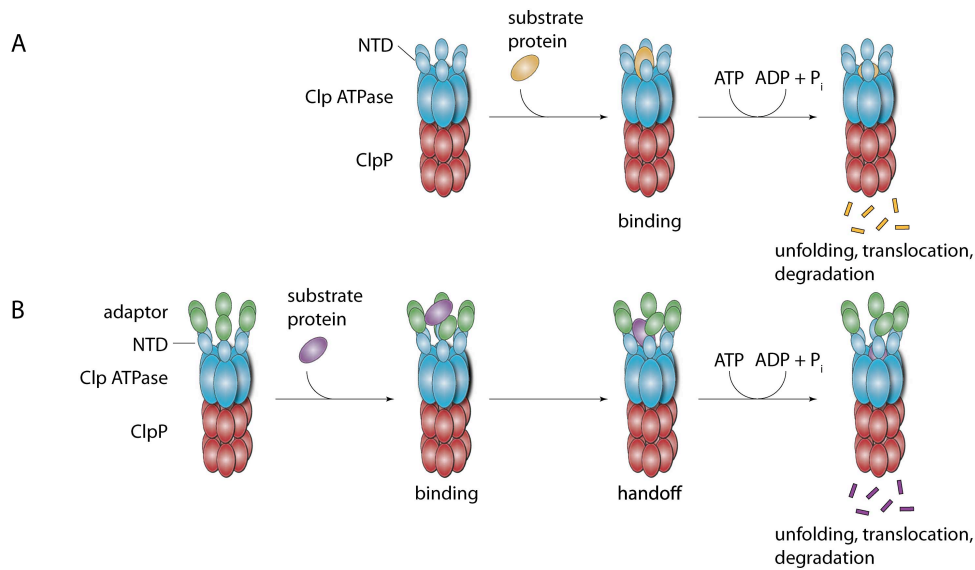
Figure 1: Mechanism of Clp/Hsp100 proteases.
A. Direct targeting of proteolysis substrates. A substrate protein (orange) binds directly to the pore loops of the Clp ATPase complex (blue). Coupled to ATP hydrolysis, the substrate is unfolded, translocated into the ClpP complex (red) and degraded. B. Adaptor protein mediated substrate targeting. A substrate protein (purple) is tethered to the Clp ATPase ring by a cognate adaptor protein (green). Subsequently, the substrate is handed off to the pore loops. Unfolding, translocation and degradation proceeds as described in A.

recognizes about 50 different substrates by 5 different degrons, 3 N–terminal and 2 C–terminal tags[66]. Some substrates also contain intrinsic degradation tags (which are not located at the N– or C–termini) as exemplified by ComK and ComS, two substrates of *B. subtilis* ClpCP[196]. Degradation tags are often unmasked by binding to interacting proteins, proteolytic cleavage or unfolding[116, 206].

Substrate recognition, unfolding and translocation   Prior to degradation, substrates are bound by conserved tyrosine residues on flexible loops lining the pore of the ATPase hexamer[91]. Subsequently, mechanical force is generated by the movement of the tyrosine pore loops, which is driven by the ATPase activity of the AAA+ subunits. This pulling force unfolds the three-dimensional structure of the substrate protein and translocates the substrate through the pore into ClpP, where it is cleaved into short peptides (Figure 1A)[91, 237, 199, 125, 206].

Adaptor protein mediated degradation   Whereas some substrates, such as casein, are directly bound by the pore loops, others require accessory domains of the AAA+ ATPases (N–terminal domain and linker if present) for binding[61, 41]. In most cases, these accessory domains serve as binding sites for adaptor proteins[41]. By binding to the AAA+ ATPase and the degradation tag of the cognate substrate, these adaptor proteins mediate tethering of the substrate to the AAA+ ATPase hexamer[116]. In this manner the local substrate concentration is increased, facilitating handoff to the pore binding sites of the ATPase complex (Figure 1B).

SspB   This mechanism was studied in great detail for *E. coli* SspB, a ClpX adaptor, which targets ssrA-tagged proteins for degradation by ClpXP[141]. The ssrA-tag is a short unstructured peptide sequence that is attached to the C–terminus of incomplete translation products on stalled ribosomes[111]. This degron features two distinct binding sites. Whereas the substrate is tethered to SspB by the N–terminal part of the tag, the C–terminus is bound by the ClpX pore loops to initiate unfolding and translocation[65].

This bipartite architecture of recognition tags is conserved in the eukaryotic ubiquitin–dependent proteasome pathway (see section 2.2.3): whereas the poly-ubiquitin tag serves to tether the substrate to the ubiquitin receptor at the 19S lid complex, a second unfolded sequence is required for engagement by the ATPases of the 19S base[195, 194]. For bacterial protease complexes it is unknown whether a distinct unfolded initiation sequence is always required in addition to the degradation tag.

RssB   Interestingly, two distinct targeting sequences were identified in the proteolysis substrate σ^S of *E. coli*[221]. In its phosphorylated form, the adaptor protein RssB binds to σ^S[13] and exposes a ClpX binding tag in the N–terminal region of σ^S[221], resulting in degradation by ClpXP.

ClpS   A different mechanism of adaptor/substrate interaction was demonstrated for ClpS[203], an adaptor protein that targets N-end rule substrates for degradation by ClpAP in *E. coli*[60]. N-end rule substrates contain a very short degron of two destabilizing amino acids at their N–terminus, which is recognized and bound by the adaptor

protein ClpS[212, 203]. ClpS also binds to the NTD of ClpA[247], leading to the formation of a low affinity ternary complex[203]. In contrast to other adaptors, ClpS has a long unstructured N–terminal extension, which interacts with ClpA pore residues, thereby stabilizing ClpS-ClpA and ClpS-substrate interaction and resulting in a high affinity ternary complex[203]. Substrate handoff from ClpS to ClpA dissolves this complex by an unknown mechanism[203]. Interestingly, ClpS cannot only target N-end rule substrates, but also unfolded and aggregated model proteins for degradation by ClpAP[51].

MecA *B. subtilis* MecA is an adaptor protein with a dual function: MecA activates ClpC by triggering the oligomerization of the ATPase[117], but also targets substrate proteins for degradation. These substrates include the competence transcription factor ComK (see section 2.3.1)[226], the unfolded protein casein and aggregated model proteins[209] for degradation by ClpCP. Similar to other adaptor proteins, MecA mediates ComK targeting by simultaneous binding to ClpC and ComK[227, 228, 117, 196]. Complex formation of MecA and ComK also inhibits the DNA binding activity of ComK[227].

Anti-adaptors In some cases, the stabilization of proteolysis substrates is mediated by anti-adaptors, which are produced in response to external signals. These proteins are themselves bound by protease complexes with high affinity, thereby competing with binding of other substrates and resulting in their stabilization[116]. For example, the small protein ComS is produced under competence-promoting conditions in *B. subtilis*. ComS binds to MecA and is targeted for degradation by ClpCP, leading to stabilization of ComK[227, 226]. A similar process has been described for the anti-adaptors IraP[20], IraD and IraM[19] of *E. coli*, which interfere with RssB-targeted σ^S proteolysis in response to stress or starvation.

2.2.3 The ubiquitin-proteasome system

Substrate selection In eukaryotes, cytosolic protein turnover is performed by the 26 S proteasome. This large complex of 33 protein subunits recognizes substrates, which are covalently linked to several copies of the small protein ubiquitin. The ubiquitin C–

terminus is activated by a single E1 ubiquitin activating enzyme, subsequently bound by one of several E2 conjugating enzymes, and finally covalently attached to lysine residues of the substrate protein by an E3 ubiquitin ligase[75]. This reaction is repeated multiple times on lysine residues of the terminal ubiquitin, resulting in a poly ubiquitin tagged substrate. In contrast to bacterial proteases that bind to recognition tags in their substrates directly or via adaptor proteins (see section 2.2.2), substrate selection in eukaryotes is mediated by a large variety of E3 ubiquitin ligases that specifically recognize structural motifs in their cognate substrates. The 26S proteasome binds ubiquitin tagged substrates, unfolds and degrades them.

Structure of the 26S proteasome   The general architecture of the proteasome is similar to Clp proteases, albeit a lot more complex. The 20S core complex consists of four stacked rings of pseudo 7–fold symmetry, two inner rings of seven different β subunits and two outer rings of seven α subunits[112]. Three of the seven β subunits are threonine proteases with distinct substrate specificities, the active sites of which are oriented to the inner surface of the barrel-like complex[112]. The α subunits serve as a gatekeeper that blocks entry of substrates into the proteolytic chamber[112].

Poly ubiquitin recognition, substrate deubiquitination, unfolding and translocation, as well as opening of the α ring gates is mediated by the 19S regulatory particle, which is further sub-divided into the base and lid complexes[112]. The base is composed of a hexameric ring of the AAA+ ATPase subunits Rpt1-6, which directly abuts the α ring of the 20S core particle, along with two other non-ATPase proteins and an ubiquitin receptor[16, 224]. This ATPase hexamer is responsible for substrate unfolding, translocation and opening of the α ring pore. The lid complex consists of ten different proteins, some of which are involved in ubiquitin binding and deubiquitination[112].

Functions of the 26S proteasome   Similar to the bacterial proteases, the 26S proteasome is important both for protein quality control[89] and for regulatory proteolysis[133], i.e. in cell cycle regulation[76], the inflammatory response[36], cancer[96] and cystic fibrosis[236]. Interestingly, a simpler form of the proteasome is also found in archea[43] and the *Actinomycetes* group of bacteria[150, 120].

2.3 Regulatory proteolysis and gene regulatory networks

In *B. subtilis* regulatory proteolysis is crucial for various differentiation and developmental processes[170]. This is exemplified by the pleiotropic phenotypes of protease mutants in this organism. For instance, a *clpP* deletion mutant is defective in competence, endospore formation, as well as swimming motility[74, 173]. In the following sections, the current knowledge about the role of proteolysis in regulatory networks of *B. subtilis* will be discussed.

2.3.1 Competence development

Genetic competence is the ability of bacterial cells to take up DNA from the environment and incorporate it into their genome by homologous recombination[55]. The biological implication of competence development is controversially discussed. One obvious advantage of competence is the incorporation of genes, which are beneficial in a stressful environment and can lead to a fitness advantage. In *B. subtilis* genetic competence is initiated under nutrient starvation conditions during the stationary phase[2] by a subpopulation of the culture[10, 151, 218].

ComK, the competence master regulator, is active in competent cells and controls the expression of downstream competence genes[229]. This transcriptional activator is present at very low concentrations during logarithmic growth due to continuous synthesis and degradation by the ClpCP protease, targeted by the adaptor protein MecA[226]. In addition, MecA inhibits the DNA-binding activity of ComK by direct protein-protein interaction[227].

When the cell density increases at the onset of the stationary phase, the quorum sensing peptides ComX and CSF trigger a signal transduction cascade that activates the expression of the *comS* gene[54, 53, 79, 219] via the two-component system ComP-ComA[239]. The phosphorylated response regulator ComA activates the expression of *comS*. Subsequently, the small protein ComS binds to MecA, leading to release, stabilization and activation of ComK[227, 226]. The *comK* gene is subject to positive autoregulation[230, 151].

In a small subpopulation of cells, ComK reaches a sufficiently high threshold level to mediate entry into the physiologically and morphologically distinct K-state by acti-

vation of its target genes. In this competent state, cells can bind and import DNA fragments from the environment and integrate them into their genome by homologous recombination[55]. ComS is also targeted for degradation by ClpCP[226]. Degradation of ComK and ComS may be important for the exit from the competent state after DNA transformation.

2.3.2   Swimming motility

Flagellar structure   The bacterial flagellum is a highly complex nanomotor, which has evolved to propel the bacterium through its liquid environment driven by the proton motive force[8, 162, 163]. Most of the experimental work on flagellar structure and assembly has been performed in the Gram–negative organisms *E. coli* and *Salmonella*. However, electron microscopy experiments have revealed a similar architecture of *Salmonella* and *B. subtilis* flagella[1]. Furthermore, many flagellar genes are highly conserved between Gram–negative model organisms and *B. subtilis*[1]. As there is currently not much information available about the *B. subtilis* flagellum, the assembly model described below is based on experimental data from *E. coli* and *Salmonella* if not stated otherwise.

The flagellum consists of a membrane embedded basal body, a flexible hook and a left-handed helical filament (Figure 2). The basal body can be divided into the C and MS rings and the rod, which is of smooth appearance in *B. subtilis* owing to the absence of the P (periplasmic) and L (outer membrane) rings[1].

Assembly of the basal body   The assembly of the basal body complex starts with the formation of the FliF 26-mer in the cytoplasmic membrane. Subsequently the proteins FliG and FliM assemble on the cytoplasmic face of the FliF ring to form the C ring[8]. FliG interacts with the MotAB channel in the mature flagellum (Figure 2), which is thought to be responsible for torque generation[250].

After completion of the C ring the flagellar type III secretion system (TTSS) assembles in the cytoplasmic membrane encased by the MS ring complex. The TTSS consists of a transmembrane part and the soluble proteins FliI, FliH and FliJ (Figure 2). FliI is an ATPase with extensive homology to the α and β subunits of the F0F1 ATPase. FliH interacts with FliI and modulates its ATPase activity[162] and FliJ interacts with
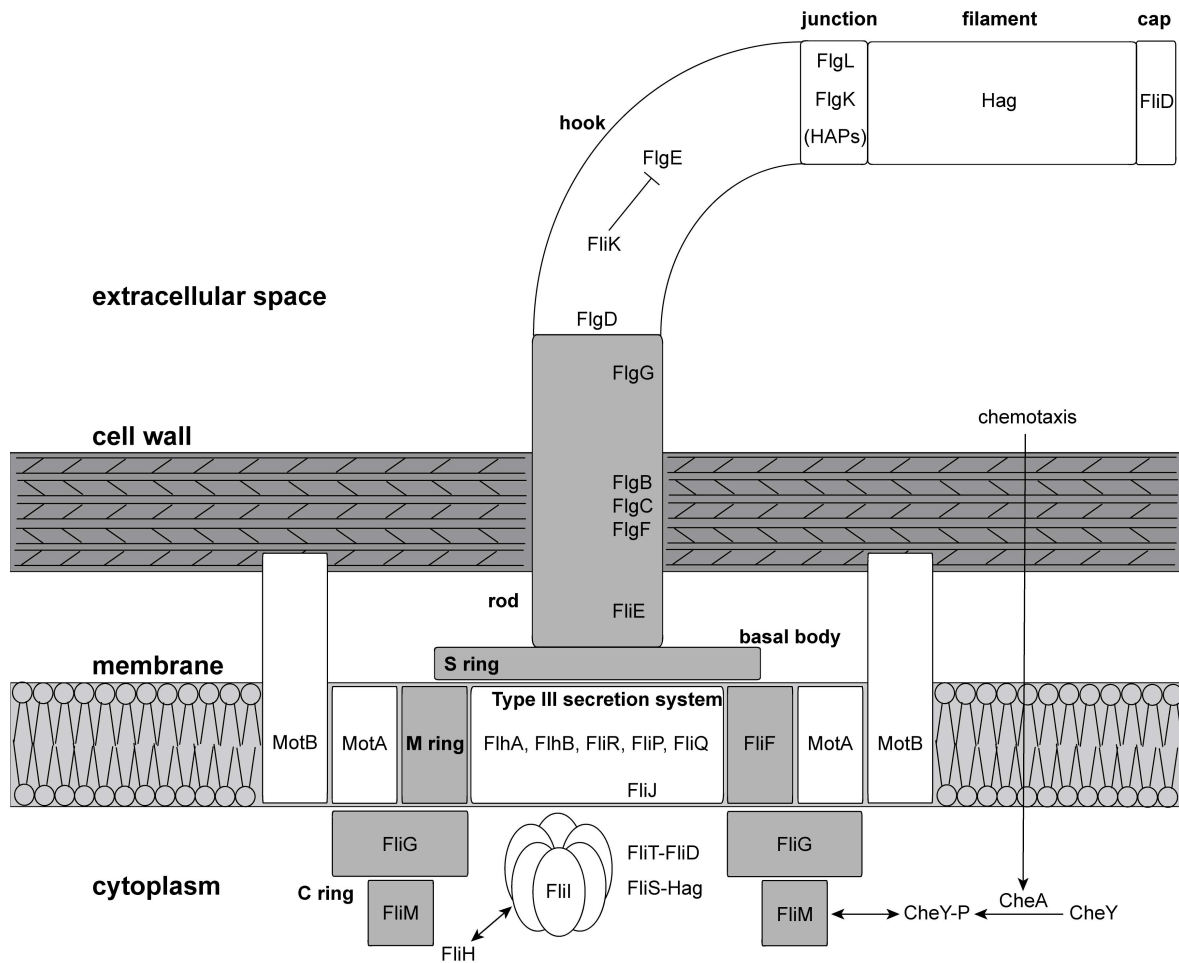
Figure 2: Flagellum of *B. subtilis*

The flagellum is anchored in the cytoplasmic membrane by the M ring complex. The C ring associates to the M ring on the cytoplasmic face of the membrane. The S ring abuts the M ring on the extracellular side. The basal body (grey) is completed by the rod. Components of the type III secretion system assemble in the cytoplasmic membrane. The flexible hook is assembled on top of the rod. Finally, Hag monomers are polymerized to form the filament, which is completed by a FliD pentamer. The MotAB complex associates with the C-ring, forms the stator that anchors the flagellum in the cell wall and functions as the motor of the flagellum. The direction of the motor is regulated by chemotaxis via the two–component system CheA-CheY, which interacts with FliM. Important proteins of the different complexes are listed. The diagram is based mostly on data from *E. coli* and *Salmonella*. Details are explained in the text.

secretion chaperones and the FlhA protein in *B. subtilis*[11]. In the presence of FliH, FliI forms a hexameric complex that binds to FlhA and FlhB[162]. It was previously suggested that FliI provides the energy for flagellar protein secretion. Since it is now clear that the proton motive force and not ATP hydrolysis is the energy source of flagellar protein export, it is more likely that FliI has a regulatory function in flagellar assembly[165, 190].

Rod and hook assembly   The components of the flagellar rod are secreted by the TTSS and assemble on top of the MS ring. Next, the hook cap protein FlgD is assembled on top of the rod. Subsequently, the hook structure is completed by secretion and polymerization of FlgE (Figure 2)[164]. How the hook length is controlled is still not completely understood. However, the protein FliK plays an important part in this process and two models, the cup filling model[155] and the tape measure model[172], have been proposed for the molecular mechanism of FliK[8]. Regardless how FliK measures the length of the hook, it is established that FliK interacts with FlhB, triggering an autocleavage event in its C–terminal domain that is thought to lead to an altered substrate specificity[164].

Filament assembly   When the hook has reached the appropriate length, the hook associated proteins (HAPs) FlgL, FlgK and FliD are assembled on top of the structure (Figure 2)[8]. FliD forms a pentamer and functions as the filament capping protein. Once the FliD cap is in place, the TTSS export apparatus switches its substrate specificity and Hag (flagellin) is polymerized to form the flagellar filament. Hag monomers are translocated through a narrow pore formed by the flagellum and assemble at the top of the structure, directly below the FliD cap[8].

Selection of secretion substrates in *B. subtilis*   A recent study has shed light on how the switch between these secretion substrates might be regulated in *B. subtilis*[11]. In the cytosol, prior to secretion, FliD and Hag both occur in a one to one complex with their cognate secretion chaperones FliT and FliS. It was demonstrated that the both the Hag-FliS and the FliD-FliT complexes are recognized by the cytosolic domain of the transmembrane protein FlhA, which forms part of the TTSS (Figure 2). Whereas Hag-

FliS is always bound with high affinity, FliD-FliT is only recognized in the presence of FliJ. Importantly, unbound FliT remains tightly bound to FlhA, so that further FliD-FliT complexes will not be secreted. Depending on the number of FlhA subunits in the secretion complex, which is not known at the time, this could provide a mechanism to ensure that only one FliD pentamer is assembled[11]. A FliS homolog FliW also forms a one to one complex with Hag and may play a role in secretion[223]. However, a recent publication suggests that FliW is rather involved in *hag* regulation[177].

Torque generation and chemotaxis   During the late stages of flagellar assembly the MotAB complex associates with the basal body. An extracellular domain anchors MotB in the peptidoglycan matrix, forming the stator of the flagellum (Figure 2). MotAB is a proton channel that converts the energy of the proton gradient into torque of the rotor[163].

The direction of the rotation is controlled by chemotaxis. 10 different chemotaxis receptors sense and integrate various attracting and repelling signals, which leads to autophosphorylation of the kinase CheA[1]. CheA in turn phosphorylates the response regulator CheY, which interacts with FliM on the flagellar C ring to reverse the direction of the motor and switch from tumbling to smooth swimming (Figure 2)[1, 193]. This system is further modulated by methylation, phosphorylation and deamidation[1, 193].

Regulation of the *fla/che* operon   A master regulator of swimming motility, similar to FlhDC in *E. coli* and *Salmonella*[148, 152], has not been identified in *B. subtilis*. However, the hierarchy of class II (dependent on the housekeeping sigma factor) and class III genes (dependent on the flagellar sigma factor σ^D)[152] is conserved in this organism (Figure 3). The class II genes are clustered in a 27 kb *fla/che* operon[3, 88], including the *sigD* gene that encodes the flagellar sigma factor σ^D. Two promoters have been identified in front of this operon[62]. Although one of these is σ^D–dependent[62], transcription of the *fla/che*-operon is almost exclusively driven by the σ^A–dependent promoter ($P_{fla/cheA}$)[110].

Transcription from the $P_{fla/cheA}$-promoter is modulated by the transcriptional repressor CodY[15], the response regulator DegU[5] and the activator of swarming motility SwrA

(Figure 3)[109, 27]. CodY is active as a repressor in the presence of GTP and branched chain amino acids and is thought to regulate the $P_{fla/che}$ promoter in response to nutrient availability[15]. Both the expression of the *fla/che* operon and the *hag* gene peak in post-exponential phase (about OD_{600} 1.0)[12, 167, 198]. This transient expression pattern was only observed in complex medium and was dependent on the presence of the *codY*[167], suggesting that it is a consequence of nutritional repression by CodY. DegU represses $P_{fla/che}$ in its phosphorylated form[5], but has also been reported to activate $P_{fla/che}$ in its unphosphorylated form[121, 225]. SwrA[109, 27] acts as a $P_{fla/che}$ activator, which is important for swarming motility (see section 2.3.4), but not for swimming motility[109].

Regulation of σ^D activity   RNA polymerase containing σ^D drives transcription of the class III genes, which are distributed in several transcriptional units[156]. Among the σ^D–dependent class III genes are *hag*, encoding flagellin, the major structural subunit of the flagellum[166] and genes encoding autolytic enzymes responsible for cell separation[156].

σ^D forms a complex with its anti-sigma factor FlgM[67], which inhibits the activity of σ^D (Figure 3)[29]. In *E. coli* and *Salmonella* FlgM is exported by the type III secretion system of the flagellar basal body complex, signaling the completion of this complex and resulting in an upregulation of class III gene expression[100]. Whether FlgM is also exported in *B. subtilis* or inactivated by another mechanism is unknown at present. Recently, the phosphorylated form of DegU has been implicated in the activation of *flgM* expression[99]. In addition to the direct repression of the *fla/che* operon, this represents another mechanism by which DegU negatively regulates motility. Interestingly, DegU and FlgM were shown to be essential for downregulation of *hag* expression, when the basal body complex is disrupted[99].

σ^D activity is also activated by SwrB, a regulator encoded by the last gene of the *fla/che* operon[108]. The mechanism of this activation is currently unclear.

Transcriptional regulation of *hag*   The *hag* gene is preceded by a relatively long untranslated region and a UP element, which enhances transcription of its σ^D–dependent promoter[30]. This promoter is repressed by ScoC (Figure 3)[123]. However, ScoC
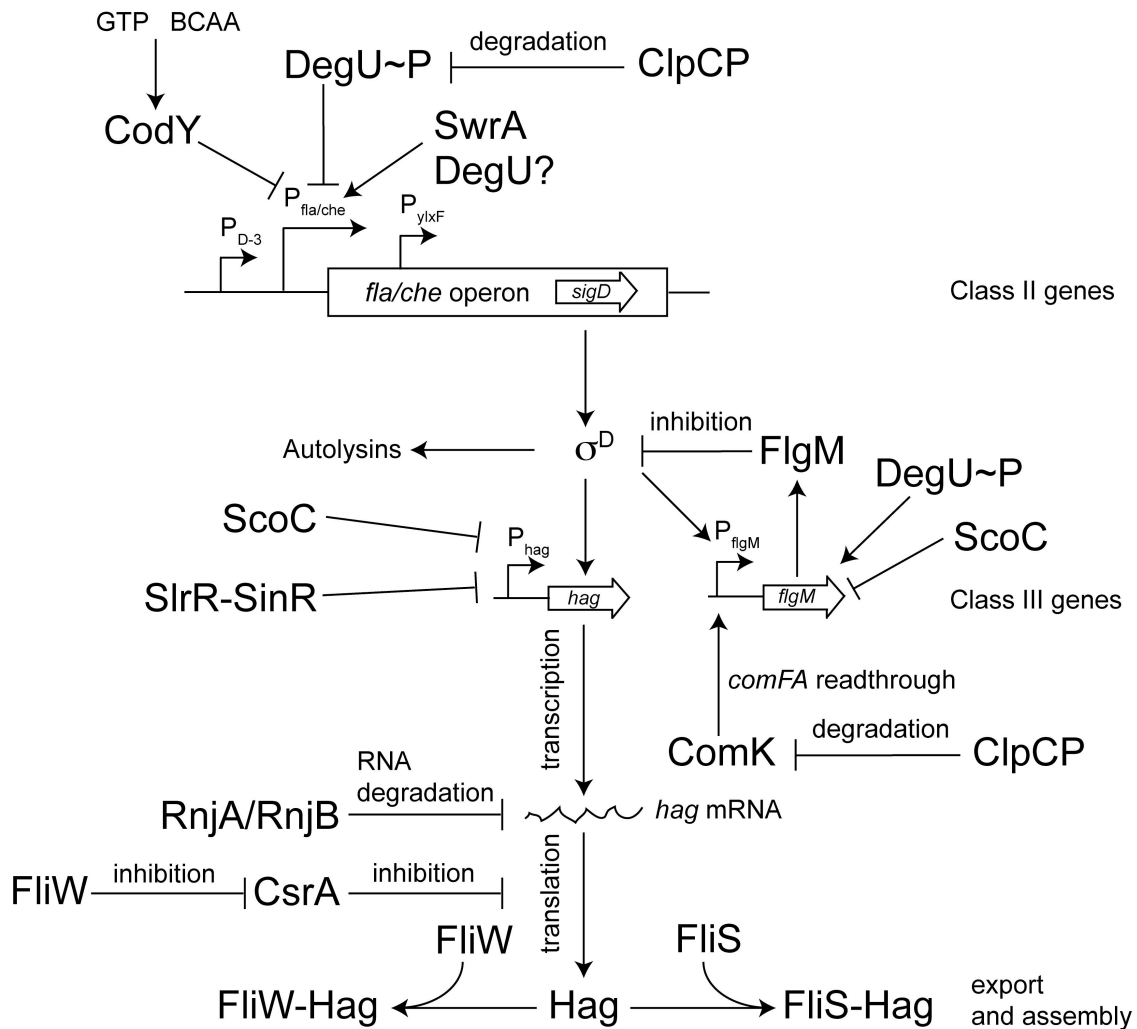
Figure 3: Regulation of flagellar gene expression in *B. subtilis.*

Flagellar genes are organized in two classes: the *fla/che* operon (class II genes) is transcribed from a σ^A–dependent promoter, whereas the class III genes, including *hag*, are controlled by σ^D. Both the *fla/che* genes and *hag* are transcriptionally and posttranscriptionally regulated by several regulator proteins (bold face). Export of Hag is regulated by FliS and FliW. Details are explained in the text.

also represses *flgM* (Figure 3), resulting in a net positive effect of ScoC on *hag* expression[123]. SlrR in complex with SinR acts as a repressor of *hag* during biofilm formation and in the subpopulation of chaining cells during exponential growth (Figure 3)[33]. YmdB, a protein of unknown function, acts as a negative regulator of *hag* through SlrR/SinR by an undefined mechanism[50].

Posttranscriptional regulation of motility   In addition, *hag* is subject to complex posttranscriptional regulation. Translation of the *hag* gene is negatively regulated by CsrA, which binds to *hag* mRNA close to the Shine Delgarno sequence and interferes with translation initiation (Figure 3)[244]. *Hag* mRNA is probably processed or turned over by RNases J1 and J2 (Figure 3)[153] and is polyadenylated at the 3'-end[28], although the functional significance of this modification is unclear.

In the cytosol, Hag is bound to its export chaperone FliS[11, 35], which escorts Hag to the type III secretion system. FliW was identified as an ortholog of FliS, which also forms a one–to–one complex with Hag and was suggested to play a role in Hag stabilization and possibly export[223]. Recently, it was demonstrated that FliW has a regulatory function[177]: FliW binds to CsrA and competes with CsrA binding to *hag* mRNA (Figure 3)[177]. According to the model of Kearns and colleagues, export of Hag during flagellar assembly results in accumulation of monomeric FliW in the cytosol. This serves as a signal that more Hag is required for export. FliW is free to interact with CsrA, thus causing the release of CsrA from *hag* mRNA and positively regulating *hag* translation[177].

Inverse regulation between competence and motility   *clpC* and *mecA* deletion mutants were found to be non-motile[147, 198]. Two groups reported that this effect is at least partially dependent on ComK[147, 198], and Zuber and colleagues went on to characterize the mechanism of this inverse regulation between motility and competence[147]. In *clpC* and *mecA* mutants the competence master regulator ComK accumulates because it is no longer degraded by ClpCP[226].

A ComK–dependent late competence gene, *comFA*, is located directly upstream of the *flgM* gene, separated by a weak transcriptional terminator. Under conditions, when ComK is active, transcription continues from *comFA* into *flgM*, which leads to

increased levels of the anti-sigma factor FlgM[147]. FlgM inhibits the activity of the flagellar sigma factor σ^D, thus negatively regulating flagellar gene expression (Figure 3)[67]. This mechanism may have evolved to ensure that competent cells, which are highly differentiated and non-dividing, shut down flagellar biosynthesis to save energy. Rashid and colleagues also reported that not only σ^D activity, but also σ^D levels are decreased in *clp* mutants, indicating that a second pathway, by which ClpCP-MecA influences motility, exists[198].

2.3.3 Biofilm formation

In recent years, the view that bacteria predominantly exist as single cells was challenged by a number of studies. Instead, the coexistence of different bacterial cells types with distinct functions in multicellular communities termed biofilms seems to be the rule and not the exception in natural habitats. For *B. subtilis* the ability to form biofilms was lost during domestication of laboratory strains and was only recently reassessed by the investigation of wild isolates of this bacterium[22, 81, 159].

In *B. subtilis* biofilms, chains of individual cells are held together laterally by an extracellular matrix composed of exopolysaccharides (EPS)[108] and amyloid-like fibers of the protein TasA[21]. The biofilm consists of a highly structured community of different cell types[22, 235]. Sporulating cells exist predominately at the tip of aerial fruiting body like structures[22], while motile cells are oriented near the base and side of the biofilm[235]. Interestingly, the extracellular matrix components are produced by a specialized subpopulation of cells[235, 149].

Regulation of biofilm formation   The operon responsible for production of the exopolysaccherides (*epsA-O*) and the operon encoding TasA (*tapA-sipW-tasA*) are both controlled by the repressor SinR[37, 108]. Under biofilm inducing conditions, Spo0A (the master regulator of sporulation, but also of other stationary phase processes) activates SinI, the antirepressor of SinR in a subpopulation of cells[31], which results in derepression of the *epsA-O* and *tapA-sipW-tasA* operons.

Inverse regulation between biofilm formation and motility   Recently, it was discovered that the gene encoding the SinR ortholog SlrR is also controlled by SinR

and derepressed during biofilm formation[38]. Interestingly, SlrR forms heterodimers with SinR, which redirects the DNA target specificity of this repressor[33]. The SlrR-SinR dimer represses the *hag* gene (Figure 3) and autolysin genes, whereas the biofilm operons *epsA-O*, *tapA-sipW-tasA* and *slrR* are derepressed[33].

This mechanism stabilizes the biofilm promoting SlrR-HIGH state, while motility is repressed and cell chaining is favored because autolysins are downregulated. The bistable distribution of single motile cells and non-motile chains during the logarithmic growth phase[110] was also shown to depend on SlrR, which is probably switched on in a small fraction of cells by stochastic fluctuations in *sinI* expression under these conditions[33]. In an investigation concerning the exit from the biofilm forming state, it was recently shown that SlrR undergoes autocleavage during transition back to the SlrR-LOW state[32]. Subsequent proteolysis of an SlrR fragment depended on the presence of ClpC, suggesting that SlrR may be a ClpCP substrate[32].

An interesting posttranscriptional cross-regulation between biofilm formation and motility was demonstrated recently. The *epsE* gene, which is part of the biofilm operon *epsA-O*, encodes a protein that interacts with FliG, a component of the flagellar rod[17]. During biofilm formation, EpsE acts as molecular clutch that uncouples the flagellum from the MotAB channel, but leaves it freely rotatable, so that it can be reused later when the same cell becomes motile[17].

2.3.4   Swarming motility

Similar to biofilm formation, swarming motility is a coordinated behavior that was lost during the domestication of laboratory strains of *B. subtilis*[109, 159]. In contrast to swimming motility of individual cells, swarming is a coordinated movement of bundles or rafts of cells over surfaces[107]. This process requires a higher number of flagella (hyperflagellation) and surfactin, a cyclic lipopeptide that reduces surface tension[107]. Swarming also depends on the presence of SwrA, a transcriptional activator of the *fla/che* operon[27, 109].

Laboratory strains of *B. subtilis* exhibit a frameshift mutation in the *swrA* gene and are thus deficient in swarming motility[109]. It is still not established if SwrA binds to the *fla/che*-promoter, but it is clear that this regulator activates the transcription of the operon, resulting in higher levels of σ^D. SwrB, a regulator encoded by the last

gene of the *fla/che*-operon is an activator of σ^D–dependent gene expression [110, 240]. This boost of σ^D-activity is required for hyperflagellation[240].

2.3.5   Degradative enzyme synthesis and other stationary phase processes

B. subtilis cultures produce a number of extracellular degradative enzymes during stationary phase. The DegS–DegU two–component system was originally discovered as a regulator pair that activates the synthesis of these enzymes[174]. Later, it turned out that DegS-DegU is involved in the control of several stationary phase processes, such as competence[80], swimming and swarming motility[5, 121, 225, 232], biofilm formation[121, 232] and poly-γ-glutamic acid production[220]. DegU is a response regulator with DNA binding affinity that is phosphorylated by the sensor histidine kinase DegS[42].

Regulation of the DegS–DegU two–component system   In contrast to most sensor kinases DegS is a soluble cytoplasmic protein. Although salt stress[131] and dissociation from the SMC-ScpA-ScpB complex responsible for DNA condensation and repair[46] have been suggested to trigger phosphorylation of DegU by DegS, the signal that activates DegS is still unknown. Phosphotransfer from DegS to DegU is stimulated by the small protein DegQ[121] and the phosphorylated form of DegU is stabilized by another small protein, DegR[176]. Thus, DegQ and DegR both contribute to a higher concentration of phosphorylated DegU. Whereas *degR* is a σ^D–dependent gene, *degQ* is activated by ComPA and is thus under the control of ComX quorum sensing. According to one publication, DNA binding activity but not the phosphorylation state of DegU is regulated by the phosphatase RapG that also dephosphorylates Spo0A[187]. RapG is inhibited by the quorum sensing peptide PhrG[187].

Regulation of target genes by DegU   Surprisingly, different levels of phosphorylated DegU affect different groups of target genes[232]. Unphosphorylated DegU activates *comK* expression[80]. According to contrasting reports, activation of swarming motility is achieved either by unphosphorylated DegU[225] or low levels of phosphorylated DegU[232]. Intermediate levels of DegU phosphorylation activate the biofilm genes *yvcA* and *yuaB*[232, 233], whereas high levels of DegU phosphorylation acti-

vate transcription of exoprotease genes and negatively regulate competence, biofilm formation, swimming and swarming motility. Accordingly, DegU has been described as a cellular rheostat that converts changes in environmental conditions into a gradual change of gene expression[178].

Such a differential response of different target gene groups to the phosphorylation state of a response regulator has also been observed for the master regulator Spo0A[69] and has been explained by different binding site affinities. For instance, a low-affinity binding site will yield a response only at high concentrations of the regulator. The negative regulation of targets at high concentrations, which are activated at low concentrations can be explained by the presence of different activating and inhibitory binding sites near the target promoters. Interestingly, two inverted repeat DegU binding sites were identified by footprinting analysis upstream of the *fla/che* promoter[225]. Whereas unphosphorylated DegU bound to both sites, *in vitro* phosphorylated DegU interacted only with one of the sequences, which may suggest such a regulation[225]. However, DegU regulation of the *fla/che* promoter appears to be complex and awaits more detailed characterization.

2.3.6   Spx and the oxidative stress response

Spx is an unusual global transcription factor, which directs the transcription of several hundred genes [182, 183, 251]. Remarkably, Spx acts both as a positive and negative transcriptional regulator. Spx positively regulates genes involved in the thiol specific oxidative stress response, including thioredoxin, thioredoxin reductase and superoxide dismutase[183]. A distinct group of genes is negatively regulated by Spx[182, 183]. Among these is the *srf* operon, which is important for competence development[53]. In contrast to most other transcriptional regulators, Spx itself has never been observed to directly bind DNA. Instead, Spx forms a complex with the C–terminal domain of the RNA polymerase α subunit (α-CTD)[135, 183, 185], which is required for both its activating and repressing activities[182, 183, 248].

Mechanism of Spx repression   Negative regulation by Spx can be explained by the interference model[182, 248]: many transcriptional activators interact with the α-CTD[26]. At high cellular concentrations of Spx, these activators are displaced

from the α-CTD by Spx binding, thereby interfering with activator–controlled gene expression[182]. Indeed, many of the negatively regulated Spx target genes require an activator for their expression. For example, the phosphorylated response regulator ComA activates the expression of the *srf* operon by interaction with the α-CTD, explaining the repression of competence development at high levels of Spx[182].

Putative mechanism of Spx activation Positive regulation by Spx is still not completely understood. Most transcriptional activators directly bind to DNA. For example, the catabolic activator protein of *E. coli* binds to DNA sequences upstream of target promoters and subsequently recruits RNAP holoenzyme to the promoter UP element[26].

In contrast, Spx has never been observed to bind DNA by itself[181]. Moreover, no evidence for Spx–DNA interaction was found in DNA-protein crosslinking experiments[201]. However, it was suggested that Spx recruits RNA polymerase to the *trxA* and *trxB* promoters[201]. In complex with the α-CTD, Spx induced binding of σ^A to the -10 region and of the $\beta\beta$' subunits to the core promoter[201]. Furthermore, a complex of α-CTD and oxidized Spx protected a DNA segment upstream of the *trxA* and *trxB* promoters in DNase I footprinting experiments[181].

Recently, evidence for sequence-specific DNA binding of the Spx-α-CTD complex was acquired for the first time[180]: purified α-CTD bound to a *trxB* promoter fragment in gel shift experiments. Notably, in the presence of Spx, a super shift could be detected. DNA binding of the complex was inhibited by addition of DTT, suggesting that oxidation of Spx is required for DNA binding. Interestingly, a comparison of the Spx-α-CTD crystal structures in the oxidized and reduced form revealed the displacement of an alpha helix, which positioned an arginine residue in an orientation that might promote DNA binding[180]. Mutation of this residue to a glutamate abolished the activating, but not the repressing function of Spx *in vivo*, indicating that Spx-α-CTD complex formation was not affected by the mutation[180]. Importantly, the mutated Spx protein was also defective in super shift formation in the *in vitro trxB* binding experiment. Furthermore, an AGCA site at positions -42 to -45 upstream of the *trxB* promoter was required for Spx–mediated activation[201, 180]. A second AGCG site at positions -34 to -31 also affected activation[201, 180]. Spx was proposed to bind to these sites

in complex with the α-CTD. An AT-rich stretch between the two putative binding sites might be bound by the α-CTD, which could explain the observed stabilization of the ternary complex[180]. If bound to this position, the α-CTD would also be appropriately oriented to promote core promoter binding by the RNA polymerase. Recently, it was demonstrated that only one Spx monomer associates with one RNA polymerase holoenzyme[144]. This excludes an activation mechanism, in which two Spx molecules associate with a promoter upstream sequence.

Transcriptional regulation of Spx   Spx is essential for survival during oxidative stress[183] and accumulates transiently after exposure to thiol oxidizing agents, such as diamide[183]. The *spx* gene is transcribed from at least five promoters[140]. One of these promoters is negatively controlled by the repressors PerR and YodR, which are inactivated by oxidative stress[139], resulting in de-repression of *spx*. However, posttranscriptional regulation of Spx appears to be more important for stress induction than transcriptional regulation[249]. Interestingly, Spx dependent gene products were shown to be induced not only by oxidative stress, but also by heat, high osmolarity and ethanol treatment by 2D gel electrophoresis [222]. If the induction of these proteins is really dependent on Spx, which was not directly addressed by the study, the results might suggest that Spx is rather a general stress regulator than a specific oxidative stress regulator.

Posttranscriptional regulation of Spx by proteolysis   The *spx* gene was originally identified by a suppressor mutation that bypasses the requirement of *clpX* and *clpP* for competence development (suppressor of *clp*P and *clp*X)[179]. Later, it was discovered that Spx is degraded by ClpXP[184]. This explains the competence defect of *clpP* and *clpX* mutants: Spx accumulates to high levels in these mutants, which interferes with ComA–dependent activation of the *srf* operon[182]. This operon encodes *comS* and is thus required for competence development[53].

Mechanism of Spx proteolysis and stabilization   An alanine asparagine sequence at the extreme C–terminus of Spx functions as a degradation tag[183]. If these amino acids are mutated to two aspartates, Spx can no longer be degraded by

ClpXP[183]. Spx proteolysis is accelerated by the adaptor protein YjbH[70, 136]. Under non–stress conditions, Spx is synthesized and rapidly turned over by ClpXP, resulting in a very low Spx protein level[183]. After treatment with thiol-oxidizing agents, Spx is transiently stabilized[183]. This stabilization appears to be a consequence of oxidative inactivation of ClpX[249] and the adaptor protein YjbH[70], which both contain a zinc binding domain. These zinc atoms are released by oxidation, leading to inactivation of ClpX and YjbH[249, 70]. Recently, the small protein YirB was identified as an anti-adaptor, which binds to YjbH and interferes with Spx targeting to ClpXP[124]. However, it is currently unknown whether YirB contributes to the stabilization of Spx under oxidative stress conditions.

Mechanism of Spx activation   In addition to transcriptional regulation and proteolysis, Spx activity is directly induced by thiol oxidative stress[181, 180]. Spx contains two conserved cysteine residues at positions 10 and 13, which form an intramolecular disulfide bond under oxidizing conditions[181, 185]. Oxidation of the disulfide bond is strictly required for the activating effect of Spx[181], but not for binding of the α-CTD[180]. This activation might be achieved by the replacement of α helix 4, which was observed by comparison of the crystal structures of the reduced and oxidized form of Spx[185, 180]. The observed conformational change leads to a movement of arginine 60, which is involved in activation and possibly in DNA binding[180].

2.4   General proteolysis and protein quality control

B. subtilis is extremely well adapted to survival in a changing and stressful environment. A major problem that cells encounter during adverse conditions, such as heat shock and oxidative stress, is protein unfolding, misfolding, oxidative protein modification and aggregation[25]. To maintain vital protein functions, cells from all kingdoms of life rely on elaborate protein quality control (PQC) systems[25]. These systems consist of a wide variety of chaperones and proteases. In order to quickly respond to stressful external conditions, the expression of chaperone and protease genes has to be regulated. In *B. subtilis*, heat shock genes are part of a complex regulatory network, which will be described in the following section.

2.4.1   Heat shock regulation in *B. subtilis*

Heat shock genes of *B. subtilis* have been classified in five groups[87]. The class I genes are controlled by the repressor HrcA and include the *dnaK* and *groES* operons[169]. The class II genes are under the control of the general stress sigma factor σ^B[86]. These genes are induced not only by heat shock, but also by a variety of other stress stimuli. This mechanism might provide cross-protection from types of stress, which the cells have not yet encountered directly, but which are likely to occur in a stressful environment.

Class III genes are repressed by CtsR and include *clpP*, *clpE* and the *ctsR-mcsA-mcsB-clpC* operon[126]. The class I and class III genes were also induced by the heterologous over–production of the outer membrane protein PorA, which forms inclusion bodies in the cytosol[103], suggesting that unfolded proteins serve as an activating signal of class I and III genes.

Heat-induced genes with an unknown induction mechanism (i.e. *htpG* and *clpX*) are grouped under class IV. Finally, class V genes are targets of the CssRS two-component system and are induced both by protein secretion stress and heat shock[44].

The class III heat shock genes are of special interest for this study because they are regulated by ClpC. Therefore, the regulation of class III heat shock genes will be described in the following section.

Regulation of class III heat shock genes   The promoters of class III heat shock genes are preceded by operator sequences, which serve as binding sites for the repressor CtsR[126]. CtsR senses heat directly and undergoes a conformational change that leads to dissociation from its binding sites on target DNA[58]. In addition, CtsR is phosphorylated by the protein arginine kinase McsB[119][68]. The kinase activity of McsB is inhibited by ClpC, activated by McsA and counter-acted by the phosphatase YwlE[119].

In its autophosphorylated, kinase active state, McsB also acts as a ClpC adaptor protein, which targets CtsR for degradation by ClpCP during heat shock[129][114]. According to recent results, neither phosphorylation by McsB nor degradation by ClpCP is strictly required for heat activation of CtsR[58] and it was suggested that phosphorylation and proteolysis serve to remove inactivated CtsR from the cell.

Interestingly, the activation of class III heat shock genes by oxidative stress follows a different route, which requires McsB and the co-adaptor McsA. McsA may be post-translationally modified by oxidation and cleaved[56][57]. McsB is also able to remove CtsR from DNA[129], which seems to play a role during oxidative stress activation[57]. McsB does not only phosphorylate CtsR, but also many other proteins. It could be recently demonstrated that 87 proteins are modified by arginine phosphorylation in *B. subtilis*, which affects the regulation of motility, competence, the stringent response and stress response[59].

2.4.2   Function of chaperones and proteases during heat stress

Chaperones   Chaperone activities can be classified into at least three partially over-lapping categories: by their holding activity, chaperones shield hydrophobic patches in unfolded or *de novo* synthesized proteins and thereby prevent them from aggregation. For example, this activity has been demonstrated for DnaK (Hsp70)[90, 71] and for ClpC in the presence of the adaptor protein MecA[209]. Folder chaperones, which actively induce folding of their bound substrates constitute the second group. For instance, GroEL/GroES provides a protected, closed-off environment for protein folding and initiates substrate folding by an ATP driven conformational change[97]. The DnaK/DnaJ/GrpE system can also actively promote folding by cyclic substrate binding and release, which is driven by ATP hydrolysis[25].

Finally, a third group of chaperones can disaggregate and refold protein aggregates. The bacterial hexameric AAA+ ATPase ClpB and the homologous Hsp104 from fungi and plants can perform this remarkable task. ClpB is very similar in sequence and structure to other Clp/Hsp100 ATPases, but lacks a ClpP binding loop in its C–terminal domain. As expected from the absence of this interaction site, ClpB retains the ATPase and unfolding activity of other Clp ATPases, but is unable to target substrates for proteolysis by ClpP[83]. Instead, ClpB unfolds substrate proteins and translocates them through the narrow pore formed by the ClpB hexamer[84]. After exit from the pore, unfolded substrates can then refold into their native structure. Interestingly, disaggregation and refolding by ClpB is assisted by the DnaK/DnaJ/GrpE system and the small heat shock proteins IbpA and IbpB, which bind to aggregates, thereby preparing them for disaggregation by DnaK/DnaJ/GrpE and ClpB[168].

Chaperone systems in *B. subtilis* protein quality control   As in most other bacteria, *groEL/groES* genes are essential in *B. subtilis*[143]. This observation might be explained by GroEL/GroES mediated folding of an unknown essential protein. Alternatively, this may be due to an important general function of the GroEL/GroES chaperone complex in protein quality control, even under non–stress conditions.

Interestingly, the *dnaK* mutant, which is highly temperature sensitive in *E. coli*, only had a slight effect on growth at high temperature in *B. subtilis*[213] and a *dnaK tig* double mutant is viable[200] in contrast to *E. coli*, where this combination is synthetically lethal under most conditions[49, 72]. The *tig* gene encodes *trigger factor*, a ribosome-associated chaperone, which is believed to shield or actively fold nascent protein chains emerging from the ribosome[92].

A ClpB homolog is not encoded in the *B. subtilis* genome. Instead, disaggregation and refolding activity was demonstrated *in vitro* for *B. subtilis* ClpC in conjunction with the adaptor protein MecA[209]. However, degradation by ClpCP-MecA was much faster than disaggregation by ClpC-MecA[209]. Therefore, it is questionable whether disaggregation by ClpC/MecA takes place *in vivo*. Alternatively, the absence of ClpB and small heat shock proteins from *B. subtilis* could be an indication that protein aggregates are rather removed by proteolysis than repaired by disaggregation and refolding in this organism.

In *E. coli*, disaggregation and refolding by ClpB is essential for thermotolerance, the ability to survive severe heat stress better if the culture is primed by a pre–shock at lower temperature[238]. Interestingly, *B. subtilis* cells become thermotolerant[234], even though they do not encode ClpB and small heat shock proteins. This observation suggests that thermotolerance is achieved by a different mechanism in this organism. This could either be disaggregation/refolding by ClpC and MecA, proteolysis, i.e. by ClpCP or ClpXP or a completely different process.

Proteases   An alternative to the chaperone activities described above is the irreversible destruction of misfolded proteins and protein aggregates, which is performed by the ATP–dependent Lon and Clp proteases in bacteria[170] and by the proteasome in eukaryotes[89].

Several observations suggest that Clp proteases play an important part in protein

quality control in *B. subtilis.* A first indication for such an involvement was the heat sensitive phenotype reported for *clpP*, *clpC* and *clpX* mutants[74, 127, 173].

The effect of Clp proteases on protein aggregation was directly tested by examining the time dependent decrease of radiolabeled aberrant translation products, which were induced by the addition of the antibiotic puromycin[128]. The half–life of the bulk radioactive peptides was significantly increased in the *clpP*, *clpC* and *clpX* mutant strains compared to the wild type, whereas the *lonA* mutant had no effect, suggesting that ClpCP and ClpXP, but not LonA, contribute to the degradation of protein aggregates in *B. subtilis*[128]. *In vitro* experiments have also shown that ClpCP can degrade aggregated model proteins, such as luciferase and malate dehydrogenase, which requires the adaptor protein MecA[209].

Localization to aggregates   Two studies have demonstrated the association of ClpP, ClpC and ClpX with insoluble proteins. Such inclusion bodies were formed by puromycyl treatment[128] or by heterologous production of the *Neisseria* outer membrane protein PorA[103]. In both cases, the Clp proteases co–localized with the inclusion bodies, as detected by immuno–gold labeling and electron microscopy[128, 103]. In more recent studies, GFP fusions to ClpP, ClpC, ClpE and ClpX were observed in clusters close to the cell poles and division sites[104, 118, 216]. These clusters, which increased in size and brightness after heat shock, co–localized with over–produced PorA, which confirms that Clp proteases localize to aggregate structures and corroborates their involvement in protein quality control[118].

2.5   Aim of this work

The general aim of this work was to better understand the function of Clp proteases in regulatory proteolysis, general proteolysis and protein quality control in *B. subtilis.* Mutants in *clpP*, *clpC* and *clpX* are non–motile, suggesting that regulators of motility gene expression are subject to regulatory proteolysis. One objective of this study was to identify these regulators and to unravel the mechanisms, by which they regulate swimming motility.

Hag, the major structural component of the flagellar filament, was previously identified as a ClpCP substrate *in vitro.* This observation suggested that Hag could be a general

proteolysis substrate. Therefore, a goal of this work was to test whether Hag is also degraded *in vivo*, and to elucidate how this proteolysis might benefit the cell.

The last part of this study was concerned with the mechanism of protein quality control, in which Clp proteases are of vital importance. The ClpCP and ClpXP protease complexes have a direct function in protein quality control, but are also involved in regulatory proteolysis. Here, it was investigated how this regulatory proteolysis influences thermotolerance, the mechanism of which is still unknown. To obtain more information about this process, several mutant strains were analyzed for their thermotolerance phenotype. Furthermore, it was investigated whether ClpC acts as a protein disaggregase *in vivo* during thermotolerance.

3   Materials and Methods

3.1   Materials

Table 2: Devices

Device	Manufacturer
Äkta purifier FPLC system	GE Healthcare (München)
Centrifuge 5804 R	Eppendorf (Hamburg)
Centrifuge Sorvall RC 6+	Thermo Scientific (Schwerte)
Fluorescence microscope Type 120 Eclipse 90i	Nikon Instruments (Japan)
Microcentrifuges Pico/Frico	Heraeus/Thermo Scientific (Schwerte)
Nanodrop spectrophotometer	Peqlab (Erlangen)
Phosphoimager Fla 2000	Fujifilm (Japan)
Pipetman pipettes	Gilson (Villiers le bel, France)
Platereader Sunrise Remote	Tecan (Grödig, Austria)
PowerPac basic power supply	Biorad (München)
Protean mini gel system	Biorad (München)
Research pro multichannel pipettes	Eppendorf (Hamburg)
Shaking incubator	Infors (Bottmingen, Switzerland)
Shaking water bath HT	Infors (Bottmingen, Switzerland)
Speed Vac lyophylizer	Eppendorf (Hamburg)
Thermo cycler T personal	Biometra (Göttingen)
Thermo shaker	Eppendorf (Hamburg)
UV Documentation station	Thermo scientific (Schwerte)

Table 3: Reagents

Manufacturer	Product
5Prime (Hamburg)	Phase Lock tubes
Applichem (Darmstadt)	acryl amide solution, PEP, IPTG
Biozym Scientific (Hessisch Oldendorf)	Phusion polymerase
Carl Roth (Karlsruhe)	basic chemicals, RotiQuant
Fermentas (Leon–Roth)	FastDigest restriction endonucleases, dNTPs
GE Healthcare (München)	ECF Western blotting kit
Hiss Diagnostics (Freiburg)	ZymoClean^{TM} Gel DNA recovery kit, DNA Clean and Concentrator kit
Millipore (Molsheim)	nitrocellulose filters
MP Biomedical (Eschwege)	FastRNA Pro Blue kit
New England Biolabs (Schwalbach)	Phusion polymerase, Chitin beads
Perkin Elmer (Waltham, USA)	^{35}S–methionine
Pineda Antikörper Service (Berlin)	polyclonal antibodies
Qiagen (Hilden)	QIAprep Spin Miniprep kit
Roche Applied Sciences (Mannheim)	CDP Star, Nylon membranes, Blocking reagent, DIG labeling kit, DIG–Easy hybridization buffer, RNase free DNase I
Sarstedt (Nümbrecht)	tubes, pipette tips, 96 well microplates
Sigma Aldrich (Seelze)	DNase I, RNase A, Proteinase K, APS, spectinomycin, erythromycin, lincomycin
Stratagene (Heidelberg)	Quikchange site–directed mutagenesis kit, *E. coli* XL–1 blue competent cells
Thermo Scientific (Schwerte)	oligonucleotides, Protein A–MagnaBeads
VWR (Darmstadt)	glassware

Table 4: *E. coli* strains

Strain	Genotype	Reference
ER2566	F- λ- *fhuA2* [*lon*] *ompT lacZ*::T7 gene 1 *gal sulA11* Δ(*mcrC-mrr*)114::IS10 R(*mcr-73*::miniTn10-Tet^S)2 R(*zgb-210*::Tn10)(Tet^S) *endA1* [*dcm*]	New England Biolabs
FI1202	*lacI^q lacL8 gln5*::Tn5 l202	[64]
W3110	F- λ- *rph*-1 INV(*rrnD, rrnE*)	[85]
XL-1 Blue	*recA1 endA1 gyrA96 thi-1 hsdR17 supE44 relA1 lac* [F *proAB lacI^{q}ZM15* Tn*10* (Tet^r)]	Stratagene

Table 5: *B. subtilis* strains

Strain	Genotype	Reference
168	*trpC2* wild type	[6]
BUG1	*trpC2* Δ*clpP*::spec	[74]
BNM102	*trpC2* Δ*clpP*::spec, suppressor mutation	this study
BNM103	*trpC2* Δ*clpP*::spec	this study
QPB418	*trpC2* Δ*clpC*::tet	[189]
BNM105	*trpC2* Δ*clpC*::tet	this study
BMM03	*trpC2* Δ*clpE*::spec	[160]
BNM106	*trpC2* Δ*clpE*::spec	this study
BEK90	*trpC2* Δ*clpX*::kan	[73]
BNM107	*trpC2* Δ*clpX*::kan	this study
ORB3834	*trpC2 pheA1* Δ*spx*::kan (JH642)	[179]
BNM111	*trpC2* Δ*spx*::kan	this study
ORB3838	*trpC2 pheA1* Δ*spx*::kan Δ*clpX*::spec	[179]
BNM112	*trpC2* Δ*spx*::kan Δ*clpX*::spec	this study
QB4652	*trpC2* Δ*mecA*::spec	[173]

BNM113	*trpC2* $\Delta mecA$::spec	this study
BNM115	*trpC2* $\Delta ypbH$::spec	[191]
BNM116	*trpC2* $\Delta mecA$::spec $\Delta ypbH$::kan	U. Gerth
BEK89	*trpC2* $\Delta mcsB$::kan	[129]
BNM117	*trpC2* $\Delta mcsB$::kan	this study
BT02	*trpC2* $\Delta dnaK$::cat	[95]
BNM 118	*trpC2* $\Delta dnaK$::cat	this study
BNM126	*trpC2* Δhag	this study
NRS1314	NCIB 3610 $\Delta degU$::cat	[232]
BNM137	*trpC2* $\Delta degU$::cat	this study
NRS1499	NCIB 3610 $\Delta degSU$::spec	N. Stanley–Wall
BNM138	*trpC2* $\Delta degSU$::spec	this study
BNM139	*trpC2* $\Delta degU$::cat $\Delta clpP$::spec	this study
BNM140	*trpC2* $\Delta degSU$::spec $\Delta clpC$::tet	this study
BNM141	*trpC2* $\Delta degU$::cat $\Delta clpE$::spec	this study
BNM142	*trpC2* $\Delta degSU$::spec $\Delta clpX$::kan	this study
BNM149	*trpC2* $\Delta comK$	A. Heinz
BNM150	*trpC2* $\Delta comK$ $\Delta clpC$::tet	A. Heinz
BNM216	*trpC2* $amyE$::P_{xyl}-*ibpA*-*gfp*::spec	this study
BNM217	*trpC2* $amyE$::P_{xyl}-*ibpB*-*gfp*::spec	this study
BNM224	*trpC2* *mdh*-*gfp*::cat	this study
BNM227	*trpC2* $\Delta dnaK$::cat $amyE$::P_{xyl}-*dnaK*-*gfp*::spec	this study
BNM233	*trpC2* *mdh*-*gfp*::cat *clpP*::spec	this study
BNM234	*trpC2* *mdh*-*gfp*::cat *clpC*::tet	this study
BNM236	*trpC2* *mdh*-*gfp*::cat *clpX*::kan	this study
YF244	*trpC2* *metC7* $\Delta iolR$::cat (60015)	[246]
BNM239	*trpC2* $\Delta iolR$::cat	this study
YF248	*trpC2* *metC7* ΔP_{iol}::cat (60015)	[246]
BNM240	*trpC2* ΔP_{iol}::cat	this study
TM044	*trpC2* *metC7* pMUTIN4-*iolX*::erm (60015)	[171]
BNM241	*trpC2* pMUTIN4-*iolX*::erm	this study

TM043	$trpC2$ $metC7$ pMUTIN2-$iolW$::erm::tet (60015)	[171]
BNM242	$trpC2$ pMUTIN2-$iolW$::erm::tet	this study
MB82	$trpC2$ $pheA1$ $\Delta gsiB$::kan (JH642)	[175]
BNM243	$trpC2$ $\Delta gsiB$::kan	this study
BNM245	$trpC2$ $clpC$(VGF::GGR)	this study
BNM253	$trpC2$ $\Delta dnaK$::cat $\Delta clpC$::tet	A. Heinz
BAE048	$trpC2$ $\Delta ywlE$::kan $amyE$::$clpE$-$bgaB$::cat	[58]
DS791	NCIB 3610 $amyE$::$P_{fla/che}$-$lacZ$::cat	[110]
BNM301	$trpC2$ $amyE$::$P_{fla/che}$-$lacZ$::cat	this study
BNM302	$trpC2$ $amyE$::$P_{fla/che}$-$lacZ$::cat $\Delta clpP$::spec	this study
BNM303	$trpC2$ $amyE$::$P_{fla/che}$-$lacZ$::cat $\Delta clpC$::tet	this study
BNM304	$trpC2$ $amyE$::$P_{fla/che}$-$lacZ$::cat $\Delta clpE$::spec	this study
BNM305	$trpC2$ $amyE$::$P_{fla/che}$-$lacZ$::cat $\Delta clpX$::kan	this study
BNM306	$trpC2$ $amyE$::$P_{fla/che}$-$lacZ$::cat $\Delta degSU$::spec	this study
BNM307	$trpC2$ $amyE$::$P_{fla/che}$-$lacZ$::cat Δspx::kan	this study
BNM308	$trpC2$ $amyE$::$P_{fla/che}$-$lacZ$::cat Δspx::kan $\Delta clpX$::spec	this study
DS793	NCIB 3610 $amyE$::P_{hag}-$lacZ$::cat	[110]
BNM328	$trpC2$ $amyE$::P_{hag}-$lacZ$::cat	this study
BNM329	$trpC2$ $amyE$::P_{hag}-$lacZ$::cat $\Delta clpP$::spec	this study
BNM330	$trpC2$ $amyE$::P_{hag}-$lacZ$::cat $\Delta clpC$::tet	this study
BNM331	$trpC2$ $amyE$::P_{hag}-$lacZ$::cat $\Delta clpE$::spec	this study
BNM332	$trpC2$ $amyE$::P_{hag}-$lacZ$::cat $\Delta clpX$::kan	this study
BNM333	$trpC2$ $amyE$::P_{hag}-$lacZ$::cat $\Delta degSU$::spec	this study
BNM334	$trpC2$ $amyE$::P_{hag}-$lacZ$::cat Δspx::kan	this study
BNM335	$trpC2$ $amyE$::P_{hag}-$lacZ$::cat Δspx::kan $\Delta clpX$::spec	this study
BNM337	$trpC2$ $amyE$::$P_{fla/che}$-$lacZ$::cat $\Delta degSU$::spec $clpC$::tet	this study
BNM338	$trpC2$ $amyE$::P_{hag}-$lacZ$::cat $\Delta degSU$::spec $clpC$::tet	this study
BNM339	$trpC2$ $amyE$::P_{hag}-$lacZ$::cat $\Delta degSU$::spec $clpX$::kan	this study
BNM341	$trpC2$ $amyE$::$P_{fla/che}$-$lacZ$::cat $\Delta degSU$::spec $clpC$::tet	this study
BNM345	$trpC2$ $amyE$::$P_{fla/che152}$-$bgaB$::cat	this study
BNM346	$trpC2$ $amyE$::$P_{fla/che152}$-$lacZ$::cat	this study

BNM347	$trpC2\ amyE::P_{fla/che152}\text{-}lacZ::\text{cat}\ \Delta degSU::\text{spec}$	this study
BNM348	$trpC2\ amyE::P_{fla/che152}\text{-}lacZ::\text{cat}\ \Delta clpC::\text{tet}$	this study
BNM349	$trpC2\ amyE::P_{fla/che152}\text{-}lacZ::\text{cat}\ \Delta degSU::\text{spec}\ \Delta clpC::\text{tet}$	this study
BNM350	$trpC2\ \Delta spx::\text{kan}\ amyE::P_{hyperspank(Hy)}\text{-}spx::\text{spec}$	this study
BNM351	$trpC2\ \Delta spx::\text{kan}\ amyE::P_{hyperspank(Hy)}\text{-}spx^{DD}::\text{spec}$	this study
BNM403	$trpC2\ \Delta fliS$	this study
BNM404	$trpC2\ \Delta fliW$	this study
BNM412	$trpC2\ \Delta fliS\ \Delta clpP::\text{spec}$	this study
BNM413	$trpC2\ \Delta fliS\ \Delta clpC::\text{tet}$	this study
BNM414	$trpC2\ \Delta fliS\ \Delta mecA::\text{spec}$	this study
BNM415	$trpC2\ \Delta fliS\ \Delta ypbH::\text{spec}$	this study
BNM421	$trpC2\ \Delta hag\ amyE::P_{xyl}\text{-}hag1::\text{cat}$	this study
BNM422	$trpC2\ \Delta hag\ amyE::P_{xyl}\text{-}hag1::\text{cat}\ \Delta clpP::\text{spec}$	this study
BNM423	$trpC2\ \Delta hag\ amyE::P_{xyl}\text{-}hag1::\text{cat}\ \Delta clpC::\text{tet}$	this study
BNM424	$trpC2\ \Delta hag\ amyE::P_{xyl}\text{-}hag1::\text{cat}\ \Delta clpE::\text{spec}$	this study
BNM425	$trpC2\ \Delta hag\ amyE::P_{xyl}\text{-}hag1::\text{cat}\ \Delta clpX::\text{spec}$	this study
BNM426	$trpC2\ \Delta hag\ amyE::P_{xyl}\text{-}hag4::\text{cat}$	this study
BNM427	$trpC2\ \Delta hag\ amyE::P_{xyl}\text{-}hag4::\text{cat}\ \Delta clpP::\text{spec}$	this study
BNM428	$trpC2\ \Delta hag\ amyE::P_{xyl}\text{-}hag4::\text{cat}\ \Delta clpC::\text{tet}$	this study
BNM430	$trpC2\ \Delta hag\ amyE::P_{xyl}\text{-}hag4::\text{cat}\ \Delta clpX::\text{spec}$	this study
BNM436	$trpC2\ \Delta hag\ amyE::P_{xyl}\text{-}hag4::\text{cat}\ \Delta spx::\text{kan}$	this study
BNM437	$trpC2\ \Delta hag\ amyE::P_{xyl}\text{-}hag4::\text{cat}\ \Delta spx::\text{kan}\ \Delta clpX::\text{spec}$	this study
BNM446	$trpC2\ \Delta hag\ amyE::P_{xyl}\text{-}hag4::\text{cat}\ \Delta fliS$	this study
BNM447	$trpC2\ \Delta hag\ amyE::P_{xyl}\text{-}hag4::\text{cat}\ \Delta fliS\ \Delta clpP::\text{spec}$	this study
BNM448	$trpC2\ \Delta hag\ amyE::P_{xyl}\text{-}hag4::\text{cat}\ \Delta fliS\ \Delta clpC::\text{tet}$	this study
BNM449	$trpC2\ \Delta hag\ amyE::P_{xyl}\text{-}hag4::\text{cat}\ \Delta fliS\ \Delta clpE::\text{spec}$	this study
BNM450	$trpC2\ \Delta hag\ amyE::P_{xyl}\text{-}hag4::\text{cat}\ \Delta fliS\ \Delta clpX::\text{kan}$	this study
BNM457	$trpC2\ amyE::P_{hyperspank(Hy)}\text{-}yhfK::\text{spec}$	this study
BNM458	$trpC2\ amyE::P_{hyperspank(Hy)}\text{-}yukF::\text{spec}$	this study

Table 6: Plasmids

Plasmid	Construction	Reference
pQE60	vector for C–terminal His$_6$ tag	Qiagen
pQE60-*fliS*	*fliS* in NcoI/BglII of pQE60	this study
pQE60-*hag*	*hag* in NcoI/BglII of pQE60	J. Kirstein
pQE60-*mecA*	*mecA* in NcoI/BglII of pQE60	[227]
pQE60-*ypbH*	*ypbH* in NcoI/BglII of pQE60	[191]
pQE70	vector for C–terminal-His$_6$ tag	Qiagen
pQE70-*clpP*	*clpP* in SphI/BglII of pQE70	[226]
pQE70-*fliW*	*fliW* in SphI/BglII of pQE60	this study
pTYB2	vector for C–terminal intein fusion	NEB
pTYB2-*clpC*	*clpC* in NdeI/SmaI of pTYB2	[227]
pTYB2-*clpC*(VGF::GGR)	*clpC*-V671G-F673G in NdeI/SmaI of pTYB2	this study
pDG268	vector for transcriptional *lacZ* fusion	[7]
pDG-*fla/che152-lacZ*	*fla/che152* in EcoRI/BamHI of pDG268	this study
pDL	vector for transcriptional *bgaB* fusion	[73]
pDL-*fla/che152-bgaB*	*fla/che152* in EcoRI/BamHI of pDL	this study
pDR111	expression from $P_{hyperspank(Hy)}$ in *amyE*	[23]
pDR111-*yhfK*	*yhfK* in HindIII/NheI of pDR111	this study
pDR111-*yukF*	*yukF* in HindIII(bl)/NheI of pDR111	this study
pMAD	vector for markerless deletion mutants	[9]
pMAD-*clpC*(ORF)	*clpC* in BamHI/NcoI of pMAD	this study
pMAD-*clpC*(VGF::GGR)	*clpC*(VGF::GGR) in BamHI/NcoI of pMAD	this study
pMAD-*fliS*	*fliS* FR in BamHI/SalI and SalI/NcoI	this study
pMAD-*fliW*	*fliW* FR in BamHI/SalI and SalI/NcoI	this study
pMAD-*hag*	*hag* FR in BamHI/SalI and SalI/NcoI	[17]
pMarB	vector carrying the TnYLB-1 transposon	[137]
pMMN521	*spx* from $P_{hyperspank(Hy)}$ in *amyE*	[182]
pSG1151	Campbell integration of C–term. GFP-fusion	[142]
pSG1151-*mdh*	*mdh* in KpnI/EcoRI of pSG1151	this study

pSG1154	C–term. GFP-fusion from P_{xyl} in *amyE*	[142]
pSG1154-*dnaK*	*dnaK* in KpnI/XhoI of pSG1154	this study
pSG1154-*ibpA*	*E. coli ibpA* in KpnI/EcoI of pSG1154	this study
pSG1154-*ibpB*	*E. coli ibpB* in KpnI/EcoI of pSG1154	this study
pSN56	spx^{DD} from $P_{hyperspank(Hy)}$ in *amyE*	[182]
pX	vector for expression from P_{xyl} in *amyE*	[113]
pX-*hag1*	*hag* in BamHI of pX	this study
pX-*hag4*	*hag* with 5'- and 3'-UTR in BamHI of pX	this study

Table 7: Primers

Primer	Amplified fragment	Sequence
158	KpnI-*dnaK* for	cccc**ggtacc**gtgagtaaagttatcggaatcgac
159	XhoI-*dnaK* rev	cccc**ctcgag**tttttttgtttttggtcgtcgtttac
165	BamHI-*hag1* for	ccc**ggatcc**atgagaattaaccacaatattgc
166	BamHI-*hag1* rev	ccc**ggatcct**taacgtaataattgaagtacgttttgc
182	KpnI-*ibpA* for	cccc**ggtacc**atgcgtaactttgatttatc
183	EcoRI-*ibpA* rev	cccc**gaattc**gttgatttcgatacggcgcg
184	KpnI-*ibpB* for	cccc**ggtacc**atgcgtaacttcgatttatc
185	EcoRI-*ibpB* rev	cccc**gaattc**gctatttaacgcgggacgttc
202	BamHI-*hag4* for	ccc**ggatcc**tgtagccgggaggaggcgca
208	BamHI-*hag4* rev	cccc**ggatcc**agaccctggcaacgccaagg
219	*hag* RNA probe for	attgaaagttgttgatgaag
224	BamHI-*fliW*-FR-p1 for	cccc**ggatcc**tggaggcacttctgaaagcg
225	SalI-*fliW*-FR-p2 rev	cccc**gtcgac**tgttcacgatccttttcttttac
227	NcoI-*fliW*-FR-p4 rev	cccc**ccatgg**cgatatcagcagtatctgctg
280	BamHI-*fliS*-FR-p1 for	cccc**ggatcc**gctgaaagaagaaaaataccgag
281	SalI-*fliS*-FR-p2 rev	cccc**gtcgac**gtgtcatcctccaaattacatttattg
283	NcoI-*fliS*-FR-p4 rev	caaa**ccatgg**gagagggaaaagagaaagagacc
284	NcoI-*fliS* for	caaa**ccatgg**cgatccaaaatccatatacagc
285	BglII-*fliS* rev	cccc**agatct**tgcgatcccgcctgatccgtg
286	SphI-*fliW* for	cccc**gcatgc**tcattcatacgaagtaccatg

287	BglII-*fliW* rev	cccc**agatct**gcatgattctcctccaatcggatg
288	KpnI-*mdh* for	cccc**ggtacc**ttgttcttgttgacattccgc
289	EcoRI-*mdh* rev	cccc**gaattc**ggataatactttcatgacatttttg
292	*clpC* VGF-GGR for	gctaaaacgcaataaatatggcggccgcaacgttcaggatgaaac
293	*clpC* VGF-GGR rev	gtttcatcctgaacgttgcggccgccatatttattgcgttttagc
298	$P_{fla/che}$-152 for	g**gaattc**ttgctgaccgtgtcggcattac
299	$P_{fla/che}$-152 rev	cg**ggatcc**gcgatattattagttatgac
300	SalI-*fliW*-FR-p3 for	cccc**gtcgac**ttggaggagaatcatgctag
301	$P_{fla/che}$ -209 to -6 for	ggaattcattttgcatttttcttcaaaaag
302	$P_{fla/che}$ -209 to -6 rev	cgggatcctattgtaagaaataacaggc
303	$P_{fla/che}$ -106 to 98 for	ggaattcctaacaatctaggactttatac
304	$P_{fla/che}$ -106 to 98 rev	cgggatcccaagattttgtatcgt
305	$P_{fla/che}$ -1 to 203 for	ggaattctatagttttacaattctcgac
306	$P_{fla/che}$ -1 to 203 rev	cgggatccaattttggaaagagactttttttg
317	SalI-*fliS*-FR-p3 for	cccc**gtcgac**atgaataatatagatcaactatacactg
318	BamHI-*clpC* for	cccc**ggatcc**atgatgtttggaagatttacag
319	NcoI-*clpC* rev	cccc**ccatgg**ttaattcgttttagcagtcg
332	HindIII-*yhfK* for	cccc**aagctt**atgaaagtgtttttaatcggag
333	NheI-*yhfK* rev	cccc**gctagc**tcatagtttcttcaatgcttcg
335	NheI-*yukF* rev	cccc**gctagc**tcacaaatccatgtgccgaag
338	*sigD* RNA probe for	ggtatgcttggtttatatgatgc
339	*sigD* RNA probe rev	gcaagctgtgcaatcagt
340	*yukF* for	tatgtcaaagagaaatcaagcacgaaaag
344	*flgB* RNA probe for	ttgagcttattttctggaacg
345	*flgB* RNA probe rev	tcattttcctcctgttaatacgg
seq44	upstream of *hag* for	atccagcgatgtgatctccg
seq45	downstream of *hag* rev	caggttgtaacgtagtgagc
seq63	upstream of *amyE* for	tgtattcactctgccaagttg
seq64	downstream of *amyE* rev	cgattaaagctactttatttac

3.2   Basic methods

Media and growth conditions   For bacteriological work, all media, buffers and materials were autoclaved at 121°C for 20 minutes prior to use. Antibiotic stock solutions and heat–sensitive media supplements were filtrated through a 0.2 μm syringe filter. *B. subtilis* stocks were stored at -80°C in LB medium + 20% glycerol. To start a culture, an aliquot from the glycerol stock was streaked on LB agar plates and grown over night at 37°C. If not otherwise indicated, 3 ml LB medium containing the appropriate antibiotics in a sterile test tube were inoculated with a single colony and grown over night at 37°C with shaking. The next morning, the optical density at 600 nm (OD_{600}) was determined using a microplate reader.

Over night cultures were diluted to OD_{600} 0.05 in fresh LB medium without antibiotics and grown at 37°C with rigorous shaking. Erlenmeyer flasks were filled with medium to a maximum of 20% of the total volume to ensure sufficient aeration. Antibiotics were used at the concentrations indicated below. Antibiotic stocks were prepared at 1000x concentration either in 50% ethanol (chloramphenicol and erythromycin), 70 % ethanol (tetracyclin) or deionized water and stored at -20°C. Erythromycin was used in combination with lincomycin at the indicated concentrations. The *erm* cassette confers resistance to both antibiotics. Strains carrying Campbell integrations (i.e. BNM205 and BNM224) were grown in the presence of antibiotics to avoid crossing out of the plasmid. Growth media were prepared as follows, supplements were filtrated and added after autoclaving.

Antibiotic	concentration [μg/ml]
ampicillin	100
chloramphenicol	10
erythromycin	1
lincomycin	25
kanamycin	10
spectinomycin	100
tetracyclin	10

LB   5 g/l yeast extract

10 g/l tryptone/peptone

5 g/l NaCl

dissolved in deionized H_2O

DYT   10 g/l yeast extract

10 g/l tryptone/peptone

5 g/l NaCl

dissolved in deionized H_2O

LB agar   5 g/l yeast extract

10 g/l tryptone/peptone

5 g/l NaCl

15 g/l agar, Kobe I

dissolved in deionized H_2O

Belitsky medium   50 mM Tris-HCl pH 7.5

1 g/l $(NH_4)_2$ SO_4

1 g/l Mg SO_4

1 g/l KCl

1 g/l tri- sodium citrate x2H_2O

Supplements   0.2% glucose

4.5 mM L-glutamate

160 μg/ml L-tryptophan

2 mM $CaCl_2$

600 μM KH_2PO_4

10 μM $MnSO_4$ x4H_2O

1 μM $FeSO_4$x7H_2O

dissolved in deionized H_2O

OD measurement   At regular intervals, 200 μl were withdrawn from growing cultures to measure OD_{600} in a microplate reader using clear flat-bottom 96 well plates (200 μl per well). Samples were diluted 10–fold in LB from an OD_{600} of 1.0 to ensure that the absorbance was in the linear range. To correct for the smaller sample density compared to cuvettes, the sample density for 200 μl in the 96 well plates was determined experimentally by parallel OD measurement of samples in a 1 cm cuvette (OD_{cuv}) and a microtiter plate (OD_{mic}). The OD_{600} was corrected for this value by the formula

$$OD_{corr} = d * OD_{mic}$$

$$d = \frac{OD_{cuv}}{OD_{mic}}.$$

Agarose gel electrophoresis   DNA fragments were mixed with 6x loading buffer and separated on 1% agarose gels without ethidium bromide in TAE buffer. Electrophoresis was run at 90 V for 45 to 90 minutes. Gels were stained in aqueous ethidium bromide solution (1 μg/ml) for 10 to 30 minutes and bands were visualized by UV irradiation. Eco130I–digested λ DNA was used as a molecular size marker.

TAE buffer   40 mM Tris-acetic acid pH 8.5
1 mM EDTA

SDS–PAGE   Tris-Glycin SDS–PAGE was performed according to the protocol of Laemmli [134]. 12.5% or 15% polyacryl amide minigels were prepared using acryl amide solution with a 37.5 to 1 ratio of acryl amide and bisacryl amide and polymerized by addition of APS solution and TEMED. 15 μl samples were mixed with 5 μl reducing 4x SDS sample buffer and boiled at 95°C for 5 minutes. 10 μl of this mixture was applied to the gels.

On gels for Coomassie staining, 5 μl protein molecular weight marker were applied as a standard. 5 μl Prestained Molecular Weight marker was used on gels for Western blotting. Electrophoresis was performed in Protean minigel chambers filled with SDS electrophoresis buffer for 45 minutes to 1 hour at a fixed current of 25 mA per gel. Gels were stained with Coomassie Brilliant Blue R250 solution for 15–30 minutes and

destained with Destain solution twice for 15 minutes. Wet SDS gels were scanned using a flat bed scanner.

12.5% separation gel solution (2 gels)	6.25 ml	30% v/v acryl amide
	3.75 ml	1.5 M Tris-HCl pH 8.8
	4.7 ml	H_2O
	150 μl	10% SDS
	150 μl	10% APS
	6 μl	TEMED
15% separation gel solution	7.5 ml	30% v/v acryl amide
	3.75 ml	1.5 M Tris-HCl pH 8.8
	3.45 ml	H_2O
	150 μl	10% SDS
	150 μl	10% APS
	6 μl	TEMED
5% sample gel solution	0.83 ml	30% v/v acryl amide
	1.25 ml	0.5 M Tris-HCl pH 6.8
	2.82 ml	H_2O
	50 μl	10% SDS
	50 μl	10% APS
SDS electrophoresis buffer	25 mM	Tris base (3 g/l)
	192 mM	Glycin (14.4 g/l)
	0.1% w/v	SDS (1 g/l)
4x SDS sample buffer	500 mM	Tris-HCl pH 6.8
	8% w/v	SDS
	40% v/v	glycerol
	20% v/v	β-mercaptoethanol
	5 mg/l	bromphenol blue

Coomassie staining solution	50% v/v	ethanol
	10% v/v	acetic acid
	250 mg/l	Coomassie Brilliant Blue R250

Destain solution	20% v/v	ethanol
	10% v/v	acetic acid

Tris–tricine SDS–PAGE   Tris–tricine gel electrophoresis was performed as described by Schägger[207]. Separation gels contained 16% v/v acryl amide and no urea. 3x Acrylamide/bisacryl amide (AB-3) solution was prepared freshly and used to prepare the gel solutions listed below. Samples were mixed with 4x Tris/Tricine sample buffer, boiled for 5 minutes at 95°C and applied to the gels. Gels were run initially at 30 V. After the samples had entered the separation gel, electrophoresis was continued for 4-5 hours at 200 V and stained.

AB-3 solution	48 g	acryl amide
	1.5 g	bisacryl amide
	ad 100 ml	deionized H_2O

3x gel buffer	3M	Tris-HCl pH 8.45
	0.3% w/v	SDS

16% separation gel solution	10 ml	AB-3 solution
	10 ml	3x gel buffer
	3 ml	glycerol
	7 ml	deionized H_2O
	100 μl	10% w/v APS
	10 μl	TEMED

4% sample gel solution	1 ml	AB-3 solution
	3 ml	gel buffer
	8 ml	deionized H_2O
	90 μl	10% w/v APS
	9 μl	TEMED
Anode buffer	100 mM	Tris-HCl pH 8.9
Cathode buffer (pH 8.25)	100 mM	Tris base
	100 mM	Tricine
	0.1% w/v	SDS
4x Tris/tricine sample buffer	150 mM	Tris-HCl pH 7.0
	12% w/v	SDS
	30% v/v	glycerol
	6% v/v	β-mercaptoethanol
	0.05% w/v	Coomassie Brilliant Blue G-250

3.3 Molecular biology techniques

3.3.1 Preparation of chromosomal DNA

To prepare chromosomal DNA, *B. subtilis* cells were grown over night in 3 ml LB (with antibiotics if applicable) at 37°C. 2 ml of the over night culture were centrifuged for one minute at 17000 *g* (13000 rpm). The pellet was resuspended in 1 ml TES buffer and centrifugation was repeated. The supernatent was discarded and the pellet was resuspended in 700 μl TES + 25 μl lysozyme solution (10 mg/ml in TES). The suspension was mixed well by inversion of the tube and incubated for 5 minutes at 37°C. Subsequently, 50 μl Proteinase K (10 mg/ml) and 150 μl Laurylsarcosine (6% w/v) were added and the mixture was incubated for 30-60 minutes at 37°C until the solution was clear, indicating complete cell lysis. For precipitation of cell debris and

proteins and extraction of DNA, 250 μl phenol (equilibrated at pH 8.0) and 250 μl chloroform were added and the sample was thoroughly mixed by inversion of the tube. To separate the aqeous from the organic phase, the sample was centrifuged for 15 minutes at 17000 g and 4°C. The upper (aqueous) phase was carefully transferred to a fresh tube without disturbing the interphase and mixed with 500 μl chloroform for a second extraction.

After centrifugation for 15 minutes at 17000 g and 4°C, 600 μl of the upper phase were transferred to a fresh tube and mixed with 1.2 ml ethanol. The sample was carefully mixed by inversion until a cloud of precipitated DNA became visible. To facilitate DNA precipitation, the sample was incubated at -20°C for at least 30 minutes. Subsequently, the DNA was pelleted by centrifugation (15 minutes at 17000g and 4°C) and washed twice with 1 ml 70% v/v ethanol. After the second centrifugation step, the pellet was dried in a SpeedVac instrument for 30 minutes at 42°C. The dried DNA pellet was resuspended in 200 μl TE buffer by mild shaking (400 rpm) for one hour at 42°C in a thermo shaker. DNA concentration was determined by absorbance at 260 nm using a Nanodrop spectrophotometer. Typical concentrations were 100-300 ng/μl.

TES buffer	10 mM Tris-HCl pH 8.0
	1 mM EDTA
	100 mM NaCl
TE buffer	10 mM Tris-HCl pH 8.0
	1 mM EDTA

3.3.2   Transformation of *E. coli*

Preparation of competent cells   To prepare heat shock competent *E. coli* cells, an over night culture was inoculated from a single colony and grown at 37°C. This culture was diluted to an OD_{600} 0.01 in 25 ml LB and grown at 37°C. At OD_{600} 0.35, 20 ml of the culture were harvested by centrifugation for 10 minutes at 5000 g and 4°C in a swingout rotor. The pellet was washed once in 10 ml ice-cold 50 mM $CaCl_2$ and then resuspended in 1.6 ml 50 mM $CaCl_2$. The cells were incubated for 60 minutes on ice, then mixed with 1 ml 50% glycerol and frozen at -80°C in 100 μl portions.

Transformation   100 μl heat competent cells were thawed on ice, mixed with 1 μl plasmid DNA (50-100 ng) or 20 μl ligation reaction and incubated for 30 minutes on ice. Subsequently, the cells were heat shocked at 42°C for 90 seconds and rapidly cooled on ice. After 10 minutes incubation on ice, 500 μl LB was added and the cells were grown with shaking for 40 minutes at 37°C. For transformation of ligation reactions, the bacteria were pelleted for 1 minute at 17000 g and resuspended in 100 μl LB. Finally, 100 μl were plated on selective agar.

3.3.3   Transformation of *B. subtilis*

A single colony from a fresh streak of *B. subtilis* cells was used to inoculate an over night culture in 10 ml CM medium with antibiotics in a 100 ml Erlenmeyer flask at 37°C. After about 16 hours, 600 μl of the over night culture was used to inoculate a 10 ml CM culture without antibiotics in a 200 or 250 ml Erlenmeyer flask. After 3 hours of growth at 37°C with rigorous shaking, the culture was diluted by addition of 10 ml starvation medium and shaking was continued for 2 hours to obtain competent cells. 400 μl of the competent cells were mixed with 300-600 ng of chromosomal DNA or 1-2 μg plasmid DNA and incubated for 1 hour at 37°C with shaking.

CM medium	14 g/l K_2HPO_4
	6 g/l KH_2PO4
	2 g/l $(NH_4)_2SO_4$
	1 g/l tri- sodium citrate $x2H_2O$
	0.2 g/l $MgSO_4x7H_2O$

Supplements	0.5% glucose
	6 mM $MgSO_4$
	1 mg/ml L-tryptophan
	0.02% casamino acids
	0.22 μg/ml ammonium iron citrate

Starvation medium   14 g/l K_2HPO_4

6 g/l KH_2PO_4

2 g/l $(NH_4)_2SO_4$

1 g/l tri- sodium citrate $x2H_2O$

0.2 g/l $MgSO_4x7H_2O$

Supplements   0.5% glucose

6 mM $MgSO_4$

3.3.4   Cloning

PCR was performed using Phusion polymerase according to the manufacturer's instructions. PCR products were purified by the Zymo DNA Clean & concentrator kit using the manufacturer's protocol. Plasmids were transformed into *E. coli* XL-1 blue for amplification and prepared from 3 ml LB over night cultures using the QIAprep Spin Miniprep kit according to the manufacturer's instructions. Plasmids and purified PCR products were digested with FastDigest restriction enzymes using FastDigest buffer for 1-2 hours at the temperature and enzyme concentration recommended by the manufacturer. Digested plasmids were purified by agarose gel electrophoresis and gel extraction using the ZymoClean^{TM} Gel DNA recovery kit following the supplied protocol. Digested PCR products were purified using the Zymo DNA Clean & concentrator kit according to the standard protocol.

For ligation, 10-50 ng of plasmid were mixed with a 3–fold to 10–fold molar excess of insert PCR product and digested with 5 units of T4 DNA Ligase. Ligation reactions (20 μl) were incubated in a 5 liter water bath starting at room temperature and cooled down to 4°C over night in the cold room. Ligation products and negative controls containing no insert DNA were transformed into 100 μl competent *E. coli* XL-1 blue by heat shock transformation (20 μl ligation product), plated on LB plates containing 100 μg/ml ampicillin and grown over night at 37°C. Clones were grown over night in 3 ml LB and plasmid was extracted (QiaPrep Spin kit). Control digestion was performed using the same restriction enzymes as for cloning and positive clones were sequenced.

All inserts were amplified by PCR using 10-30 ng chromosomal DNA extracted from the *B. subtilis* 168 wild type strain as a template, except for *ibpA* and *ibpB*, which were amplified from *E. coli* W3110 chromosomal DNA. Primer sequences are listed in Table 7. Restriction digests and ligation reactions were performed as described in section 3.3.4, page 58. The restriction sites that were used for each plasmid are listed in Table 6.

pDR-*yhfK* To obtain plasmid pDR-*yhfK*, plasmid pSN56 (which is identical to pDR111 with spx^{DD}[182] in HindIII/NheI) was digested with HindIII and NheI to cut out the *spxDD* insert, gel-purified and ligated with the HindIII/NheI-digested *yhfK* insert. Due to a HindIII restriction site in the *yukF* gene, this strategy was not possible for pDR-*yukF*. Therefore, pSN56 was linearized with HindIII and blunted with T4 DNA Polymerase according to the manufacturer's protocol. The linear blunted plasmid was then digested with NheI to cut out the spx^{DD} insert and gel extracted. The *yukF* gene was amplified with a 5'-phosphorylated forward primer (340) and a reverse primer carrying a NheI restriction site (335). This fragment was ligated into the linear blunted plasmid resulting in pDR-*yukF*. The HindIII restriction site in this plasmid was reconstituted by additional residues on primer 340.

pMAD plasmids For plasmids pMAD-*fliS* and pMAD-*fliW*, the 1000 kb upstream and downstream flanking regions of the *fliS* and *fliW* genes were amplified by PCR using the primer pairs 280/281 and 317/283 (*fliS*) and 224/225 and 300/227 (*fliW*). The *fliS* gene is positioned in the *fliDST* operon and the *fliS* ORF is translationally coupled to *fliT*[130]. Likewise, *fliW* is translationally coupled to the downstream *csrA* gene[177]. The primers 300 and 317 are designed to preserve these adjacent genes to avoid polar effects. The upstream fragments were digested with BamHI and SalI and the downstream regions were cut with SalI and NcoI. To facilitate digestion, the pMAD-*hag* plasmid was used for cloning instead of empty pMAD. After digestion with BamHI and NcoI, the plasmid was purified by extraction from an agarose gel and ligated with both the upstream and downstream flanking reagions in a single reaction.

pTYB2-*clpC*(VGF::GGR) and pMAD-clpC(VGF::GGR)   To obtain plasmid
pTYB2-*clpC*(VGF::GGR), pTYB2-*clpC* was mutagenized using the Quikchange Site
Directed Mutagenesis Kit and primers 292 and 293, encoding the amino acid exchanges
V671G and F673R and an additional NotI restriction site. For construction of the
pMAD-*clpC*(VGF::GGR), which is designed to introduce the point mutations into
the chromosome-encoded *clpC* gene, the wild type *clpC* gene was first cloned into the
BamHI and NcoI sites of pMAD to obtain pMAD-*clpC*(ORF). Quikchange mutagenesis
was attempted with this plasmid, however no positive clones were obtained, possibly
due to the size of this plasmid (12,5 kb). Therefore, primers 318 and 319 were used
to amplify the mutated *clpC* gene from plasmid pTYB2-*clpC*(VGF::GGR) and the
product was ligated into the BamHI and NcoI sites of pMAD, resulting in pMAD-
clpC(VGF::GGR).

3.3.5   Strain construction

All *in vivo* experiments were performed in the *B. subtilis* 168 (*trpC2*) background[6].
Strains obtained from other laboratories were crossed into this background. To this
end, the recipient strains were made competent and transformed with chromosomal
DNA prepared from the donor strains. For example, strain BNM103 was obtained by
crossing of chromosomal DNA from strain BUG1 (U. Gerth, University of Greifswald)
into 168. Double and triple mutants were generated in a step–wise manner, in which
one single mutant was transformed with chromosomal DNA of the other single mutant.

***clp* mutants**   ClpP, *clpC* and *clpX*, *degU* mutations were always introduced last
because of competence defects and/or growth problems in competence medium of
these strains and to avoid the selection of suppressor mutants. The *clpC degSU* and
clpX degSU double mutants were obtained by simultaneous transformation with two
chromosomal DNA samples and selection for two antibiotics.

GFP fusion strains   Strains BNM224 were constructed by transformation of the
pSG1151-*mdh* plasmid into strain 168 and selection for chloramphenicol. Strains
BNM216, BNM217 were constructed by transformation of plasmids pSG1154-*ibpA*
and pSG1154-*ibpB* in strain 168 and selection for spectinomycin. Strain BNM227

was constructed by transformation of plasmid pSG1154-*dnaK* into strain BNM118 (Δ*dnaK*::cat) and selection for chloramphenicol and spectinomycin.

amyE insertions   Strains BNM345, BNM346, BNM421, BNM426 were obtained by transforming plasmids pDL-*fla/che*152-*bgaB*, pDR-*fla/che152-lacZ*, pX-*hag1* and pX-*hag4*, respectively, into the wild type strain and selection for chloramphenicol. These plasmids integrate into the *amyE* locus by double homologous recombination, thus inactivating the *amyE* gene. This knockout was confirmed by an amylase assay. To this end, the strains were patched on LB agar plates containing 1% starch. After over night incubation, the plates were placed over a plastic lid containing a few iodine crystals. After a few minutes, iodine staining of the starch plates was observed. Amylase positive strains produce a non–stained halo around the patch, wheras successful *amyE* insertions lack this zone of starch degradation.

Combination of strains   Strain BNM111 was transformed with plasmids pMMN521 and pSN56 to obtain BNM350 and BNM351. Strains BNM301 and BNM328, which were constructed by transformation of chromosomal DNA from strains DS791 and DS793 (D. Kearns), were also tested for amylase activity. Strains BNM302 to BNM308 and BNM337 are derivatives of BNM301 obtained by transformation of chromosomal DNA from the respective single mutants. Likewise BNM329 to BNM335, BNM338 and BNM339 are derivatives of BNM328 and BNM347 to BNM349 are derived from BNM346.

Construction of markerless deletions and chromosomal point mutations
To obtain the markerless deletion mutants BNM126 (Δ*hag*), BNM403 (Δ*fliS*) and BNM404 (Δ*fliW*), plasmids pMAD-*hag* (kindly provided by D. Kearns, University of Atlanta, USA), pMAD-*fliS* and pMAD-*fliW*, respectively, were transformed into strain 168 at 37°C by natural competence, selecting for the erythromycin/lincomycin (ery/linc) marker to force an unstable Campbell integration of the plasmid into one of the flanking regions[9]. Two to three single clones were picked from the ery/linc plates and grown over night at 22°C in LB without antibiotics. The culture was diluted 1:100 in fresh LB medium and over night cultivation at 22°C was repeated. By this proce-

dure, the plasmid was forced to cross out of the chromosome and was lost due to the absence of ery/linc[9]. Subsequently, a dilution series (10^4 to 10^7) was plated on LB plates without antibiotics and inbubated at 37°C over night.

Approximately 8 to 16 clones were picked from the plates and replica-plated on LB plates with and without ery/linc. Sensitivity to ery/linc indicates a successful loss of the pMAD plasmid. To screen the ery/linc sensitive clones for deletions of *hag*, *fliS* and *fliW*, chromosomal DNA was extracted from a number of clones and used as a template for control PCR reactions with primers that bind 1000 bases upstream and downstream of the gene of interest (primers 280/283 for *fliS*, 224/227 for *fliW* and seq44/seq45 for *hag*). The PCR products were digested with SalI and their size was analyzed by agarose gel electrophoresis and ethidium bromide staining. A successful deletion event by pMAD generates a SalI restriction site in place of the gene and is thus indicated by two 1000 bp fragments after the SalI digest.

Combination of markerless deletions with other strains   To obtain strain BNM446, the pMAD-*fliS* plasmid was transformed into strain BNM126 (Δ*hag*) and crossed out to produce a Δ*hag* Δ*fliS* double mutant. Subsequently, plasmid pX-*hag4* was transformed into this strain to yield strain BNM446. Strains BNM412 to BNM415, BNM422 to BNM425, BNM427 to BNM430 and BNM447 to BNM450 were constructed by transformation of chromosomal DNA from *clp* mutants (BNM103, BNM105, BNM106, BNM107) and the *ypbH* mutant (BNM115) into strains BNM403 (Δ*fliS*), BNM421 (Δ*hag amyE*::P_{xyl}-*hag1*::cat), BNM426 (Δ*hag amyE*::P_{xyl}-*hag4*::cat) and BNM446 (Δ*fliS* Δ*hag amyE*::P_{xyl}-*hag4*::cat), respectively.

Chromosomal *clpC* point mutant   To obtain strain BNM245, plasmid pMAD-*clpC*(VGF::GGR), carrying the entire *clpC* gene with point mutations encoding a NotI restriction site was transformed into the 168 strain, selecting for ery/linc. Negative selection at 22°C was performed as described above. Chromosomal DNA from ery/linc sensitive clones was used as a template for a control PCR reaction with primers 318 and 319, generating a 2.4 kb *clpC* fragment. The successful introduction of the point mutations was confirmed by NotI digestion of the fragment and gel electrophoresis.

3.4   Genetic screens

Construction of a transposon library   To isolate motile suppressor mutants from strain BNM351 and non-motile mutants from BNM301, the strains were transformed with plasmid pMarB[137], harboring a mariner transposon, as described in section 3.3.3, selecting for kanamycin resistance. The kanamycin resistance cassette is located in the transposon, wheras an erythromycin/lincomycin (ery/linc) cassette is situated outside of the transposon. Plates were incubated at 30°C for 2 days to avoid transposition of the mariner transposon at this step. 24 clones were replica–plated on kanamycin and ery/linc. 8 clones that were resistant to both antibiotics, indicating the presence of a complete pMarB plasmid, were grown in 10 ml LB medium without antibiotics at 37°C for 8 hours to reduce the copy number of the plasmid. Aliquots of these cultures were frozen in 20% glycerol and stored at -80°C.

For each clone, a dilution series (10^0 to 10^{-3}) was plated on kanamycin and on ery/linc plates and the plates were incubated over night at 50°C to initiate transposition (the transposase gene is under the control of a heat–inducible σ^B–dependent promoter on plasmid pMarB[137]). The next day, colonies were counted and the ratio of kanamycin resistant colonies to ery/linc resistant colonies was determined for each clone. The clone with the highest ratio (indicating the largest percentage of complete transposition events) was selected for construction of a transposon library. To this end, the strain was plated on 10 large LB plates, aiming for 2500 colonies per plate (library of 25000 clones) and incubated at 50°C over night for transposition. The colonies were scraped from the plates and resuspended in 5 ml LB each. The suspensions were pooled and centrifuged for 10 minutes at 4500g and 4°C and resuspended in LB + 20% glycerol. The cells were resuspended carefully by vortexing and subsequently mixed on an orbital rotator for 30 minutes at 4°C. The library was aliquoted in 1 ml portions, frozen in liquid nitrogen and stored at -80°C.

Screen for suppressors of spx^{DD}   To determine the number of colony forming units (CFU) in the library pools, aliquots of the library were thawed and plated on LB without antibiotics at dilutions of 10^0 to 10^{-9}, incubated over night at 37°C and colonies were counted. For the BNM351 suppressor screen, 200 3 μl samples from the transposon library were used to inoculate swim plates (section 3.9) containing 0.1 mM IPTG. Under

these conditions, the parent strain BNM351 is non-motile. Swim plates were incubated for 8 hours at 37°C and left over night at room temperature. Motile suppressors were picked and streaked to single colonies on LB plates and the motility phenotype was verified by motlity assays. Chromosomal DNA was isolated from 25 candidate clones (section 3.3.1) and backcrossed into the parent strain BNM351, selecting for kanamycin resistance (section 3.3.3) to separate multiple transposon insertions.

Four colonies from each backcross were tested for motility in the presence of 0.1 mM IPTG, resulting in 70 non-motile candidates with a single transposon insertion. Chromosomal DNA was extracted from these clones and used as a template for a control PCR with primers seq63/seq64 to amplify the *amyE* locus and verify if the transposon had inserted into this locus. Insertion into this locus could result in rescue of the motility phenotype by inactivation of the $P_{hyperspank(Hy)}$-*spx*-::spec construct. 53 out of the 70 backcrossed clones from 22 out of 25 original clones had no insertion in the *amyE* locus, indicating correct second site suppressor mutations. Chromosomal DNA from these clones will be sequenced for mapping of the transposon insertion site.

Screen for positive regulators of *fla/che* To screen for positive regulators of the *fla/che* operon, the transposon library constructed from BNM30, carrying a $P_{fla/che}$-*lacZ* fusion, was plated on LB agar plates containing 0.02% X-Gal and incubated over night at 37°C. 40000 colonies (10 plates harboring 4000 colonies each) were screened and 167 white colonies were picked and restreaked on 0.02% X-Gal. 78 clones appeared white compared to the parent strain and were tested for swimming motility, thus eliminating transposon insertions in the *lacZ* gene. 14 clones were compromised in swimming motility. From these clones, chromosomal DNA was extracted and backcrossed into the parent strain BNM301 to separate mutlitple transposon insertions. Four clones from each backcross were tested for swimming motility. DNA was extracted from the clones exhibiting a motility defect and will be sequenced for mapping of the transposon insertion site.

3.5   Protoplast preparation

30 ml of a growing *B. subtilis* culture were collected and centrifuged for 10-15 minutes at 4500g and 4°C in a swingout rotor centrifuge. Pellets were frozen and stored at

-20°C for 1-3 days or immediately used for protoplast preparation. The pellets were resuspended in 1 ml STM buffer containing sucrose and centrifuged for 15 minutes at 17000g and 4°C. The supernatant was discarded and the washing procedure was repeated once. Subsequently, the pellet was resuspended in 200 μl STM buffer + 0.3 mg/ml lysozyme and incubated for 30 minutes at 37°C to obtain protoplasts. The protoplasts were carefully resuspended in 1 ml STM by vortexing and centrifuged for 15 minutes at 17000g and 4°C. After repeating this washing procedure once, the protoplasts were lysed by resuspension in 200 μl TM buffer with DNase and RNase and incubated on ice for 30 minutes for DNA and RNA degradation. Finally, the lysate was centrifuged for 20 minutes at 17000g and 4°C to separate cell debris and unlysed protoplasts and the supernatent was transferred to a fresh tube.

Total protein concentration of the lysate was determined by the Bradford assay, using Rotiquant solution. 5 μl of protein lysate (diluted in TM buffer if necessary) was transferred to a flat-bottom 96-well plate and mixed with 250 μl Rotiquant solution diluted 1:5. Absorbance at 495 nm was measured and concentration was determined according to a BSA calibration using TM buffer as a blank sample. Typical concentrations were 5-10 mg/ml total protein from a 30 ml *B. subtilis* sample grown to OD 1.0.

3.6   Western blot analysis

SDS–PAGE gels loaded with 2.5 to 10 μg protein lysate per lane were run at 25 mA per gel for 45 minutes to 1 hour and subsequently incubated in Transblot buffer for 2 minutes. A stack of 4 3MM Whatman papers were drenched in Transblot buffer and placed on the lower electrode of a semidry blotting chamber. A PVDF membrane was quickly submerged in methanol, incubated in Transblot buffer for 2 minutes and then placed onto the Whatman papers. Next, the SDS–PAGE gel was placed onto the PVDF membrane and topped with another stack of 4 Whatman papers drenched in Transblot buffer. After careful removal of air bubbles, the blotting chamber was closed by attachment of the upper electrode. The blotting chamber was connected to a power supply and electroblotting was performed at a fixed current of 1 mA per cm^2 (typically 50 mA per gel) for 1 hour.

Transblot buffer (pH 8.2)	20 mM	Tris base
	150 mM	glycine
	20% w/v	methanol
TBS buffer	50 mM	Tris-HCl pH 8.0
	150 mM	NaCl
TBS-T buffer	50 mM	Tris-HCl pH 8.0
	150 mM	NaCl
	0.5% w/v	Tween-20
Blocking buffer (TBS-M)	50 mM	Tris-HCl pH 8.0
	150 mM	NaCl
	5% w/v	skim milk pouder
Alkaline phosphatase (AP) buffer	100 mM	Tris-HCl pH 9.5
	100 mM	NaCl
	5 mM	$MgCl_2$
NBT	5% w/v	in 70% v/v dimethyl formamide
BCIP	5% w/v	in dimethyl formamide

After disassemby of the blotting chamber, the PVDF membrane was incubated with 10-20 ml TBS-M blocking buffer over night at 4°C with shaking. Subsequently, the PVDF membrane was incubated with primary antibodies against the protein of interest diluted in 10-20 ml TBS-M for 1-3 hours at room temperature. Origin and dilutions for the antibodies used are listed in Table 11. The blot was washed twice in TBS-T buffer for 10 minutes to remove the primary antibodies and then incubated with secondary antibodies (goat anti–rabbit or rabbit anti–sheep) conjugated to alkaline phosphatase for 1 hour at room temperature. The secondary antibodies were removed by washing twice in TBS buffer. Finally, the membrane was incubated in 20 ml AP buffer for

10 minutes. Western blots were developed either by addition of 66 μl BCIP and 132 μl NBT in 20 ml AP buffer or by the ECF Western blotting kit. ECF substrate is dephosphorylated by alkaline phosphatase, resulting in fluorescence, which was scanned using a Phosphoimager.

Table 11: Antibodies

Detected epitope	Dilution	Source	Supplied by
CodY	1:10000	rabbit	A.L. Sonenshein (Tufts University)
DegU	1:5000	sheep	N. Stanley-Wall (University of Dundee, UK)
Digoxigenin	1:5000	sheep	Roche Applied Science
Hag	1:40000	rabbit	Pineda Antibody Service
MDH	1:10000	rabbit	Pineda Antibody Service
Rabbit IgG	1:10000	goat	GE Healthcare
RnjA/B	1:10000	rabbit	H. Putzer (University of Paris)
SigD	1:5000	rabbit	J. Helmann (Cornell University, USA)
Spx	1:1000	rabbit	P. Zuber (University of Oregon, USA)
Sheep IgG	1:10000	rabbit	Antikoerper Online

3.7 Northern blot analysis

RNA preparation To avoid contaminations with RNases, plastic tubes were autoclaved twice, sterile RNase free pipette tips were used and latex gloves were worn for all RNA experiments. All buffers were either stirred over night with 0.1% DEPC and autoclaved or autoclaved twice (i.e. Tris buffers). RNA was extracted from *B. subtilis* cultures using the FastRNA Pro Blue kit. 30 ml cultures were harvested by centrifugation for 10 minutes at 4500g and 4°C in a swingout rotor centrifuge. Pellets were resuspended in 1 ml RNA*pro*^{TM} containing acidic phenol and transferred to a screw-cap tube containing Lysing Matrix B.

The cells were lysed by shaking in a Retsch mill for 10 minutes at a frequency of 30 s^{-1}. The samples were then centrifuged for 5 minutes at 17000g to pellet beads and unlysed cells and the supernatent was transferred to fresh tubes. After incubation for 5 minutes at room temperature, the lysate was mixed with 300 μl chloroform, vortexed for 10

seconds and incubated for 5 minutes at room temperature to facilitate dissociation of protein-RNA complexes. After centrifugation for 5 minutes at 17000g and 4°C, the upper phase was transferred to a fresh tube. 500 μl cold ethanol were added to precipitate the RNA and the solution was mixed by inversion of the tube.

To facilitate precipitation, the samples were incubated at -20°C for 30 minutes. Subsequently, the samples were centrifuged for 15 minutes at 17000g and 4°C. After this step, RNA was visible as a white pellet at the bottom of the tube. The precipitated RNA was washed once with 500μl 70% v/v ethanol diluted in DEPC-H_2O. The pellet was air-dried for 5 minutes at room temperature under a flow hood and finally resuspended in 100 μl DEPC-H_2O. RNA concentration was measured by absorbance at 260 nm using a NanoDrop spectrophotometer. The RNA was stored at -80°C or at -20°C for shorter periods.

DNase digestion   In order to eliminate contaminations with genomic DNA, the RNA samples were digested with RNase free DNase I according to the following scheme and incubated for 1 hour at 37°C.

DNase I digest

87 μl	RNA in DEPC-H_2O
10 μl	10x DNase I buffer
3 μl (30 U)	RNase free DNase I

DNase I was inactivated for 20 minutes at 75°C. After this step, 1.5 ml Phase Lock tubes were prepared by short centrifugation to allow the Phase Lock material to settle at the bottom of the tubes. 100 μl DEPC-H_2O were added to the RNA, the samples were mixed and transferred to Phase Lock tubes. Subsequently, 200 μl phenol:chloroform:isoamyl alcohol (25:24:1, PCI) was added to the tubes. The samples were mixed by inverting 10 times and centrifuged for 5 minutes at 17000g and 4°C. The phenolic phase was retained under the Phase Lock gel matrix in this step, wheras the aqueous phase was on top of the gel matrix. 200 μl chloroform:isoamyl alcohol (24:1) were added to this upper phase and the tubes were inverted 10 times for mixing. After centrifugation for 5 minutes at 17000g and 4°C, the upper phase (200 μl) was carefully removed and transferred to a fresh tube. 20 μl 3 M sodium acetate (pH 5.2) and 600 μl cold ethanol were added to this solution and the sample was incubated for

30 minutes at -80°C to allow RNA precipitation. The pellet was washed twice with 70% ethanol in DEPC-H$_2$O and air dried under a flow hood. The RNA was resuspended in 100 μl DEPC-H$_2$O for 2 hours at 4°C. RNA concentration was measured in a NanoDrop spectrophotometer and was typically 1-5 μg/μl from a 30 ml culture grown to OD$_{600}$ 1.0. In addition, RNA quality was checked by agarose gel electrophoresis and ethidium bromide staining to visualize ribosomal RNAs.

Denaturing formaldehyde gel elecrophoresis   A horizontal elecrophoresis chamber was cleaned by over night incubation in hypochloride solution and the chamber was rinsed in DEPC-H$_2$O. To prepare a 1.2 % agarose gel, 1.2 g agarose were dissolved in 72 ml DEPC-H$_2$O in a microwave oven and cooled to about 50°C. Subsequently, 10 ml 10x MOPS buffer and 18 ml 37% formaldehyde solution were mixed with this solution and the gel mix was poured into the chamber and allowed to solidify. The gel chamber was filled with 1x MOPS buffer. RNA samples were diluted in DEPC-H$_2$O, mixed 1:1 with 2x RNA sample buffer and heated to 65°C for 10 minutes to denature secondary structures.

10x MOPS buffer	400 mM	MOPS
	50 mM	sodium acetate
	10 mM	EDTA
	0.1% v/v	DEPC

2x RNA sample buffer	1.5x	MOPS buffer
	75% v/v	formamide
	3.33% w/v	formaldehyde
	3% w/v	Ficoll 70
	0.02% w/v	Bromphenol blue

20x SSC	300 mM	tri-sodium citrate pH 7.0
	3 M	NaCl
	0.1%	DEPC

An appropriate volume to yield 200 ng to 10 μg/lane total RNA was applied to the pockets of the gel. 10 μl RNA Molecular Weight Marker III was mixed 1:1 with 2x RNA

sample buffer and applied to the gel as a size standard. Electrophoresis was performed at a fixed voltage of 80 V for 2 hours and 45 minutes. Subsequently, the gel was rinsed three times in DEPC-H$_2$O and and formaldehyde was removed by incubation in 20x SSC twice for 15 minutes with mild shaking.

Vacuum blotting   A positively charged nylon membrane was shortly drenched in DEPC-H$_2$O, incubated in 10x SSC for 5 minutes and then placed on top of a Whatman paper drenched in DEPC-H$_2$O on a vacuum blotter. A plastic membrane with a cut-out space (mask) the size of the nylon membrane was adjusted on top and locked. Next, the agarose gel was placed on the nylon membrane so that the mask was covered completely and the gel was covered in 10x SSC. After removal of air bubbles, a vacuum pump was connected to the system and vacuum blotting was performed for 1.5 hours at a pressure of 5 mm Hg. The level of 10x SSC was checked in regular intervals and 10x SSC was added if necessary to cover the gel. After transfer of the RNA the nylon membrane was washed twice for 5 minutes in 2x SSC, dried for 5 minutes and then UV irradiated for 10 minutes at 328 nm to crosslink the RNA to the nylon membrane. Subsequently, the blot was stained in methylen blue solution for 5 minutes to visualize the 23S, 16S and 5S ribosomal RNAs as a control for equal sample application and blotting. The membrane was destained in Bleaching buffer twice for 15 minutes and re-equilibrated in 2x SSC twice for 5 minutes.

10x SSC	150 mM	tri-sodium citrate pH 7.0
	1.5 M	NaCl
	0.1%	DEPC
2x SSC	30 mM	tri-sodium citrate pH 7.0
	300 mM	NaCl
	0.1%	DEPC
Methylene blue solution	0.02%	methylene blue
	300 mM	sodium acetate pH 5.5
	0.1%	DEPC

Bleaching buffer	0.2x	SSC
	1% w/v	SDS
	0.1%	DEPC

Preparation of the hybridization probes Digoxigenin (DIG) labeled DNA probes were prepared by PCR using PCR DIG labeling mix containing DIG-dUTP. PCR was performed with Phusion polymerase and primers 219/166 (*hag* probe), 338/339 (*sigD* probe) and 334/335 (*flgB* probe, see Table 7 for sequences). A first round of PCR was performed with chromosomal DNA as a template without DIG labeling mix. The product of this reaction was used as a template for a second round of PCR in the presence of DIG labeling mix. The PCR products were purified by gel extraction using the ZymoClean^{TM} Gel DNA recovery kit and eluted in 20 μl DEPC-H$_2$O. The probes were denatured for 5 minutes at 95°C and cooled rapidly on ice.

Northern hybridization The nylon membrane was transferred to a hybridization glass tube and incubated with 20 ml DIG Easy Hybridization solution for 1 hour at 47°C with rotation in a hybridization oven. 20 μl DIG-labeled probe was diluted in 20 ml DIG Easy Hybridization solution and the membrane was hybridized with this solution over night at 47°C with rotation. The next day, the blot was washed twice with 20 ml wash buffer 1 for 5 minutes at 47°C and twice with wash buffer 2 for 30 minutes (also at 47°C) to wash off unbound probe.

Wash buffer 1	2x	SSC
	0.1%	SDS
	0.1%	DEPC

Wash buffer 2	0.1x	SSC
	0.1%	SDS
	0.1%	DEPC

Detection with anti-DIG antibodies   The blot membrane was transferred to a
Petri dish and rinsed in Detection buffer 1. Next, the membrane was blocked in Block-
ing buffer for 30 minutes at room temperature. Anti-digoxigen antibodies conjugated
to alkaline phosphatase were diluted 1:5000 in Blocking buffer and applied to the blot
for 1.5 hours at room temperature. Subsequently, the blot was washed twice for 15
minutes in Detection buffer 1 and finally equilibrated in Detection buffer 2 for 2 min-
utes. Detection was performed either with CDP Star solution followed by development
of X-ray films or by the ECF Western blotting kit and fluorescence scanning using a
phosphoimager (used for quantification of the RNA stability experiments).

Detection buffer 1	100 mM	maleic acid pH 7.5
	150 mM	NaCl
Blocking buffer	100 mM	maleic acid pH 7.5
	150 mM	NaCl
	1% w/v	Blocking reagent
Detection buffer 2	100 mM	Tris-HCl
	100 mM	NaCl
	5 mM	$MgCl_2$

3.8   RNA stability experiments

A culture of *B. subtilis* strain BNM351 was inoculated to OD_{600} 0.05 in 200 ml LB in
a 2 l flask and grown at 37°C. At OD_{600} 0.5, the culture was split in 2 100 ml cultures
in 500 ml flasks. IPTG was added to a concentration of 1 mM to one of the cultures,
while the second culture was not induced and shaking was continued for either 10 or 30
minutes. At this time, rifampicin was added to both cultures to a final concentration of
100 μg/ml to inhibit the RNA polymerase. 10 ml samples were removed immediately
from both cultures, rapidly mixed with 1.25 ml Stop solution (5% phenol diluted in
ethanol) and stored on ice. Shaking at 37°C was continued and further samples were
withdrawn after 2, 4, 6, 8, 10, 20 and 40 minutes, mixed with Stop solution and
stored on ice. Samples were centrifuged at 4500g in a swingout rotor centrifuge for 10
minutes at 4°C. The supernatent was removed and pellets were stored at -20°C. RNA

preparation from the cell pellets and Northern blotting was performed as described in section 3.7.

3.9 Motility assay

Over night cultures were grown in 3 ml LB with antibiotics at 37°C. The next day, OD_{600} was determined and the cultures were diluted to OD_{600} 2.0 in fresh LB medium. Swim plates were freshly prepared in large Petri dishes (100 ml Swim plate agar per plate) and dried at room temperature with closed lids. 3 μl of the diluted cultures were pipetted under the surface of the swim plates and the plates were incubated at 37°C for 6-8 hours.

Swim plate agar	10 g/l	tryptone/peptone
	5 g/l	NaCl
	3 g/l	agar, bacteriologic
		dissolved in deionized H_2O

3.10 β-galactosidase assay

1 ml samples of a growing *B. subtilis* carrying a *lacZ* fusion were collected and centrifuged for 5 minutes at 17000g. The supernatent was discarded and the pellets were frozen at -20°C. OD_{600} was determined in parallel as described above. At lower OD values, sample volumes were adjusted to 2 ml or 5 ml to increase the number of cells for a higher β-galactosidase activity. The sample volume was included in the formula for the determination of β -galactosidase activity.

For the β-galactosidase measurement, the cell pellets were thawed on ice and resuspended in 500 μl freshly prepared Z buffer. 10 μl toluene were added to make the cells permeable for the ONPG substrate. The samples were vortexed for 15 seconds and incubated on ice for 30 minutes. For the assay, 150 μl Z buffer were transferred into the wells of a flat–bottom 96 well plate using a 8–channel multi–pipette. Subsequently, 50 μlof the samples were added to these wells and mixed by pipetting.

To start the assay, 50 μl ONPG (4 mg/ml in Z buffer) were added to the wells by a 8–channel multi–pipette, the 96 well plate (with lid attached) was quickly inserted into the slot of a microplate reader and a kinetic measurement (absorbance at 420 nm,

measurement every 60 seconds for 15 minutes, shaking between the measurements, room temperature) was started. The β-galactosidase activity (in Miller Units[161]) was calculated from the linear slope of the absorbance at 420 nm over time ($\frac{dA_{420}}{dt}$) according to the following formula:

$$activity[MU] = 1000 * \frac{dA_{420}}{dt} * \frac{f * d}{OD_{600} * V_s[ml]} = 20000 * \frac{\frac{dA_{420}}{dt}}{OD_{600} * V_s[ml]}$$

f is a dilution factor obtained by the ratio of the total sample in Z buffer (500 μl) and the sample used for the assay (50 μl). d is factor that takes into account the difference of the sample thickness between a 250 μl sample in a microplate well and a regular 1 cm cuvette and was determined experimentally to 2.0 (measured as described above in section 3.2).

Z buffer	100 mM	NaPO$_4$ pH 7.0
	1 mM	MgSO$_4$
	100 mM	β-mercaptoethanol

For comparison of β-galactosidase activities of strains exhibiting lag phases in growth (i.e. *clpP* and *clpX* mutants), the time axis was normalized to T0, the point of deviation from exponential growth.

3.11   *Pulse chase* labeling and immunoprecipitation

Cells were grown in Belitsky minimal medium (see section 3.2) to OD$_{600}$ 0.7 at 37°C. 3.5 ml bacteria were removed and pulse labeled with 30 μCi L-^{35}S-methionine for 10 minutes at 37°C. The chase was started by addition of 100 μl L-methionine and 400 μl samples were taken after different times (typically 0, 5, 10, 20, 40 and 60 minutes) and mixed with 50 μl TCA. TCA-precipitated samples were incubated on ice for 10 minutes and centrifuged for 15 minutes at 17000g and 4°C. The pellets were washed twice in 1 ml acetone, air-dried shortly and resuspended in 20 μl lysis buffer containing SDS. Next, the samples were boiled for 3 minutes at 95°C to denature proteins. 270 μl KI buffer was added and the samples were incubated on ice for 15 minutes.

Remaining precipitate was separated by centrifugation for 15 minutes at 17000g and 4°C and 100 μl of the supernatent were mixed with 2 μl polyclonal anti-Hag antiserum

and incubated over night at 4°C for immunoprecipitation. The next day, 8 μl ProteinA-Magnabeads were added to the solution and mixed. The magnetic beads with bound Hag antibodies and immunoprecipitated Hag were washed twice in 200 μl KI buffer using a magnet. Subsequently, the magnetic beads were resuspended in 20 μl 4x SDS sample buffer (see section 3.2), boiled for 3 minutes at 95°C and applied to 12.5% SDS–PAGE gels (see section 3.2). After electrophoresis at 25 mA per gel for 1 hour, gels were vacuum dried on Whatman paper for 2 hours at 85°C. The dried gels were placed on a phosphoimager screen for at one day and screens were scanned on a phosphoimager.

3.12   Light microscopy

B. subtilis cultures were grown in LB to mid–exponential phase at 37°C. 0.5 μl samples were removed and applied to a microscope glass slide covered with 1% agarose. The slides were briefly air-dried and a cover slip was attached. Microscopy was performed using a fluorescence microscope equipped with a 100x oil immersion phase contrast objective and standard GFP excitation and emission filters. Pictures were taken with a CCD camera. A typical exposure time was 1.5 seconds.

3.13   Protein production and purification

Purification of ClpP, MecA, YpbH, Hag, FliS, FliW and MDH   ClpP, MecA, YpbH, Hag, FliS, FliW and MDH were produced as C–terminal fusions to a hexahistidine tag under the control of the IPTG–inducible T5 promoter (pQE-60 and pQE70 plasmids) in *E. coli* FI1202 (Table 4). 1.5 l (ClpP, Hag and MDH) or 3 l (MecA, YpbH, FliS and FliW) DYT medium (see section 3.2) in 5 l flasks were inoculated 1:100 with over night cultures grown in LB with 100 μg/ml ampicillin and cultivated at 37°C and 170 rpm with 100 μg/ml ampicillin. At OD_{600} 0.6-0.8, protein production was induced by addition of 1 mM IPTG and growth was continued for 3 hours at 37°C. Cells were harvested by centrifugation and resuspended in 10 ml Ni-NTA lysis buffer per liter culture. The cell suspension was passed through a 40 ml French Pressure Cell 3 times at 18000 psi for lysis. The cell lysate was cleared by centrifugation for 45 minutes at 20000g and 4°C (SS-34 rotor).

The supernatent containing soluble proteins was passed over a 1 ml Ni-NTA column

equilibrated in Ni-NTA lysis buffer. To remove unspecifically bound proteins, the column was washed in 20-50 ml Ni-NTA wash buffer. Proteins were eluted with 3 ml Ni-NTA elution buffer. The raw extract, flow through, wash and elution fractions were analyzed by SDS–PAGE (see section 3.2). The eluted proteins were dialyzed twice against 2l Dialysis buffer at 4°C to remove the imidazol. Protein concentration was determined by the Bradford assay using RotiQuant solution and aliquots were frozen in liquid N_2 and stored at -80°C.

Ni-NTA lysis buffer	50 mM	Tris-HCl pH 8.0
	300 mM	NaCl
	5 mM	$MgCl_2$
	1 mM	β-mercaptoethanol
	10 mM	imidazol
	1 tablet/50 ml	cOmplete EDTA-free Protease Inhibitor
	5 μg/ml	DNase I
Ni-NTA wash buffer	50 mM	Tris-HCl pH 8.0
	300 mM	NaCl
	5 mM	$MgCl_2$
	1 mM	β-mercaptoethanol
	20 mM	imidazol
Ni-NTA elution buffer	50 mM	Tris-HCl pH 8.0
	300 mM	NaCl
	5 mM	$MgCl_2$
	1 mM	β-mercaptoethanol
	250 mM	imidazol
Dialysis buffer	50 mM	Tris-HCl pH 8.0
	300 mM	NaCl
	5 mM	$MgCl_2$
	1 mM	β-mercaptoethanol

Purification of ClpC   ClpC was produced from pTYB-clpC as a C–terminal intein fusion to a chitin binding protein under the control of a T7 promoter in *E. coli* ER2566 (Table 4). 6 l DYT were inoculated 1:100 with an LB over night culture and grown at 37°C and 170 rpm with 100 μg/ml ampicillin. At OD_{600} 0.7 cells were shifted to 16°C and induced with 1 mM IPTG over night. Cells were harvested by centrifugation and resuspended in 10 ml chitin lysis buffer per liter culture.

The cell suspension was passed through a 40 ml French Pressure Cell 3 times at 18000 psi for lysis. The cell lysate was cleared by centrifugation for 45 minutes at 20000g and 4°C (SS-34 rotor). The cleared lysate was bound to a 3 ml chitin column and the column was washed with 20-50 ml chitin column buffer. Subsequently, 10 ml intein cleavage buffer, containing DTT were quickly passed through the column, the column was closed and incubated at 4°C over night. The next day, the protein was eluted in 10 ml chitin column buffer.

To remove two lower molecular weight contaminations and to remove DTT, gel filtration chromatography was performed as a second purification step. To this end, ClpC eluted from the chitin column was loaded onto a High Load Superdex 75 16/60 gel filtration column equilibrated in gel filtration buffer and connected to an Äkta Purifier FPLC system. Fractions were analyzed by SDS–PAGE.

The fractions containing ClpC were diluted to a final volume of 50 ml in Q1 buffer A and loaded on a 1 ml Resource Q column equilibrated in Q1 buffer A for concentration and further purification. Anion exchange chromatography was performed using an Äkta Purifier FPLC system with a gradient from 0 to 1 M KCl (Q1 buffer B) and 0.6 ml fractions were collected. ClpC eluted from the column (at a concentration of about 200 mM KCl) was aliquoted, frozen in liquid N_2 and stored at -80°C.

Chitin lysis buffer	50 mM	Tris-HCl pH 8.0
	300 mM	NaCl
	5 mM	$MgCl_2$
	1 tablet/50 ml	cOmplete EDTA-free Protease Inhibitor
	5 μg/ml	DNase I

Chitin column buffer	50 mM	Tris-HCl pH 8.0
	300 mM	NaCl
	5 mM	MgCl$_2$
Intein cleavage buffer	50 mM	Tris-HCl pH 8.0
	300 mM	NaCl
	5 mM	MgCl$_2$
	30 mM	DTT
Gel filtration buffer	20 mM	Bicin pH 8.9
	200 mM	KCl
	5 mM	MgCl$_2$
Q1 buffer A	20 mM	Bicin pH 8.9
	5 mM	MgCl$_2$
Q1 buffer B	20 mM	Bicin pH 8.9
	1 M	KCl
	5 mM	MgCl$_2$

3.14   *In vitro* degradation assay

ClpC, MecA and substrate (casein or Hag) were diluted to 1 μM monomer concentration in Degradation buffer in the presence of 5 mM ATP and a pyruvate kinase/PEP ATP regeneration system and incubated for 5 minutes at 37°C to initiate oligomerization of the ClpC-MecA. Degradation was then started by addition of 1 μM ClpP and the reaction mix was incubated at 37°C. 15 μl samples were taken immediately and after 15, 30, 60 and 90 minutes and mixed with 5 μl 4x SDS sample buffer. Samples were heated to 95°C for 5 minutes and then applied to 12.5% or 15% Tris-Glycine SDS–PAGE gels or 16% Tris-Tricine gels depending on the proteins separated. Gels

were stained with Coomassie Brilliant Blue, destained and scanned.

Degradation buffer	50 mM	Tris-HCl pH 8.0
	300 mM	KCl
	20 mM	$MgCl_2$
	15% v/v	glycerol
	5 mM	DTT
	5 mM	ATP
	2 mM	PEP
	66 μg/ml	pyruvate kinase

3.15   Thermotolerance experiments

20 ml LB medium was inoculated to OD_{600} 0.05 from an overnight culture and grown at 37°C to OD_{600} 0.5-0.7. The culture was split in two 10 ml cultures in prewarmed 100 ml flasks. One 10 ml culture was placed in a shaking water bath preheated to 48°C and cultivated for 15 minutes, whereas the other half of the culture was left at 37°C with shaking. After the preshock, both 10 ml cultures were placed in a shaking water bath preheated to 53°C and grown for 2 hours. 100 μl samples were removed before transfer to 53°C and after 30, 60 and 120 minutes and dilution series were plated on LB plates and incubated over night at 37°C. Typical dilutions were 10^{-3} to 10^{-8} with pre–shock and 10^{0} to 10^{-4} without pre–shock depending on the mutants used. Colonies were counted the next day and colony forming units (CFU) were determined for each sample. The data were normalized to the CFU at time 0 at 53°C separately for the cultures with and without preshock at 48°C.

3.16   Aggregate preparation

Cells were grown in 500 ml LB to OD_{600} 0.5 at 37°C and heat shocked as indicated. 30 ml samples were withdrawn, pelleted by centrifugation for 10 minutes at $4500g$ and frozen at -20°C. Pellets were thawed on ice, washed once in 5 ml phosphate buffer and resuspended in aggregate lysis buffer containing lysozyme, DNase I and RNase A. The suspension was incubated for 20 minutes at 37°C for lysozyme digestion of the cell wall. Subsequently, the samples were passed through a French Pressure Cell three times at

18000 psi. 100 μl of the lysate were collected and frozen (total cell extract). The lysate was centrifuged for 15 minutes at 1500g (4000 rpm) in a microcentrifuge at 4°C to pellet unlysed cells. Next, the supernatent was centrifuged for 30 minutes at 17000g (13000 rpm) in a microcentrifuge. The supernatent of this centrifugation step was removed and samples were frozen (soluble extract). The pellet was resuspended in the same volume of aggregate wash buffer + 1% v/v Triton X-100 and incubated for two hours at 4°C with mixing every 15 minutes to solubilize membrane proteins. Subsequently, the samples were centrifuged again for 30 minutes at 16000g and resuspended in aggregate wash buffer + 0.5 % v/v Triton X-100 and the solubilization procedure was repeated. The samples were washed with aggregate wash buffer without Triton X-100 and insoluble aggregates were resuspended in Rehydration buffer and subjected to SDS–PAGE and Coomassie staining or Western blotting.

Phosphate buffer	50 mM	Na_3PO_4 pH 7.0
Aggregate lysis buffer	50 mM	Na_3PO_4 pH 7.0
	10 μg/ml	lysozyme
	10 μg/ml	DNase I
	5 μg/ml	RNase I
Aggregate wash buffer	50 mM	Tris pH 8.0
	150 mM	NaCl
Rehydration buffer	7 M	urea
	2 M	thiourea
	4% w/v	CHAPS
	100 mM	DTT

3.17   Electron microscopy

1 ml over night culture was pelleted by centrifugation and resuspended in 100 μl TBS buffer (50 mM Tris-HCl pH 8.0, 150 mM NaCl). The samples were stained with 0.2% w/v ammonium molybdate and observed by transmission electron microscopy at 2000x magnification. Experiments were performed with the help of Beatrix Fauler and Professor Dr. Rudi Lurz at the Max Planck Institute for Molecular Genetics in Berlin.

4   Results

4.1   The effect of Clp proteases on the regulation of swimming motility

Hag (flagellin) was identified as a putative ClpC interaction partner in a co–immuno-precipitation experiment (J. Kirstein and K. Turgay, unpublished). Subsequently, Hag was over–produced in *E. coli*, purified and *in vitro* degradation assays were performed with Hag as a substrate (J. Kirstein, unpublished). Hag was degraded *in vitro* by ClpCP in the presence of the adaptor protein YpbH, but much slower in the presence of MecA (J. Kirstein, unpublished data and Figure 36). This observation raised the question whether Hag is also degraded by ClpCP *in vivo*.

One indication of *in vivo* Hag proteolysis by ClpCP could be accumulation of Hag in *clpC* and *clpP* mutant cells. To investigate whether Hag levels are higher in these mutants compared to the wild type, protoplasts were prepared from exponentially growing cultures of wild type and *clp* mutant cells and lysed. The cell lysates were then separated by SDS–PAGE and analyzed by Western blot using Hag antibodies (Figure 4). Unexpectedly, the Western blot analysis revealed strongly reduced Hag protein levels in the *clpP*, *clpC* and *clpX* mutants, but not in the *clpE* mutant compared to wild type cells (Figure 4).
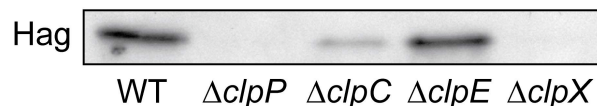
Figure 4: Hag levels in wild type and *clp* mutant cells.
Hag Western blot. Strains 168, BNM103 ($\Delta clpP$::spec), BNM105 ($\Delta clpC$::tet), BNM106 ($\Delta clpE$::spec) and BNM107 ($\Delta clpX$::kan) were grown in LB to OD_{600} 1.0 at 37°C and harvested for protoplast preparation. Protoplasts were lysed and the lysates (2.5 μg total protein per lane) were separated by SDS–PAGE and subjected to Western blotting. Hag levels are strongly reduced in the *clpP*, *clpC* and *clpX* mutants.

These data suggest that *clp* mutant cells are unable to synthesize Hag. To analyze whether this also affects swimming motility, motility assays were performed with wild type and mutant cells. To this end, the different strains were spotted on soft agar plates and the plates were incubated at 37°C for several hours. Whereas the wild type

and the *clpE* mutant produced circular halos around the point of inoculation, which indicate swimming through the soft agar, the *clpC* mutant spread to a much smaller area and the *clpP* and *clpX* mutants only formed a small colony at the inoculation point (Figure 5).
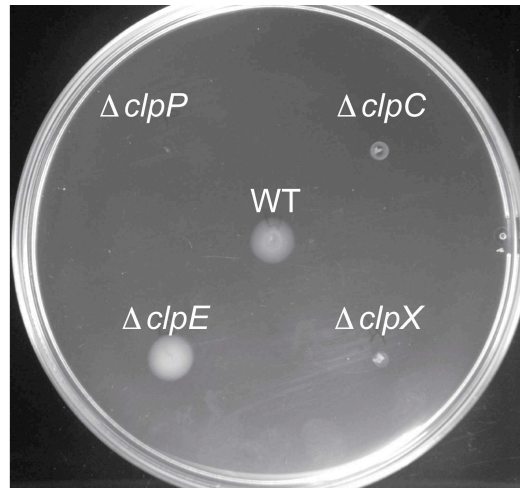
Figure 5: Swimming motility in wild type and *clp* mutant cells.
Swim plates were inoculated with cultures of strains 168 (wild type), BNM103 ($\Delta clpP$::spec), BNM105 ($\Delta clpC$::tet), BNM106 ($\Delta clpE$::spec) and BNM107 ($\Delta clpX$::kan) and incubated for 6 hours at 37°C. Wild type and *clpE* mutant cells were motile, *clpP*, *clpC* and *clpX* mutants were non-motile.

This indicates that the *clpP* and *clpX* mutants are non-motile and that the *clpC* mutant displays strongly reduced motility, consistant with the observation that these mutants do not produce flagellin (Figure 4). To investigate whether this defect in Hag synthesis interferes with the synthesis of flagella, electron microscopy of the wild type and *clpP* mutant strains was performed. As expected, the wild type was flagellated, whereas no flagellar structures were visible on the cell surface of the *clpP* mutant and the *hag* mutant, which was used as negative control (Figure 6). The *clpP* mutant also appeared elongated (Figure 6) as described previously [74, 173].

Impact of adaptor protein mutants on swimming motility   A *mecA* mutant has previously been described as non–motile[198, 147], which was partially due to MecA–mediated targeting of ComK to ClpCP (see sections 2.3.2 and 4.1.1)[147]. In order to investigate which ClpC adaptor protein is responsible for the motility functions of ClpC, swimming motility assays were performed with cells mutated in adaptor protein

A   B   C

WT   ΔclpP   Δhag
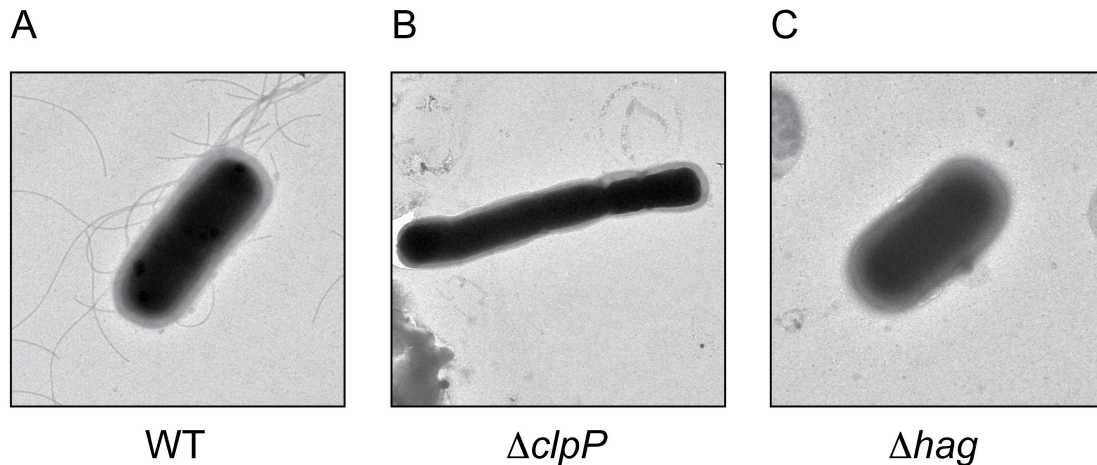
Figure 6: Electron microscopy of wild type and *clpP* mutant cells.
Over night cultures of strains 168 (wild type, A), BNM103 (Δ*clpP*::spec, B) and
BNM126 (Δ*hag*, C) were stained with 0.2% ammonium molybdate and subjected
to transmission electron microscopy. Flagella could be observed on wild type cells,
whereas *clpP* and *hag* mutant cells were non-flagellated. Pictures were taken with the
help of Beatrix Fauler and Rudi Lurz (MPI for Molecular Genetics, Berlin).

genes. As shown in Figure 7, *mecA* mutants exhibit reduced motility, as previously
observed[198, 147], whereas the *ypbH* and *mcsB* mutations have no effect on swimming.
These data suggest that MecA is the only known adaptor protein required for motility.
Interestingly, the *mecA ypbH* double mutant appears to partially suppress the motility
phenotype of the *mecA* mutant. Possibly, this phenotype might be the consequence of
YpbH–mediated Hag proteolysis. However, the *pulse chase* results presented in section
4.2 argue against this hypothesis.

The observed motility phenotypes of *clp* mutants had been reported in previous stu-
dies[147, 173, 198]. However, except for the effect of *clpC* and *mecA*, which is dependent
on *comK* and *flgM* (see sections 2.3.2 and 4.1.1)[147], the motility defect of the *clp*
mutants was not further characterized. Furthermore, a second, *comK*-independent
effect of *clpC* was described but not further investigated[198]. Therefore, the details
of this regulatory proteolysis were further investigated here. In addition, proteolysis of
Hag itself was studied by *in vivo pulse chase* analysis, the results of which are described
in section 4.2.

So far, the results shown above indicate that ClpCP and ClpXP positively regulate
hag expression and swimming motility. Since Clp proteases are involved in cellular
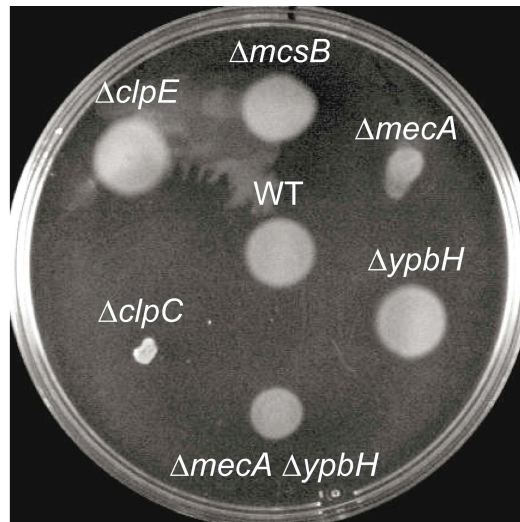
Figure 7: Swimming motility in ClpC adaptor mutants.
Swim plates were inoculated with cultures of strains 168 (wild type), BNM106 ($\Delta clpE$::spec), BNM113 ($\Delta mecA$::spec), BNM115 ($\Delta ypbH$::spec), BNM116 ($\Delta mecA$::kan $\Delta ypbH$::spec) and BNM117 ($\Delta mcsB$::kan) and incubated over night at 37°C. Only the *mecA* mutant and the *mecA ypbH* double mutant exhibited reduced swimming motility. The experiment was performed with the help of Jörn Hossmann.

regulation by degradation of regulators, it was hypothesized that ClpCP and ClpXP degrade one or several negative regulators of swimming motility. Inactivation of the proteases by mutation would then result in accumulation of the negative regulator and inhibition of motility.

Flagellar gene expression studies   In order to investigate which process in flagellar gene expression is influenced by ClpCP and ClpXP, it was first analyzed whether transcription initiation from the $P_{fla/che}$ and P_{hag} promoters is affected by *clp* mutations. To this end, *clpP*, *clpC*, *clpE* and *clpX* mutants were crossed with the *lacZ* reporter strains $P_{fla/che}$-*lacZ* and P_{hag}-*lacZ* (kindly provided by D. Kearns, Indiana University) and β-galactosidase activities were measured along the growth curve.

In the wild type background, as well as in the *clpE* mutant, the characteristic postexponential expression peak was observed for both promoter *lacZ* fusions. However, as demonstrated in Figure 8 A and Figure 9, the *clpP* and *clpX* mutations resulted in a strong downregulation of $P_{fla/che}$ and P_{hag} promoter activities at all measured timepoints. The *clpC* mutant exhibited reduced P_{hag} promoter activity, but had no effect on the $P_{fla/che} - lacZ$ fusion. Notably, the postexponential expression peak was
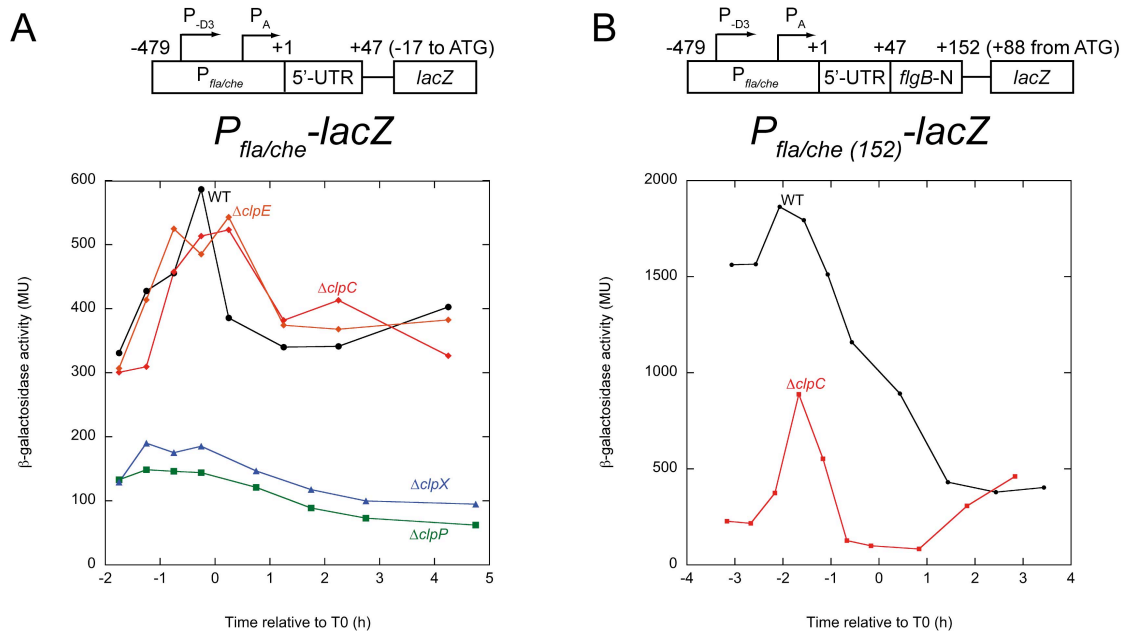
Figure 8: β-galactosidase assays of $P_{fla/che}$-$lacZ$ fusions in wild type and clp mutant cells.

A. β-galactosidase assay of $amyE$::$P_{fla/che}$-$lacZ$::cat strains BNM301 (wild type, black circles), BNM302 ($\Delta clpP$::spec, green squares), BNM303 ($\Delta clpC$::tet, red diamonds), BNM304 ($\Delta clpE$::spec, orange diamonds) and BNM305 ($\Delta clpX$::kan, blue triangles). β-galactosidase activity is strongly reduced in $clpP$ and $clpX$ mutants. B. β-galactosidase assay of $amyE$::$P_{fla/che152}$-$lacZ$::cat strains BNM346 (wild type, black circles) and BNM348 ($\Delta clpC$::tet, red squares), carrying a longer $lacZ$-fusion. β-galactosidase activity of this fusion was reduced by the $clpC$ mutation.

still detected in the $clpC$ mutant, but not in the $clpP$ and $clpX$ mutants.

Interestingly, a different $lacZ$ fusion, which extended further into the first open reading frame of the fla/che operon ($P_{fla/che152}$-$lacZ$) was downregulated in the $clpC$ mutant background (Figure 8 B) in contrast to the shorter fusion (Figure 8 A). These data imply that DNA sequences downstream of the transcriptional start site are required for repression of $P_{fla/che}$ promoter activity in the $clpC$ mutant.
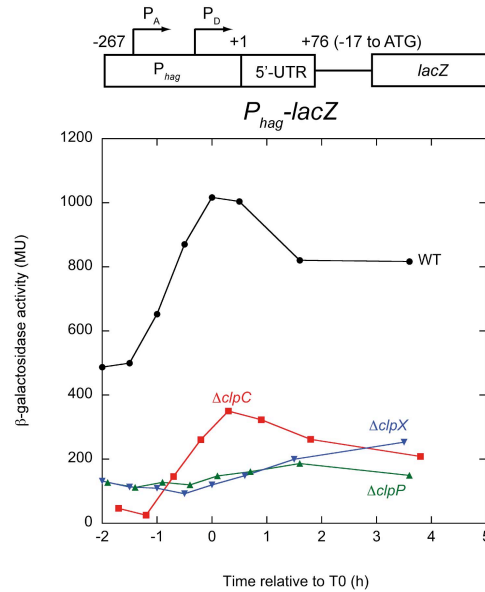
Figure 9: β-galactosidase assays of a P_{hag}-$lacZ$ fusion in wild type and clp mutant cells.
$amyE$::P_{hag}-$lacZ$::cat strains BNM328 (wild type, black circles), BNM329 ($\Delta clpP$::spec, green squares), BNM330 ($\Delta clpC$::tet, red squares) and BNM332 ($\Delta clpX$::kan, blue triangles) were assayed for β-galactosidase activity. Activity was strongly reduced in $clpP$, $clpC$ and $clpX$ mutants.

As a control, flagellar transcripts were directly visualized by Northern blot analysis. For these experiments, total RNA was extracted from wild type and clp mutant strains grown to postexponential phase. The samples were then separated by denaturing agarose gel electrophoresis, blotted on nylon membranes and hybridized to digoxigenin labeled DNA probes. These probes were designed to hybridize to the hag, $flgB$ (the first gene of the fla/che operon) and $sigD$ (the second to last gene of the fla/che operon encoding the flagellar sigma factor σ^D) transcripts (Figure 10).

For each probe, a band of the expected size was detected in the sample from the wild type strain, but was absent or strongly reduced in the $clpP$, $clpC$ and $clpX$ mutant
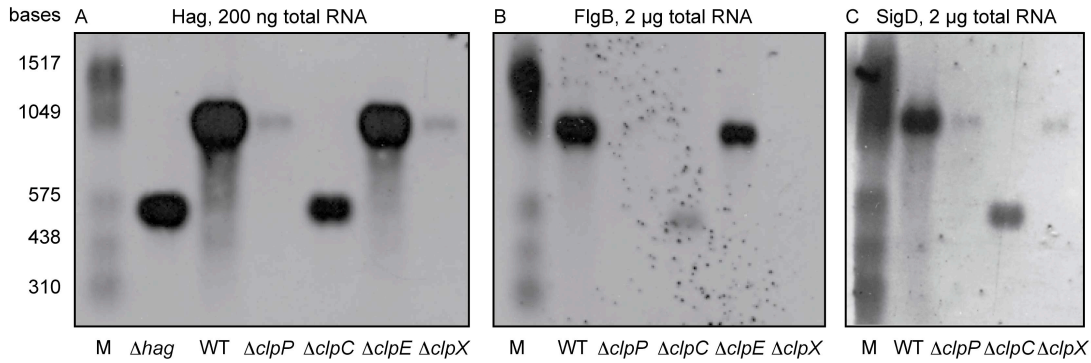
Figure 10: Analysis of flagellar transcript levels in *clp* mutant cells.
RNA extracted from strains 168 (wild type), BNM103 ($\Delta clpP$::spec), BNM105 ($\Delta clpC$::tet), BNM106 ($\Delta clpE$::spec), BNM107 ($\Delta clpX$::kan) and BNM126 (Δhag) grown to OD_{600} 1.0 at 37°C in LB was subjected to Northern blot analysis with DIG-labeled DNA probes against *hag* (A), *flgB* (B) or *sigD* (C). The levels of all three mRNAs were strongly reduced in the *clpP*, *clpC* and *clpX* mutants. A smaller band of approximately 500 bases was observed in *hag* and *clpC* mutants.

samples. Interestingly, the Northern blot experiments revealed the accumulation of small RNA fragments of about 500 bases length in the *clpC* mutant and in the *hag* mutant in the presence of all three RNA probes (Figure 10). The reason for this observation is unknown at the moment.

Additionally, it was tested whether the levels of the flagellar sigma factor σ^D in wild type and *clp* mutant strains reflect the pattern observed in the $P_{fla/che}$ reporter gene studies and in the *sigD* Northern blot. The Western blot experiments with σ^D antibodies demonstrated that σ^D protein levels are downregulated in the *clpP*, *clpC* and *clpX* mutants as expected (Figure 11).
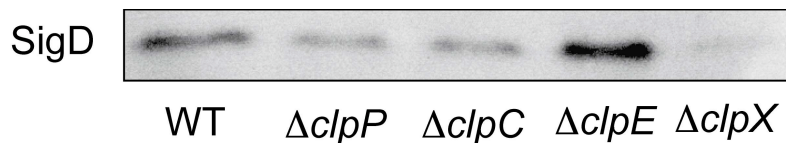
Figure 11: σ^D Western blot in wild type and *clp* mutant cells.
Protoplast lysates (LB, OD_{600} 1.0, 10 μg total protein per lane) of strains 168 (wild type), BNM103 ($\Delta clpP$::spec), BNM105 ($\Delta clpC$::tet), BNM106 ($\Delta clpE$::spec) and BNM107 ($\Delta clpX$::kan) were subjected to Western blot analysis with antibodies against σ^D. σ^D levels were reduced in *clpP*, *clpC* and *clpX* mutants.

In summary, it can be inferred from these data that the $P_{fla/che}$ promoter activity is reduced by mutation of *clpP*, *clpC* and *clpX*, which results in a low abundance of the

flgB and *sigD* transcripts and low σ^D protein levels. The reduced cellular concentration of σ^D in turn leads to reduced transcription initiation from the P_{hag} promoter, resulting in low levels of *hag* mRNA and Hag protein and the inability to assemble flagella. One possible explanation of these data is regulatory proteolysis of a negative regulator of $P_{fla/che}$ by ClpCP and ClpXP.

4.1.1   Investigation of ClpCP substrates, which regulate swimming motility

The results shown in the previous section gave rise to the hypothesis that negative regulators of the $P_{fla/che}$ promoter might be proteolysis substrates of ClpCP and ClpXP. To identify these proteolysis targets, strains mutated in genes encoding known negative regulators of motility, such as ComK, DegU (this study), FlgM and CsrA (Jörn Hossmann, diploma thesis) were constructed and combined with the *clpC* and *clpX* mutants. Suppression of the motility phenotype in the double mutant suggests that the effect of the *clp* mutation is caused by the accumulation of the corresponding regulator.

In the motility and reporter gene studies, it was noticed that although both the *clpC* mutant and the *clpX* mutant interfere with $P_{fla/che}$ promoter activity and swimming motility, they have slightly different phenotypes. For instance, only the activity of the longer $P_{fla/che}$-*lacZ* fusion is altered in the *clpC* mutant, whereas both $P_{fla/che}$-*lacZ* fusions are downregulated in the *clpX* mutant (Figure 8 and data not shown). Moreover, the effect of the *clpC* mutant on motility, *hag* expression and $P_{fla/che}$ promoter activity is weaker than the effect of the *clpX* mutant. Therefore, it appears likely that distinct negative regulators of motility are degraded by ClpCP and ClpXP.

ComK/FlgM   Zuber and colleagues demonstrated that the motility phenotype of the *mecA* mutant is suppressed by *comK*[147]. This was explained by upregulation of *flgM*, coding for FlgM, the anti–sigma factor of σ^D, by transcriptional read–through from a ComK activated gene. ComK is targeted for ClpCP degradation by the adaptor protein MecA[226]. Therefore, deletion of *clpC* or *mecA* results in elevated ComK levels, which lead to higher FlgM levels and a subsequent downregulation of σ^D dependent genes. To investigate whether ComK contributes to the motility defect of the *clpC* mutant, which was not directly demonstrated by Liu and Zuber[147], a *comK clpC* double

mutant was constructed and assayed for swimming motility and Hag levels. Indeed, swimming motility and Hag protein levels were upregulated in the double mutant compared to the *clpC* single mutant (Figure 12). The *comK* single mutant had no effect on motility or Hag concentration (Figure 12).
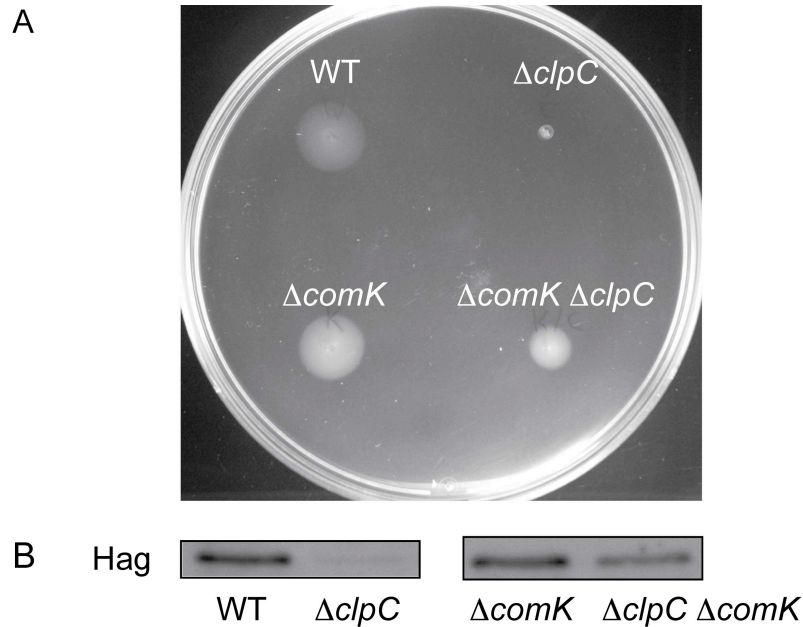
Figure 12: The motility defect of a *clpC* mutant is partially suppressed by a *comK* mutation.
A. Swim plates were inoculated with cultures of strains 168, BNM105 ($\Delta clpC$::tet), BNM149 ($\Delta comK$) and BNM150 ($\Delta comK$ $\Delta clpC$::tet) and incubated for 6 hours at 37°C. The wild type and *comK* mutant were motile, the *clpC* mutant was non-motile and the *comK clpC* double mutant was motile, albeit less than the wild type. B. Hag Western blot of strains 168, BNM105, BNM149 and BNM150. Hag levels were restored partially in the *comK clpC* double mutant compared to the *clpC* single mutant.

These results demonstrate that ComK is involved in downregulation of motility in the *clpC* mutant. In addition, there is evidence that the *clpC* motility defect is also suppressed by a *flgM* mutation (Jörn Hossmann, unpublished), implying that ClpC acts on motility through ComK and FlgM as suggested previously[147].

DegU   FlgM directly inhibits the activity of the flagellar sigma factor σ^D, which initiates transcription of flagellar class III genes, but not of the *fla/che* operon[110]. Nevertheless, a downregulation of the $P_{fla/che152}$-*lacZ* fusion (Figure 8 B), *flgB* and *sigD* transcript levels (Figure 10) and σ^D protein levels (Figure 11) was observed in

the *clpC* mutant. In addition, swimming motility and Hag protein levels were only partially restored in the *clpC comK* double mutant (Figure 12).
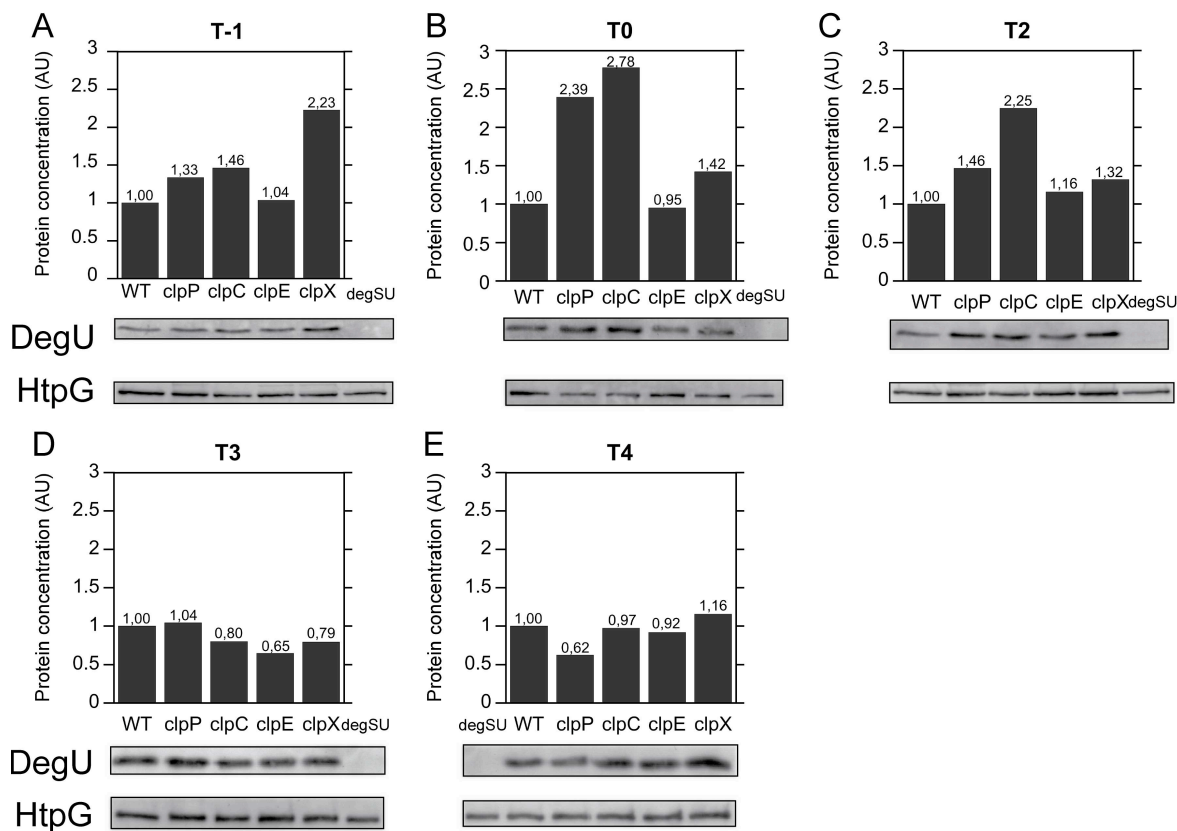
Figure 13: DegU levels in wild type and *clp* mutant cells.
Protoplast lysates were prepared from samples of strains 168 (wild type), BNM103 (Δ*clpP*::spec), BNM105 (Δ*clpC*::tet), BNM106 (Δ*clpE*::spec), BNM 107 (Δ*clpX*::kan) and BNM138 (Δ*degSU*::spec) at different points during growth in LB at 37°C. A: 1 hour prior to the end of exponential growth (T-1), B: at the end of exponential growth (T0), C: T0 + 2 hours (T2), D: T0 + 3 hours (T3), E: T0 + 4 hours (T4). 5 μg total protein per lane was separated by SDS–PAGE and blotted. Blots were cut and the upper half was incubated with HtpG antibodies as a loading control, whereas the lower half was probed with DegU antibodies. Band intensities were quantified and normalized to HtpG band intensities. DegU levels were higher in the *clpX* mutant at T-1 and in the *clpC* and *clpP* mutants at T0 and T2 compared to the wild type.

These observations suggested that a second ClpCP substrate negatively regulates the $P_{fla/che}$ promoter. One candidate was DegU, which has been shown to repress the $P_{fla/che}$ promoter in its phosphorylated form[5] and was recently identified as a substrate of ClpCP[188].

In order to investigate the levels of DegU in wild type and *clp* mutant strains, quantitative Western blot experiments were performed with DegU antibodies (Figure 13). As

reported in a recent publication[188], DegU was produced in higher amounts in *clpC* and *clpP* mutant cells. This effect was only observed from postexponential phase (T0) until 2 hours into stationary phase (T2, Figure 13). Interestingly, DegU protein levels were also increased in a *clpX* mutant during exponential phase. The reason for this effect is currently unknown.
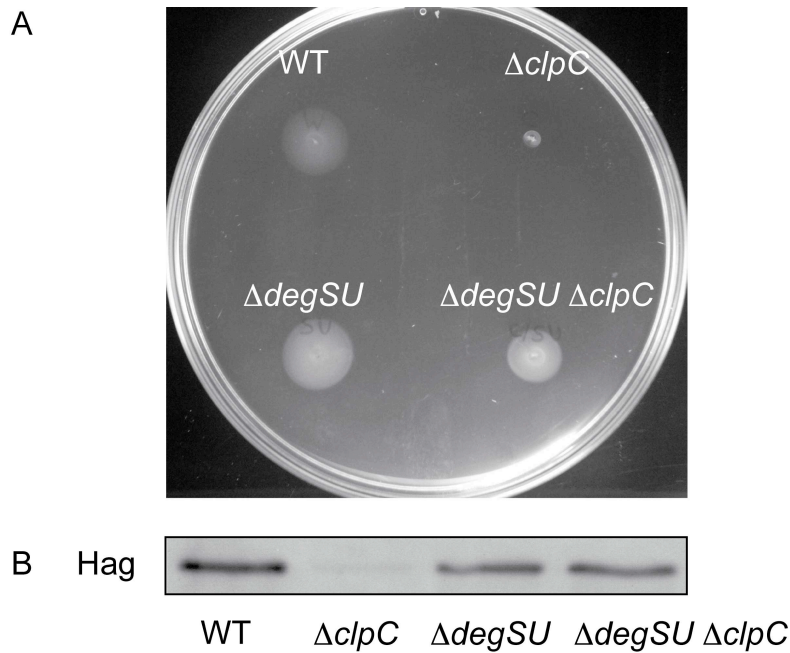
Figure 14: The motility defect of a *clpC* mutant is partially suppressed by mutation of *degSU*.
A. Swim plates were inoculated with cultures of strains 168, BNM105 (Δ*clpC*::tet), BNM138 (Δ*degSU*::spec) and BNM140 (Δ*degSU*::spec Δ*clpC*::tet) and incubated for 6 hours at 37°C. The *degSU clpC* double mutant suppressed the motility phenotype of the *clpC* mutant. B. Hag Western blot of strains 168, BNM105, BNM138 and BNM140. Hag levels are restored in the *degSU clpC* double mutant compared to the *clpC* single mutant.

To test the assumption that *clpC* acts on motility via *degU*, a *degSU clpC* double mutant was constructed and analyzed by motility assays and Hag Western blots. Similar to the *comK clpC* double mutant, both swimming motility (Figure 14 A) and Hag levels (Figure 14 B) were partially restored in the *degSU clpC* double mutant.

Furthermore, the activity of the $P_{fla/che152}$-*lacZ* reporter gene fusion was upregulated almost to wild type levels in the *degSU clpC* double mutant compared to the *clpC* single mutant (Figure 15 A). Interestingly, the P_{hag}-*lacZ* fusion was only slightly upregulated in this strain (Figure 15 B). As a control, the β-galactosidase activity of the P_{hag}-*lacZ*-

fusion was measured in the *clpX* and *degSU clpX* double mutant (Figure 15B). The *degSU* mutation was insufficient to suppress the phenotype of the *clpX* mutant (Figure 15), suggesting that *clpX* does not act on motility genes via *degU*.
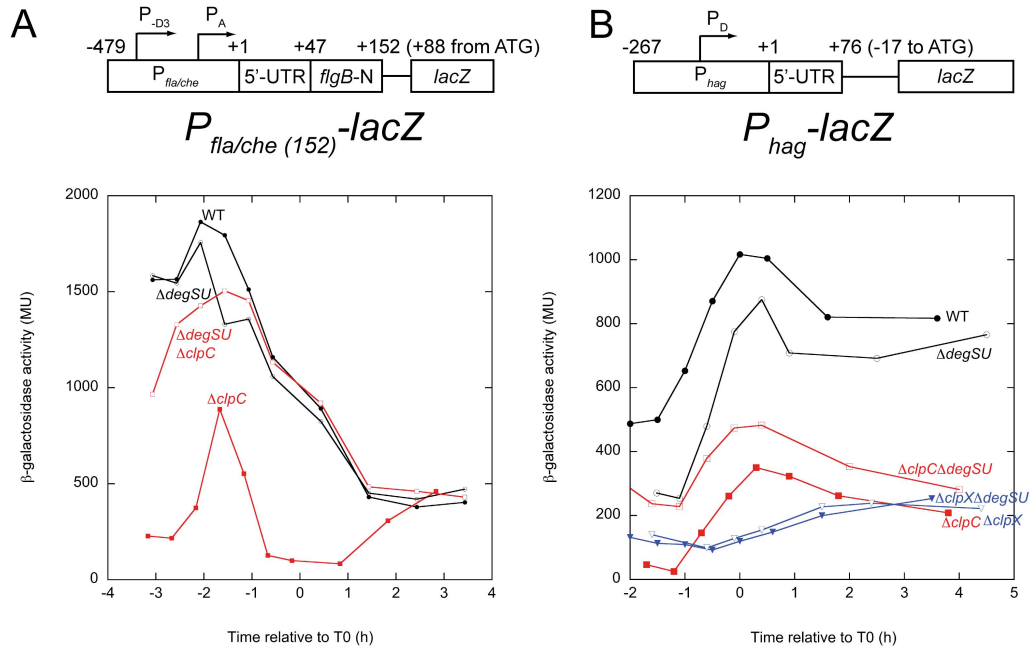
Figure 15: *β*-galactosidase assays in *clpC degSU* mutant cells.
A. *β*-galactosidase assay of *amyE*::$P_{fla/che152}$-*lacZ*::cat strains BNM346 (wild type, closed black circles), BNM347 ($\Delta degSU$::spec, open black circles), BNM348 ($\Delta clpC$::tet, closed red squares) and BNM349 ($\Delta degSU$::spec $\Delta clpC$::tet, open red squares). Mutation of *degSU* suppresses the effect of *clpC* on the $P_{fla/che152}$-*lacZ* fusion. B. *β*-galactosidase assay of *amyE*::P_{hag}-*lacZ*::cat strains BNM328 (wild type, closed black circles), BNM333 ($\Delta degSU$::spec, open black circles), BNM330 ($\Delta clpC$::tet, closed red squares), BNM332 ($\Delta clpX$::kan, closed inverse blue triangles), BNM338 ($\Delta degSU$::spec $\Delta clpC$::tet, open red squares) and BNM339 ($\Delta degSU$::spec $\Delta clpX$::kan, open inverse blue triangles). *β*-galactosidase activity of the *clpC* mutant, but not the *clpX* mutant was partially restored by mutation of *degSU*.

CodY Like DegU, CodY is a transcriptional repressor of the *fla/che* operon[15]. Therefore, it was important to establish whether CodY might be a ClpCP or ClpXP substrate and whether the *clpC* or *clpX* mutants act on motility through *codY*. Unfortunately, the attempts to construct *codY clpC* and *codY clpX* double mutants failed. However, it was demonstrated by Western blot analysis that CodY levels are equal in wild type cells and all *clp* mutant strains (Figure 16). In addition, preliminary *in vivo* stability experiments suggested that CodY is a stable protein (data not shown).

Therefore, it can be inferred that neither ClpCP nor ClpXP are involved in CodY degradation and that their effect on swimming motility is independent of CodY.
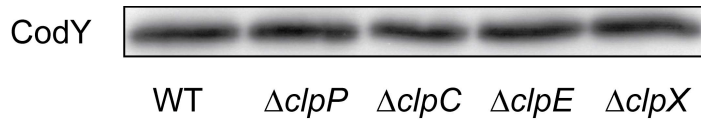
Figure 16: CodY Western blot of wild type and *clp* mutant cells.
10 μg total protein per lane from protoplast lysates of strains 168 (wild type), BNM103 ($\Delta clpP$::spec), BNM105 ($\Delta clpC$::tet), BNM106 ($\Delta clpE$::spec), BNM107 ($\Delta clpX$::kan) was separated by SDS–PAGE, blotted and probed with CodY antibodies. CodY levels were equal in all strains.

In summary, the data presented here are consistant with the model that ClpC influences transcription from the $P_{fla/che}$ promoter by degradation of DegU, which acts as a *fla/che* repressor. In addition, *clpC* regulates σ^D activity by proteolysis of ComK, which activates *flgM*.

4.1.2   Negative regulation of swimming motility by the ClpXP substrate Spx

During the initial characterization of the *clp* motility phenotype it was noticed that the *clpP* mutant strain frequently picked up suppressor mutations that resulted in restoration of swimming motility and Hag levels (Figure 17 C). Such a suppressor mutant, which exhibited a larger colony size on LB plates, was further characterized by analysis of its growth behavior and cell morphology. As shown in Figure 17, this strain grew as quickly as the wild type in LB medium (Figure 17 A) and was morphologically indistinguishable from wild type cells (Figure 17 B), whereas a freshly transformed *clpP* mutant displayed a lag phase of about four hours during growth in LB (Figure 17 A) and formed long chains (Figure 17 B).

The transcriptional regulator Spx is a substrate of ClpXP and accumulates to high levels in *clpP* and *clpX* mutants[179]. Because high levels of the normally tightly controlled stress regulator Spx interfere with normal growth, suppressor mutations in *spx* are easily acquired by these mutants[179]. To investigate whether the suppressor mutation in the motile *clpP* strain might have occurred in *spx*, Western blot analysis was performed with lysates from wild type, *clpP* mutant and *clpP* suppressor strains.
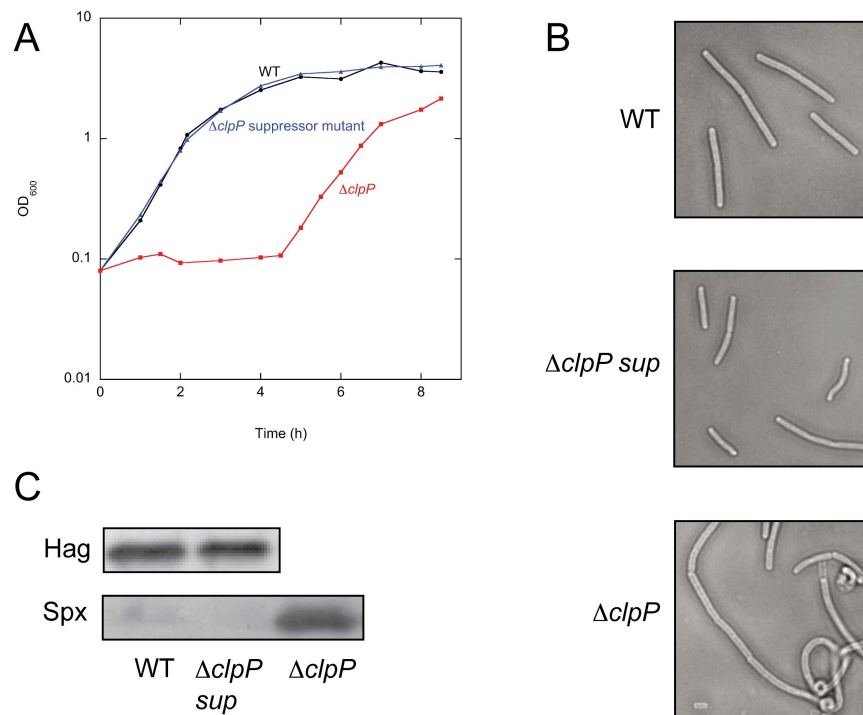
Figure 17: Growth, cell morphology and Spx levels of a *clpP* suppressor mutant.
A. Strains 168 (wild type, black circles), BNM102 ($\Delta clpP$::spec, suppressor, blue triangles) and BNM103 ($\Delta clpP$::spec, red squares) were inoculated to OD_{600} 0.05 and grown in LB at 37°C. Strain BNM103 displayed a lag phase of approximately 4 hours, wheras BNM102 grew as fast as the wild type. B. Phase contrast microscopy of strains 168 (upper), BNM102 (middle) and BNM103 (lower) grown in LB to OD_{600} 0.4-0.6. BNM103 formed long chains and exhibited aberrant cell morphology, BNM102 was indistinguishable from the wild type. C. Hag and Spx Western blots of samples from 168 (wild type), BNM102 and BNM103. Spx was barely detectable in the wild type and strain BNM103 displayed high levels of Spx. Spx was not visible in BNM102.

Spx accumulated to high levels in the *clpP* mutant and was barely detectable in the wild type strain as expected under non–stress conditions (Figure 17 C). In contrast, no Spx was detected in the suppressor mutant (Figure 17 C), suggesting that the mutation occured either in the *spx* ORF, in its promoter region, or in a gene required for the expression of *spx*.

To test directly, whether the motility defect of *clpP* and *clpX* mutants is caused by Spx accumulation, a *spx clpX* double mutant was constructed and motility assays and Hag Western blots were performed with the strain. As shown in Figure 18 A, the wild type and the *spx* mutant were motile, whereas the *clpX* mutant was non-motile. Notably, the *spx clpX* double mutant was motile (although slightly less than the wild type, Figure 18 A).
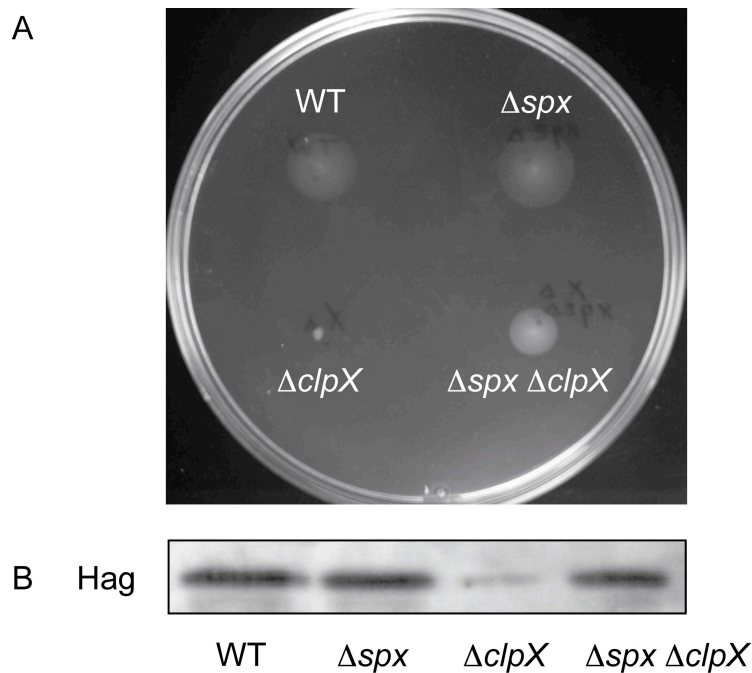
Figure 18: Suppression of the *clpX* motility phenotype by mutation of *spx*.
A. Swim plates were inoculated with cultures of strains 168 (wild type), BNM107 (Δ*clpX*::kan), BNM111 (Δ*spx*::kan) and BNM112 (Δ*spx*::kan Δ*clpX*::spec) and incubated for 6 hours at 37°C. Mutation of *spx* suppressed the motility phenotype of the *clpX* mutant. B. Hag Western blot. Strains 168, BNM107, BNM111 and BNM112 were grown in LB to OD$_{600}$ 1.0 at 37°C and harvested for protoplast preparation. Protoplasts were lysed and the lysates (2.5 μg total protein per lane) were separated by SDS–PAGE and subjected to Western blotting. Hag levels were restored in the *spx clpX* double mutant compared to the *clpX* single mutant.

Analogous results were obtained by Hag Western blot experiments (Figure 18 B): the

spx mutant produced wild type levels of Hag. In contrast, very low amounts of Hag were detected in the *clpX* mutant. Importantly, the *spx clpX* double completely suppressed the phenotype of the *clpX* mutant (Figure 18 B), suggesting that *clpX* downregulates motility and Hag production via *spx*.
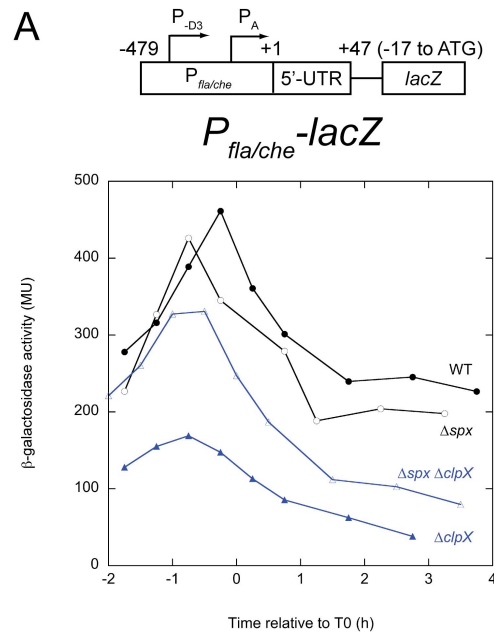
Figure 19: Expression of $P_{fla/che}$-*lacZ* is restored in a *clpX spx* double mutant. β-galactosidase assay of $amyE$::$P_{fla/che}$-*lacZ*::cat strains BNM301 (wild type, closed black circles), BNM305 ($\Delta clpX$::kan, closed blue triangles), BNM307 (Δspx::kan, open black circles), BNM308 (Δspx::kan $\Delta clpX$::spec, open blue triangles).

To investigate whether the *spx clpX* also restores $P_{fla/che}$ and P_{hag} promoter activities, reporter gene studies were performed in the single and double mutant strains. Notably, the β-galactosidase activities of the $P_{fla/che}$-*lacZ* (Figure 19) and P_{hag}-*lacZ* (Figure 20) fusions were partially restored compared to the *clpX* single mutant.

Furthermore, the mRNA levels of *hag* and other flagellar transcripts were also upregulated in the *spx clpX* double mutant compared to the *clpX* single mutant in microarray experiments (K. Turgay, unpublished data), demonstrating that *clpX* acts globally on motility genes via *spx*. These results strongly suggest that the motility defect of the *clpP* and *clpX* mutants is a result of Spx accumulation. This would imply that Spx acts as a negative regulator of motility genes, which has not been reported previously. Moreover, it can be inferred from the reporter gene studies (Figure 19) that Spx acts on motility at the level of the $P_{fla/che}$ promoter.
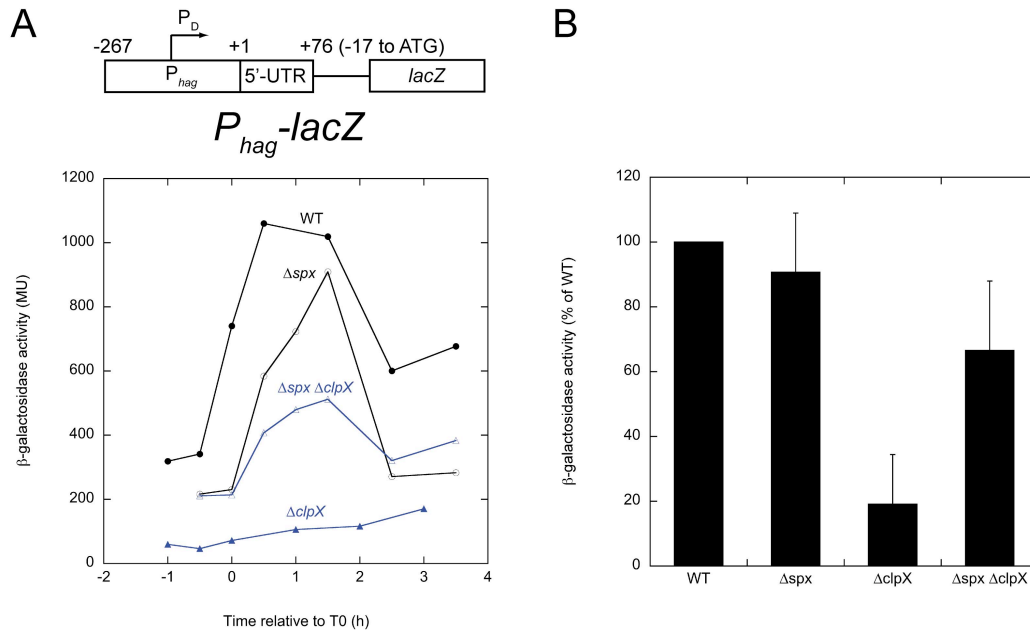
Figure 20: Expression of P_{hag}-$lacZ$ is restored in a $clpX$ spx double mutant.
A. β-galactosidase assay of $amyE$::P_{hag}-$lacZ$::cat strains BNM328 (wild type, closed black circles), BNM332 ($\Delta clpX$::kan, closed blue triangles), BNM334 (Δspx::kan, open black circles), BNM335 (Δspx::kan $\Delta clpX$::spec, open blue triangles). For both constructs, β-galactosidase activity was reduced in the $clpX$ mutant and partially restored in the spx $clpX$ double mutant. B. Mean β-galactosidase activities of strains BNM328, BNM332, BNM334 and BNM335 at the postexpontial peak (around OD_{600} 1.0) were determined from 3 independent experiments and normalized separately to wild type activity. Error bars indicate standard deviations.

Induction of proteolysis–resistant Spx   To show whether Spx production is suffi-
cient for the inhibition of motility in a $clpX^+$ background, two strains (kindly provided
by P. Zuber, University of Oregon) were used, in which spx is placed under the control
of an IPTG–inducible promoter[182]. In strain BNM350, wild type Spx is produced,
whereas in strain BNM351 the C–terminal ClpXP degradation tag of Spx is mutated
(spx^{DD}), resulting in stabilization of Spx and accumulation to higher levels (Figure 22
A)[182].

Swim plates containing 0.1 mM IPTG or no inducer were inoculated with these strains
to test swimming motility. Interestingly, strain BNM351, but not strain BNM350 was
motile without IPTG (Figure 21 A), but non–motile in the presence of IPTG (Figure 21
B), suggesting that high levels of Spx are sufficient to downregulate swimming motility
and confirming that Spx acts as a negative regulator of motility genes.
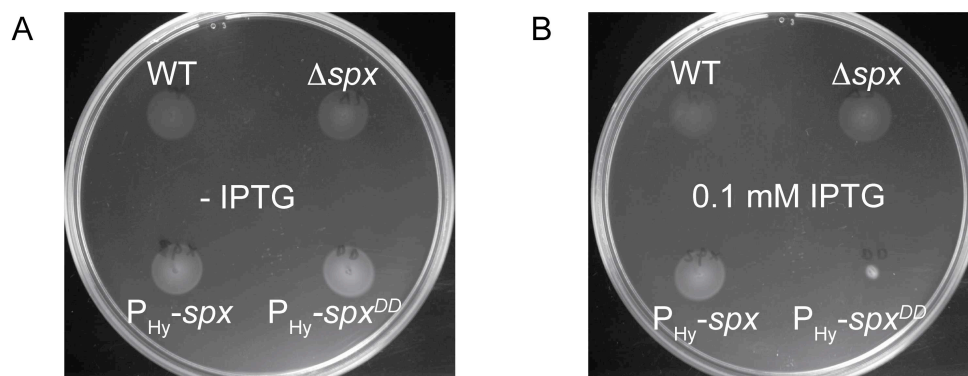
Figure 21: Swimming motility is inhibited by Spx.
Swim plates without IPTG (A) or with 0.1 mM IPTG (B) were inoculated with strains
168 (wild type), BNM111 (Δspx::kan), BNM350 (Δspx::kan $amyE$:: $P_{hyperspank(Hy)}$-
spx::spec) and BNM351 (Δspx::kan $amyE$::$P_{hyperspank(Hy)}$-spx^{DD}::spec) and grown for
6 hours at 37°C. BNM351 was non-motile in the presence of IPTG.

Spx and Spx^{DD} were also induced by IPTG addition in liquid medium and samples
were analyzed by Western blot (Figure 22) and Northern blot (Figure 23). Hag protein
concentration (Figure 22) as well as hag and $sigD$ transcript levels (Figure 23) were
measured after 30 and 60 minutes of induction.

As shown in Figure 22, Hag protein levels decreased to about 50% of the initial level
after 60 minutes of induction. For hag and $sigD$ mRNA, the effect was much stronger:
after 30 mintues of Spx^{DD} induction, both transcripts were below the detection level
of the Northern blot experiment (Figure 23). The different results obtained in Western

A

+ 1 mM IPTG

P_{Hy}-*spx* P_{Hy}-*spx*^{DD}

Spx

Hag

0   30   60   0   30   60

B

P_{Hy}-*spx* P_{Hy}-*spx*^{DD}

- IPTG   + IPTG   - IPTG   + IPTG

Hag

Δ*spx* 0   30   60   30   60   0   30   60   30   60
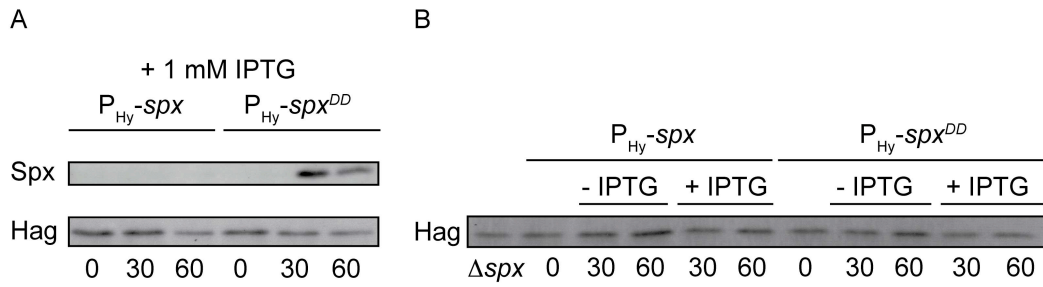
Figure 22: Spx inhibits Hag production.
Strains BNM350 (Δ*spx*::kan *amyE*::$P_{hyperspank(Hy)}$-*spx*::spec) and BNM351 (Δ*spx*::kan *amyE*::$P_{hyperspank(Hy)}$-*spx*^{DD}::spec) were grown to OD$_{600}$ 0.3 in LB at 37°C and *spx* expression was induced by addition of 1 mM IPTG. Samples were withdrawn before induction and 30 and 60 minutes thereafter, protoplasted and lysed. Lysates were separated by SDS–PAGE, blotted and developed with Hag and Spx antibodies (A) or Hag antibodies (B). Hag levels decreased to about 50% of the initial value after IPTG induction.

and Northern blot experiments were probably due to the higher stability of Hag protein compared to *hag* and *sigD* mRNAs.

Δ*spx amyE*   ::P$_{Hy}$-*spx*^{DD}

hag

sigD

0   30   60   0   30   60   min
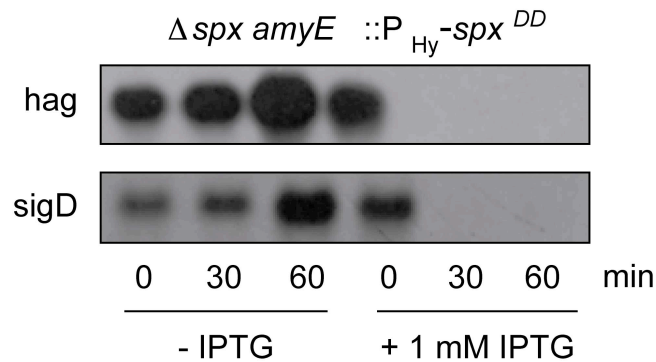
- IPTG   + 1 mM IPTG

Figure 23: Spx inhibits transcription of *hag* and *sigD*.
Strain BNM351(Δ*spx*::kan *amyE*::$P_{hyperspank(Hy)}$-*spx*^{DD}::spec) were grown to OD$_{600}$ 0.3 in LB at 37°C and *spx* expression was induced by addition of 1 mM IPTG. Total RNA was prepared from samples taken before and 30 and 60 minutes after induction and 2 μg RNA were separated on denaturing agarose gels and subjected to Northern blot analysis. Blots were hybridized with DIG-labeled DNA probes against *hag* (upper) and *sigD* (lower). Both transcripts were undetectable after 30 and 60 minutes induction.

Motility regulation during stress   In wild type cells, Spx is quickly degraded by ClpXP under non–stress conditions and only accumulates after oxidative stress. Therefore, it was investigated whether Spx affects swimming motility during its natural induction by oxidative stess. To this end, the *lacZ* reporter strains $P_{fla/che}$-*lacZ* and

P_{hag}-*lacZ* were grown to early exponential phase, the culture was split and diamide (an oxidaizing agent that causes the formation of disulfide bonds in cytoplasmic proteins) was added to one half of the culture. Samples were removed after the shock and β-galactosidase activites were measured. The same samples were used to determine Spx levels by Western blot analysis.

As shown in Figure 24, both the $P_{fla/che}$ and P_{hag} promoters were strongly downregulated for approximately one hour in the presence of diamide. After this period, the promoter activity increased and displayed the usual peak that is observed in postexponential phase in the absence of stress. Interestingly, Spx protein accumulated at exactly the same time, at which the promoters were downregulated. Unfortunately, these experiments yielded inconclusive results in *spx* mutant cells, because the *spx* mutant did not survive the diamide shock (data not shown). Therefore, it cannot be directly inferred that downregulation of motility genes during oxidative stress depends on *spx*, although this hypothesis is strongly favored.

Spx appears to be induced not only by oxidative stress, but also by heat stress (A. Heinz & K. Turgay, microarray experiments, S. Runde, Western blot analysis). Therefore, it was tested whether the $P_{fla/che}$ promoter activity was downregulated by heat stress. A fusion of the long $P_{fla/che}$ promoter fragment (identical to the one used for strain BNM346) to the heat stable β-galactosidase BgaB from *Bacillus stearothermophilus* was constructed, grown at 37°C and 48°C and BgaB acivity was determined.

BgaB is more stable than LacZ at 37°C. Therefore, the expression peak in postexponential phase was less well defined than with the *lacZ* fusions and BgaB activity increased further after the peak (Figure 25, closed black circles). At 48°C however, the $P_{fla/che}$-*bgaB* fusion was completely inactive, demonstrating that motility genes are downregulated at high temperature, possibly by Spx. Confirming this result, motility genes were strongly downregulated in microarray experiment in response to heat shock (A. Heinz & K. Turgay, unpublished data).

Investigation of the Spx repression mechanism Spx is an unusual transcriptional regulator that can act as an activator or repressor on distinct target genes[182, 183]. Interestingly, Spx itself has never been observed to bind DNA[181], but interacts with the C–terminal domain of the RNA polymerase α subunit (α-CTD), which is re-
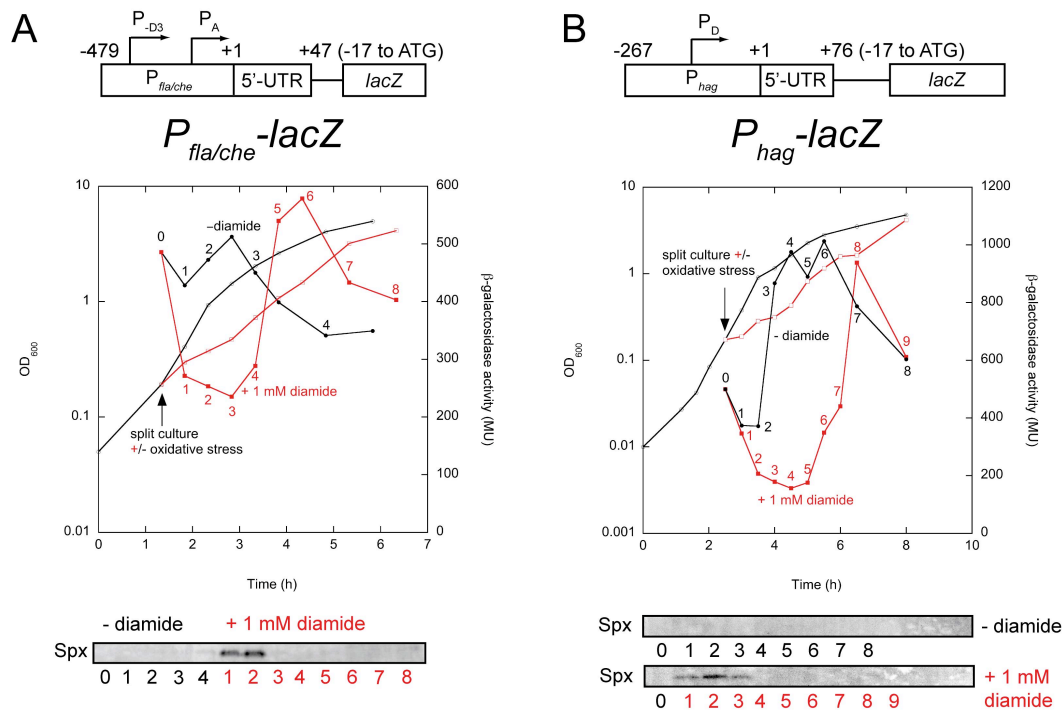
Figure 24: Oxidative stress leads to transient downregulation of motility genes.
Strains BNM301 ($amyE::P_{fla/che}$-$lacZ$::cat, A) and BNM328 ($amyE::P_{hag}$-$lacZ$::cat, B) were grown in LB to early exponential phase (OD_{600} 0.15-0.3) and split into two smaller cultures. 1 mM diamide was added to one of these cultures (red squares), the other was grown in the absence of diamide (black circles) and samples were taken for measurement of β-galactosidase activity and Spx Western blot (lower panel). Open symbols indicate OD_{600} and closed symbols indicate β-galactosidase activities. Both $lacZ$ fusions were transiently downregulated after diamide treatment, which correlates with accumulation of Spx.
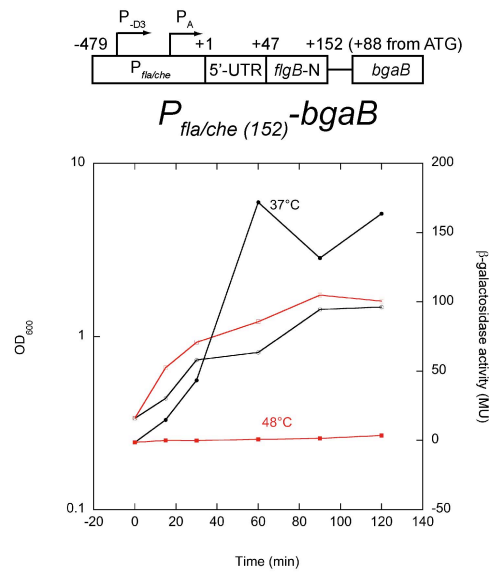
Figure 25: Heat stress downregulates the $P_{fla/che}$ promoter. Strain BNM345 ($amyE$::$P_{fla/che152}$-$bgaB$::cat) was grown at 37°C (black circles) or 48°C (red squares). Open symbols: OD_{600}, closed symbols: $bgaB$ activity. Promoter activity was inhibited throughout growth at 48°C. The experiment was performed by Ingke Marg.

quired both for activation and repression[182, 201, 180]. According to the interference model, Spx represses activator–controlled genes by competition with activators, such as ComA, for binding to the α-CTD[182]. Activation requires binding of the Spx-α-CTD complex to sequences upstream of the core promoter of the regulated genes[201, 180].

The negative regulation of the $P_{fla/che}$ promoter observed in this study (Figure 19) might be explained by interference of Spx with an α-CTD binding $P_{fla/che}$ activator. However, such an activator has never been described, raising the possibility that Spx regulates $P_{fla/che}$ by a different mechanism.

In order to rule out that Spx binds directly to the $P_{fla/che}$ promoter, Spx was over–produced in $E.\ coli$ with a C–terminal His–tag and purified by affinity chromatography. Subsequently, electrophoretic mobility shift assays were performed with purified Spx protein and 3 overlapping DNA fragments (generated by PCR), which cover the entire $P_{fla/che}$ promoter and part of the $flgB$ open reading frame. As shown in Figure 26, even at high protein concentrations, no Spx bound to the DNA fragments, in line with previous reports that Spx alone does not bind to DNA[181]. These results suggest that Spx does not repress $P_{fla/che}$ by direct binding. However, interference of Spx with an
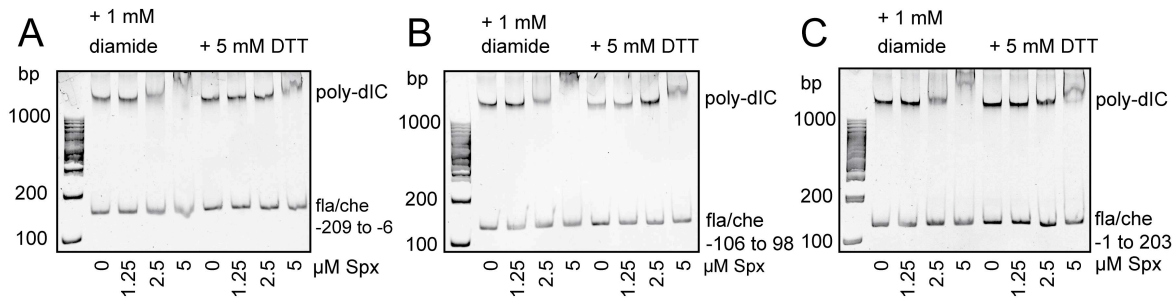
Figure 26: Spx does not directly bind to the *fla/che* promoter region. Purified Spx protein was mixed with different DNA fragments close to the *fla/che* promoter (A: -209 to -6, B: -106 to 98, C: -1 to 203 relative to the *flgB* transcription start site) in the presence of poly d-IC under oxidizing (left) and reducing conditions (right). After incubation, the samples were separated on an acryl amide gel and stained with ethidium bromide. Spx bound to neither of the promoter fragments, but caused a shift of the poly d-IC band at high protein concentrations.

unknown transcriptional activator of $P_{fla/che}$ cannot be ruled out by the data presented here.

Alternatively, Spx may regulate the $P_{fla/che}$ promoter indirectly by transcriptional activation of a $P_{fla/che}$ repressor. Microarray experiments of RNA from a *spx clpX* double mutant compared to the *clpX* single mutant revealed several genes that were upregulated by Spx (K. Turgay, unpublished). These microarray data were searched for putative transcription factors. Two candidate genes of unknown function, *yhfK* and *yukF* were identified. These genes were cloned and expressed in *B. subtilis* from an IPTG–inducible promoter. The respective strains were assayed for swimming motility on swim plates containing 1 mM IPTG (Figure 27). In contrast to *spxDD*, over-expression of both genes had no effect on swimming motility, excluding them as negative regulators of $P_{fla/che}$.

In order to identify negative regulators of $P_{fla/che}$, which are activated by Spx, a genetic suppressor screen was performed. To this end, a transposon insertion library was constructed from a strain expressing spx^{DD} from an IPTG–inducible promoter. As shown in Figure 21, this strain is non-motile in the presence of IPTG, very likely due to Spx–mediated repression of $P_{fla/che}$. This library was screened for clones, which restore swimming motility in the presence of IPTG.

In a second screen for novel activators of $P_{fla/che}$, strain BNM301, expressing a transcriptional *lacZ*-fusion to $P_{fla/che}$, was transposon mutagenized and the transposon
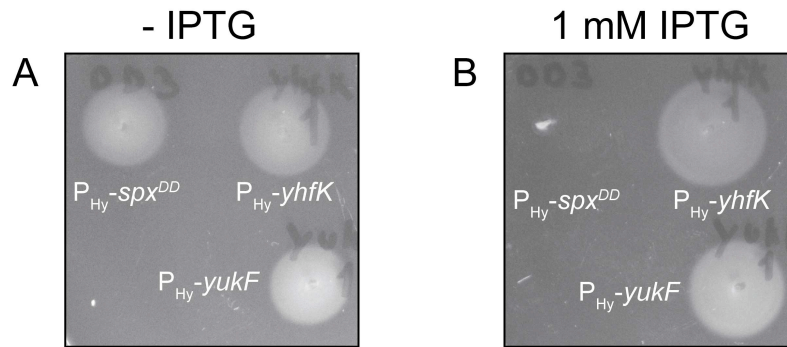
Figure 27: YhfK and YukF are not involved in downregulation of swimming motility. Strains BNM351 (Δspx::kan $amyE$::$P_{hyperspank(Hy)}$-spx^{DD}::spec), BNM457 ($amyE$::$P_{hyperspank(Hy)}$-$yhfK$::spec) and BNM458 ($amyE$::$P_{hyperspank(Hy)}$-$yukF$::spec) were spotted on swim plates in the absence (A) or presence (B) of 1 mM IPTG and incubated at 37°C for 6 hours. Production of YhfK or YukF did not interfere with swimming motility.

library was screened for clones, in which $P_{fla/che}$ and swimming motility are downregulated. The identification of such an activator might help to explain the Spx–mediated repression of $P_{fla/che}$ by interference with the α-CTD. Chromosomal DNA of clones from both screens is currently being sequenced to map the transposon insertion sites.

4.1.3   Possible posttranscriptional regulation of motility by ClpXP/Spx

The data presented in section 4.1 clearly indicate that the expression of the *hag* gene is downregulated in *clpP*, *clpC* and *clpX* mutants. These effects were due to repression of the $P_{fla/che}$ promoter by DegU (for the *clpC* mutant) and by Spx (in case of the *clpX* mutant), resulting in lower levels of σ^D (see section 4.1.1). In addition, the *clpC* mutant was shown to downregulate σ^D activity via ComK and FlgM (see section 4.1.1)[147]. Notably, *hag* is not only regulated at the transcriptional level, but is also subject to posttranscriptional regulation (see section 2.3.2 and Figure 3). For instance, *hag* mRNA might be processed by RNases J1 and J2[153] and translation initiation of *hag* is inhibited by CsrA[244].

In order to investigate whether transcriptional regulation is the only step influenced by the Clp proteases or whether posttranscriptional regulation of *hag* is also affected, *hag* expression was uncoupled from transcriptional regulation by σ^D. To this end, *hag* was placed under the control of the xylose–inducible promoter P_{xyl} in the *amyE* locus of a *hag* mutant (strain *hag1*, Figure 28 A). If only the transcriptional regulation of

hag was regulated by ClpCP and ClpXP, *clp* mutations introduced into strain *hag1* would be expected to no longer influence Hag protein levels. Uncoupling *hag* from σ^D regulation also proved useful for *in vivo* studies of Hag proteolysis (see section 4.2).

It is also possible that the *fla/che* operon is regulated posttranscriptionally. Indeed, the observation that RNA probes against both *flgB* and *sigD* detected a much smaller RNA fragment than the expected 27 kb full length transcript (Figure 10) strongly suggests that this transcript is processed after transcription. This assumption might be directly tested either by ectopic expression of the entire 27 kb *fla/che* operon or by replacement of the *fla/che* promoters i.e. by a P_{xyl} promoter.
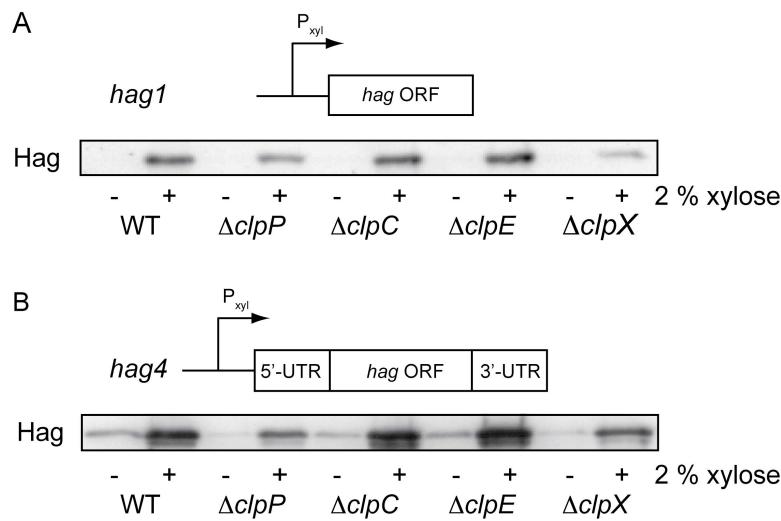
Figure 28: Uncoupling of *hag* expression from flagellar regulation.
A. *hag* was expressed from a xylose–inducible promoter in a *hag* deletion background and combined with *clp* mutants. BNM421 (Δhag $amyE$::P_{xyl}-*hag1*::cat), BNM422 (*hag1* $\Delta clpP$::spec), BNM423 (*hag1* $\Delta clpC$::tet), BNM424 (*hag1* $\Delta clpE$::spec) and BNM425 (*hag1* $\Delta clpX$::kan). B. Hag was expressed with 5'- and 3'-untranslated regions from an xylose–inducible promoter. BNM426 (Δhag $amyE$::P_{xyl}-*hag4*::cat), BNM427 (*hag4* $\Delta clpP$::spec), BNM428 (*hag4* $\Delta clpC$::tet), BNM429 (*hag4* $\Delta clpE$::spec) and BNM430 (*hag4* $\Delta clpX$::kan). Strains were grown in LB with 2% xylose to OD_{600} 1.0 and protoplast extacts were subjected to Hag Western blot. Hag levels were equal to the wild type in *clpC* and *clpE* mutants after xylose induction, but were strongly reduced in *clpP* and *clpX* mutants.

However, since the observed pattern of P_{hag} promoter activity in wild type and *clp* mutant cells (Figure 9) was very similar to $P_{fla/che}$ activity (Figure 8), *flgB* and *sigD* transcripts (Figure 10) and σ^D protein levels (Figure 11), posttranscriptional regulation of the *fla/che* operon does not appear to play a role in the motility regulation by ClpCP

and ClpXP and was not further investigated in this study.

Hag levels in the *hag1* strain   Hag levels were analyzed by Western blot in the strain with a xylose–inducible copy of *hag* (*hag1*) combined with *clp* mutants (Figure 28). Induction with 2% xylose resulted in lower Hag levels than in the wild type strain 168 (data not shown). As shown in Figure 28 A, the *clpC* mutant displayed the same Hag level as the wild type in the *hag1* background, demonstrating that *hag* expression was independent of *clpC*. This result confirms that *clpC* acts upstream of *hag* transcription, which is consistant with the data presented above (section 4.1). However, the *clpP* and *clpX* mutants still displayed lower levels of Hag protein than the wild type in the *hag1* background (Figure 28 A), suggesting that *hag* under control of the P_{xyl} promoter is still regulated by *clpP* and *clpX*.
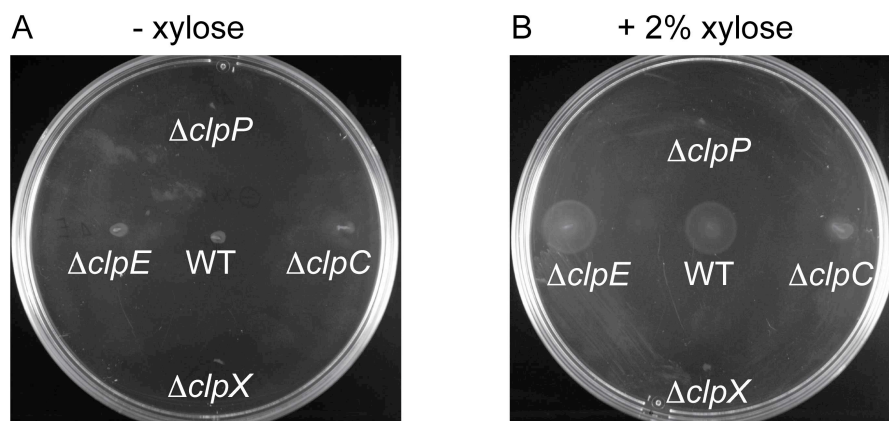
Figure 29: Motility of the *hag4* strain
Swim plates of strains BNM426 (Δhag $amyE$::P_{xyl}-*hag4*::cat), BNM427 (*hag4* $\Delta clpP$::spec), BNM428 (*hag4* $\Delta clpC$::tet), BNM429 (*hag4* $\Delta clpE$::spec) and BNM430 (*hag4* $\Delta clpX$::kan) in the absence (A) or presence of 2% xylose (B). All strains were non-motile in the absence of xylose (A). In the presence of xylose (B), BNM426 and BNM429 were motile, whereas BNM428 displayed reduced motility and strains BNM427 and BNM428 were non-motile. Experiments performed by Jörn Hossmann.

Hag levels in the *hag4* strain   Since the *hag1* strain turned out to be non-motile for unknown reasons (data not shown), strain BNM426 (*hag4*), which contains non-translated upstream and downstream sequences in addition to the *hag* open reading frame, was constructed (Figure 28 B). Hag levels were similar to or slightly higher in *hag4* than in the wild type strain 168 (data not shown). Interestingly, this strain was
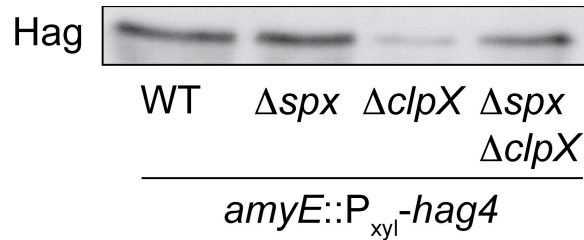
Figure 30: Suppression of a posttranscriptional *clpX* effect by mutation of *spx*. Δhag $amyE$::P_{xyl}-$hag4$::cat strains BNM426 (WT), BNM430 ($\Delta clpX$::kan), BNM436 (Δspx::kan) and BNM437 (Δspx::kan $\Delta clpX$::spec) were grown in LB with 2% w/v xylose to OD_{600} 1.0 at 37°C and harvested for protoplast preparation. Protoplast lysates (2.5 μg total protein per lane) were separated by SDS–PAGE and subjected to Western blotting. Hag levels were restored in the *spx clpX* double mutant compared to the *clpX* single mutant.

motile in the wild type background, but not combined with the *clpP*, *clpC* and *clpX* mutants (Figure 29).

These data suggest that untranslated regions upstream or downstream of the *hag* gene are strictly required for motility. The lack of complementation of the motility phenotype in the *clpP*, *clpC* and *clpX* mutants (Figure 29) was expected because other components of the flagellum cannot be produced at sufficient levels in these strains due to the downregulation of the *fla/che* operon.

When strain BNM426 was combined with the *clpC* mutant and Hag levels were analyzed by Western blot after xylose induction, Hag accumulated to wild type levels (Figure 28 B) as for the *hag1* strain background. It could be confirmed by these data that *clpC* acts on motility at or upstream of the P_{hag} promoter, consistant with the results shown in section 4.1.1.

However, less protein was detected in the *clpP* and *clpX* mutants similar to the *hag1* strain (Figure 28 B). It can be inferred from these results that either the P_{xyl} promoter is downregulated in the *clpP* and *clpX* mutants, or that a negative posttranscriptional regulator of Hag is upregulated in these mutants.

Spx dependence of the putative posttranscriptional ClpXP effect   To elucidate the mechanism, by which *clpP* and *clpX* influence *hag* expression from the P_{xyl} promoter, it was tested whether Spx is responsible for the observed effect. To this end, the *spx* and *spx clpX* mutations were introduced into the *hag4* background and
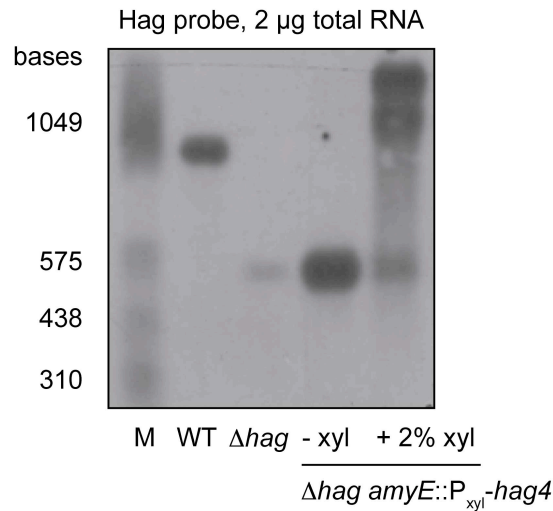
Figure 31: Northern blot analysis of wild type and xylose-induced *hag* transcripts. Northern blot of total RNA (2 µg/lane) from strains 168 (wild type), BNM126 (Δ*hag*) and BNM426 (Δ*hag amyE*::P_{xyl}-*hag4*::cat with or without 2% xylose) grown in LB at 37°C to OD_{600} 1.0. RNA from strains BNM126 and BNM426 without xylose exhibited a small RNA species of about 500 bases, which was bound by the *hag* probe. In the presence of xylose, RNA from strain BNM426 exhibited two *hag* bands, which were larger than the single *hag* band in the wild type strain.

Hag Western blots were performed with lysates of the *hag4* strain in the wild type, *spx*, *clpX* and *spx clpX* backgrounds after xylose induction (Figure 30). Indeed, Hag was restored to wild type levels in the *spx clpX* double mutant compared to the *clpX* single mutant (Figure 30), suggesting that the effect of *clpX* on *hag* is dependent on Spx, even in the *hag4* strain, in which *hag* expression is uncoupled from σ^D control. Next, it was important to determine, how Spx exerts this putative posttranscriptional control.

Northern blot analysis of strain *hag4* To analyze whether Spx acts on *hag* expression at the mRNA level or the protein level, Northern blots of RNA extracted from the xylose induced *hag4* strain were performed.

As depicted in Figure 31, two bands above 1.5 kb were detected by the probe in the presence of xylose in contrast to the wild type strain, which displayed only one band of roughly 1 kb. The greater length of the ectopically produced *hag* transcript may be the result of a *xylA* linker downstream of the P_{xyl} promoter [113]. However, the reason for the second band is unknown. In addition, a band of about 500 bases was observed

Hag probe, 2 µg total RNA

Δ*hag* WT Δ*clpP* Δ*clpC* Δ*clpE* Δ*clpX* Δ*spx* Δ*spx* Δ*clpX*

Δ*hag amyE*::P   *hag4* + 2% xylose
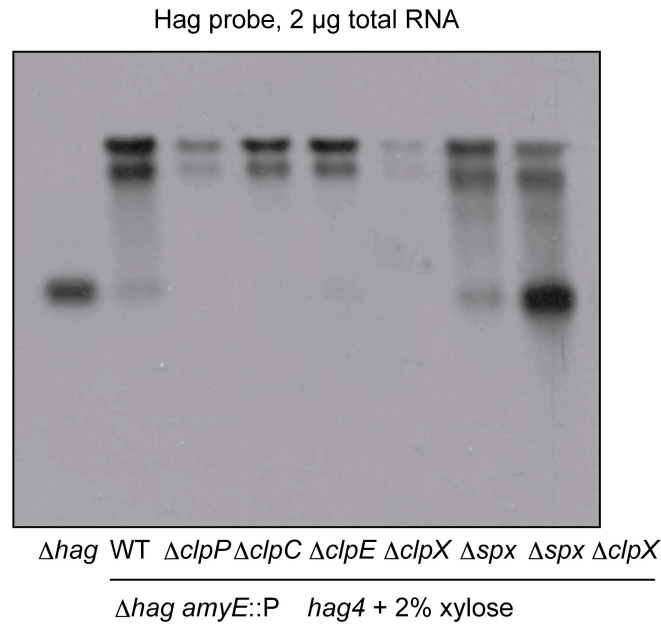
Figure 32: Spx influences xylose-induced *hag* mRNA levels.
Northern blot of total RNA (2 µg/lane) from strains BNM126 (Δ*hag*), BNM426 (Δ*hag amyE*::P_{xyl}-*hag4*::cat), BNM427 (Δ*hag amyE*::P_{xyl}-*hag4*::cat Δ*clpP*::spec), BNM428 (Δ*hag amyE*::P_{xyl}-*hag4*::cat Δ*clpC*::tet), BNM429 (Δ*hag amyE*::P_{xyl}-*hag4*::cat Δ*clpE*::spec), BNM430 (Δ*hag amyE*::P_{xyl}-*hag4*::cat Δ*clpX*::kan), BNM436 (Δ*hag amyE*::P_{xyl}-*hag4*::cat Δ*spx*::kan) and BNM437 (Δ*hag amyE*::P_{xyl}-*hag4*::cat Δ*spx*::kan Δ*clpX*::spec) grown in LB with 2% w/v xylose to OD_{600} 1.0 at 37°C. Hag transcript levels were reduced in the *clpP* and *clpX* mutants and restored in the *clpX spx* double mutant.

in the *hag4* strain without xylose and in the *hag* mutant.

A Northern blot with RNA samples extracted from wild type and *clp* mutant strains, as well as the *spx* and *spx clpX* mutants revealed that *hag* transcript levels are significantly lowered in the *clpP* and *clpX* mutants compared to the wild type (Figure 32). Furthermore, transcript levels were restored in a *spx clpX* double mutant (Figure 32). These data indicate that Spx acts on *hag* at the mRNA level.

This implies that Spx influences either transcription initiation from the P_{xyl} promoter or a step downstream of *hag* transcription initiation and upstream of translation initiation.

RNaseJ   These steps could be either transcription elongation or mRNA degradation. If the regulated step was mRNA stability, the regulator of interest could be an RNA degrading enzyme that is upregulated by Spx. One candidate for such an enzyme was identified in microarray experiments (K. Turgay, unpublished): the transcript levels of
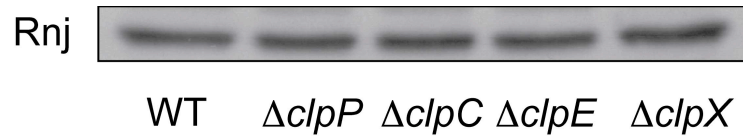
Figure 33: RNaseJ Western blot of wild type and *clp* mutant cells.
Lysates from strains 168 (wild type), BNM103 ($\Delta clpP$::spec), BNM105 ($\Delta clpC$::tet), BNM106 ($\Delta clpE$::spec) and BNM107 ($\Delta clpX$::kan) grown to OD_{600} 1.0 in LB at 37°C were separated by SDS–PAGE, blotted and probed with antibodies against RnjA/RnjB. The *clpX* mutant had slightly higher levels of RNaseJ than the wild type. All other mutants were equal to the wild type.

rnjA encoding RNaseJ1 were 3–fold upregulated in the *clpX* single mutant compared to the *spx clpX* double mutant.

RNaseJ1 and RNaseJ2 have been implicated in the degradation of flagellar transcripts[153]. Unfortunately, construction of a *rnjA clpX* double mutant, which could have unambiguously demonstrated whether *clpX* acts via *rnjA* was not possible, because *rnjA* is an essential gene[122].
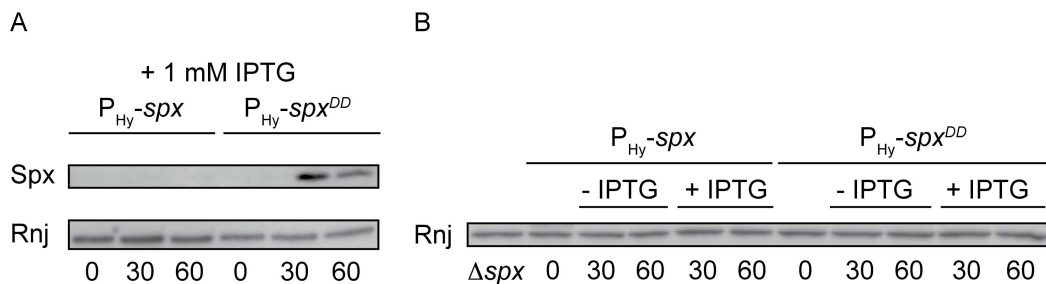
Figure 34: RNaseJ production is not activated by Spx.
Strains BNM350 (Δspx::kan $amyE$::$P_{hyperspank(Hy)}$-*spx*::spec) and BNM351(Δspx::kan $amyE$::$P_{hyperspank(Hy)}$-*spx* ^{DD}::spec) were grown to OD_{600} 0.3 in LB at 37°C and *spx* expression was induced by addition of 1 mM IPTG. Samples were withdrawn before induction and 30 and 60 minutes thereafter, protoplasted and lysed. Lysates were separated by SDS–PAGE, blotted and developed with RnjA/B and Spx antibodies (A) or RnjA/B antibodies (B). RNaseJ levels did not change after induction of Spx or Spx^{DD}.

Instead, it was tested whether RNase J protein levels are affected by *clp* mutations in the wild type background (with *hag* under control of its native promoter). To this end, RNase J Western blots were performed with lysates from wild type and *clp* mutant strains. The RNase J polyclonal antiserum (kindly provided by H. Putzer, University of Paris), detects both isoforms of RNase J, which appear as one band on SDS–PAGE

gels. As shown in Figure 33, RNaseJ levels were slightly elevated in the *clpX* mutant, but not in the *clpP*, *clpC* and *clpE* mutants.

Because of this ambiguous result, it was directly investigated whether RNaseJ is induced by Spx. To this end, RNaseJ levels were measured in strains BNM350 and BNM351 (IPTG–inducible *spx* or *spx^{DD}*) 30 and 60 minutes after IPTG induction. The Western blot shown in Figure 34 revealed that RNase J protein levels were unchanged by Spx or Spx^{DD} induction.

In summary, although RNases J1 and J2 may be involved in the processing or turnover of flagellar RNAs[153], these enzymes do not appear to be degraded by Clp proteases and their cellular levels are not affected by Spx, judging by the data shown here.
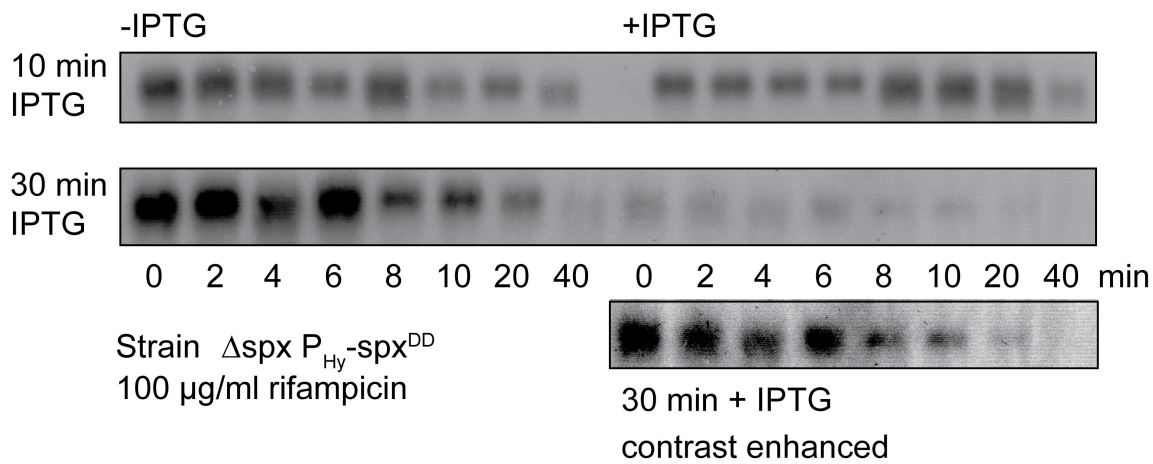
Figure 35: Transcript stability of *hag* is not influenced by Spx.
Strain BNM351 (Δspx::kan $amyE$::$P_{hyperspank(Hy)}$-spx^{DD}::spec) was grown to OD$_{600}$ 0.5 in LB at 37°C and split into two cultures. 1 mM IPTG was added to one culture, and shaking was continued for either 10 minutes (upper) or 30 minutes (lower). Subsequently, rifampicin was added to both cultures to a final concentration of 100 μg/ml and samples were removed at different times for RNA preparation. Total RNA (2 μg/lane) was subjected to Northern blot analysis. The *hag* transcript was degraded with a half–life between 10 and 20 minutes independently from IPTG induction of *spx^{DD}*, even though *hag* RNA levels at time 0 were strongly reduced after 30 minutes induction.

RNA stability experiments   To directly test whether Spx affects *hag* mRNA degradation, RNA stability assays were performed. Strain BNM351 (harboring IPTG–inducible *spx^{DD}*) was grown to OD$_{600}$ 0.5 and the culture was split. One half was induced with IPTG for either 10 minutes or 30 minutes to produce Spx^{DD}. Subse-

quently, rifampicin was added to both cultures to inhibit RNA synthesis and samples were removed at different timepoints for RNA extraction and Northern blot analysis. As shown in Figure 35, the half–life of RNA turnover was in the range of 10-20 minutes without IPTG induction, as previously described for the *hag* transcript[50]. Importantly, the transcript half–life did not change significantly after IPTG induction of Spx^{DD} (Figure 35). When Spx^{DD} was induced for 30 minutes, *hag* mRNA levels were already very low at the time of rifampicin addition, probably due to the negative effect of Spx on *hag* transcription (see Figure 23). Nevertheless, analysis of the data at increased contrast revealed that the half–life of the *hag* transcript was unaffected by induction of Spx^{DD} also in this experiment.

It can be concluded from these data that the putative posttranscriptional regulation of *hag* by Spx occurs either at the level of transcription elongation or that the observed effect is a consequence of Spx–dependent downregulation of the P_{xyl} promoter.

In accordance with this hypothesis, it was demonstrated that Hag levels in the *hag4 clpP* and *hag4 clpX* are unaffected by mutation of *csrA* (J. Hossmann, unpublished), thus suggesting that regulation of translation initiation by CsrA is not involved in the putative postranscriptional regulation of *hag*.

4.2 Putative general proteolysis of flagellin (Hag)

Hag was identified as an interaction partner of ClpC in a pulldown experiment. Subsequently it was shown that recombinant purified Hag is a substrate of the ClpCP protease complex, which is targeted for degradation by the adaptor protein YpbH (Janine Kirstein, unpublished data). This result was reproduced here and it was confirmed that Hag is targeted for degradation by ClpCP specifically by YpbH (Figure 36).

In order to investigate whether Hag is also degraded *in vivo*, *pulse chase* labeling experiments were performed in the wild type strain 168. To this end, cells were grown to late exponential phase (the growth phase of maximal *hag* expression) in minimal medium, newly synthesized proteins were labeled with radioactive methionine for 10 minutes and subsequently an excess of unlabeled methionine was added (chase). Samples were taken at different times and TCA–precipitated. Hag protein was enriched from these samples by immunoprecipitation with Hag antibodies and protein A–coated magnetic
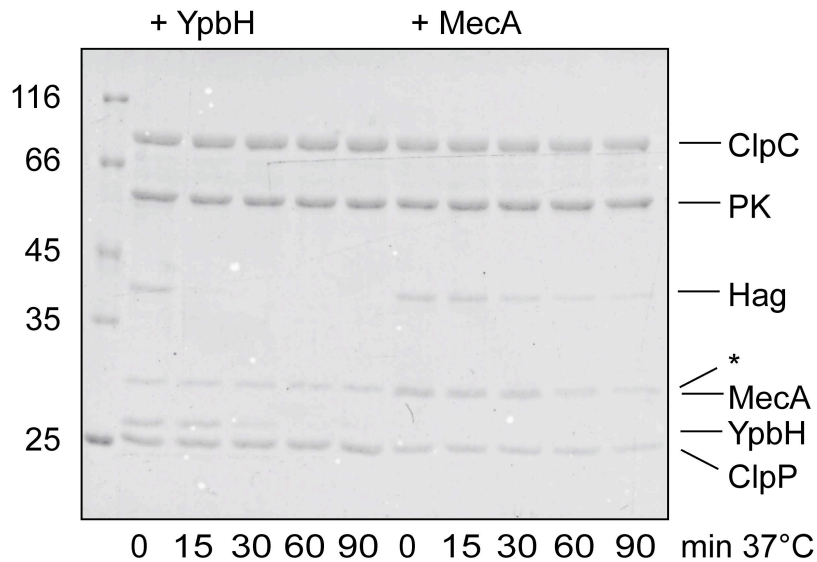
Figure 36: Hag proteolysis by ClpCP-YpbH *in vitro.*
1 μM purified ClpC, ClpP, Hag and MecA or YpbH were incubated at 37°C in degradation buffer containing ATP and pyruvate kinase (PK)/PEP as an ATP regeneration system. Samples were removed at the times indicated and analyzed by Tris-Tricine SDS–PAGE. The asterix indicates a minor protein band from the pyruvate kinase preparation, which runs at the same height as MecA. Hag was rapidly degraded by ClpCP in the presence of the adaptor YpbH (left), but not MecA (right).

beads and subjected to SDS–PAGE and autoradiography. As shown in Figure 37, Hag was successfully labeled and immunoprecipitated, but remained relatively stable up to one hour after the chase.

Hag degradation assays during stress A possible explanation of these data is that the ClpCP protease is capable of Hag degradation, but not under the conditions of the *in vivo pulse chase* experiment. The crystal structure of flagellin from *Salmonella* suggest that flagellin confers unfolded stretches at the N– and C–termini[245]. It was hypothesized that these unfolded regions may lead to Hag aggregation under stress conditions. In addition, ClpC, ClpP and YpbH are produced in higher amounts during stress, which might favor general proteolysis of Hag.

Therefore, *in vivo pulse chase* experiments were performed at elevated temperatures and during oxidative stress. Hag was completely stable at 50°C (Figure 38) and after addition of diamide, an oxidizing agent, which results in the formation of disulfide bonds (Figure 39). Hag was also not degraded during stationary phase (data not
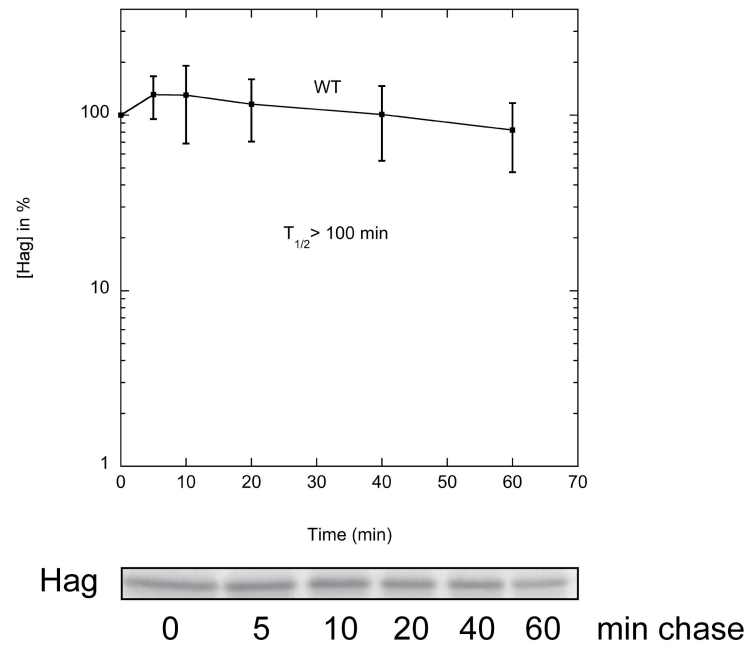
Figure 37: *In vivo pulse chase* analysis of Hag.
Wild type *B. subtilis* cells were grown to late exponential phase in Belitsky minimal medium at 37°C and pulse labelled with 25 μCi L-^{35}S-methionine for 10 minutes. Following a chase with non-labelled L-methionine, Hag was immunoprecipitated and visualized by SDS–PAGE and autoradiography. The data were quantified and normalized to the band intensity at time 0. The upper plot shows mean values from 6 independent experiments. Error bars indicate standard deviations. Hag protein appeared stable over a timecourse of 60 minutes.
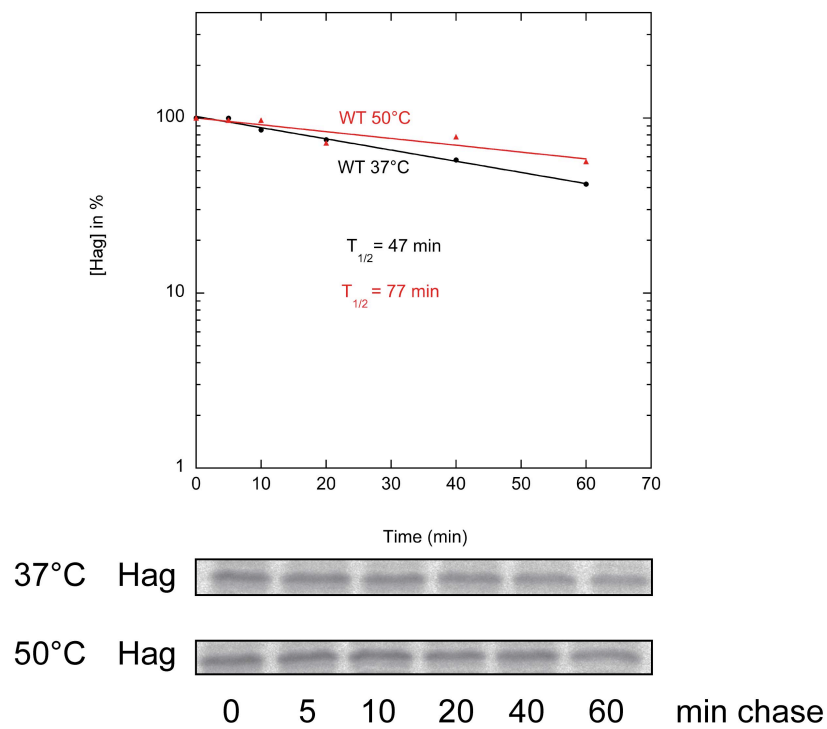
Figure 38: Hag *pulse chase* analysis under heat stress conditions.
Wild type *B. subtilis* cells were grown to late exponential phase in Belitsky minimal medium at 37°C, pulse labelled with 25 μCi L-^{35}S-methionine for 10 minutes at 37°C (upper, black circles) or 50°C (lower, red triangles) and treated as described above. Hag was stable both at 37 and 50°C.

shown).
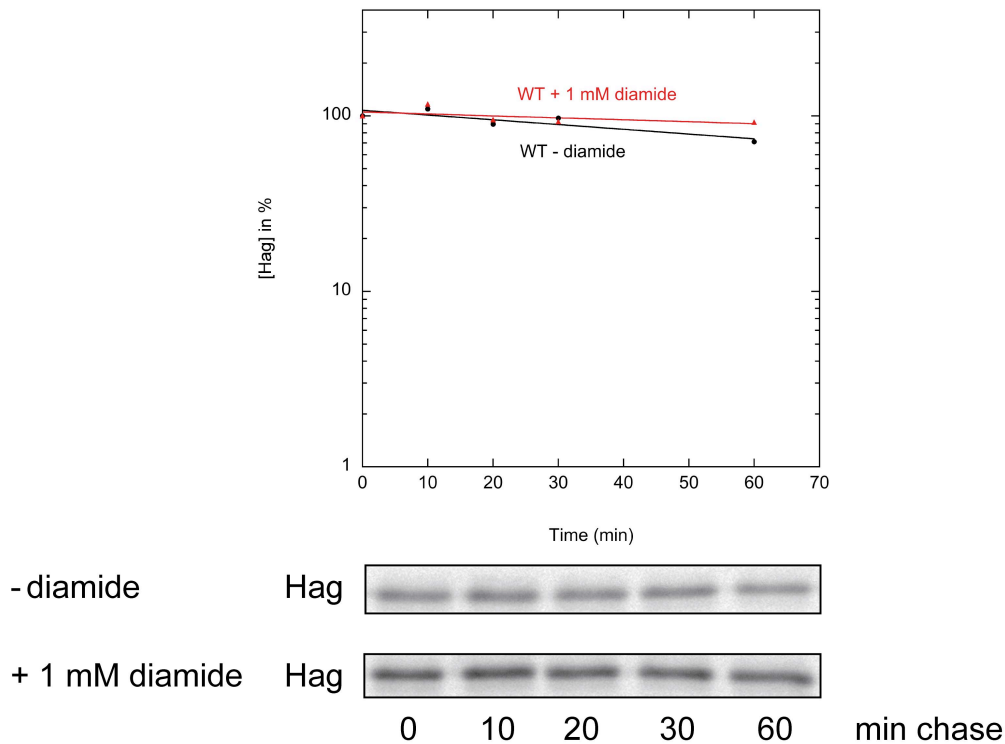
Figure 39: Hag *pulse chase* analysis during oxidative stress.
Wild type *B. subtilis* cells were grown to late exponential phase in Belitsky minimal medium at 37°C and pulse labelled with 25 μCi L-^{35}S–methionine for 10 minutes at 37°C (upper, black circles) in the presence (lower, red triangles) or absence (upper, black circles) of 1 mM diamide and treated as described above. Hag was stable during oxidative stress.

Effect of secretion chaperones on Hag degradation   Since stress was insufficient to induce Hag degradation *in vivo*, it was surmised that the degradation tag in this protein might be masked by the interaction with other factors. Two candidates for such an interaction were the export chaperone FliS and the FliS homolog FliW, which have both been shown to form a complex with Hag[11, 177, 223]. FliS and FliW were produced in *E. coli* and purified by affinity chromatography.

The interaction of both proteins with Hag was tested by analytical size exclusion chromatography (Figure 40). FliS eluted from the gel filtration column in two peaks for an unknown reason. However, in the presence of Hag, these peaks were clearly shifted to a smaller retention volume and FliS was detected in the high molecular peak by SDS–PAGE and Coomassie staining (Figure 40 A). FliW eluted in a single peak, which was
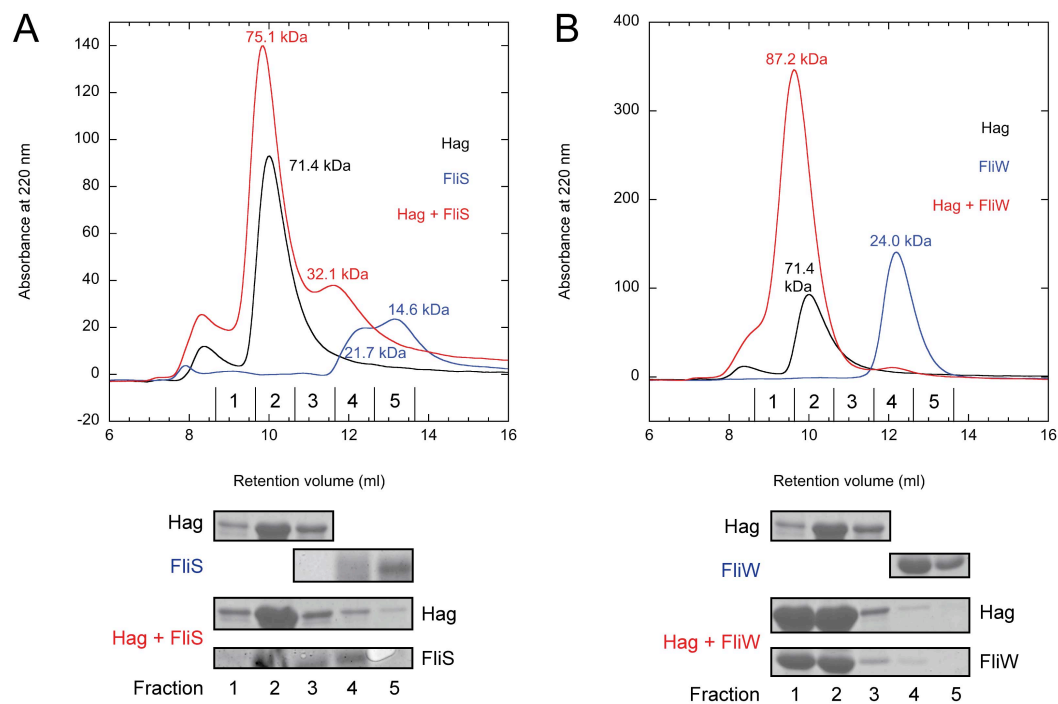
Figure 40: Analytical gel filtration of FliS-Hag and FliW-Hag complexes.
5 μM Hag was mixed with either 5 μM FliS (A) or 5 μM FliW (B) and pre-incubated for 15 minutes at room temperature. 100 μl of each sample was loaded onto a Superdex 75 10/300 GL gel filtration column and chromatography was performed as described in Materials and Methods. As a control, 5 μM Hag, FliS and FliW alone were loaded onto the column. Retention profiles were measured by UV absorbance at 220 nm. 1 ml fractions were collected from each run, acetone precipitated and analyzed by Tris-Glycine SDS–PAGE (15% v/v acryl amide). Hag formed a higher molecular weight complex with both FliS and FliW.

completely shifted to a higher molecular weight in the presence of Hag (Figure 40 B), indicating that the two proteins formed a stable complex.
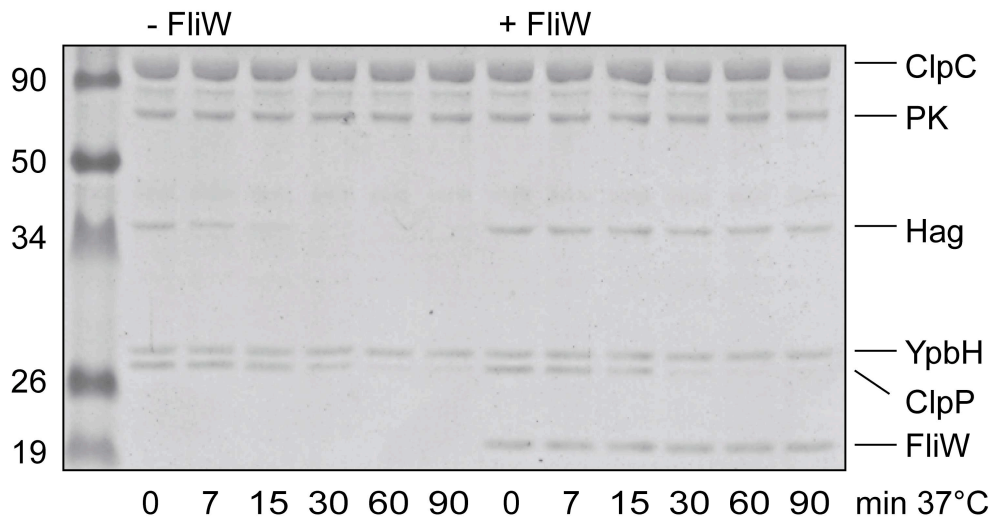
Figure 41: Hag proteolysis is inhibited by FliW *in vitro*.
1 μM Hag was preincubated for 15 minutes at room temperature with 1 μM FliW (right) or without FliW (left) and subsequently mixed with 1 μM ClpC, ClpP and YpbH for *in vitro* degradation at 37°C. Samples were analyzed by Tris-Tricine SDS–PAGE at the timepoints indicated. Hag proteolysis was strongly inhibited in the presence of FliW, whereas YpbH proteolysis was unaffected by FliW.

In order to investigate whether FliS and FliW affect Hag degradation by ClpCP-YpbH, *in vitro* degradation assays were performed. As shown in Figure 41, FliW premixed with Hag at a 1:1 ratio was sufficient to stabilize Hag over a timecourse of 1.5 hours. In contrast, even a 5–fold excess of FliS had no effect on Hag proteolysis (Figure 42 B). When both proteins were added to Hag, proteolysis was inhibited as with FliW alone (Figure 42 A).

To determine whether FliS and FliW are required for protection of Hag from proteolysis *in vivo*, markerless deletion mutants of *fliS* and *fliW* were constructed. In order to prevent polar effects on the adjacent genes *fliT* (for *fliS*) and *csrA* (for *fliW*), which are translationally coupled to *fliS* and *fliW*, the mutants were constructed in a way to preserve the *fliT* and *csrA* coding regions (see section 3.3.4).

The *fliS* mutant was non-motile, whereas the *fliW* mutant displayed normal swimming motility (Figure 43). Hag levels measured by Western blot in the *fliS* mutant were reduced to roughly 50% of the wild type (Figure 45). In contrast to previous
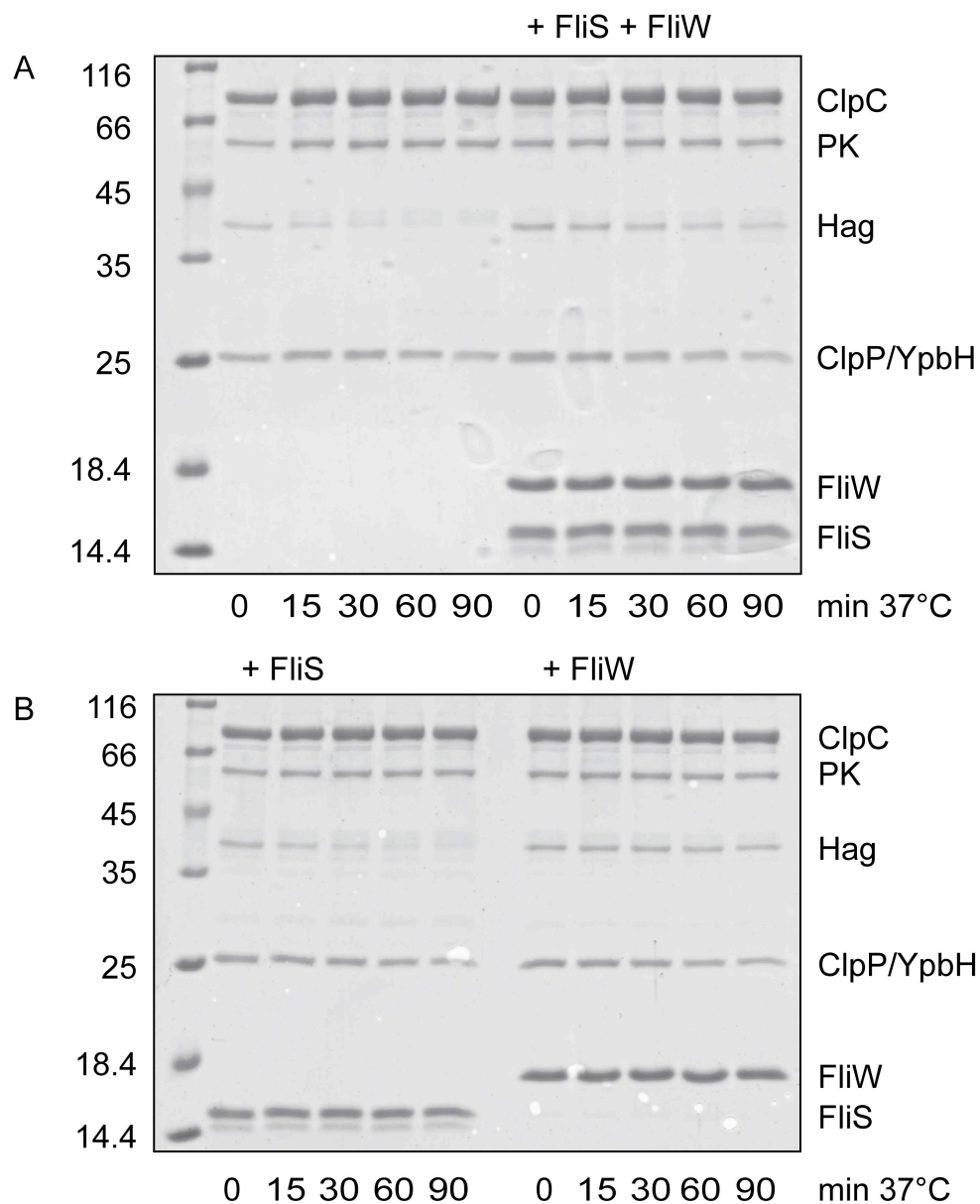
Figure 42: Hag proteolysis in the presence of FliS and FliW.
1 μM Hag was preincubated for 15 minutes at room temperature alone (A, left), with
5 μM FliS and 5 μM FliW (A, right), with 5 μM FliS (B, left) or with 5 μM FliW (B,
right) and subsequently mixed with 1 μM ClpC, ClpP and YpbH complex for *in vitro*
degradation at 37°C. Samples were removed at the times indicated and analyzed by
Tris-Glycine SDS–PAGE (15% v/v acryl amide). ClpP ran at exactly the same size as
YpbH under these electrophoresis conditions.
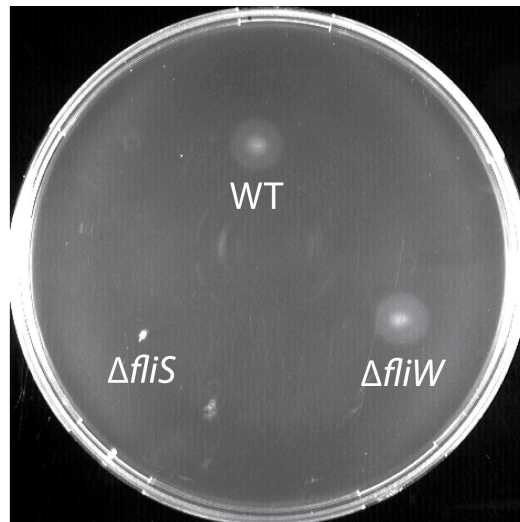
Figure 43: Swimming motility of *fliS* and *fliW* mutants.
Swim plates were inoculated with cultures of strains 168 (wild type), BNM403 (Δ*fliS*) and BNM404 (Δ*fliW*) and grown for 8 hours at 37°C. Wild type and Δ*fliW* mutant cells were motile, strain BNM403 (Δ*fliS*) was non-motile.

observations [177, 223], the *fliW* mutant exhibited the same amount of Hag as the wild type (Figure 44).
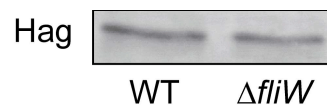
Figure 44: Hag levels in wild type and *fliW* mutant cells.
Strains 168 (wild type) and BNM404 (Δ*fliW*) were grown to OD_{600} 1.0 in LB, protoplasted and lysed. Lysates (2.5 μg total protein per lane) were separated on SDS–PAGE gels and Western blot with anti-Hag antiserum was performed. Hag levels were approximately equal in wild type and *fliW* mutant cells.

Interestingly, *pulse chase* analysis of the *fliS* and *fliW* mutant strains revealed that Hag is quickly degraded in the *fliS* mutant, but not in the *fliW* mutant (Figure 46). This result was unexpected because the *in vitro* data suggested that Hag is protected from proteolysis by FliW, but not by FliS, whereas the *in vivo* data are in accordance with protection of Hag by FliS.

ClpCP-YpbH dependence of Hag degradation *in vivo*   It was further investigated whether ClpCP and YpbH are responsible for Hag degradation in the *fliS* mutant. To this end, *fliS ypbH* and *fliS mecA* double mutants were constructed and *pulse chase*
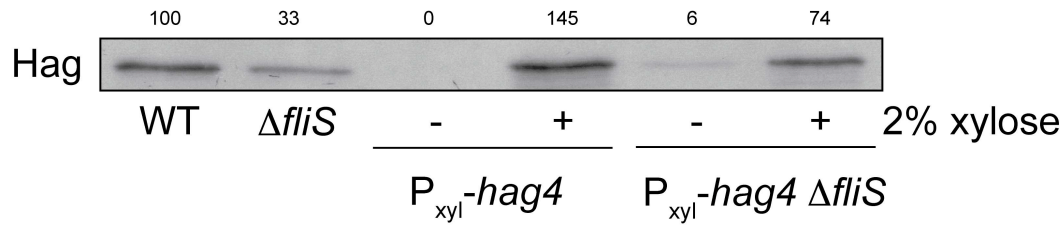
Figure 45: Hag levels in *fliS* mutants with xylose–inducible *hag*.
Strains 168 (wild type), BNM403 (Δ*fliS*), BNM426 (Δ*hag amyE::P_{xyl}-hag4*::cat) or BNM446 (Δ*hag amyE::P_{xyl}- hag4*::cat Δ*fliS*) were grown to OD_{600} 1.0 in LB or Belitsky medium as indicated, lysed and protoplasted. Samples of 2.5 μg total protein per lane were separated on SDS–PAGE gels and Western blot with anti-Hag antiserum was performed. Hag levels are 3–fold lower in *fliS* mutant cells compared to the wild type. Hag was slightly over–produced (1.5–fold) by xylose induction and Hag levels were still reduced 2–fold in the *fliS* mutant in this background.

analysis was performed with these strains. Hag appeared slightly stabilized both in the *ypbH* mutant and the *mecA* mutant (Figure 47). However, quantification of the data revealed more subtle differences between the three strains: Hag was indeed degraded slightly slower in the *ypbH* mutant (half–life 20 minutes compared to 17 minutes in the wild type, Figure 47).

In contrast, Hag was even degraded faster in the *mecA* mutant (half–life 13 minutes, Figure 47). Nevertheless, these data should be judged with caution, because the experimental error was relatively large. It can be concluded that *ypbH* exerts a small positive effect on Hag proteolysis, whereas *mecA* has a small negative effect.

Pulse chase experiments were also attempted with *fliS clpP*, *fliS clpC* and *fliS clpX* double mutants to directly show if Hag degradation in a *fliS* mutant background requires ClpCP or ClpXP. However, these experiments were technically very challenging for two reasons: first, due to amino acid auxotrophies, *clp* mutants grow poorly in minimal medium, which is required for labeling with ^{35}S-methionine. Second, both *clp* mutants and *fliS* mutants exhibit reduced Hag levels (see section 4.1), resulting in extremely weak signals.

To circumvent the auxotrophy problem, Belitsky medium with 0.01% yeast extract was used, which restored growth, but may have made labeling less efficient because yeast extract may contain unlabeled methionine. For better *hag* expression, strain BNM426 was used, in which the *hag* gene is placed under the control of a xylose–
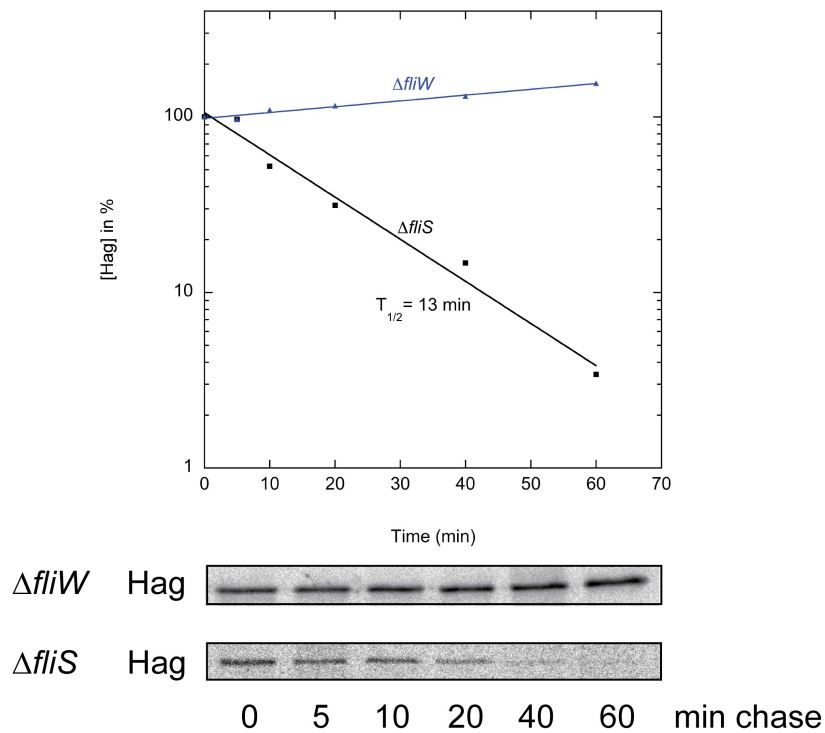
Figure 46: Hag is degraded in a *fliS* mutant.
Pulse chase analysis of strains BNM403 (Δ*fliS*, lower, black circles) and BNM404 (Δ*fliW*, upper, blue triangles). Hag was degraded with a half–life of 15-20 minutes in the *fliS* mutant, but was stable in the *fliW* mutant.
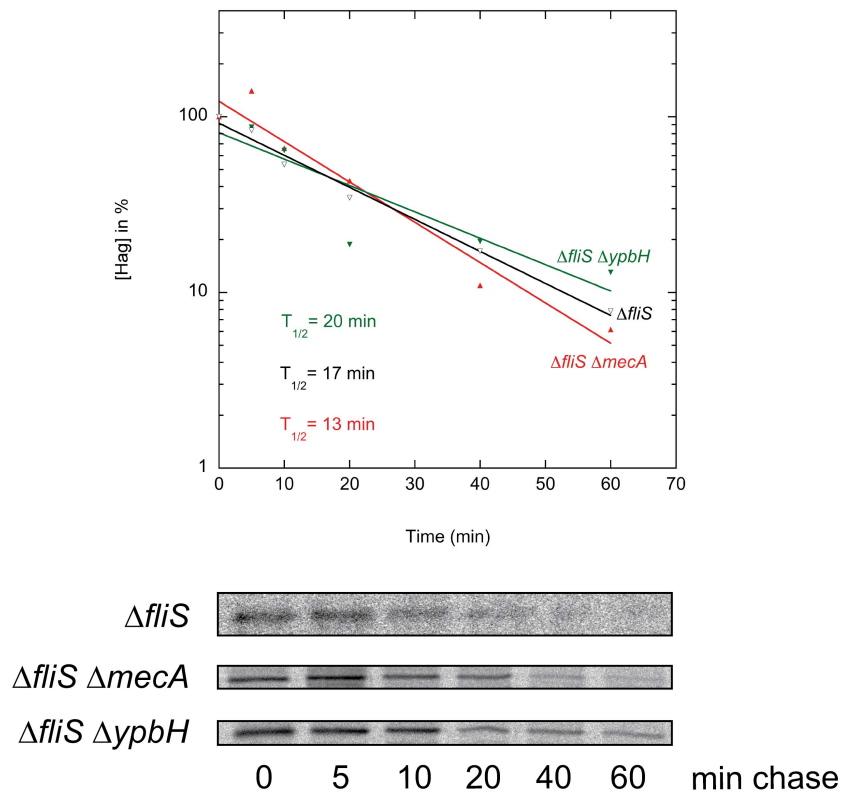
Figure 47: Hag proteolysis *in vivo* is independent of YpbH and MecA.
Pulse chase analysis of strains BNM403 ($\Delta fliS$, open black inverse triangles), BNM414
($\Delta fliS$ $\Delta mecA$, closed red triangles) and BNM415 ($\Delta fliS$ $\Delta ypbH$, closed green inverse
triangles). Hag was degraded in all three strains.

inducible promoter (described in section 4.1.3). Although *hag* expression is uncoupled from transcriptional control in this strain, the *clpP* and *clpX* mutations still result in lower Hag levels due to an unknown posttranscriptional effect (section 4.1.3). Hag was only slightly over–produced (150% of the wild type level, Figure 45) in BNM426 in the presence of 2% xylose. Strain BNM426 was first subjected to *pulse chase* analysis in the wild type background. As shown in Figure 48, Hag was stable under these conditions as expected.
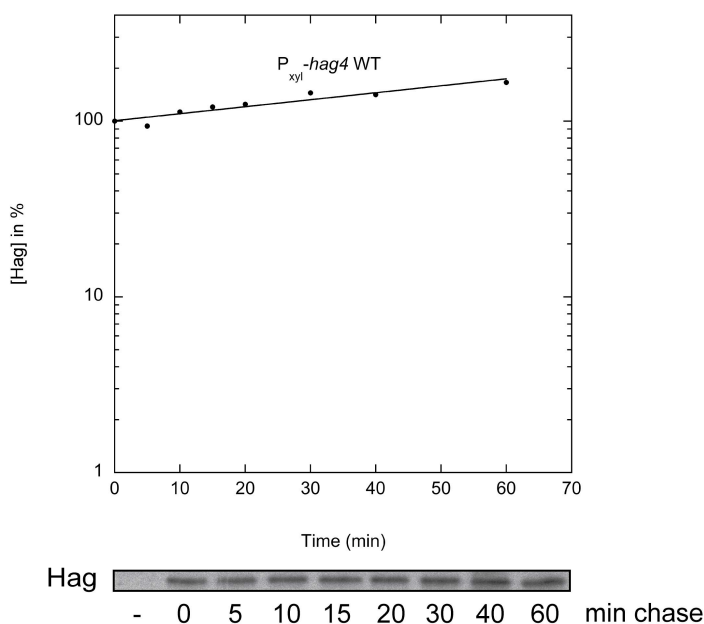
Figure 48: Hag *pulse chase* analysis with xylose–inducible *hag*.
Pulse chase analysis of strain BNM426 ($\Delta hag\ amyE$::P_{xyl}-*hag4*::cat). Cells were grown at 37°C in Belitsky Medium to OD_{600} 0.3-0.4. Expression of *hag* was induced by addition of 2% w/v xylose. Growth was continued for one hour and pulse labeling was performed as described above. Hag was stable in strain BNM426.

Next, a markerless *fliS* deletion was introduced into strain BNM426. Hag levels were still reduced to about 50% of the wild type level in this background (Figure 45). Mutations in *clpP*, *clpC* and *clpX* were introduced into this mutant and the resulting strains were tested for Hag stability by *pulse chase* analysis. As shown in Figure 49, Hag is degraded in the *fliS* mutant as well as in all *fliS clp* double mutants. Unfortunately, quantification of these data was unreliable due to weak signal intensities and large experimental errors, so that small effects on Hag stability could not be measured.

In order to assay Hag degradation by a second independent method, non–radioactive
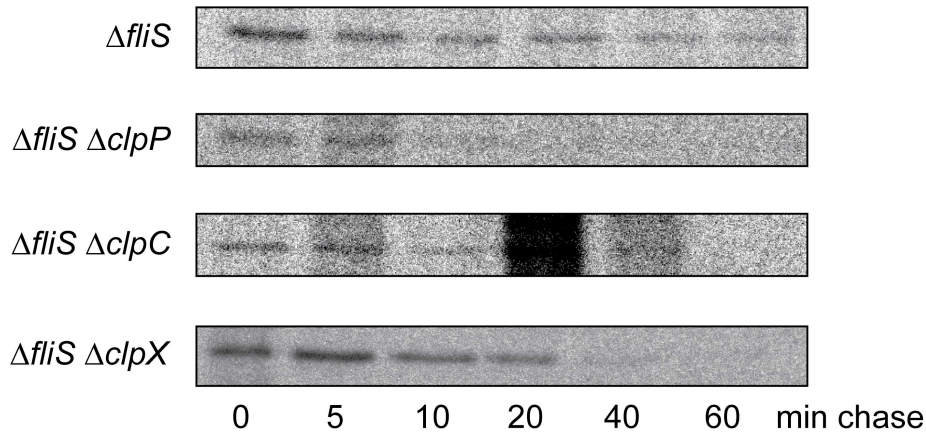
Figure 49: Hag degradation *in vivo* is independent of ClpCP and ClpXP.
Pulse chase analysis of strains BNM426 ($\Delta hag\ amyE$::P_{xyl}-*hag4*::cat), BNM427 (Δhag
$amyE$::P_{xyl}-*hag4*::cat $\Delta clpP$::spec), BNM428 ($\Delta hag\ amyE$::P_{xyl}-*hag4*::cat $\Delta clpC$::tet)
and BNM430 ($\Delta hag\ amyE$::P_{xyl}-*hag4*::cat $\Delta clpX$::kan). The cells were grown in Be-
litsky Medium containing 0.01 % w/v yeast extract to alleviate growth problems of the
clp mutants. Hag was degraded in all strains.

stability experiments were performed with the *fliS* and *fliS clpP* mutants in the xylose–
inducible *hag* background. To this end, bacteria were grown in LB in the presence of
xylose and tetracyline was added to inhibit protein synthesis. Samples removed at
different times after addition of the antibiotic were analyzed by Western blot against
Hag. As shown in Figure 50, Hag degradation appears slower under these conditions.
However, Hag proteolysis is clearly not blocked in the *clpP* mutant. Taken together,
the data strongly suggest that Hag is degraded predominantly by proteases distinct
from ClpP in the absence of FliS *in vivo*. In addition, a second general proteolysis
pathway of Hag may be relevant under yet undefined conditions. It is possible that
this degradation is mediated by ClpCP-YpbH, as suggested by the *in vitro* results
presented here.

Motility regulation and general proteolysis by ClpCP and ClpXP   In sum-
mary, the results presented here indicate that ClpCP regulates transcription from the
$P_{fla/che}$ promoter by degradation of the repressor DegU. In addition, ClpCP regulates
transcription from the P_{hag} promoter by proteolysis of ComK, which acts on σ^D activity
via FlgM. ClpCP does not affect any step downstream from *hag* transcription, as *hag*
expression from a xylose–inducible promoter was completely uncoupled of *clpC* control.

P_{xyl}-*hag4* Δ*fliS*

Hag

\- 0 5 10 15 20 30 40 60 min chase

P_{xyl}-*hag4* Δ*fliS* Δ*clpP*

Hag

\- 0 5 10 15 20 30 40 60 min chase
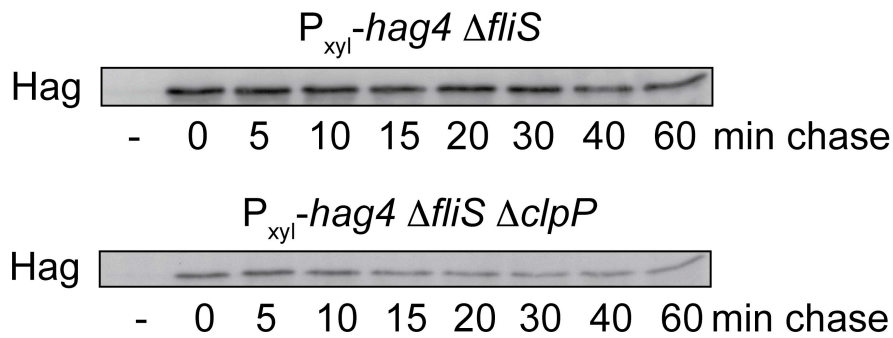
Figure 50: Non-radioactive Hag degradation assay in wild type and *clpP* mutant cells. Strains BNM426 (Δ*hag amyE*::P_{xyl}-*hag4*::cat) and BNM427 (Δ*hag amyE*::P_{xyl}-*hag4*::cat Δ*clpP*::spec) were grown in LB medium at 37°C to OD_{600} 0.3-0.4. Expression of *hag* was induced by addition of 2% w/v xylose and growth was continued for one hour. To inhibit protein synthesis, tetracycline was added to the cultures to a final concentration of 200 μg/ml. Hag degradation appeared slightly slower compared to the *pulse chase* experiments in minimal medium, but could be observed in wild type and *clpP* mutant cells.

ClpXP affects transcription from the $P_{fla/che}$ promoter by degradation of Spx, which acts as a negative regulator at this promoter by a yet undefined mechanism. ClpXP also influences either transcription from the P_{xyl} promoter or transcription elongation of the *hag* transcript. The observation that Hag interacts with ClpC and is targeted by the adaptor protein YpbH for degradation by ClpCP *in vitro* suggests that Hag might be a general proteolysis substrate of ClpCP *in vivo*. This could serve as a mechanism to prevent the aggregation or premature polymerization of Hag monomers in the cytosol.

Unexpectedly, Hag was found to be relatively stable *in vivo* under non–stress conditions as well as during heat and oxidative stress. However, evidence is presented here for rapid *in vivo* degradation of Hag in the absence of the export chaperone FliS, which is probably independent of ClpCP and YpbH. Therefore, the results presented here might suggest that Hag is degraded by two general proteolysis pathways. Whereas degradation in the absence of FliS might be mediated by an unknown protease, the observed *in vitro* degradation of Hag by ClpCP raises the possibility that ClpCP may be responsible for *in vivo* proteolysis of Hag by a second pathway under yet unknown conditions.

4.3   *In vivo* investigation of protein quality control

Clp proteases have a strong impact on protein quality control and thermal stress management in *B. subtilis*[127, 103, 128], suggesting that misfolded and aggregated proteins are degraded by these proteases. For ClpCP, this activity was directly demonstrated *in vitro*[209]. However, both ClpCP and ClpXP are involved in regulatory proteolysis (see section 4.1), which also influences stress response pathways.

For example, ClpXP degrades Spx, a transcriptional regulator of oxidative stress genes[179]. It could recently be demonstrated that Spx–dependent genes are induced during heat stress, suggesting that some of these target genes are required for thermal stress management and possibly protein quality control (A. Heinz & K. Turgay, unpublished data).

Likewise, ClpCP modulates the expression of class III heat shock genes by degradation of the transcriptional repressor CtsR[129, 114]. This process requires the adaptor protein McsB[114], which is also a protein arginine kinase[68]. To gain more insight in the significance of direct and regulatory effects of Clp proteases on protein quality control, thermotolerance experiments were performed in wild type and mutant *B. subtilis* cells.

4.3.1   Interplay of protein quality control and regulation

Thermotolerance is a priming process, in which cells exposed to a sublethal pre–heat shock survive a more severe heat shock better than cells directly shifted to the high temperature. In *E. coli*, protein disaggregation by ClpB, DnaK and small heat shock proteins is required for thermotolerance[238]. *B. subtilis* cells also exhibit thermotolerance[234], but the molecular mechansim of this process is unclear. Anja Heinz and Kürşad Turgay have recently analyzed various protease and chaperone mutants for their thermotolerance phenotypes (Anja Heinz, Master Thesis, unpublished).

Involvement of Spx in thermotolerance   According to their data, mutants in *dnaK* and *clpC* negatively affect thermotolerance development. In contrast, *clpX* and *clpP* mutants were equivalent to the wild type or even more thermotolerant and survived better than the wild type in the absence of a pre–heat shock (see also Figure 57 B). These results suggest that regulatory proteolysis of a stress regulator by ClpXP

might be more important than the direct effect of ClpXP on protein unfolding and aggregation during thermotolerance development. Based on the results presented above (see section 4.1), the proteolysis substrate Spx, a transcriptional regulator of the oxidative stress response, was an obvious candidate for such a regulator. Indeed, *spx* mutants were found to heat sensitive, also in combination with a *clpX* mutation (A. Heinz, unpublished).

Therefore, the effect of Spx on thermotolerance was tested. To this end, thermotolerance measurements were performed in wild type and *spx* mutant cells complemented with ectopically expressed Spx or Spx^{DD}(see section 4.1.2). The strains were grown at 37°C to mid–exponential phase and production of Spx or Spx^{DD} was induced for 15 minutes by addition of IPTG. Subsequently, the cultures were split and one half was incubated at 48°C for 15 minutes, while the other half was cultivated at 37°C. Next, all cultures were transferred to 53°C and aliquots were plated for determination of colony forming units (CFU).

As demonstrated in Figure 51 A, the *spx* mutation almost completely abolished thermotolerance. The *spx* phenotype was partially complemented by IPTG induction of either Spx or Spx^{DD} for 15 minutes before the pre–shock (Figure 51). The complementation effect was most apparent up to 30 minutes after the shift to 53°C (Figure 51). After 60 and 120 minutes at 53°C, survival rates dropped sharply. At the 60 minutes timepoint, the strain, in which Spx^{DD} was induced, still survived 10–fold better with preshock than without preshock, but 3 orders of magnitude worse than the wild type, whereas production of Spx induction had no effect at this timepoint (Figure 51). After 120 minutes, the survival rate of the Spx^{DD} strain decreased to the level of the culture without preshock. Furthermore, both the *spx* and the *spx^{DD}* expressing strain displayed a slight complementation effect without IPTG induction (Figure 51).

As a control experiment, wild type and *spx* mutant cells with and without complementation were incubated at 48°C for up to one hour and colony forming units (CFU) were determined. As shown in Figure 52, all strains survived as well as the wild type in the presence and absence of IPTG. These results demonstrate that the effect of Spx on thermotolerance (Figure 51) is not due to a survival defect during the 48°C pre–shock. The data presented here indicate that Spx is essential for thermotolerance development. Importantly, Spx is not sufficient for this process, because induction of Spx did not
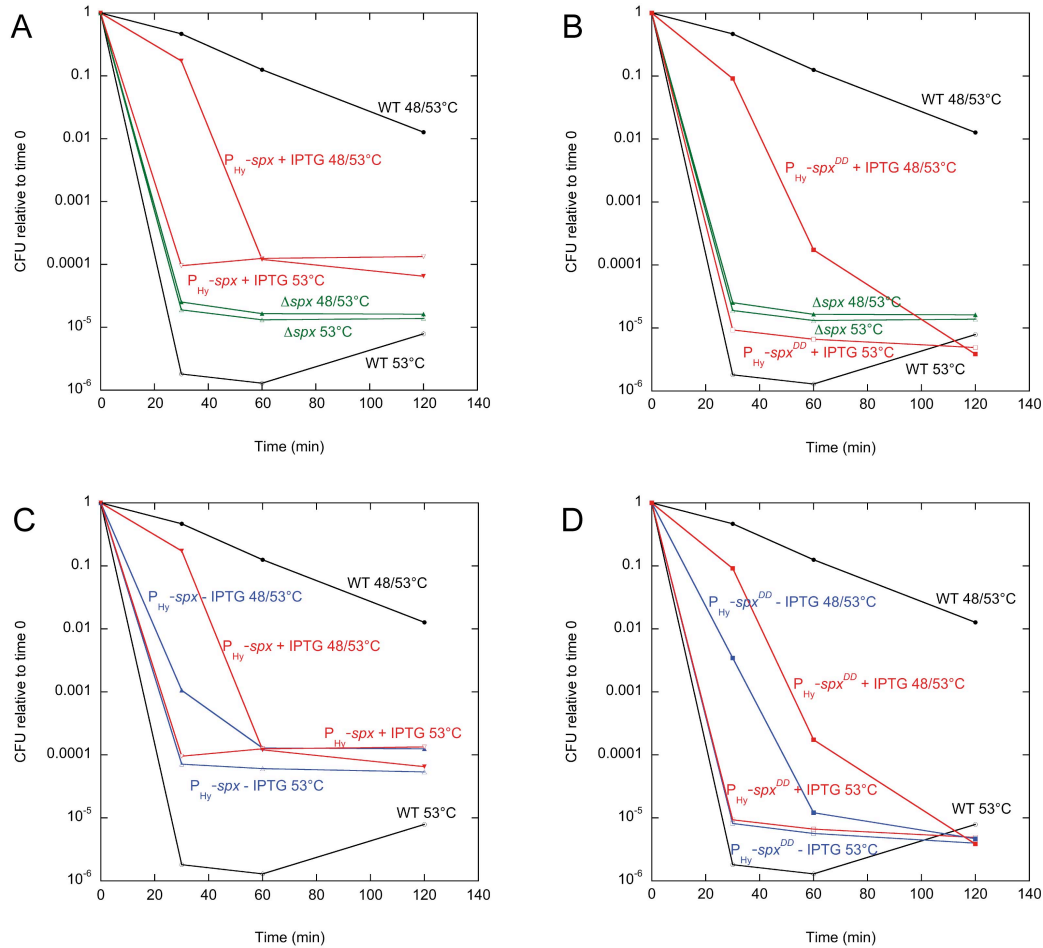
Figure 51: Spx is required for thermotolerance

Strains 168 (wild type, black circles), BNM111 (Δspx::kan, green triangles in A and B), BNM350 (Δspx::kan $amyE$::$P_{hyperspank(Hy)}$-spx::spec, red inverse triangles in A and C, blue triangles in C) and BNM351 (Δspx::kan $amyE$::$P_{hyperspank(Hy)}$-spx^{DD}::spec, red squares in B and D, blue squares in D) were grown in LB at 37°C to OD_{600} 0.4-0.6. Strains BNM350 and BNM351 were split into two 20 ml cultures and one half was induced with 1 mM IPTG for 15 minutes (C+D: red symbols + IPTG, blue symbols -IPTG). Subsequently, thermotolerance assays were performed (see Materials and Methods). Open symbols, no pre–shock; closed symbols: 15 minutes pre–shock at 48°C. The spx mutant was defective in thermotolerance. This phenotype was partially complemented by expression of spx or spx^{DD} from an IPTG–inducible promoter.
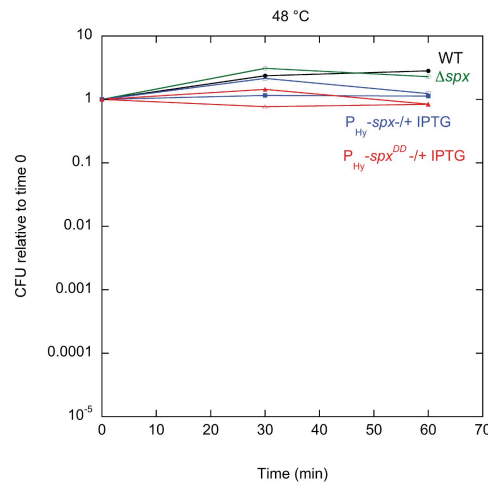
Figure 52: Spx does not influence growth at 48°C

Cultures of strains 168 (wild type, black circles), BNM111 (Δspx::kan, open green circles), BNM350 (Δspx::kan $amyE$::$P_{hyperspank(Hy)}$-spx::spec, blue squares) and BNM351 (Δspx::kan $amyE$::$P_{hyperspank(Hy)}$-spx^{DD}::spec, red triangles) were grown at 37°C to OD_{600} 0.4-0.6. BNM350 and BNM351 were split and one half was induced with 1 mM IPTG for 15 minutes (open symbols: -IPTG, closed symbols: +IPTG). The cultures were then transferred to 48°C and grown for one hour. Colony forming units were determined before the heat shock, 30 and 60 minutes thereafter. All strains grew equally well at 48°C.

substitute for a 48°C preshock (compare i.e. samples +/- IPTG without preshock; red and blue open symbols in Figure 51 D). Moreover, the natural heat induction of Spx (in the wild type strain) was much more efficient than artificial induction of the regulator.

The results shown above provide a possible explanation for the positive effect of $clpP$ and $clpX$ mutants on thermotolerance: as regulatory proteolysis of Spx is blocked in these mutants, cells prematurely activate the Spx–dependent stress response during normal growth, which could be advantageous during subsequent heat stress.

Interestingly, a different effect of $clpP$ and $clpX$ mutants was observed during growth at high temperatures (A. Heinz and N. Molière). These mutants displayed slow growth at 50°C and this phenotype was aggravated in the $dnaK$ $clpP$ and $dnaK$ $clpX$ double mutants, suggesting that ClpX and ClpP positively influence protein quality control under these conditions, probably by general proteolysis.

These observations imply that $clpP$ and $clpX$ mutants differentially affect thermotolerance and growth at high temperatures. The experimental conditions of both assays

are quite different: whereas cells are subjected to a temperature shift at relatively high density and followed for up to two hours in thermotolerance assays, bacteria encounter heat stress at low OD and for 8 to 10 hours during growth experiments. Furthermore, a heat shock at 53°C was applied during thermotolerance measurements, whereas growth curves were performed at up to 50°C. While *clpP* and *clpX* mutants appear to influence thermotolerance positively because Spx accumulates in these mutants (Figure 57 B), these mutants could negatively affect growth at high temperatures due to reduced general proteolysis of aggregates.
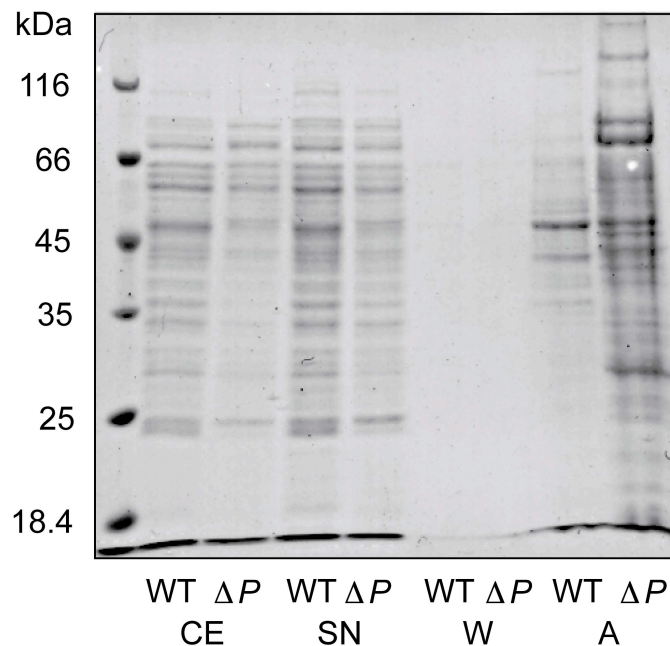
Figure 53: Protein aggregates in wild type and *clpP* mutant cells.
Strains 168 (wild type) and BNM103 (Δ*clpP*::spec) were grown to mid–exponential phase at 37°C and heat–shocked at 50°C for 30 minutes. Aggregates were prepared as described in Materials and Methods. CE: total cellular extract, SN: supernatent after centrifugation, W: wash, A: aggregate fraction. An increased amount of aggregated proteins was detected in the Δ*clpP* lysate compared to the wild type.

To verify whether ClpP is directly involved in aggregate removal as described previously [128], aggregated protein fractions were prepared from wild type and *clpP* mutant cells (see section 3.16) after a heat shock for 30 minutes at 50°C. As shown in Figure 53, more proteins were detected in the aggregate fraction of the *clpP* mutant compared to the wild type. These results suggest that ClpP is indeed involved in the removal of protein aggregates under certain conditions.

In summary, it can be proposed that ClpP is involved in heat stress management both by general proteolysis of aggregated proteins and by regulatory proteolysis of Spx. The importance of these pathways is apparently determined by the experimental conditions: during thermotolerance, regulatory proteolysis is more important, whereas during growth at high temperatures general proteolysis prevails.

Involvement of McsB and YwlE in thermotolerance   The protein arginine kinase McsB and the phosphatase YwlE are involved in the regulation of the class III heat shock genes[114, 129]. McsB also acts as an adaptor protein for ClpC, which targets CtsR for degradation[116]. Furthermore, *mcsB* is itself a class III heat shock gene. Thus, the effect of *mscB* and *ywlE* mutants on thermotolerance of *mscB* and *ywlE* mutant cells was examined.
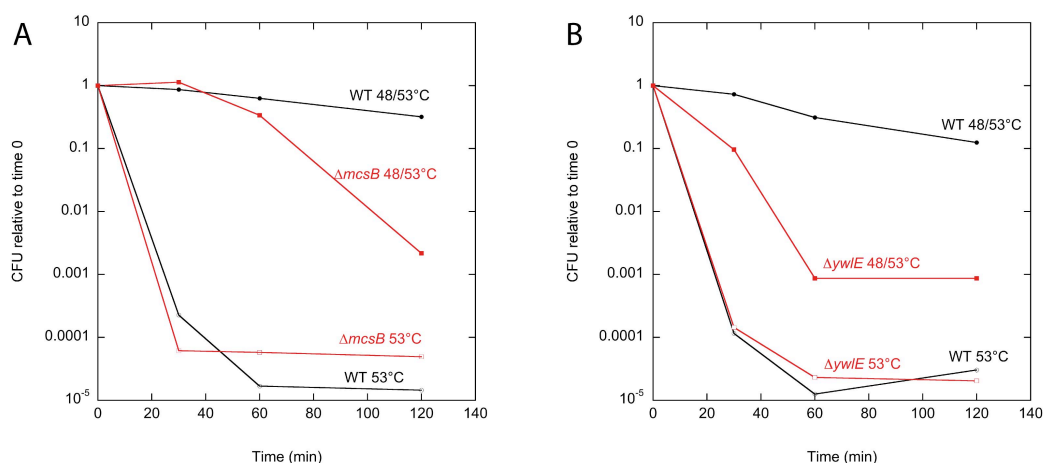
Figure 54: Both McsB and YwlE are involved in thermotolerance. Thermotolerance assays were performed as described with strains 168 (wild type, black circles), BNM117 (*mcsB*::kan, red squares in A) and BAE048 (*ywlE*::kan, red squares in B). Open symbols: no pre–shock; closed symbols: 15 minutes pre–shock at 48°C. Both mutants displayed reduced thermotolerance.

As demonstrated in Figure 54, both mutants displayed a reduction in survival rates at 53°C following a 48°C pre–shock, but colony forming units (CFU) were unchanged without the pre–shock. The effect of the *mcsB* mutant was moderate (Figure 54 A), whereas the *ywlE* mutant displayed a strong thermotolerance phenotype (Figure 54 B).

These results imply that McsB and YwlE are involved in thermotolerance development,

although the mechansim of this effect awaits further characterization. It can be concluded that regulatory effects by Spx and by the kinase/phosphatase pair McsB/YwlE play an important part in thermotolerance development. Furthermore, thermotolerance appears to be more complex than previously anticipated, justifying a more detailed analysis of this process.

4.3.2   Involvement of *gsiB* and inositol catabolic genes in thermotolerance

Recently, microarray experiments were performed under thermotolerance conditions to distinguish between genes, which are activated during the 48°C pre-heat shock, at 53°C or at 53°C following the pre–shock (A. Heinz & K. Turgay, unpublished). Among the genes, which were upregulated at 48°C compared to 37°C and were further upregulated during incubation at 53°C after the pre–shock, were *gsiB* and the *iol* operon comprising *mmsA-iolBCDEFGHIJ*.

Involvement of *gsiB* in thermotolerance   *gsiB* is a σ^B–dependent gene of unknown function. The amino acid sequence of GsiB features 5 repeats of almost identical primary sequence separated by putative glycine–rich linkers. In addition, GsiB has been implicated in salt tolerance, suggesting that the protein may have a stress tolerance related function[105].

As shown in Figure 55, the *gsiB* mutant displayed reduced survival at 53°C following a pre-heat shock compared to the wild type. These data suggest that the *gsiB* mutant exhibits a moderate thermotolerance defect. However, the *gsiB* mutant displayed a growth phenotype on agar plates. Therefore, more experiments are required to show that the thermotolerance effect of the mutant is not a result of this growth defect.

Inositol as a putative chemical chaperone in thermotolerance   The *iol* genes are involved in inositol catabolism. *Myo*-inositol can be taken up from the growth medium and utilized as a carbon source[246]. Interestingly, *scyllo*-inositol, a stereo isomer of *myo*-inositol, which can also be catabolized by *B. subtilis*[171], has been implicated as a chemical chaperone that inhibits the formation of amyloid fibers *in vitro*[158]. The *iol* operon is controlled by the transcriptional repressor IolR.

Because the *iol* genes are strongly induced under thermotolerance conditions (A. Heinz,
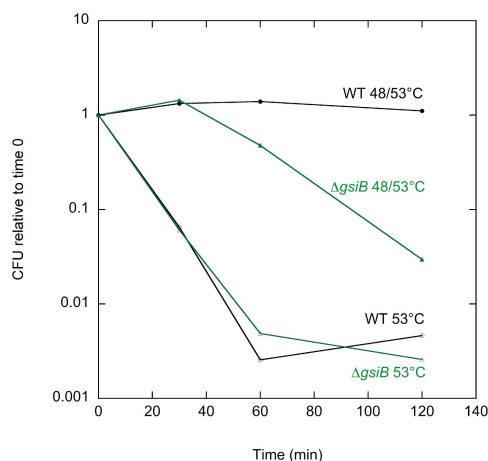
Figure 55: Thermotolerance of wild type and *gsiB* mutant cells.
Strains 168 (wild type, black circles) and BNM243 ($\Delta gsiB$::kan, green triangles) were tested for thermotolerance as described. Open symbols: no pre–shock; closed symbols: 15 minutes pre–shock at 48°C. The *gsiB* mutant displayed reduced thermotolerance.

unpublished), it was investigated whether inositol plays a role as a chemical chaperone during thermotolerance. To this end, thermotolerance assays were performed with mutants, in which either the *iol* promoter (ΔP_{iol}) or the repressor IolR was removed ($\Delta iolR$). The ΔP_{iol} strain is unable to metabolize inositol, whereas the inositol catabolic enzymes are over–produced in $\Delta iolR$. In addition, mutants in *iolX* and *iolW*, encoding two *scyllo*-inositol dehydrogenases that are responsible for interconversion between *scyllo*-inositol and *scyllo*-inosose, a reaction intermediate of the *myo*-inositol catabolic pathway[171], were examined for their thermotolerance phenotype.

As depicted in Figure 56 A, thermotolerance of the wild type strain was slightly enhanced in the presence of 25 mM inositol. However, this effect was not observed in all experiments (see Figure 56 D).

Surprisingly, the *iolR* mutant displayed reduced thermotolerance in the absence of inositol (Figure 56 A) and did not grow in the presence of 25 mM *myo*-inositol (data not shown). The ΔP_{iol} mutant did not influence thermotolerance both with and without inositol in the growth medium (Figure 56 B+C). Furthermore, the *iolX* and *iolW* mutants did not display any thermotolerance phenotype (Figure 56 C+D).

The small effect of *myo*-inositol on thermotolerance might suggest that this compound might act as a chemical chaperone during thermotolerance, although it was not reproduced in all experiments. However, conversion of *myo*-inositol into *scyllo*-inositol or
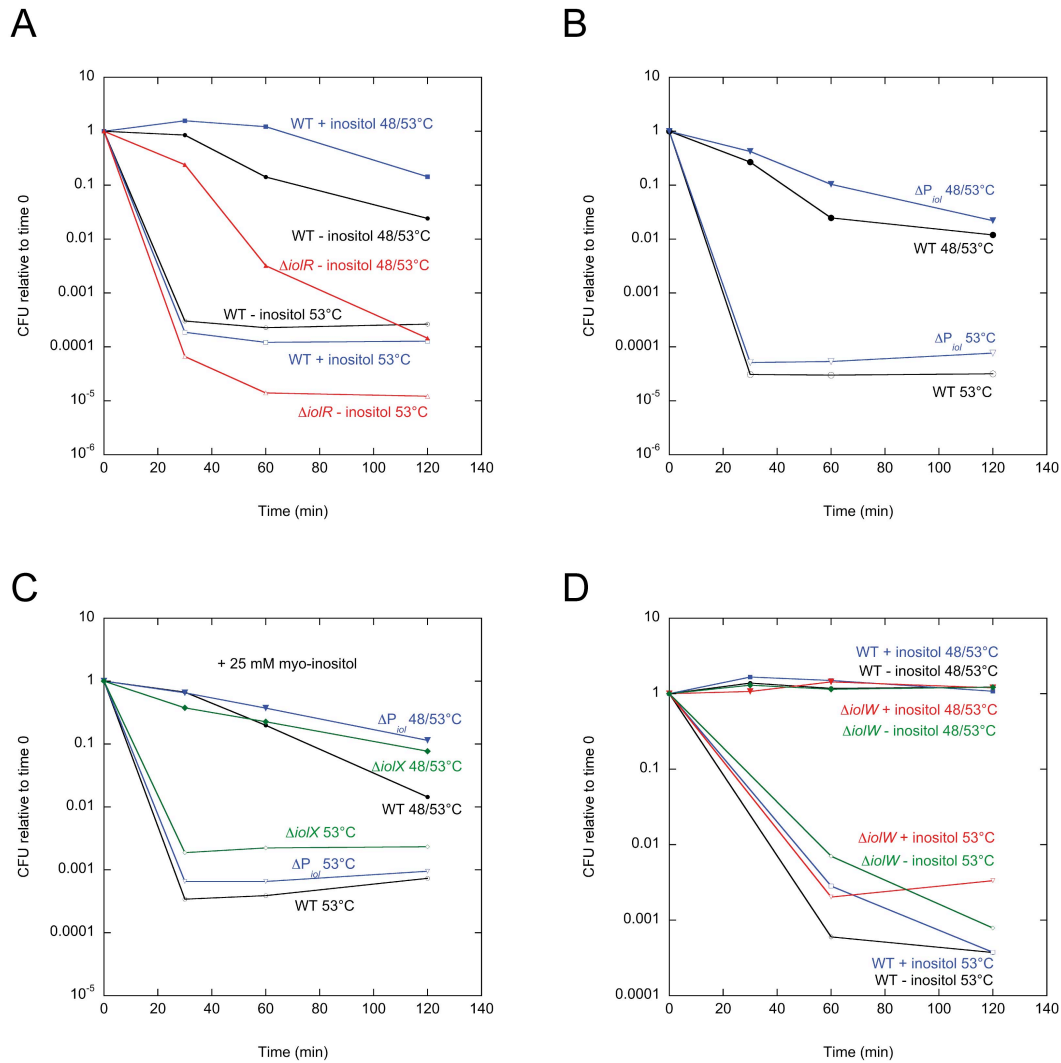
Figure 56: Thermotolerance of wild type and *iol* mutant cells.
Strains 168 (wild type, black circles or blue squares in A and D), BNM239 ($\Delta iolR$, red triangles), BNM240 (ΔP_{iol}, blue inverse triangles), BNM241 ($\Delta iolX$, green diamonds in C) and BNM242 ($\Delta iolW$, green diamonds in D) were tested for thermotolerance in LB medium or LB + 25 mM *myo*-inositol as indicated. The $\Delta iolR$ mutant was defective in thermotolerance in the absence of *myo*-inositol (A). The ΔP_{iol} mutant had no influence on thermotolerance (B, C). $\Delta iolX$ and $\Delta iolW$ did also not affect thermotolerance development (C, D).

other compounds does not seem to be important, because the absence of the inositol catabolic pathway (in the ΔP_{iol} mutant) had no effect. The growth and thermotolerance defects of the *iolR* mutant imply that high levels of inositol catabolic enzymes are detrimental to cell growth and survival during thermotolerance.

4.3.3   Possible ClpP–independent function of ClpC in thermotolerance

Thermotolerance in *E. coli*, yeast and plants requires the Clp/Hsp100 ATPase ClpB or its homolog Hsp104[204, 138, 208, 238]. ClpB is a special Hsp100 protein that lacks the residues responsible for interaction with ClpP and is able to disaggregate and refold protein aggregates aided by DnaK/Hsp70 and small heat shock proteins[238, 84, 83]. Interestingly, both ClpB and small heat shock proteins are not encoded in the *B. subtilis* genome. In contrast, ClpC exhibits protein disaggregase activity *in vitro*[209], suggesting that ClpC could substitute for the function of ClpB in *B. subtilis*.
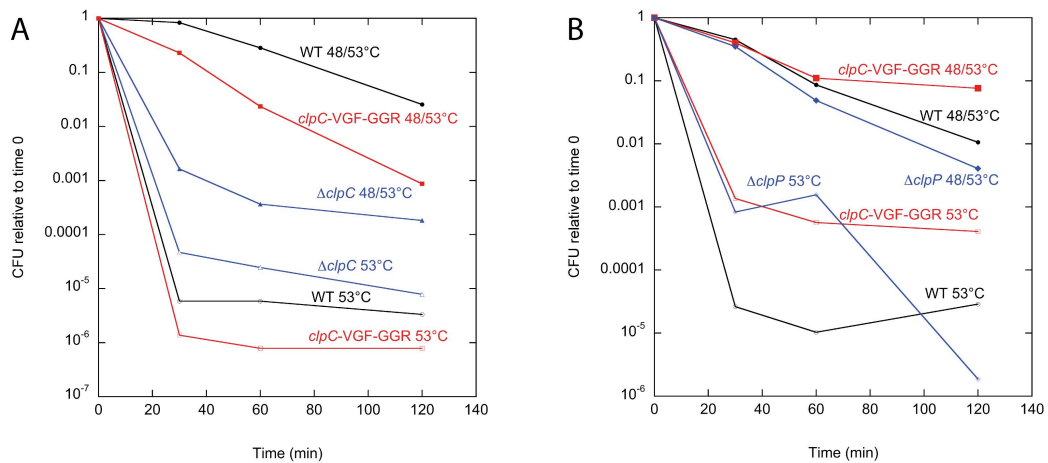
Figure 57: ClpC allows thermotolerance independent of ClpP.
Thermotolerance experiment performed with strains 168 (wild type, black circles), BNM103 ($\Delta clpP$::spec, blue diamonds in B), BNM105 ($\Delta clpC$::tet, blue triangles in A) and BNM245 (*clpC*(VGF::GGR), red squares). Open symbols: no preshock; closed symbols: 15 minutes pre–shock at 48°C. Strain BNM245 was more thermotolerant than the *clpC* mutant (A). The *clpP* mutant survived as well as the wild type after a preshock and even better than the wild type without preshock (B).

To directly test whether ClpC can facilitate thermotolerance by disaggregation in the absence of ClpP, a mutant was constructed, in which the peptide loop in ClpC that is responsible for ClpP binding is mutated in the native chromosomal *clpC* locus. This strain (BNM245, VGF loop mutant) was assayed for thermotolerance.

As displayed in Figure 57 A, the VGF loop mutant was only slightly less thermotolerant than the wild type, whereas the *clpC* deletion mutant exhibited a strong thermotolerance defect. As previously observed, a *clpP* mutant displayed no thermotolerance phenotype (Figure 57 B). These results suggest that ClpC might exert a ClpP independent chaperone function *in vivo* during thermotolerance. However, it should be considered that the VGF loop mutant affects regulatory proteolysis mediated by ClpCP and adaptor proteins, which might influence thermotolerance development.

Heat sensitivity of a *dnaK clpC* double mutant   In *E. coli*, ClpB cooperates with DnaK in protein disaggregation during thermotolerance. To elucidate whether ClpC might cooperate with DnaK in *B. subtilis*, a *dnaK clpC* double mutant was constructed (A. Heinz & N. Molière, unpublished) and growth curves were measured at different temperatures.

As shown in Figure 58, at 47-49°C growth temperature, the *dnaK* single mutant had only a minor effect on growth. At 50°C, this mutant displayed slightly delayed growth compared to the wild type, suggesting that the cells are only slightly more heat sensitive in the absence of DnaK, as observed previously[213]. In contrast, the *clpC* mutant grew markedly slower than the wild type at 49°C and was unable to grow at 50°C, confirming earlier reports that ClpC is very important during heat stress[127].

The *dnaK clpC* double mutant, however, grew significantly slower than both single mutants at 47-49°C (Figure 58 B and C). These data corroborate that DnaK and ClpC are both important for growth during heat stress and suggest that the removal of both components strongly reduces the capacity of the protein quality network to cope with heat stress. Whether DnaK and ClpC actually cooperate during the stress response and whether the function of ClpC in thermal stress management is degradation or disaggregation cannot be answered by the studies performed here.

In summary, the results of this section suggest that both degradation and disaggregation contribute to protein quality control in *B. subtilis*. To further investigate the mechanism of aggregate removal at the single cell level, GFP–tagged marker proteins were developed as described in the following section.
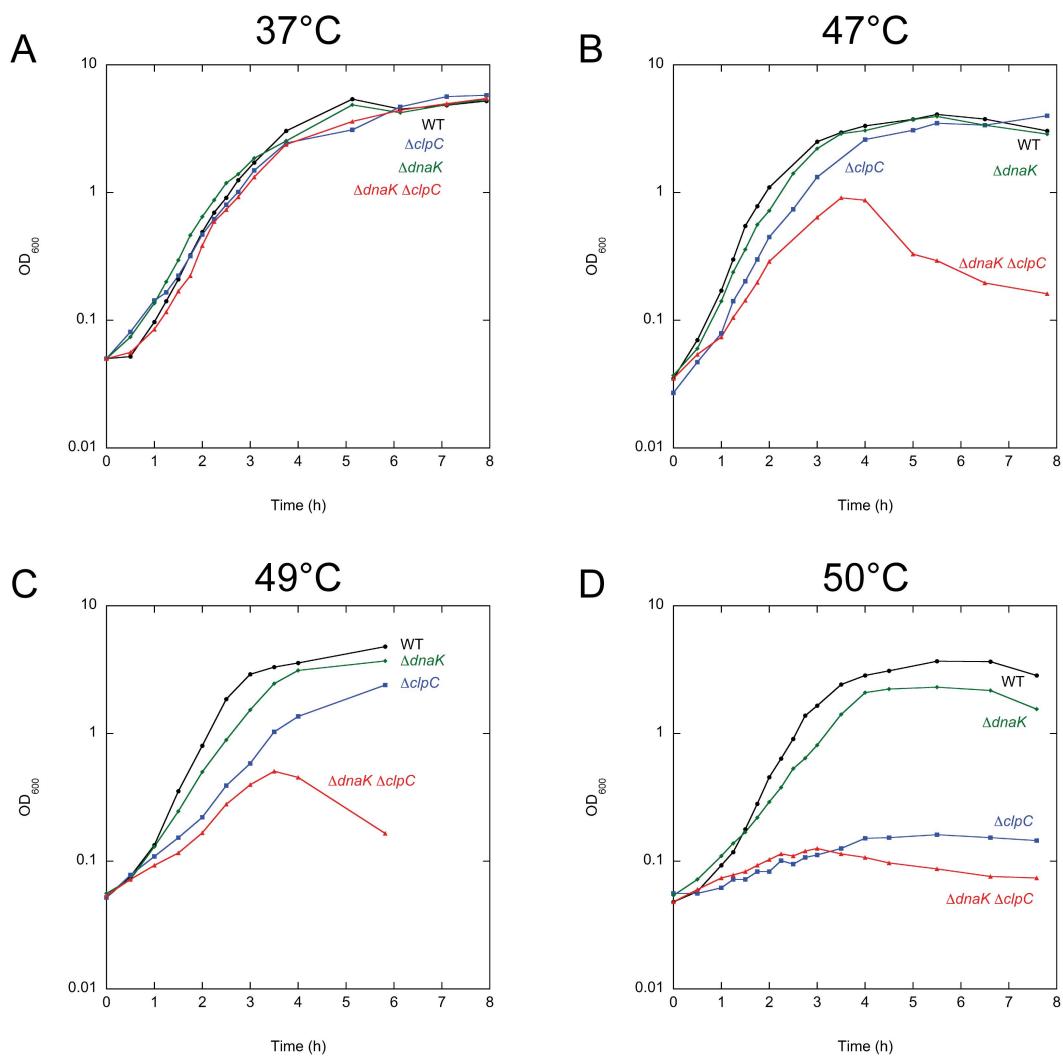
Figure 58: Growth of *dnaK clpC* double mutant cells at high temperature.
Strains 168 (wild type, black circles), BNM105 ($\Delta clpC$::tet, blue squares), BNM118
($\Delta dnaK$::cat, green diamonds) and BNM253 ($\Delta dnaK$::cat $\Delta clpC$::tet, red triangles)
were grown in LB medium at 37°C (A), 47°C (B), 49°C (C) and 50°C (D). The *dnaK*
clpC double mutant was more thermosensitive than the *dnaK* and *clpC* single mutants
(B, C).

4.3.4   Development of *in vivo* markers of protein aggregation

The effect of Clp proteases on protein aggregates has only been studied using over–produced heterologous model proteins, such as PorA[103] or aggregation–prone peptides produced by puromycyl treatment[128]. To study aggregates from intrinsic *B. subtilis* proteins, three types of GFP–tagged marker proteins were designed and tested. In one construct, *B. subtilis* DnaK was tagged with GFP to serve as a marker protein for aggregates. The small heat shock proteins IbpA and IbpB from *E. coli* were also GFP–tagged and used as external aggregate binding markers, which do not naturally occur in *B. subtilis*. As an endogenous aggregation–prone protein from *B. subtilis*, malate dehydrogenase (MDH) was chosen. Eukaryotic MDH is a heat–sensitive protein that has been used as a model protein for *in vitro* aggregation studies and is degraded by ClpCP[209]. Furthermore, MDH interacted with ClpC in co–immunoprecipitation experiments (Janine Kirstein, unpublished).

DnaK–GFP   DnaK–GFP was expressed from a xylose–inducible promoter in a *dnaK* mutant background in order to preserve the *dnaK* operon, which contains the co-chaperone genes *dnaJ* and *grpE*. Cells were grown to mid–exponential phase in the presence of inducer and observed by fluorescence microscopy before and after heat shock at 50°C. As shown in Figure 59, DnaK–GFP localized in foci and patches already at 30°C. After the heat shock, the localization pattern did not change significantly. The localization pattern of DnaK is similar, but slightly distinct from that observed for ClpP–GFP, ClpC–GFP and ClpX–GFP[118]. DnaK–GFP foci appear to be more heterogeneous in size and shape and are not restricted to polar and mid–cell locations, but occur along the whole length of the cell.

The fact that the intensity of DnaK foci did not change after heat shock is not suprising considering that the gene fusion was expressed from an artificial promoter, which is not upregulated by heat stress. Nevertheless, the patchy localization of the DnaK–GFP before the heat shock suggests that DnaK either binds to aggregates that are already present at ambient temperatures or that the chaperone is part of a pre–formed higher order structure, to which aggregated proteins might be targeted.
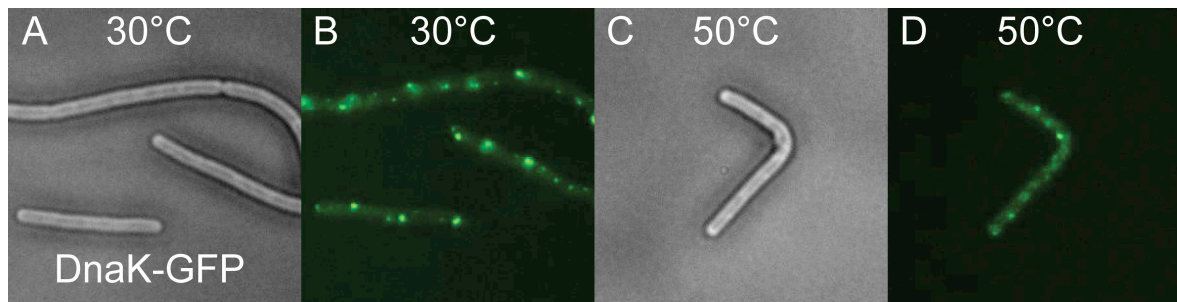
Figure 59: Localization of DnaK–GFP.
Strain BNM227 ($\Delta dnaK$::cat $amyE$::P_{xyl}-$dnaK$-gfp::spec) was grown in LB medium with 2% w/v xylose at 30°C to OD_{600} 0.4-0.6 and heat shocked for 10 minutes at 50°C. Samples were analyzed by phase contrast and fluorescence microscopy before (A and B) and after heat shock (C and D). Xylose-induced DnaK–GFP formed several foci per cell at 30°C, which did not change in size or number after heat shock.
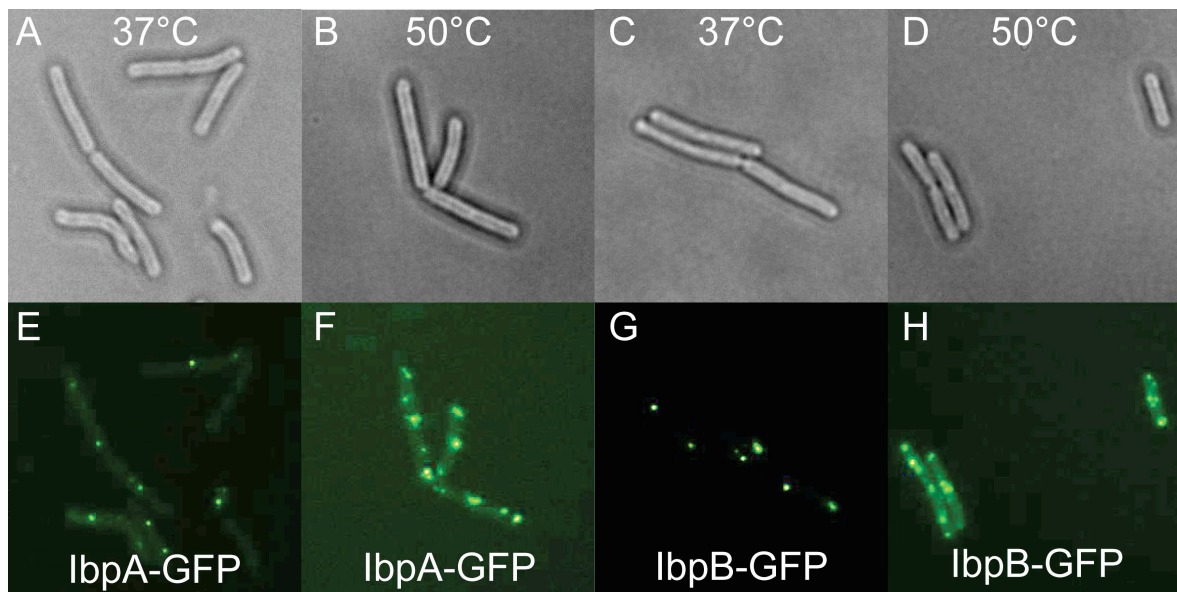
Figure 60: Localization of IbpA–GFP and IbpB–GFP.
Strains BNM216 ($amyE$::P_{xyl}-$ibpA$-gfp::spec, A, B, E, F) and BNM217 ($amyE$::P_{xyl}-$ibpB$-gfp::spec, C, D, G, H) were grown in LB with 2% w/v xylose at at 37°C to OD_{600} 0.4-0.6 and heat shocked for 10 minutes at 50°C. Samples were analyzed by phase contrast and fluorescence microscopy before (A, E, C, G) and after heat shock (B, F, D, H). Both IbpA–GFP and IbpB–GFP formed foci at the cell poles and at mid–cell before heat shock. After heat shock, the number and size of the foci increased.

Small heat shock proteins fused to GFP   The small heat shock proteins IbpA and IbpB bind to protein aggregates and contribute to protein disaggregation together with ClpB and DnaK in *E. coli*[168]. IbpA and IbpB were successfully applied as aggregate markers previously[145]. The *ibpA* and *ibpB* genes were expressed from a xylose–inducible promoter in the ectopic *amyE* locus as C–terminal GFP fusions. Cells grown in the presence of xylose were heat shocked at 50°C in exponential phase and observed by fluorescence microscopy before and after the heat shock. Both GFP fusions were localized in predominantly polar foci at 37°C (Figure 60 E and G). IbpA–GFP foci have previously been observed in non–stressed bacteria[145] and were interpreted as protein aggregates. These aggregates could result from small amounts of unfolded proteins, which are present under non–stress conditions and had escaped detection by less sensitive methods, such as phase contrast microscopy.

In contrast to the DnaK–GFP fusion, both size and number of these foci increased after heat shock (Figure 60 F and H), suggesting that the small heat shock proteins bound to additional protein aggregates formed in response to the heat stress. The IbpA–GFP and IbpB–GFP fusions have been characterized in detail by Etienne Maisonneuve and Kürşad Turgay (unpublished work) and were also successfully applied as aggregate markers during thermotolerance experiments (Anja Heinz, Master thesis, and Stephanie Runde, unpublished).

MDH–GFP   *B. subtilis* MDH gene was C–terminally fused to GFP and the gene fusion was inserted into the genome as a Campbell integration under the control of its natural promoter. During the exponential phase in LB medium at 37°C MDH–GFP displayed a weak but homogeneously distributed fluorescence signal (Figure 61 F). After heat shock at 50°C some MDH–GFP localized to polar foci, whereas the majority of the fusion protein remained homogeneously localized (Figure 61 G). Following a more severe heat shock at 53°C, several MDH–GFP patches of different sizes and shapes became visible (Figure 61 H), suggesting that MDH–GFP aggregates under these conditions. These patches were even visible as dark structures in phase contrast microscopy (Figure 61 C). Interestingly, a stronger MDH–GFP fluorescence signal was observed in Belitsky minimal medium at 37°C (Figure 61 I) and foci were much more clearly visible already after heat shock at 50°C (Figure 61 J).

Since GFP alone does not form foci after heat shock (Stephanie Runde, unpublished results), the MDH–GFP foci observed in the fluorescence microscopy experiments can be interpreted as MDH aggregates. However, the fact that MDH–GFP is only partially localized in these aggregates suggests that *B. subtilis* MDH is more heat stable than anticipated. To test MDH heat sensitivity directly, a His–tagged variant of MDH was produced in *E. coli* and purified. To determine MDH activity *in vitro*, the rate of oxalo acetate reduction to malate was measured by monitoring the decrease of NADH fluorescence at 455 nm during oxidation to NAD^+.
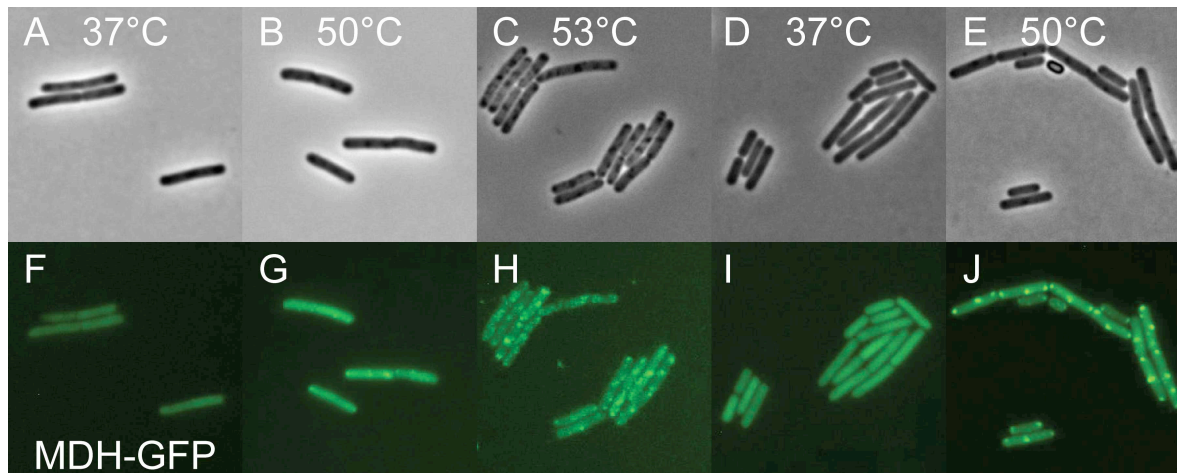
Figure 61: Localization of MDH–GFP

Strain BNM224 (*mdh-gfp*::cat) was grown in LB or Belitsky Medium to OD_{600} 0.4-0.6 at 37°C and heat–shocked for 10 minutes at 50°C or 53°C. Samples were analyzed by phase contrast and fluorescence microscopy before and after heat shock. MDH–GFP was homogeneously localized prior to heat shock (F, I). A heat shock at 50°C resulted in a mixture of foci at polar and mid–cell location and cytoplasmic localization (G), with brighter foci in cells grown in Belitsky Medium than in LB (J). At 53°C, MDH–GFP formed brighter foci of more heterogeneous size and shape all along the cell (H). These foci co-localized with phase-dark structures visible by phase contrast microscopy (C).

At room temperature, the enzyme activity *B. subtilis* MDH was similar to that of pig MDH (Figure 62). In order to heat inactivate *B. subtilis* MDH, the enzyme was incubated for 30 minutes at different temperatures at a concentration of 2 µM. As demonstrated in Figure 62 B, *B. subtilis* MDH was still about 80% active after incubation at 47°C, a temperature commonly used to inactivate pig MDH[209]. Even at 53°C, which is more than the maximum temperature at which *B. subtilis* 168 can grow, MDH was still about 40% active. Complete inactivation of the enzyme was only

achieved at 55°C (Figure 62).
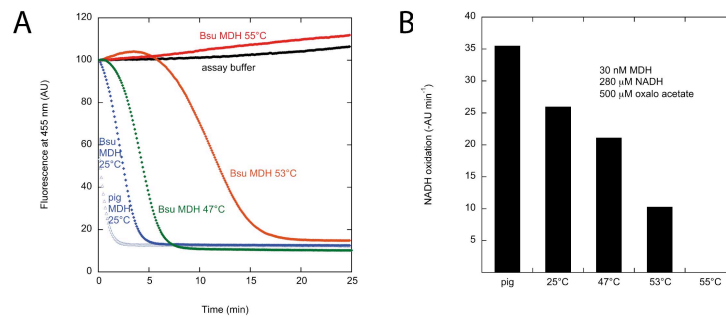
Figure 62: Heat inactivation of *B. subtilis* MDH.
For determination of MDH activity, 50 nM purified MDH from *B. subtilis* or pig MDH
were mixed with 280 μM NADH and 500 μM oxalo acetate and the decrease of NADH
fluorescence was monitored for 25 minutes at 455 nm (A). Slopes were determined
from the phase of linear decrease and used to calculate MDH activities (B). For heat
inactivation, MDH was incubated at a concentration of 2 μM for 30 minutes at the
indicated temperatures and MDH activity was determined. *B. subtilis* MDH was still
more than 80% active at 47°C and was completely inactivated by incubation at 55°C
(B).

To investigate whether *B. subtilis* heat inactivated MDH is degraded by ClpCP, as
demonstrated for pig MDH[209], *in vitro* degradation assays with ClpCP, MecA and
MDH from *B. subtilis* were performed (Figure 63). Both MDH kept at room tempera-
ture and heat inactivated for 30 minutes at 55°C were stable for over 1.5 hours in the
presence of ClpCP-MecA complex (Figure 63). The Clp protease complex was highly
active, as demonstrated by MecA degradation on the same gel and casein degradation
in a parallel experiment (Figure 63). ClpCP-YpbH was also insufficient to degrade
B. subtilis MDH *in vitro* (data not shown). It can be concluded that MDH is either
targeted for degradation by a different adaptor protein, such as McsB or an unknown
adaptor, or is not targeted for degradation by ClpCP at all.
In summary, IbpA–GFP and IbpB–GFP appear to be well suited as aggregate markers
at least for some applications, as suggested previously for *E. coli* cells[145]. The obser-
vation that foci containing these GFP fusions were already visible in non–stressed cells
may be due to a small amount of aggregates in the absence of stress. However, this high
sensitivity of aggregate detection might be a disadvantage for some experiments (see
section 4.3.5). Importantly, the number and intensity of IbpA–GFP and IbpB–GFP
foci increased after heat shock, presumably due to the accumulation of heat aggregated

proteins, in contrast to the DnaK–GFP fusion, which displayed a similar localization pattern before and after heat stress.
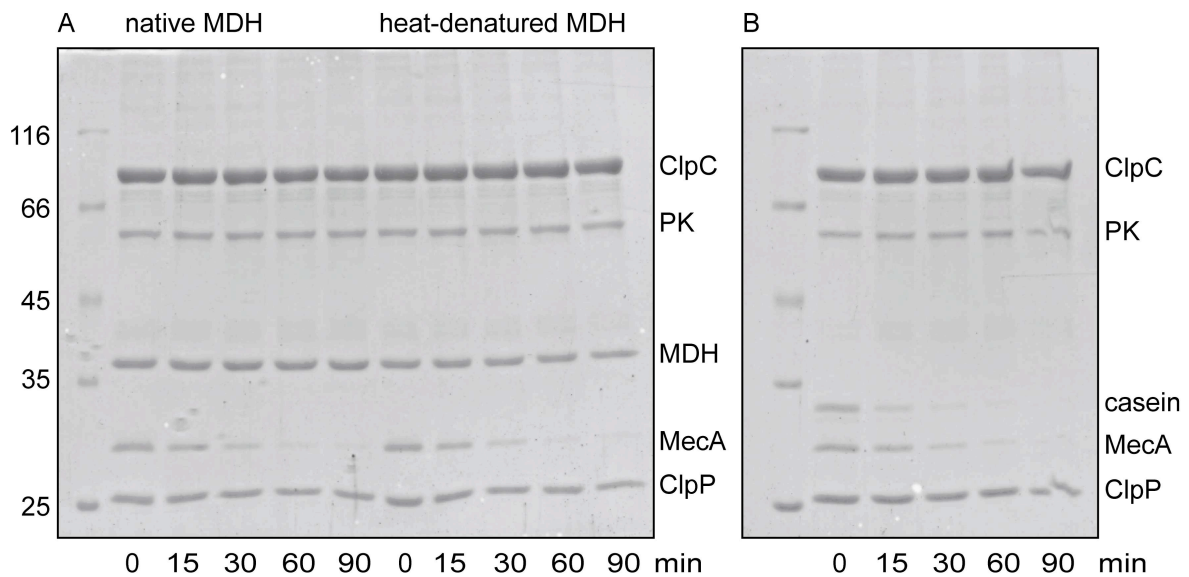
Figure 63: *B. subtilis* MDH is not degraded by ClpCP *in vitro*.
Purified *B. subtilis* MDH was incubated at room temperature (A, left) or at 55°C (A, right) for 30 minutes and then added to purified ClpP, ClpC and MecA (1 μM monomer each) with ATP and pyruvate kinase/PEP as ATP regenerating system for *in vitro* degradation at 37°C. As a control for ClpCP-MecA activity, casein was used as a substrate (B). Reaction products were removed at different times and analyzed by SDS–PAGE and Coomassie staining. MDH was not degraded by ClpCP-MecA over a time course of 1.5 hours (A). In contrast, casein (B) and MecA (A, B) were quickly degraded.

MDH–GFP aggregated exclusively during heat shock, but was comparably thermostable, so that only a small fraction of the protein formed aggregates even at temperatures of 53°C. Since a GFP fusion to a more unstable endogenous protein of *B. subtilis* appears to be required for some experiments (see section 4.3.5), future experiments will be aimed at identifying such a protein.

4.3.5   Single cell investigation of protein aggregation using MDH–GFP

Localization of MDH–GFP in *clp* mutant strains   Although the MDH–GFP fusion is far from an ideal aggragate marker, this fusion was utilized for a preliminary investigation of the influence of Clp proteases on protein aggregation at the single cell level.   MDH–GFP was preferred to IbpA–GFP or IbpB–GFP for two reasons: first,

the small heat shock proteins IbpA and IbpB do not naturally occur in *B. subtilis* and might alter the effect of Clp proteins on the aggregates as well as aggregate removal, whereas MDH can be expected to naturally occur in aggregates. Second, the presence of IbpA–GFP or IbpB–GFP foci under non–stressed conditions might complicate studies on aggregate removal because the foci might not competely disappear during recovery from heat shock.

Therefore, *clp* mutants were introduced into the MDH–GFP strain and cells were observed by fluorescence microscopy at 37°C and after heat shock at 50°C. To obtain a better signal, these experiments were performed in Belitsky Medium (with 0.05% w/v casamino acids to circumvent growth problems of the *clp* mutants).

Unexpectedly, the *clpP* mutant displayed a MDH–GFP localization similar to the wild type both before and after heat shock (Figure 64). In constrast, the *clpC* mutant had highly aberrant cell morphology and displayed very small dispersed foci in a number of cells, whereas other cells exhibited a homogeneous GFP signal. After the heat shock, the localization pattern was very similar, although a few more aggregates were observed. Interestingly, in the *clpX* mutant MDH–GFP was weakly detectable, but homogeneous both before and after heat stress.

The results in the *clpP* and *clpX* mutants correlate with the observation that these mutants were equally or more thermotolerant compared to the wild type (see section 4.3.1). The significance of the dramatically altered MDH–GFP localization in the *clpC* mutant is currently unknown, but possible explanations will be discussed (see section 5.3).

Heat shock recovery experiments   Thermotolerance experiments with a ClpC–VGF loop mutant indicated that ClpC may have a ClpP–independent function as a disaggregase *in vivo* (Figure 57). Since *clpC* also affected the localization of MDH–GFP, an interesting question was whether MDH aggregates are degraded or disaggregated and refolded.

To investigate this, cells producing GFP–tagged MDH were heat shocked for 15 minutes at 50°C, transferred back to 37°C and the cells were observed by fluorescence microscopy (Figure 65). This experiment was repeated in the presence of spectinomycin to inhibit protein synthesis during the recovery phase (Figure 66). In both cases, the
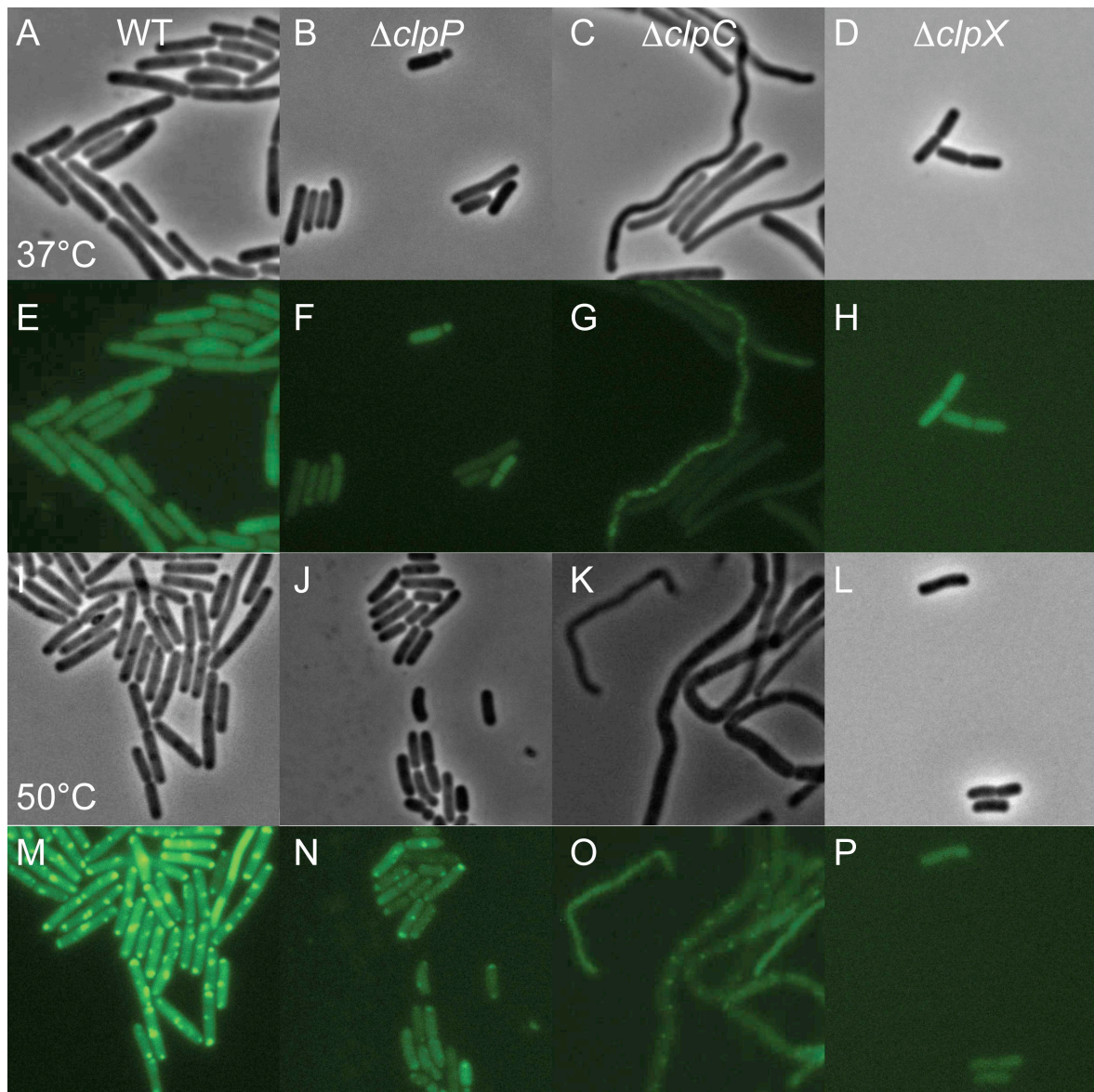
Figure 64: MDH–GFP localization in wild type and *clp* mutants.
mdh-gfp::cat strains BNM224 (WT), BNM233 ($\Delta clpP$::spec), BNM234 ($\Delta clpC$::tet) and BNM236 ($\Delta clpX$::kan) were grown in Belitsky Medium + 0.05% casamino acids to OD_{600} 0.4-0.6 at 37°C and heat–shocked for 10 minutes at 50°C. Samples were analyzed by phase contrast and fluorescence microscopy before (A-H) and after heat shock (I-P). The *clpP* mutant displayed a localization pattern that was similar to the wild type (F, N). In contrast, MDH–GFP in the *clpC* mutant (G, O) exhibited a heterogeneous patchy localization pattern before heat shock, which changed only slightly after heat shock. In the *clpX* mutant, MDH–GFP was homogeneously localized in the cytoplasm both before and after heatshock (H, P).
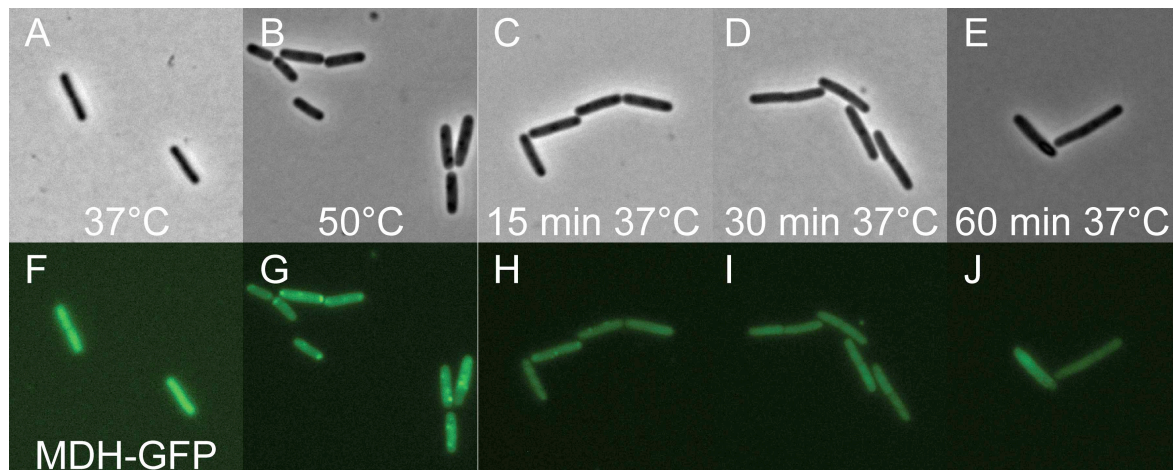
Figure 65: MDH–GFP localization during recovery from heat shock
Strain BNM224 (*mdh-gfp*::cat) was grown to OD$_{600}$ 0.4-0.6 in Belitsky Minimal Medium
at 37°C (A, F), heat–shocked for 15 minutes at 50°C (B, G) and then transferred back
to 37°C (C-E, H-J). Samples were analyzed by phase contrast (A-E) and fluorescence
microscopy (F-J). MDH–GFP foci decreased in intensity after 15 minutes at 37°C (H)
and were undetectable after 30 minutes at 37°C (I).
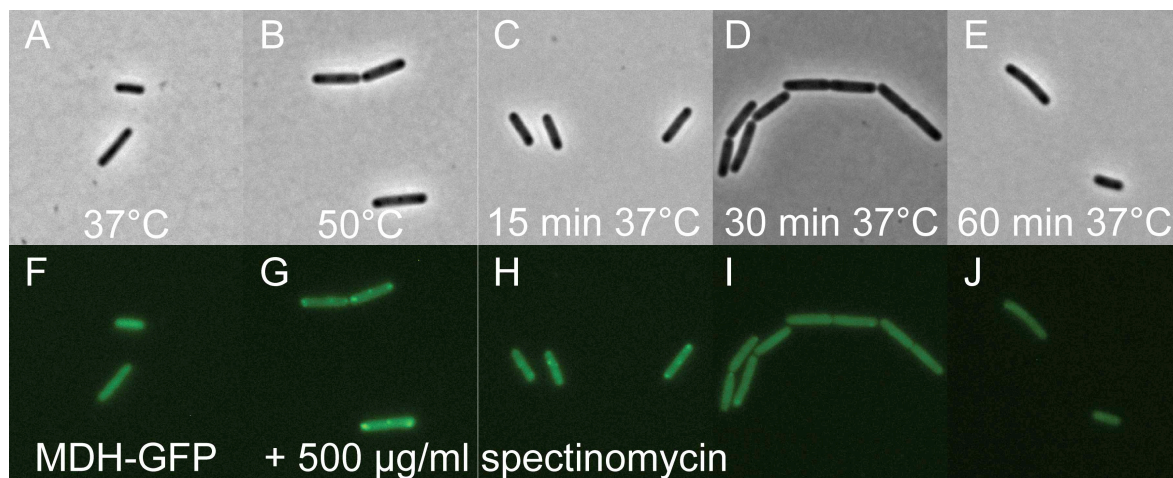
Figure 66: MDH–GFP localization during recovery from heat shock (with inhibition
of protein synthesis)
Strain BNM224 (*mdh-gfp*::cat) was grown to OD$_{600}$ 0.4-0.6 in Belitsky Minimal Medium
at 37°C (A, F) and heat–shocked for 15 minutes at 50°C (B, G). 500 μg/ml specti-
nomycin was added to inhibit protein synthesis and the culture was transferred back
to 37°C (C-E, H-J). Samples were analyzed by phase contrast (A-E) and fluorescence
microscopy (F-J). MDH–GFP foci decreased in intensity after 15 minutes at 37°C (H)
and were almost undetectable after 30 minutes at 37°C (I).

majority of MDH–GFP foci that were formed during the heat shock disappeared after 15 minutes of recovery (Figures 65 F to J and 66 F to J).

If MDH–GFP was predominantly disaggregated, an increase of the homogeneously localized fluorescence signal would be expected in parallel with an intensity decrease of the MDH–GFP foci. In contrast, MDH–GFP degradation would simply result in a loss of total fluorescence. Unfortunately, quantification of the GFP fluorescence was difficult due to the relatively weak signals against the background of homogeneously localized fluorescence. Therefore, it could not be deduced from these experiments whether MDH–GFP in the foci is disaggregated or degraded.
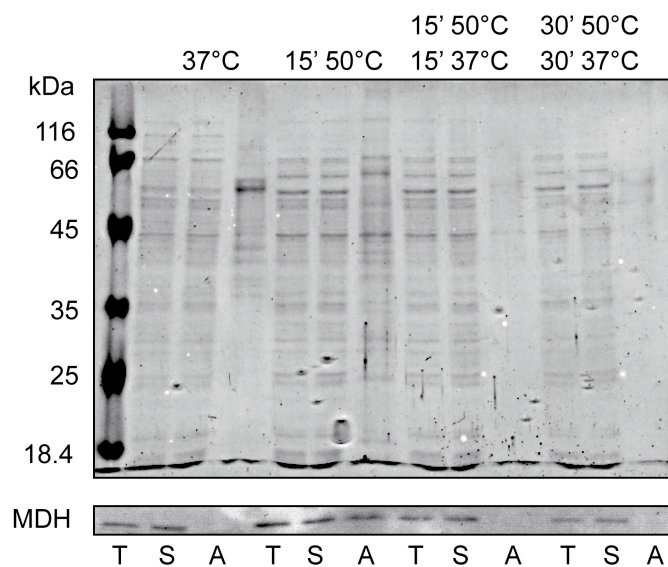
Figure 67: Effect of recovery from heat shock on protein aggregates.
Wild type cells (strain 168) were grown in LB to OD_{600} 0.4-0.6 at 37°C, heat shocked for 15 minutes at 50°C and transferred back to 37°C. Samples were removed for aggregate preparation (Material and Methods) at the timepoints indicated. Aggregate preparations were separated by SDS–PAGE and stained with Coomassie Brilliant Blue (upper) or subjected to Western blotting with anti-MDH antibodies (lower). T: total extract, S: soluble fraction after centrifugation, A: aggregates. Aggregated proteins were undetectable after 15 minutes at 37°C. MDH could be detected in the aggregate fraction after heat shock, but not after recovery for 15 minutes at 37°C.

In a different approach, wild type cells were subjected to a heat shock for 15 minutes at 50°C followed by a recovery phase at 37°C and samples were collected for aggregate preparations. Purified aggregates were separated by SDS–PAGE and analyzed by Coomassie staining and MDH Western blot. As shown in Figure 67, aggregates accumulated after the heat shock and disappeared during the recovery phase. In addition,

MDH could be detected in the aggregate fraction as well as in the soluble fraction after heat shock. During recovery, MDH was removed from the aggregate fraction. However, due to the relatively low yield of aggregated proteins (aggregates were concentrated 100–fold compared to soluble fractions) it was impossible to determine whether MDH was refolded or degraded.

In future studies, these experiments should be repeated with an aggregate marker protein, which quantitatively aggregates during heat shock. This will hopefully provide information about the relative importance of disaggregation and degradation in *B. subtilis*.

5 Discussion

In this work, different aspects of proteolysis by ClpCP and ClpXP in *B. subtilis* were studied. In the first part of the study, it was investigated how these proteases influence swimming motility by regulatory proteolysis. The results presented here suggest that ClpCP contributes to motility by regulatory proteolysis of the response regulator DegU, a negative regulator of the *fla/che* operon. ClpXP affects swimming motility by degradation of the stress regulator Spx. Like DegU, Spx appears to act as a negative regulator of the *fla/che* operon by an unknown mechanism, which could be important to downregulate swimming motility during stress.

Clp proteases also contribute to general proteolysis by removal of aggregated or damaged protein substrates. Hag, the major structural subunit of the flagellum, may be subject to general proteolysis in the cytosol prior to its secretion and assembly under certain conditions. Here, evidence is presented that two general proteolysis pathways of Hag might exist, one of which may depend on ClpCP and the adaptor protein YpbH. *B. subtilis* cells become tolerant to severe heat stress, when they are primed by a mild heat shock, a phenomenon known as thermotolerance. Previous results suggested that general proteolysis by Clp proteases is important during the heat stress response[128, 209]. Surprisingly *B. subtilis clpP* and *clpX* mutants appear to be as thermotolerant as the wild type. It could be demonstrated in this work that this effect is due to regulatory proteolysis of Spx by ClpXP. Furthermore, the data shown here indicate that the Spx regulon contributes to the heat stress response.

Surprisingly, thermotolerance experiments with a strain, in which ClpC could no longer target substrates to ClpP, revealed a putative ClpP–independent function of ClpC in thermotolerance, possibly disaggregation and refolding of aggregated proteins. Subsequently, experimental tools were developed to specifically study protein disaggregation and aggregate degradation *in vivo*.

Taken together the results shown here demonstrate that the function of Clp proteins in protein quality control and the heat stress response are more complex than anticipated. In addition to general proteolysis, regulatory proteolysis is intricately involved in protein quality control.

The common theme of many results presented in this study is the interconnection be-

tween gene regulation (including regulatory proteolysis) and the stress response (general proteolysis and protein quality control). For instance, swimming motility is influenced by oxidative stress and heat shock through Spx, whereas thermotolerance is strongly influenced by regulatory proteolysis of Spx.

Furthermore, the putative ClpP–independent activity of ClpC might represent a novel aspect of protein quality control in *B. subtilis*.

5.1   Motility regulation

The motility defect of *clpP*, *clpC* and *clpX* mutants was described previously[173, 198]. However, the molecular details of this effect were only partially characterized[147, 198]. Therefore, the motility regulation by the ClpCP and ClpXP proteases was analyzed in detail.

As demonstrated previously[147] and consistant with the results presented here, ClpCP regulates σ^D activity through ComK and FlgM. In addition, it could be established that ClpCP and ClpXP positively regulate transcription of the *fla/che* operon. These data led to the hypothesis that ClpCP and ClpXP proteolytically degrade negative transcriptional regulators of the *fla/che* promoter, which accumulate in the absence of the proteases and repress the *fla/che* promoter.

Motility regulation by ClpCP via DegU   In order to identify the regulator responsible for ClpCP–mediated motility regulation, mutants of known negative *fla/che* regulators were combined with *clp* mutations. The resulting double mutants were tested for suppression of the *clp* mutant phenotype. Using this method, it could be demonstrated that the effect of ClpCP on the *fla/che* promoter is due to its substrate DegU (Figure 14), which acts as a transcriptional repressor of *fla/che*[5]. CodY, another *fla/che* repressor is unlikely to play a role in this process, because this regulator did not accumulate in *clp* mutants (Figure 16). It was also previously demonstrated that SwrA is not directly involved, as *clp* mutants still had an effect on swimming in a strain, in which functional *swrA* is reconstituted in *B. subtilis* 168 (J. Hossmann, unpublished).

Function of DegU in motility regulation   DegU regulation of the *fla/che* operon
is complex and still controversially discussed[121, 225, 232]. At high concentrations
phosphorylated DegU acts as a repressor of *fla/che*[5], whereas either unphosphory-
lated DegU or low concentrations of phosphorylated DegU act as an activator of the
operon[121, 225, 232]. The activator function of DegU is more significant in strains
with a functional copy of the swarming regulator SwrA[225] and activation by DegU
is required for swarming motility, but not for swimming motility[232].

The results presented in this work confirm that only the repressor function of DegU
is relevant for swimming motility in the non–swarming strain 168, because *degSU* and
degU mutants were motile (Figure 14) and expressed flagellar genes normally (Figure
15). Reporter gene studies (Figure 8) revealed that *clpC* specifically affects a *lacZ*
fusion to a *fla/che* fragment that extends into the *flgB* open reading frame (to position
+152 relative to the transcription start), but not a shorter fusion (+47). Interestingly,
this additional DNA fragment contains an inverted repeat sequence, to which DegU
bound *in vitro*[225] (BR2, position +119 to +136). These data suggest that DegU
binding to BR2 is responsible for the repressing effect on *fla/che*. This is consistant
with the observation that BR2 is required for downregulation of the *fla/che* promoter
in a hyperphosphorylated *degU* mutant[225]. More experiments are required to clarify
whether a second upstream inverted repeat sequence (BR1, position -95 to -69) also
contributes to repression of $P_{fla/che}$.

Notably, BR2 is situated far downstream from the core promoter sequence, which
suggests that DegU does not repress *fla/che* transcription by restricting access of RNA
polymerase to the core promoter sequence, but acts by a distinct mechanism. Recently,
such a mechanism was demonstrated for the repressor CodY[14]. CodY binds to a site
80 nucleotides downstream of the *ybgE* transcription start and represses transcription
by a roadblock mechanism, resulting in a short terminated transcript. Interestingly, a
small RNA fragment was detected by *flgB* specific probe in Northern blot experiments
(Figure 10). This fragment may represent a terminated transcript resulting from a
DegU–mediated roadblock of *fla/che* transcription. Future experiments may elucidate
whether DegU indeed regulates *fla/che* transcription by this mechanism.

Function of DegU proteolysis   Recently, DegU was identified as a proteolysis sub-
strate of ClpCP[188] *in vitro* and *in vivo*. According to the *in vitro* data, phosphory-
lated DegU was preferentially degraded. The ClpC adaptor protein MecA was sufficient
to target DegU for degradation by ClpCP. However, other adaptor proteins were not
tested in this study[188].

The rationale of DegU degradation is currently unclear. It has been suggested that
DegU proteolysis by ClpCP prevents the premature accumulation of phosphorylated
DegU during exponential growth[188]. The *degSU* operon features an internal pro-
moter in the intergenic region between *degS* and *degU* that is positively auto-regulated
by phosphorylated DegU[188]. This regulatory circuit would result in a high level of
phosphorylated DegU in the absence of a proteolytic mechanism. In stationary phase,
an unknown signal was suggested to activate DegS and possibly stabilize DegU, leading
to induction of phosphorylated DegU[188]. ClpCP was reported to preferentially de-
grade phosphorylated DegU[188]. The finding that deletion of *clpC* leads to repression
of motility by DegU is consistant with this model.

The biological significance of motility regulation by ClpCP through DegU is difficult
to assess, because the activating signal for the DegS histidine kinase, which in turn
phosphorylates DegU, is still elusive. However, it is known that distinct levels of
DegU phosphorylation regulate important stationary phase processes, such as biofilm
formation and degradative enzyme synthesis[174, 232]. One function of ClpCP may
be to keep the concentration of phosphorylated DegU below a threshold level to al-
low motility gene expression during postexponential phase, but high enough to allow
transcriptional activation of other genes. Interestingly, the largest differences in DegU
levels between wild type and *clpC* mutant strains were observed between T0 and T2
(Figure 13). At later time points, when DegU accumulated to higher levels also in
wild type cells, DegU levels were no longer affected by mutation of *clpC*, suggesting
that either DegU is stabilized by an unknown mechanism or that the ClpCP protease
is titrated by other substrates. However, accumulation of DegU in stationary phase
is not the reason for downregulation of motility genes in stationary phase because the
characteristic postexponential peak expression pattern of class II and class III genes
was preserved in the *degSU* mutant (Figure 15). This observation is consistant with
reports that nutritional repression by CodY contributes to the postexponential peak

of motility gene expression[15].

Regulation of FlgM by DegU Interestingly, a recent publication showed that phosphorylated DegU activates the transcription of *flgM*[99]. Through this pathway, DegU negatively regulates σ^D activity. As demonstrated previously, flagellar genes are downregulated by disruption of the basal body structure (i.e. by mutation of a basal body component)[12]. This effect was shown to be dependent on *flgM* activation by DegU[99]. Therefore, DegS was proposed to sense the integrity of the basal body complex and regulate flagellar gene expression via DegU and FlgM, a mechanism, which could substitute for export of FlgM through the flagellar type III secretion system[99]. FlgM export is important for flagellar gene regulation in Gram–negative organisms[132], but has never been demonstrated in *B. subtilis*.

Direct regulation of DegU at $P_{fla/che}$ and indirect regulation via FlgM constitute a coherent negative feed–forward loop. These network motifs often act as noise filters in signaling pathways, which ensure that a pathway is only activated if a consistant signal is present[4]. The DegU– σ^D feed forward loop could act as such a noise filter that integrates an unknown FliS activating signal. This regulatory circuit could then be modulated by proteolysis of DegU[188] and ComK[226, 147].

Motility regulation by SlrR and putative influence of ClpC Another regulator of *hag* expression is the biofilm regulator SlrR[33], which downregulates *hag* in complex with SinR during biofilm formation and also in the chaining subpopulation during exponential growth. According to a recent publication, SlrR is more stable in a *clpC* mutant, suggesting that SlrR might be degraded by ClpCP[32]. However, elevated SlrR levels could not be observed in a *clpC* mutant in postexponential phase (Jörn Hossmann, Diploma Thesis), implying that SlrR accumulation is not the reason for repression of *hag* in the *clpC* mutant under these conditions. More experimental data are required to assess the function of ClpC on motility regulation by SlrR.

Motility regulation by ClpXP via Spx The motility phenotype of the *clpX* mutant was clearly separable from that of the *clpC* mutant and was not suppressed by mutation of *degU*. In contrast, all motility-related functions were restored in a *clpX spx*

double mutant (Figures 18, 19 and 20). It could also be directly shown that ectopically produced proteolysis–resistant Spx downregulates *fla/che* transcription (Figure 23) and inhibits swimming motility (Figure 21). Furthermore, it was demonstrated that motility genes are downregulated by oxidative stress (Figure 24) and heat shock (Figure 25), conditions under which Spx is induced (S. Runde, unpublished)[183, 249]. These data suggested that accumulation of the oxidative stress regulator Spx interferes with expression of the *fla/che* operon. Under normal growth conditions, this is prevented by the ClpXP protease, which degrades Spx (Figure 68)[179].
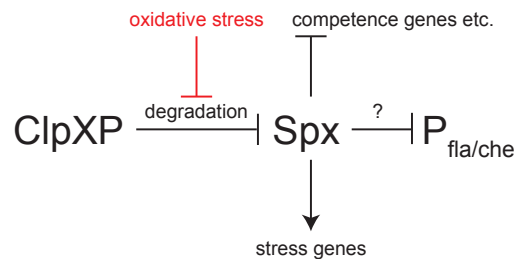
Figure 68: Model of gene regulation by Spx.
Under non–stress conditions, Spx is degraded by ClpXP. Oxidative stress leads to stabilization and activation of Spx, which activates stress genes and inhibits the expression of activator–controlled genes and motility genes.

Interestingly, heat–mediated downregulation of the $P_{fla/che}$ promoter persisted throughout the experiment (Figure 25), whereas $P_{fla/che}$ was only transiently downregulated by oxidative stress (Figure 24). One possible explanation of these data is that oxidizing radicals are enzymatically removed over time, resulting in a relaxation from the stressed state, whereas heat stress requires continuous chaperone and protease activity, as well as new synthesis of degraded proteins. These processes would consume energy, justifying the continuous downregulation of motility gene expression in order to save energy.

It was also noticed here that the characteristic lag phase of *clpP* (Figure 17) and *clpX* mutants (data not shown) is a consequence of Spx accumulation. How Spx causes this growth arrest is not known. The data shown in this work also suggest that the chaining phenotype of the *clpP* mutant (Figure 17) is suppressed by mutation of *spx*. Notably, autolytic enzymes are under control of σ^D[198], implying that cell chaining in the *clpP* mutant might be caused by Spx–mediated downregulation of autolysins.

Mechanism of motility regulation by Spx Three alternative mechanisms for *fla/che* regulation by Spx could be imagined. The first possibility is direct binding of Spx and repression at the *fla/che* promoter. This scenario is unlikely because Spx–DNA interaction has only been observed in complex with the α subunit of RNA polymerase[201, 180]. As expected, no evidence for Spx binding to the *fla/che* promoter was found in gel shift experiments (Figure 26). Nevertheless, the possibility that direct Spx binding and repression of the $P_{fla/che}$ promoter requires additional proteins should not be excluded.

Another possible mechanism of negative regulation by Spx is interference with a transcriptional activator by titration of the RNA polymerase α subunit. Such a pathway has been demonstrated i.e. for the response regulator ComA, which results in downregulation of competence development in the presence of high levels of Spx[183]. However, according to current knowledge, expression of the *fla/che* operon is not dependent on transcriptional activators. The only known *fla/che* activator is SwrA[109, 27], which is required for swarming but not swimming motility and is not expressed in the *B. subtilis* strain used in this study[109]. Still, it should be considered that Spx may interfere with activation by unknown positive regulars of $P_{fla/che}$. A genetic screen aiming for the identification of novel activators of flagellar gene expression is currently being performed (see section 4.1.2).

Finally, Spx could indirectly downregulate the *fla/che* promoter by activation of a negative regulator. Two putative transcription factors, YhfK and YukF could be ruled out as negative regulators of motility, because they do not interfere with swimming motility when over–produced (Figure 27).

Recently, the *ytpQ* gene was identified as a Spx–activated gene that enhances the redox sensitivity of the *spx* mutant when deleted and seems to play a part in iron homeostasis[252]. Interestingly, *hag* transcription was strongly upregulated in the *ytpQ* mutant, suggesting that *ytpQ* constitutes a link between Spx and swimming motility. Since the function of *ytpQ* is unknown and the YtpQ sequence is not similar to genes of known function, the mechanism of *hag* regulation by *ytpQ* is still elusive.

A genetic screen for suppressor mutants that restore motility in the presence of proteolysis–resistant Spx is presently being performed. Further candidates for Spx–activated negative regulators of motility may be identified in this screen (see section 4.1.2).

Biological function of motility repression during stress   Why is motility gene expression downregulated under stress conditions? At first glance, it appears more logical for a bacterial cell to upregulate swimming motility under these conditions in order to swim faster and escape a local source of stress. However, chemotactic repulsion by heat or oxidative stress has never been observed. In contrast, *B. subtilis* cells use aerotaxis mediated by the oxygen sensor protein HemAT to swim in the direction of higher oxygen concentration[98].

Interestingly, *hemAT* belongs to the σ^D regulon and is strongly downregulated by heat shock and in a *clpX* mutant compared to a *clpX spx* double mutant (A. Heinz and K. Turgay, unpublished microarray data). As aerotaxis may accidentally direct cells towards a local source of oxidizing radicals, stress–induced downregulation of *hemAT* may be beneficial for survival.

The results presented here suggest that motility genes are only transiently inhibited during oxidative stress (Figure 24). Therefore, it can be assumed that the cells merely downregulate new synthesis of flagella and are still able to swim during a redox shock using existing flagella, if these are stable enough to resist shearing forces, unfolding and extracellular proteases. The most obvious advantage of halting flagellar assembly during stress is to save metabolic energy for the expression of stress genes, which is crucial for survival during adverse conditions.

Putative posttranscriptional motility regulation by Spx   In addition to regulation of the $P_{fla/che}$ promoter, evidence that ClpXP influences the expression of *hag* from a xylose–inducible promoter is presented in this work. Spx is responsible for this effect (Figure 32), whereas regulation of translation initiation by CsrA (results by Jörn Hossmann, unpublished) and regulation of RNA stability (Figure 35) are not involved. An effect of ClpXP via RNases J1 and J2 is also unlikely because the levels of these RNases are only slightly affected by a *clpX* mutation (Figure 33) and independent of Spx (Figure 34). By demonstrating that Spx acts at the mRNA level, but does not affect *hag* mRNA stability, the process affected by Spx could be narrowed down to either transcriptional elongation or initiation from the P_{xyl}-promoter. Recently, transcriptional units of *B. subtilis* were accurately defined by a tiled microarray approach[186]. In this work, the effect of Rho–dependent transcription termination on mRNA elonga-

tion was investigated on a global scale. By this method, the *hag* gene was found to be Rho–independent[186], which implies that *hag* transcript elongation is not regulated by Rho at least under non–stress conditions.

Nevertheless, *hag* transcription elongation could be downregulated by a different Spx–dependent mechansim. If this is the case, various molecular mechanisms for this process can be imagined. For example, Spx may inhibit elongation factors required for the transcription of the *hag* gene. Alternatively, Spx might induce the formation of a stable hairpin structure in the *hag* gene. In this case, it is unlikely that this structure is formed in the 5'- or 3'-UTR, because the effect of *clpP* and *clpX* on *hag* expression is also observed when the *hag* open reading frame without the untranslated regions is expressed from the P_{xyl}-promoter (Figure 28).

In addition to the effect of Spx on *hag* mRNA levels, Hag protein levels in the xylose–inducible strains are expected to be lowered by Hag degradation, because the expression of *fliS*, a class II flagellar gene, should be downregulated by Spx–mediated repression of the *fla/che* promoter, which could result in Hag proteolysis (Figure 46).

Effect of the untranslated regions of *hag* on swimming motility   Interestingly, the experiments with the xylose–inducible *hag* strain also revealed that either the 5'- or the 3'-untranslated regions of *hag* are required for swimming motility. When only the *hag* ORF was expressed from P_{xyl}, Hag protein levels were reduced to about 40-50% of the wild type level, whereas Hag concentrations were about equal in the wild type and the strain, in which *hag* with 5' and 3'-UTRs is expressed from P_{xyl} (Figure 28). One possible explanation of these data is that the untranslated regions contribute to *hag* expression. This would explain the effect on motility, if a certain threshold concentration of Hag is required for efficient export by the flagellar type III secretion system. Mechanistically, the 5'- or 3'-UTR could be required for mRNA stabilization or mRNA targeting to a specific location in the cell, i.e. close to the membrane. This mechanism could ensure that translation of Hag occurs close to the site of secretion.

fla/che and _hag_ RNA fragments detected in Northern blot experiments
The accumulation of a small RNA band of around 500 bases length was observed by Northern blot analysis in the *clpC* mutant by three independent RNA probes (*hag*,

flgB and *sigD*). Therefore, it can be assumed that these bands are three distinct RNA fragments of similar size. Unexpectedly, the fragment detected by the *hag* probe also accumulated in the *hag* mutant and in the *hag* P_{xyl}-*hag4 spx clpX* mutant. This fragment could be the mRNA of the *hag* homolog *yvcZ* (with a function in dendritic swarming[82]), which could be recognized by the *hag* probe in the absence of the *hag* transcript. The *yvcZ* gene may be upregulated in the absence of *hag* and repressed (as all other flagellar genes) in the presence of high Spx levels.

The *flgB* and *sigD* fragments may constitute stable mRNA processing products from different segments of the polycistronic *fla/che* mRNA. At least in case of *flgB*, the first gene of the *fla/che*-operon, this RNA fragment could also be a terminated mRNA, which is still transcribed in the presence of high DegU levels, perhaps due to an elongation "roadblock", as suggested for CodY repression of *ybgE*[14]. Because a double stranded DIG-labeled PCR product was used as a RNA probe, it is also possible that antisense RNA fragments were detected. However, antisense RNA was not detected in this area of the *fla/che* operon in a recent study[186]. More experimental work is required to clarify the nature of the RNA fragments accumulating in the *clpC* and *hag* mutants.

Inverse regulation in cellular differentiation   Inverse regulation of differentiation processes appears to be a common mechanism in bacterial cells[17, 192, 231, 235, 149, 18, 33, 50]. For example in *E. coli*, motility and biofilm formation are mutually exclusive due to regulation at two levels. Biofilm genes, which are dependent on the alternative sigma factor σ^S, are downregulated by the FlhDC-controlled regulator FliZ[192]. In addition, the second messenger cyclic di-GMP downregulates motility and activates the expression of biofilm genes[192]. One target of cyclic di-GMP is YcgR, a protein that interacts with MotA in the presence of the second messenger to inhibit the rotation of flagella[18].

In *B. subtilis*, an analogous system exists: at the level of gene expression, the SlrR-SinR heterodimer, an activator of biofilm genes, represses the *hag* promoter, thereby negatively regulating motility[33] and YmdB is a negative regulator of motility that apparently acts via SlrR[50]. At the posttranscriptional level, EpsE, encoded in a biofilm operon, interacts with FliG and acts as a molecular clutch, thus resulting in an

uncoupled flagellar rotation[17].

DegU repression of motility genes might also play a role during differentiation into specialized cell types[231, 235, 149]. Phosphorylated DegU is an activator of exoenzyme genes[174]. One study has shown that *degU* expression levels are broadly distributed among individual cells and that DegU is involved in differentiation into specialized exoenzyme producing cells by a bistable switch[231]. It may be beneficial to the bacterial colony to downregulate motility genes in these "miner" cells in order to keep them in close vicinity to the biofilm to scavenge nutrients[149]. In structured biofilms, this phenomenon has actually been observed, as exoenzyme producing cells localized in patches, whereas motile cells were situated at the base and rim of the community[235]. DegU proteolysis could be important in multicellular communities of *B. subtilis* to stablize the motile subpopulation or to regulate the exit from the exoenzyme producing state as suggested previously[231].

A similar kind of mutually exclusive gene expression between competent and motile cells may be mediated by transcriptional readthrough of *flgM* at high ComK levels[147]. In competent cells, ComK accumulates to high levels, which would be expected to activate *flgM* expression and downregulate swimming motility. Whether such an inverse regulation exists in individual cells remains to be shown experimentally.

An inverse regulation between swimming motility and stress, mediated by Spx, was also observed in this work. During oxidative stress or heat shock, motility genes were repressed (Figures 24 and 25). However, it is currently unknown whether this regulation occurs in the whole population or whether distinct subpopulations expressing either motility genes or stress response genes form in response to the stress.

5.2   General proteolysis of Hag

There is some evidence that Hag might be a general proteolysis substrate of the ClpCP protease. Hag interacted with ClpC in a pulldown experiment (Janine Kirstein, unpublished), was degraded *in vitro* by ClpCP and specifically targeted by the adaptor protein YpbH (Figure 36). This is the first account of a YpbH-specific ClpCP substrate. In contrast, the *pulse chase* results presented here revealed that Hag is a relatively stable protein *in vivo* both under normal growth conditions and during stress (Figures

37, 38 and 39). These experiments were performed at OD_{600} 0.7, at the time of maximal *hag* expression. Hag also remained stable after pulse labeling at OD_{600} 2.5 (data not shown). However, these results do not rule out that Hag is degraded under growth conditions not tested here.

Furthermore, it should be kept in mind that Hag is a secreted protein that is only accessible to cytoplasmic proteases during the time between its ribosomal synthesis and its translocation by the the flagellar type III secretion system. This protein export could apparently stabilize Hag, because newly synthesized labeled protein could escape from degradation by secretion.

It is also possible that Hag proteolysis is only of relevance *in vivo* when secretion is blocked. Indeed, Hag was rapidly degraded when the secretion chaperone FliS was removed by mutation (Figure 46). This could be explained by a model, according to which monomeric Hag molecules are degraded quickly to prevent aggregation or premature filament formation. During secretion stress, the accumulation of Hag monomers in the cytoplasm would be counteracted by degradation.

Putative molecular mechanism of Hag protection from proteolysis   The difference in Hag stability between the *fliS* mutant and the wild type (Figure 46) could be explained by two different models. Physical interaction of FliS with Hag could mask a putative degradation tag or stabilize the three dimensional structure of the protein. Alternatively, Hag could be degraded because it accumulates to high levels due to the Hag secretion defect of the *fliS* mutant. Therefore, it was attempted to assay Hag degradation in a *fliI* knockout strain, in which FliS is still able to form a complex with Hag, but chaperone subunit complexes can no longer be delivered to the TTSS. Unfortunately, Hag levels in this mutant were extermely low, preventing the acquisition of meaningful *pulse chase* data. This effect may be due to a feedback on *hag* transcription or translation or could be a hint that Hag is indeed degraded when protein translocation is blocked.

Influence of FliW on Hag proteolysis   FliW was previously reported to form a complex with Hag[223]. In the same study, it was reported that a *fliW* mutant displays lower Hag levels than the wild type strain[223]. This was interpreted as evidence that

FliW might protect Hag from proteolysis[223].

It was recently demonstrated in another publication that FliW exerts a regulatory effect on *hag* translation[177]. FliW was shown to bind to CsrA, thereby interfering with binding of CsrA to *hag* mRNA and facilitating *hag* translation[177]. Although interaction of Hag and FliW was also confirmed by Kearns and colleagues[177], inhibition of CsrA by FliW provided an alternative explanation for the motility defect and low Hag levels observed in the *fliW* mutant[177].

In accordance with both reports, a FliW-Hag complex could be detected *in vitro* by gel filtration in this study (Figure 40). Furthermore, FliW stabilized Hag from YpbH–mediated proteolysis by ClpCP *in vitro* (Figure 41).

In contrast, a *fliW* deletion mutant did not destabilize Hag *in vivo* (Figure 46), suggesting that Hag protection by FliW is not relevant *in vivo*. Alternatively, it is possible that an unknown suppressor mutation occurred in the *fliW* mutant used in this study. Notably, the phenotype of the *fliW* mutant constructed in this work is different from that reported by two publications[223, 177]. Whereas the mutants used by the Kearns and Uetz groups displayed a defect in swimming motility and Hag production[223, 177], the strain used here was motile (Figure 43) and exhibited wild type Hag levels (Figure 44).

Like the two previously described mutants, the *fliW* mutant used here was constructed to preserve the downstream *csrA* gene, which is translationally coupled to *fliW*[244]. Importantly, Kearns et al. reported that a mutation in *csrA* suppressed the motility phenotype and restored Hag levels of the *fliW* mutant[177]. Although the *csrA* open reading frame is intact in the *fliW* mutant used in this study, it is still possible that a spontaneous loss of function mutation occurred in *csrA* or other genes, thereby restoring motility and Hag protein levels.

Whether this putative suppressor mutation could also stabilize Hag from proteolysis *in vivo* is not known. In case of a mutation in *csrA*, Hag stabilization appears unlikely because the only known activity of *csrA* in *B. subtilis* is inhibition of *hag* translation[244]. Although the data presented in this study seem to suggest that FliW is not involved in Hag stabilization from proteolysis *in vivo*, more experiments will be required to answer this question. Most importantly, the *fliW* mutant used here should be carefully examined for suppressor mutations. In addition, it should be investigated whether Hag

stability is further reduced in a *fliS fliW* double mutant. If this turns out to be true, it could be argued that FliS and FliW both contribute to Hag stability *in vivo*. Interestingly, *in vitro* degradation by ClpCP-YpbH was almost completely inhibited by FliW, but was not influenced by addition of FliS. This result was unexpected, because a *fliS* mutant destabilized Hag *in vivo* (Figure 46). To explain these data, it should not be excluded that in the *in vitro* assay FliS interacted with Hag in a different way than *in vivo*. This should be tested for expample by co–expression of FliS and Hag, purification of homogeneous one–to–one FliS-Hag complex and *in vitro* degradation assays.

Evidence for two pathways of Hag proteolysis   The results of the *in vivo* stability experiments in *clp* mutants suggest that Hag degradation in a *fliS* mutant is independent of YpbH, ClpC, ClpP or ClpX (Figures 47 and 49). According to these data, it could be assumed that Hag is degraded by another protease, such as LonA, LonB, ClpYQ or FtsH in the absence of FliS or when secretion is blocked (Figure 46). ClpCP-YpbH clearly targeted Hag for degradation *in vitro*, but could not be observed *in vivo* so far. Therefore, it might be possible that two distinct mechanisms of Hag proteolysis exist: ClpCP-YpbH dependent Hag degradation, which is inhibited by FliW, but not FliS, and ClpP–independent Hag proteolysis, blocked by FliS. Distinct degradation tags in Hag, which are specifically recognized by the two proteases and masked by either FliS or FliW, could explain the *in vitro* data.

In future experiments, Hag degradation should be assayed in other protease mutant strains to determine which proteolytic system is responsible for this process. The respective protease should then be purified and tested in Hag *in vitro* degradation assays with and without FliS. In order to elucidate whether ClpCP–dependent proteolysis is relevant *in vivo*, *pulse chase* experiments should be performed under various conditions. It will be interesting to determine the molecular details and biological significance of both pathways in more detail in future studies.

5.3   Protein quality control

Effect of Spx on thermotolerance   In addition to their function in regulatory proteolysis, Clp proteases influence protein quality control directly by degradation of aggregated proteins (Figure 53)[128, 103, 209]. In this work, it was demonstrated that ClpXP indirectly influences thermotolerance by regulatory proteolysis of Spx (Figure 57 B). Spx accumulates in *clpX* and *clpP* mutants[179], which interferes with growth (Figure 17), motility (Figure 18) and competence development[179] under non–stress conditions, but appears to be beneficial during thermotolerance (Figure 51). In these mutants, the thermotolerance defect, which is expected to result from the inability to degrade protein aggregates, seems to be balanced by Spx accumulation, explaining the unexpected observation that the *clpX* and *clpP* mutants are normally thermotolerant. Consistant with this hypothesis, *spx* mutants were unable to develop thermotolerance, which could be partially complemented by ectopic expression of *spx* (Figure 51).
Spx–dependent gene expression is induced by thiol oxidative stress[182]. However, the results of a proteomics study suggest that Spx–dependent genes are also upregulated by salt, ethanol and heat stress[222]. Furthermore, Spx accumulates during heat stress (S. Runde, unpublished data) and the expression of Spx–dependent genes is upregulated under thermotolerance conditions (A. Heinz & K. Turgay, unpublished microarray data). These observations suggest that Spx is not a specific oxidative stress regulator, as previously assumed[182], but rather a general stress regulator. Spx activates a large number of genes, which include for example *trxA* and *trxB*, encoding thioredoxin and thioredoxin reductase and *sodA*, encoding superoxide dismutase, but also many functionally uncharacterized genes[182]. It will be interesting to determine which target genes are required for thermotolerance and how they influence thermotolerance development.

Effect of McsB and YwlE on thermotolerance   Interestingly, it could be demonstrated in this study that both the protein arginine kinase McsB and its cognate phosphatase YwlE contribute to thermotolerance (Figure 54). Both effects may either depend on the function of McsB as a ClpC adaptor protein or on its arginine kinase function. McsB might be required to target aggregated substrates for degradation by ClpCP or disaggregation by ClpC. Alternatively, McsB could phosphorylate substrate

proteins, which may stablize them or even mark them for degradation or disaggregation. The fact that YwlE affects thermotolerance suggests that high levels of arginine phosphorylation are detrimental to thermotolerance development. Furthermore, it should be considered that McsB and YwlE influence thermotolerance by an indirect regulatory effect. Indeed, it was recently demonstrated that arginine phosphorylation has an effect on gene expression on a global scale[59].

Effect of McsB and ClpC on cluster formation   An *mcsB* mutation dramatically alters the localization of the IbpA–GFP (Etienne Maisonneuve, unpublished data) and MDH–GFP fusions (Stephanie Runde, unpublished data). In these strains, the GFP fusion proteins localize as extremely bright polar foci. A similar localization has been observed for the competence protein ComGA in the *mcsB* mutant[78]. Interestingly, the opposite phenotype was observed here for MDH–GFP in a *clpC* mutant (Figure 64). After heat shock, no polar foci were visible in this strain. Instead smaller aggregates were dispersed throughout the cell. Possibly, small protein aggregates are more toxic to the cell than large clusters, in which the surface area and therefore the potential to co–aggregate other proteins is minimized. Interestingly, it has been shown for yeast prion proteins that small amyloid fibrils seed the formation of larger aggregates and that the ClpB homolog Hsp104 is involved both in the breakdown of these aggregates and in prion propagation[215].

On the basis of the current data, it can be hypothesized that ClpC is involved in stablization of these polar clusters, whereas McsB is involved in breakdown of the clusters. Interestingly, both ClpC and McsB localize to polar foci themselves[118]. Detailed characterization of the impact of cluster formation and protein arginine phosphorylation may help to better understand the mechanisms of protein aggregate removal in *B. subtilis*.

Role of GsiB in thermotolerance   With the aim to identify additional determinants of thermotolerance in *B. subtilis*, genes, which are upregulated during thermotolerance on a global scale were identified by microarray experiments (Anja Heinz, unpublished). In these studies, *gsiB*, a σ^B–dependent gene of unknown function was identified. It could be demonstrated here that *gsiB* influences thermotolerance (Figure

55). GsiB has an interesting repeat structure of extremely homologous 20 amino acid stretches separated by glycine pairs, which may constitute flexible linkers. Interestingly, proteins with homology to GsiB conferred salt tolerance to *E. coli* cells[105]. Therefore, it is tempting to speculate that GsiB acts as chaperone that protects proteins from salt and heat stress. It will be very interesting to further study the function of GsiB in stress tolerance *in vitro* and *in vivo*.

Putative effect of chemical chaperones on thermotolerance The *iol* operon, which mediates inositol catabolism, was also strongly upregulated under thermotolerance conditions (A. Heinz, unppublished). Interestingy, *scyllo*-inositol inhibits the aggregation of amyloid fibers *in vitro*[158], suggesting that this compound may also be important for the bacterial cell as a chemical chaperone during heat-induced protein folding stress. Other chemical chaperones, such as glycine betaine and proline have been shown to influence tolerance to heat, salt and cold stress in *B. subtilis*[243, 94, 93]. Indeed, a slight positive effect on thermotolerance could be observed in some experiments when *myo*-inositol was added to the medium (Figure 56 A). However, deletion of the *iol* promoter had no effect on thermotolerance under the conditions tested (Figure 56 B and C) and deletion of the repressor *iolR* even negatively influenced growth and thermotolerance (Figure 56 A). Furthermore, the enzymes, which interconvert the *myo* and *scyllo* isoforms of inositol, were not required for thermotolerance (Figure 56 C and D). However, it is possible that the complex growth medium that was used for the thermotolerance experiments is not optimal for the utilization of inositol. Therefore, it will be important to repeat these experiments in minimal medium.

Evidence for a ClpP independent function of ClpC In *E. coli*, thermotolerance requires ClpB, an AAA+ ATPase with protein disaggregase activity, which is unable to interact with ClpP[238]. As ClpC displays disaggregase activity *in vitro*[209] and is involved in thermotolerance (A. Heinz & K. Turgay, unpublished), it was tempting to speculate that ClpC is involved in protein disaggregation during thermotolerance development in *B. subtilis*. In this work, evidence for *in vivo* disaggregation by ClpC during thermotolerance was acquired: a strain, in which the ClpP binding loop in ClpC was mutated (VGF loop mutant), was as thermotolerant as the wild type, whereas the

clpC mutant had a significant thermotolerance defect.

More experiments will be required to demonstrate whether the observed effect of the VGF loop mutant is a consequence of ClpC disaggregase activity or is at least partially due to an indirect regulatory effect. In principle, the VGF loop mutant should result in accumulation of ClpCP proteolysis substrates, similar to the *clpC* deletion mutant. However, it is possible that ClpC and its adaptor proteins also exert a ClpP–independent regulatory effect on thermotolerance development. Furthermore, it will have to be investigated whether the VGF loop mutant is unable to interact with ClpP *in vitro* and whether this protein has *in vitro* disaggregation activity.

Although a number of control experiments are missing at this time, it can be tentatively suggested that ClpC might have a dual function in protein quality control and specifically thermotolerance. According to this model, ClpC could associate with ClpP to degrade aggregates or could act independently of ClpP to disaggregate and refold aggregated substrates.

Disaggregase activity of ClpC in wild type cells could only be relevant if a significant fraction of ClpC exists as hexamers, unbound to ClpP. This fraction should depend on the relative abundance of ClpP and Clp ATPases and on the protease/ATPase binding affinities and kinetics. In one study, cellular levels of ClpP and its three associated ATPases were measured by quantitative Western blot analysis[73]. According to this publication, 1200 ClpP tetradecamers, 250 ClpC complexes, 100 ClpE hexamers and 1400 ClpX hexamers per cell can be detected under non–stress conditions. After heat shock, these numbers increased to 2500 ClpP complexes, 1000 ClpC complexes and 450 ClpE complexes per cell, whereas the ClpX level remained constant[73]. In another publication, 670 to 1300 ClpC molecules per cell were detected in minimal medium containing glucose[226].

According to *in vitro* data, two ClpC hexamers form a complex with one ClpP tetradecamer[117]. Therefore, the Western blot results by Gerth et al. would suggest that ClpP is present in excess over ATPase hexamers both under non–stress conditions and after heat shock[73]. However, it has been demonstrated that *E. coli* ClpXP complexes consist of a a mixture of 1 to 1 and 2 to 1 complexes[154] and the situation could be similar for ClpCP *in vivo*. Furthermore, depending on binding affinities, a significant fraction of unassembled Clp hexamers might exist at equilibrium, even though excess

ClpP is available for complex formation. Finally, the calculated protein levels after heat shock may be an underestimation, because ClpP and its ATPases localize to insoluble aggregates under these conditions[73]. Therefore, it can be concluded that the actual abundance of ClpC hexamers without associated ClpP is a matter of speculation at present.

If protein disaggregation plays a role in *B. subtilis*, it will be highly interesting to study how substrates are selected for disaggregation or degradation *in vivo*. Mechanistically, this is a very interesting question, especially for ClpC, which appears to mediate both disaggregation and degradation. In principle, a substrate, which is unfolded by ClpC, should always be translocated into ClpP and degraded if ClpP is associated with this particular ClpC hexamer. Therefore, the decision between disaggregation and degradation could be expected to depend only on association of ClpC and ClpP complexes and not on the sequence or structure of the substrate, except if the substrate or another factor actively inhibits ClpP or interferes with ClpC-ClpP complex formation. To experimentally distinguish between disaggregation and degradation, GFP–tagged substrates can be followed by fluorescence microscopy after recovery from heat shock. Alternatively, proteins can be detected by Western blotting of aggregate preparations. Both experiments were performed with MDH in this work (Figures 65, 66 and 67). However, due to the low relative amount of aggregated *B. subtilis* MDH after heat shock, the data were inconclusive. Therefore, an important task for future work will be to identify a heat unstable *B. subtilis* protein, which completely aggregates during heat stress. This protein could then be tagged to GFP and used to monitor the fate of aggregates after recovery from heat shock.

Cooperation of chaperone and protease systems in protein quality control
Since ClpB cooperates with the DnaK system in *E. coli*, it is possible that ClpC is also functionally connected to other chaperones in *B. subtilis*. The data shown in this work suggest that the combined function of ClpC and DnaK is important for protein quality control, as the *dnaK clpC* double mutant is highly temperature sensitive (Figure 58). This double mutant should also be tested for its thermotolerance phenotype. Furthermore, it will be very interesting to investigate if and how these two proteins cooperate in protein quality control. It could be imagined that DnaK directly

binds to ClpC to deliver substrates or modulate its activity. Alternatively, DnaK might prepare substrates for unfolding by ClpC. Moreover, it is possible that some substrates, which are stabilized or refolded by DnaK can also be degraded or refolded by ClpC.

5.4   Summary and conclusion

The work presented here was originally prompted by the observation that Hag, the structural subunit of the flagellum interacts with the Hsp100/Clp ATPase ClpC in co–immunoprecipitation experiments (J. Kirstein, unpublished). Indeed, Hag was degraded by ClpCP *in vitro*, which corroborated that this interaction is functional and that Hag is a general proteolysis substrate. However, Hag was shown to be stable *in vivo* except if the export chaperone FliS was mutated. Even in this case, Hag degradation did not depend on ClpCP, suggesting the existance of two proteolytic pathways. One of these pathways is ClpCP–dependent and occurs under yet unknown conditions *in vivo*, whereas the other is mediated by a protease distinct from ClpP and may represent general proteolysis to remove cytosolic Hag when secretion is compromised. Furthermore, Western blot analysis revealed that Hag does not accumulate in *clp* mutant strains as expected for a proteolysis substrate. In contrast, Hag levels were lower in these strains, demonstrating that regulatory proteolysis of upstream regulators is involved in the synthesis of Hag. Subsequenty, these regulators were identified by genetic methods: ClpCP degrades DegU, a negative regulator of the flagellar *fla/che* operon. Likewise, Spx, a proteolysis substrate of ClpXP, downregulates motility, although the molecular mechanism of this process is not clear at the moment. These results indicate that Clp proteases affect swimming motility by general and regulatory proteolysis at different levels.

Further experiments demonstrated that Clp proteases also act on protein quality control and specifically thermotolerance by general and regulatory proteolysis. ClpXP acts on protein quality control directly by degradation of aggregated proteins. At the same time, ClpXP indirectly influences thermotolerance by proteolysis of Spx, a regulator, which is required for thermotolerance. By regulatory proteolysis of CtsR together with McsB and by McsB inhibition[119], ClpC might also exert a regulatory effect on thermotolerance and protein quality control. ClpC contributes to these processes by

general proteolysis and possibly protein disaggregation independent of ClpP.

It is interesting to note that MDH, which, like Hag, was identified as a ClpC interaction partner in a co–immunoprecipitation experiment (J. Kirstein, unpublished) could not be degraded by ClpCP *in vitro*, at least with the adaptor proteins tested. However, an *in vivo* effect of ClpC on aggregated MDH–GFP was observed, suggesting that the interaction of the two proteins might have some functional significance.

Taken together, both the studies on swimming motility and on thermotolerance show that Clp proteases are part of a highly complex network, in which general and regulatory proteolysis are interconnected. These interconnections should always be taken into account, when effects of the pleiotrophic Clp proteases are investigated. However, in spite of the apparent complexity of these protease systems, it appears that general and regulatory effects can be distinguished experimentally by appropriate methods.

Proteolysis and protein quality are involved in a plethora of cellular activities in organisms from all kingdoms of life. Insight into the complex and highly regulated network of proteases and chaperones is crucial for the better understanding of the bacterial cell and its various ways to respond to stress and differentiate into specialized cell forms. Better knowledge of these pathways may spark new ideas for antibiotics against bacterial pathogens as well as for industrial applications. Finally, many concepts of bacterial proteolysis and protein quality control can also be applied to eukaryotic cells and have proven to be valuable in the battle against human diseases.

References

[1] S.-I. Aizawa, I. B. Zhulin, L. Márquez-Magaña, and G. W. Ordal. Chemotaxis and motility. *Bacillus subtilis and its closest relatives - from genes to cells, ASM press, Washington D.C.; Editors Abraham L. Sonenshein, James A. Hoch, Richard Losick*, pages 437–452, 2002.

[2] M. Albano, J. Hahn, and D. Dubnau. Expression of competence genes in *Bacillus subtilis*. *J Bacteriol*, 169(7):3110–3117, Jul 1987.

[3] A. M. Albertini, T. Caramori, W. D. Crabb, F. Scoffone, and A. Galizzi. The *flaA* locus of *Bacillus subtilis* is part of a large operon coding for flagellar structures, motility functions, and an ATPase-like polypeptide. *J Bacteriol*, 173(11):3573–3579, Jun 1991.

[4] U. Alon. Network motifs: theory and experimental approaches. *Nat Rev Genet*, 8(6):450–461, Jun 2007.

[5] G. Amati, P. Bisicchia, and A. Galizzi. DegU-P represses expression of the motility *fla-che* operon in *Bacillus subtilis*. *J Bacteriol*, 186(18):6003–6014, Sep 2004.

[6] C. Anagnostopoulos and J. Spizizen. Requirements for transformation in *Bacillus subtilis*. *J Bacteriol*, 81(5):741–746, May 1961.

[7] C. Antoniewski, B. Savelli, and P. Stragier. The *spoIIJ* gene, which regulates early developmental steps in *Bacillus subtilis*, belongs to a class of environmentally responsive genes. *J Bacteriol*, 172(1):86–93, Jan 1990.

[8] D. Apel and M. G. Surette. Bringing order to a complex molecular machine: the assembly of the bacterial flagella. *Biochim Biophys Acta*, 1778(9):1851–1858, Sep 2008.

[9] M. Arnaud, A. Chastanet, and M. Débarbouillé. New vector for efficient allelic replacement in naturally nontransformable, low-GC-content, gram-positive bacteria. *Appl Environ Microbiol*, 70(11):6887–6891, Nov 2004.

[10] S. V. Avery. Cell individuality: the bistability of competence development. *Trends Microbiol*, 13(10):459–462, Oct 2005.

[11] G. Bange, N. Kümmerer, C. Engel, G. Bozkurt, K. Wild, and I. Sinning. FlhA provides the adaptor for coordinated delivery of late flagella building blocks to the type III secretion system. *Proc Natl Acad Sci U S A*, 107(25):11295–11300, Jun 2010.

[12] D. Barilla, T. Caramori, and A. Galizzi. Coupling of flagellin gene transcription to flagellar assembly in *Bacillus subtilis*. *J Bacteriol*, 176(15):4558–4564, Aug 1994.

[13] G. Becker, E. Klauck, and R. Hengge-Aronis. Regulation of RpoS proteolysis in *Escherichia coli*: the response regulator RssB is a recognition factor that interacts with the turnover element in RpoS. *Proc Natl Acad Sci U S A*, 96(11):6439–6444, May 1999.

[14] B. R. Belitsky and A. L. Sonenshein. Roadblock repression of transcription by *Bacillus subtilis* CodY. *J Mol Biol*, 411(4):729–743, Aug 2011.

[15] F. Bergara, C. Ibarra, J. Iwamasa, J. C. Patarroyo, R. Aguilera, and L. M. Márquez-Magaña. CodY is a nutritional repressor of flagellar gene expression in *Bacillus subtilis*. *J Bacteriol*, 185(10):3118–3126, May 2003.

[16] H. C. Besche, A. Peth, and A. L. Goldberg. Getting to first base in proteasome assembly. *Cell*, 138(1):25–28, Jul 2009.

[17] K. M. Blair, L. Turner, J. T. Winkelman, H. C. Berg, and D. B. Kearns. A molecular clutch disables flagella in the *Bacillus subtilis* biofilm. *Science*, 320(5883):1636–1638, Jun 2008.

[18] A. Boehm, M. Kaiser, H. Li, C. Spangler, C. A. Kasper, M. Ackermann, V. Kaever, V. Sourjik, V. Roth, and U. Jenal. Second messenger-mediated adjustment of bacterial swimming velocity. *Cell*, 141(1):107–116, Apr 2010.

[19] A. Bougdour, C. Cunning, P. J. Baptiste, T. Elliott, and S. Gottesman. Multiple pathways for regulation of sigmaS (RpoS) stability in *Escherichia coli* via the action of multiple anti-adaptors. *Mol Microbiol*, 68(2):298–313, Apr 2008.

[20] A. Bougdour, S. Wickner, and S. Gottesman. Modulating RssB activity: IraP, a novel regulator of sigma(S) stability in *Escherichia coli*. *Genes Dev*, 20(7):884–897, Apr 2006.

[21] S. S. Branda, F. Chu, D. B. Kearns, R. Losick, and R. Kolter. A major protein component of the *Bacillus subtilis* biofilm matrix. *Mol Microbiol*, 59(4):1229–1238, Feb 2006.

[22] S. S. Branda, J. E. González-Pastor, S. Ben-Yehuda, R. Losick, and R. Kolter. Fruiting body formation by *Bacillus subtilis*. *Proc Natl Acad Sci U S A*, 98(20):11621–11626, Sep 2001.

[23] R. A. Britton, P. Eichenberger, J. E. Gonzalez-Pastor, P. Fawcett, R. Monson, R. Losick, and A. D. Grossman. Genome-wide analysis of the stationary-phase sigma factor (σ^H) regulon of *Bacillus subtilis*. *J Bacteriol*, 184(17):4881–4890, Sep 2002.

[24] H. Brötz-Oesterhelt, D. Beyer, H.-P. Kroll, R. Endermann, C. Ladel, W. Schroeder, B. Hinzen, S. Raddatz, H. Paulsen, K. Henninger, J. E. Bandow, H.-G. Sahl, and H. Labischinski. Dysregulation of bacterial proteolytic machinery by a new class of antibiotics. *Nat Med*, 11(10):1082–1087, Oct 2005.

[25] B. Bukau, J. Weissman, and A. Horwich. Molecular chaperones and protein quality control. *Cell*, 125(3):443–451, May 2006.

[26] S. Busby and R. H. Ebright. Transcription activation by catabolite activator protein (CAP). *J Mol Biol*, 293(2):199–213, Oct 1999.

[27] C. Calvio, F. Celandroni, E. Ghelardi, G. Amati, S. Salvetti, F. Ceciliani, A. Galizzi, and S. Senesi. Swarming differentiation and swimming motility in *Bacillus subtilis* are controlled by *swrA*, a newly identified dicistronic operon. *J Bacteriol*, 187(15):5356–5366, Aug 2005.

[28] G. J. Cao and N. Sarkar. Poly(A) RNA in *Bacillus subtilis*: identification of the polyadenylylation site of flagellin mRNA. *FEMS Microbiol Lett*, 108(3):281–285, Apr 1993.

[29] T. Caramori, D. Barilla, C. Nessi, L. Sacchi, and A. Galizzi. Role of FlgM in σ^D-dependent gene expression in *Bacillus subtilis*. *J Bacteriol*, 178(11):3113–3118, Jun 1996.

[30] T. Caramori and A. Galizzi. The UP element of the promoter for the flagellin gene, *hag*, stimulates transcription from both SigD- and SigA-dependent promoters in *Bacillus subtilis*. *Mol Gen Genet*, 258(4):385–388, May 1998.

[31] Y. Chai, F. Chu, R. Kolter, and R. Losick. Bistability and biofilm formation in *Bacillus subtilis*. *Mol Microbiol*, 67(2):254–263, Jan 2008.

[32] Y. Chai, R. Kolter, and R. Losick. Reversal of an epigenetic switch governing cell chaining in *Bacillus subtilis* by protein instability. *Mol Microbiol*, 78(1):218–229, Oct 2010.

[33] Y. Chai, T. Norman, R. Kolter, and R. Losick. An epigenetic switch governing daughter cell separation in *Bacillus subtilis*. *Genes Dev*, 24(8):754–765, Apr 2010.

[34] M. F. Charette, G. W. Henderson, and A. Markovitz. ATP hydrolysis-dependent protease activity of the Lon (CapR) protein of *Escherichia coli* K-12. *Proc Natl Acad Sci U S A*, 78(8):4728–4732, Aug 1981.

[35] L. Chen and J. D. Helmann. The *Bacillus subtilis* σ^D-dependent operon encoding the flagellar proteins FliD, FliS, and FliT. *J Bacteriol*, 176(11):3093–3101, Jun 1994.

[36] Z. Chen, J. Hagler, V. J. Palombella, F. Melandri, D. Scherer, D. Ballard, and T. Maniatis. Signal-induced site-specific phosphorylation targets IκB-α to the ubiquitin-proteasome pathway. *Genes Dev*, 9(13):1586–1597, Jul 1995.

[37] F. Chu, D. B. Kearns, S. S. Branda, R. Kolter, and R. Losick. Targets of the master regulator of biofilm formation in *Bacillus subtilis*. *Mol Microbiol*, 59(4):1216–1228, Feb 2006.

[38] F. Chu, D. B. Kearns, A. McLoon, Y. Chai, R. Kolter, and R. Losick. A novel regulatory protein governing biofilm formation in *Bacillus subtilis*. *Mol Microbiol*, 68(5):1117–1127, Jun 2008.

[39] C. H. Chung and A. L. Goldberg. The product of the *lon* (*capR*) gene in *Escherichia coli* is the ATP-dependent protease, protease La. *Proc Natl Acad Sci U S A*, 78(8):4931–4935, Aug 1981.

[40] A. Ciechanover. Proteolysis: from the lysosome to ubiquitin and the proteasome. *Nat Rev Mol Cell Biol*, 6(1):79–87, Jan 2005.

[41] S. Cranz-Mileva, F. Imkamp, K. Kolygo, Z. Maglica, W. Kress, and E. Weber-Ban. The flexible attachment of the N-domains to the ClpA ring body allows their use on demand. *J Mol Biol*, 378(2):412–424, Apr 2008.

[42] M. K. Dahl, T. Msadek, F. Kunst, and G. Rapoport. Mutational analysis of the *Bacillus subtilis* DegU regulator and its phosphorylation by the DegS protein kinase. *J Bacteriol*, 173(8):2539–2547, Apr 1991.

[43] B. Dahlmann, F. Kopp, L. Kuehn, B. Niedel, G. Pfeifer, R. Hegerl, and W. Baumeister. The multicatalytic proteinase (prosome) is ubiquitous from eukaryotes to archaebacteria. *FEBS Lett*, 251(1-2):125–131, Jul 1989.

[44] E. Darmon, D. Noone, A. Masson, S. Bron, O. P. Kuipers, K. M. Devine, and J. M. van Dijl. A novel class of heat and secretion stress-responsive genes is controlled by the autoregulated CssRS two-component system of *Bacillus subtilis*. *J Bacteriol*, 184(20):5661–5671, Oct 2002.

[45] C. De Duve, R. Gianetto, F. Appelmans, and R. Wattiaux. Enzymic content of the mitochondria fraction. *Nature*, 172(4390):1143–1144, Dec 1953.

[46] E. Dervyn, M.-F. Noirot-Gros, P. Mervelet, S. McGovern, S. D. Ehrlich, P. Polard, and P. Noirot. The bacterial condensin/cohesin-like protein complex acts in DNA repair and regulation of gene expression. *Mol Microbiol*, 51(6):1629–1640, Mar 2004.

[47] E. Deuerling, A. Mogk, C. Richter, M. Purucker, and W. Schumann. The *ftsH* gene of *Bacillus subtilis* is involved in major cellular processes such as sporulation, stress adaptation and secretion. *Mol Microbiol*, 23(5):921–933, Mar 1997.

[48] E. Deuerling, B. Paeslack, and W. Schumann. The *ftsH* gene of *Bacillus subtilis* is transiently induced after osmotic and temperature upshift. *J Bacteriol*, 177(14):4105–4112, Jul 1995.

[49] E. Deuerling, A. Schulze-Specking, T. Tomoyasu, A. Mogk, and B. Bukau. Trigger factor and DnaK cooperate in folding of newly synthesized proteins. *Nature*, 400(6745):693–696, Aug 1999.

[50] C. Diethmaier, N. Pietack, K. Gunka, C. Wrede, M. Lehnik-Habrink, C. Herzberg, S. Hübner, and J. Stülke. A novel factor controlling bistability in *Bacillus subtilis*: the YmdB protein affects flagellin expression and biofilm formation. *J Bacteriol*, 193(21):5997–6007, Nov 2011.

[51] D. A. Dougan, B. G. Reid, A. L. Horwich, and B. Bukau. ClpS, a substrate modulator of the ClpAP machine. *Mol Cell*, 9(3):673–683, Mar 2002.

[52] J. Driscoll and A. L. Goldberg. Skeletal muscle proteasome can degrade proteins in an ATP-dependent process that does not require ubiquitin. *Proc Natl Acad Sci U S A*, 86(3):787–791, Feb 1989.

[53] C. D'Souza, M. M. Nakano, D. L. Frisby, and P. Zuber. Translation of the open reading frame encoded by *comS*, a gene of the *srf* operon, is necessary for the development of genetic competence, but not surfactin biosynthesis, in *Bacillus subtilis*. *J Bacteriol*, 177(14):4144–4148, Jul 1995.

[54] C. D'Souza, M. M. Nakano, and P. Zuber. Identification of *comS*, a gene of the *srfA* operon that regulates the establishment of genetic competence in *Bacillus subtilis*. *Proc Natl Acad Sci U S A*, 91(20):9397–9401, Sep 1994.

[55] D. Dubnau. DNA uptake in bacteria. *Annu Rev Microbiol*, 53:217–244, 1999.

[56] A. K. W. Elsholz, K. Hempel, S. Michalik, K. Gronau, D. Becher, M. Hecker, and U. Gerth. Activity control of the ClpC adaptor McsB in *Bacillus subtilis*. *J Bacteriol*, 193(15):3887–3893, Aug 2011.

[57] A. K. W. Elsholz, K. Hempel, D.-C. Pöther, D. Becher, M. Hecker, and U. Gerth. CtsR inactivation during thiol-specific stress in low GC, Gram+ bacteria. *Mol Microbiol*, 79(3):772–785, Feb 2011.

[58] A. K. W. Elsholz, S. Michalik, D. Zühlke, M. Hecker, and U. Gerth. CtsR, the Gram-positive master regulator of protein quality control, feels the heat. *EMBO J*, 29(21):3621–3629, Nov 2010.

[59] A. K. W. Elsholz, K. Turgay, S. Michalik, B. Hessling, K. Gronau, D. Oertel, U. Mäder, J. Bernhardt, D. Becher, M. Hecker, and U. Gerth. Global impact of protein arginine phosphorylation on the physiology of *Bacillus subtilis*. *Proc Natl Acad Sci U S A*, in press, 2012.

[60] A. Erbse, R. Schmidt, T. Bornemann, J. Schneider-Mergener, A. Mogk, R. Zahn, D. A. Dougan, and B. Bukau. ClpS is an essential component of the N-end rule pathway in *Escherichia coli*. *Nature*, 439(7077):753–756, Feb 2006.

[61] A. H. Erbse, J. N. Wagner, K. N. Truscott, S. K. Spall, J. Kirstein, K. Zeth, K. Turgay, A. Mogk, B. Bukau, and D. A. Dougan. Conserved residues in the N-domain of the AAA+ chaperone ClpA regulate substrate recognition and unfolding. *FEBS J*, 275(7):1400–1410, Apr 2008.

[62] W. Estacio, S. S. Anna-Arriola, M. Adedipe, and L. M. Márquez-Magaña. Dual promoters are responsible for transcription initiation of the *fla/che* operon in *Bacillus subtilis*. *J Bacteriol*, 180(14):3548–3555, Jul 1998.

[63] J. D. Etlinger and A. L. Goldberg. A soluble ATP-dependent proteolytic system responsible for the degradation of abnormal proteins in reticulocytes. *Proc Natl Acad Sci U S A*, 74(1):54–58, Jan 1977.

[64] U. Fiedler and V. Weiss. A common switch in activation of the response regulators NtrC and PhoB: phosphorylation induces dimerization of the receiver modules. *EMBO J*, 14(15):3696–3705, Aug 1995.

[65] J. M. Flynn, I. Levchenko, M. Seidel, S. H. Wickner, R. T. Sauer, and T. A. Baker. Overlapping recognition determinants within the ssrA degradation tag allow modulation of proteolysis. *Proc Natl Acad Sci U S A*, 98(19):10584–10589, Sep 2001.

[66] J. M. Flynn, S. B. Neher, Y. I. Kim, R. T. Sauer, and T. A. Baker. Proteomic discovery of cellular substrates of the ClpXP protease reveals five classes of ClpX-recognition signals. *Mol Cell*, 11(3):671–683, Mar 2003.

[67] K. Fredrick and J. D. Helmann. FlgM is a primary regulator of σ^D activity, and its absence restores motility to a *sinR* mutant. *J Bacteriol*, 178(23):7010–7013, Dec 1996.

[68] J. Fuhrmann, A. Schmidt, S. Spiess, A. Lehner, K. Turgay, K. Mechtler, E. Charpentier, and T. Clausen. McsB is a protein arginine kinase that phosphorylates and inhibits the heat-shock regulator CtsR. *Science*, 324(5932):1323–1327, Jun 2009.

[69] M. Fujita, J. E. González-Pastor, and R. Losick. High- and low-threshold genes in the Spo0A regulon of *Bacillus subtilis*. *J Bacteriol*, 187(4):1357–1368, Feb 2005.

[70] S. K. Garg, S. Kommineni, L. Henslee, Y. Zhang, and P. Zuber. The YjbH protein of *Bacillus subtilis* enhances ClpXP-catalyzed proteolysis of Spx. *J Bacteriol*, 191(4):1268–1277, Feb 2009.

[71] P. Genevaux, C. Georgopoulos, and W. L. Kelley. The Hsp70 chaperone machines of *Escherichia coli*: a paradigm for the repartition of chaperone functions. *Mol Microbiol*, 66(4):840–857, Nov 2007.

[72] P. Genevaux, F. Keppel, F. Schwager, P. S. Langendijk-Genevaux, F. U. Hartl, and C. Georgopoulos. *In vivo* analysis of the overlapping functions of DnaK and trigger factor. *EMBO Rep*, 5(2):195–200, Feb 2004.

[73] U. Gerth, J. Kirstein, J. Mostertz, T. Waldminghaus, M. Miethke, H. Kock, and M. Hecker. Fine-tuning in regulation of Clp protein content in *Bacillus subtilis*. *J Bacteriol*, 186(1):179–191, Jan 2004.

[74] U. Gerth, E. Krüger, I. Derré, T. Msadek, and M. Hecker. Stress induction of the *Bacillus subtilis clpP* gene encoding a homologue of the proteolytic component of the Clp protease and the involvement of ClpP and ClpX in stress tolerance. *Mol Microbiol*, 28(4):787–802, May 1998.

[75] M. H. Glickman and A. Ciechanover. The ubiquitin-proteasome proteolytic pathway: destruction for the sake of construction. *Physiol Rev*, 82(2):373–428, Apr 2002.

[76] M. Glotzer, A. W. Murray, and M. W. Kirschner. Cyclin is degraded by the ubiquitin pathway. *Nature*, 349(6305):132–138, Jan 1991.

[77] A. L. Goldberg and A. C. St John. Intracellular protein degradation in mammalian and bacterial cells: Part 2. *Annu Rev Biochem*, 45:747–803, 1976.

[78] J. Hahn, N. Kramer, K. Briley, Jr, and D. Dubnau. McsA and B mediate the delocalization of competence proteins from the cell poles of *Bacillus subtilis. Mol Microbiol*, 72(1):202–215, Apr 2009.

[79] L. W. Hamoen, H. Eshuis, J. Jongbloed, G. Venema, and D. van Sinderen. A small gene, designated *comS*, located within the coding region of the fourth amino acid-activation domain of *srfA*, is required for competence development in *Bacillus subtilis. Mol Microbiol*, 15(1):55–63, Jan 1995.

[80] L. W. Hamoen, A. F. Van Werkhoven, G. Venema, and D. Dubnau. The pleiotropic response regulator DegU functions as a priming protein in competence development in *Bacillus subtilis. Proc Natl Acad Sci U S A*, 97(16):9246–9251, Aug 2000.

[81] M. A. Hamon and B. A. Lazazzera. The sporulation transcription factor Spo0A is required for biofilm development in *Bacillus subtilis. Mol Microbiol*, 42(5):1199–1209, Dec 2001.

[82] K. Hamze, D. Julkowska, S. Autret, K. Hinc, K. Nagorska, A. Sekowska, I. B. Holland, and S. J. Séror. Identification of genes required for different stages of dendritic swarming in *Bacillus subtilis*, with a novel role for *phrC. Microbiology*, 155(Pt 2):398–412, Feb 2009.

[83] T. Haslberger, B. Bukau, and A. Mogk. Towards a unifying mechanism for ClpB/Hsp104-mediated protein disaggregation and prion propagation. *Biochem Cell Biol*, 88(1):63–75, Feb 2010.

[84] T. Haslberger, A. Zdanowicz, I. Brand, J. Kirstein, K. Turgay, A. Mogk, and B. Bukau. Protein disaggregation by the AAA+ chaperone ClpB involves partial threading of looped polypeptide segments. *Nat Struct Mol Biol*, 15(6):641–650, Jun 2008.

[85] K. Hayashi, N. Morooka, Y. Yamamoto, K. Fujita, K. Isono, S. Choi, E. Ohtsubo, T. Baba, B. L. Wanner, H. Mori, and T. Horiuchi. Highly accurate genome sequences of *Escherichia coli* K-12 strains MG1655 and W3110. *Mol Syst Biol*, 2:2006.0007, 2006.

[86] M. Hecker, J. Pané-Farré, and U. Völker. SigB-dependent general stress response in *Bacillus subtilis* and related gram-positive bacteria. *Annu Rev Microbiol*, 61:215–236, 2007.

[87] M. Hecker, W. Schumann, and U. Völker. Heat-shock and general stress response in *Bacillus subtilis*. *Mol Microbiol*, 19(3):417–428, Feb 1996.

[88] J. D. Helmann, L. M. Márquez, and M. J. Chamberlin. Cloning, sequencing, and disruption of the *Bacillus subtilis* σ^{28} gene. *J Bacteriol*, 170(4):1568–1574, Apr 1988.

[89] A. Hershko, E. Eytan, A. Ciechanover, and A. L. Haas. Immunochemical analysis of the turnover of ubiquitin-protein conjugates in intact cells. Relationship to the breakdown of abnormal proteins. *J Biol Chem*, 257(23):13964–13970, Dec 1982.

[90] T. Hesterkamp and B. Bukau. Role of the DnaK and HscA homologs of Hsp70 chaperones in protein folding in *E.coli*. *EMBO J*, 17(16):4818–4828, Aug 1998.

[91] J. Hinnerwisch, W. A. Fenton, K. J. Furtak, G. W. Farr, and A. L. Horwich. Loops in the central channel of ClpA chaperone mediate protein binding, unfolding, and translocation. *Cell*, 121(7):1029–1041, Jul 2005.

[92] A. Hoffmann, B. Bukau, and G. Kramer. Structure and function of the molecular chaperone Trigger Factor. *Biochim Biophys Acta*, 1803(6):650–661, Jun 2010.

[93] T. Hoffmann and E. Bremer. Protection of *Bacillus subtilis* against cold stress via compatible-solute acquisition. *J Bacteriol*, 193(7):1552–1562, Apr 2011.

[94] G. Holtmann and E. Bremer. Thermoprotection of *Bacillus subtilis* by exogenously provided glycine betaine and structurally related compatible solutes: involvement of Opu transporters. *J Bacteriol*, 186(6):1683–1693, Mar 2004.

[95] G. Homuth, S. Masuda, A. Mogk, Y. Kobayashi, and W. Schumann. The *dnaK* operon of *Bacillus subtilis* is heptacistronic. *J Bacteriol*, 179(4):1153–1164, Feb 1997.

[96] R. Honda, H. Tanaka, and H. Yasuda. Oncoprotein MDM2 is a ubiquitin ligase E3 for tumor suppressor p53. *FEBS Lett*, 420(1):25–27, Dec 1997.

[97] A. L. Horwich, A. C. Apetri, and W. A. Fenton. The GroEL/GroES cis cavity as a passive anti-aggregation device. *FEBS Lett*, 583(16):2654–2662, Aug 2009.

[98] S. Hou, R. W. Larsen, D. Boudko, C. W. Riley, E. Karatan, M. Zimmer, G. W. Ordal, and M. Alam. Myoglobin-like aerotaxis transducers in archaea and bacteria. *Nature*, 403(6769):540–544, Feb 2000.

[99] Y.-H. Hsueh, L. M. Cozy, L.-T. Sham, R. A. Calvo, A. D. Gutu, M. E. Winkler, and D. B. Kearns. DegU-phosphate activates expression of the anti-sigma factor FlgM in *Bacillus subtilis*. *Mol Microbiol*, 81(4):1092–1108, Aug 2011.

[100] K. T. Hughes, K. L. Gillen, M. J. Semon, and J. E. Karlinsey. Sensing structural intermediates in bacterial flagellar assembly by export of a negative regulator. *Science*, 262(5137):1277–1280, Nov 1993.

[101] B. J. Hwang, W. J. Park, C. H. Chung, and A. L. Goldberg. *Escherichia coli* contains a soluble ATP-dependent protease (Ti) distinct from protease La. *Proc Natl Acad Sci U S A*, 84(16):5550–5554, Aug 1987.

[102] A. S. Jarnagin and E. Ferrari. Extracellular enzymes: gene regulation and structure function relationship studies. *Biotechnology*, 22:189–217, 1992.

[103] B. Jürgen, R. Hanschke, M. Sarvas, M. Hecker, and T. Schweder. Proteome and transcriptome based analysis of *Bacillus subtilis* cells overproducing an insoluble heterologous protein. *Appl Microbiol Biotechnol*, 55(3):326–332, Apr 2001.

[104] J. Kain, G. G. He, and R. Losick. Polar localization and compartmentalization of ClpP proteases during growth and sporulation in *Bacillus subtilis*. *J Bacteriol*, 190(20):6749–6757, Oct 2008.

[105] R. K. Kapardar, R. Ranjan, A. Grover, M. Puri, and R. Sharma. Identification and characterization of genes conferring salt tolerance to *Escherichia coli* from pond water metagenome. *Bioresour Technol*, 101(11):3917–3924, Jun 2010.

[106] Y. Katayama-Fujimura, S. Gottesman, and M. R. Maurizi. A multiple-component, ATP-dependent protease from *Escherichia coli*. *J Biol Chem*, 262(10):4477–4485, Apr 1987.

[107] D. B. Kearns. A field guide to bacterial swarming motility. *Nat Rev Microbiol*, 8(9):634–644, Sep 2010.

[108] D. B. Kearns, F. Chu, S. S. Branda, R. Kolter, and R. Losick. A master regulator for biofilm formation by *Bacillus subtilis*. *Mol Microbiol*, 55(3):739–749, Feb 2005.

[109] D. B. Kearns, F. Chu, R. Rudner, and R. Losick. Genes governing swarming in *Bacillus subtilis* and evidence for a phase variation mechanism controlling surface motility. *Mol Microbiol*, 52(2):357–369, Apr 2004.

[110] D. B. Kearns and R. Losick. Cell population heterogeneity during growth of *Bacillus subtilis*. *Genes Dev*, 19(24):3083–3094, Dec 2005.

[111] K. C. Keiler, P. R. Waller, and R. T. Sauer. Role of a peptide tagging system in degradation of proteins synthesized from damaged messenger RNA. *Science*, 271(5251):990–993, Feb 1996.

[112] H. M. Kim, Y. Yu, and Y. Cheng. Structure characterization of the 26S proteasome. *Biochim Biophys Acta*, 1809(2):67–79, Feb 2011.

[113] L. Kim, A. Mogk, and W. Schumann. A xylose-inducible *Bacillus subtilis* integration vector and its application. *Gene*, 181(1-2):71–76, Nov 1996.

[114] J. Kirstein, D. A. Dougan, U. Gerth, M. Hecker, and K. Turgay. The tyrosine kinase McsB is a regulated adaptor protein for ClpCP. *EMBO J*, 26(8):2061–2070, Apr 2007.

[115] J. Kirstein, A. Hoffmann, H. Lilie, R. Schmidt, H. Rübsamen-Waigmann, H. Brötz-Oesterhelt, A. Mogk, and K. Turgay. The antibiotic ADEP reprogrammes ClpP, switching it from a regulated to an uncontrolled protease. *EMBO Mol Med*, 1(1):37–49, Apr 2009.

[116] J. Kirstein, N. Molière, D. A. Dougan, and K. Turgay. Adapting the machine: adaptor proteins for Hsp100/Clp and AAA+ proteases. *Nat Rev Microbiol*, 7(8):589–599, Aug 2009.

[117] J. Kirstein, T. Schlothauer, D. A. Dougan, H. Lilie, G. Tischendorf, A. Mogk, B. Bukau, and K. Turgay. Adaptor protein controlled oligomerization activates the AAA+ protein ClpC. *EMBO J*, 25(7):1481–1491, Apr 2006.

[118] J. Kirstein, H. Strahl, N. Molière, L. W. Hamoen, and K. Turgay. Localization of general and regulatory proteolysis in *Bacillus subtilis* cells. *Mol Microbiol*, 70(3):682–694, Nov 2008.

[119] J. Kirstein, D. Zühlke, U. Gerth, K. Turgay, and M. Hecker. A tyrosine kinase and its activator control the activity of the CtsR heat shock repressor in *B. subtilis*. *EMBO J*, 24(19):3435–3445, Oct 2005.

[120] N. Knipfer and T. E. Shrader. Inactivation of the 20S proteasome in *Mycobacterium smegmatis*. *Mol Microbiol*, 25(2):375–383, Jul 1997.

[121] K. Kobayashi. Gradual activation of the response regulator DegU controls serial expression of genes for flagellum formation and biofilm formation in *Bacillus subtilis*. *Mol Microbiol*, 66(2):395–409, Oct 2007.

[122] K. Kobayashi, S. D. Ehrlich, A. Albertini, G. Amati, K. K. Andersen, M. Arnaud, K. Asai, S. Ashikaga, S. Aymerich, P. Bessieres, F. Boland, S. C. Brignell, S. Bron, K. Bunai, J. Chapuis, L. C. Christiansen, A. Danchin, M. Débarbouille, E. Dervyn, E. Deuerling, K. Devine, S. K. Devine, O. Dreesen, J. Errington, S. Fillinger, S. J. Foster, Y. Fujita, A. Galizzi, R. Gardan, C. Eschevins,

T. Fukushima, K. Haga, C. R. Harwood, M. Hecker, D. Hosoya, M. F. Hullo, H. Kakeshita, D. Karamata, Y. Kasahara, F. Kawamura, K. Koga, P. Koski, R. Kuwana, D. Imamura, M. Ishimaru, S. Ishikawa, I. Ishio, D. Le Coq, A. Masson, C. Mauël, R. Meima, R. P. Mellado, A. Moir, S. Moriya, E. Nagakawa, H. Nanamiya, S. Nakai, P. Nygaard, M. Ogura, T. Ohanan, M. O'Reilly, M. O'Rourke, Z. Pragai, H. M. Pooley, G. Rapoport, J. P. Rawlins, L. A. Rivas, C. Rivolta, A. Sadaie, Y. Sadaie, M. Sarvas, T. Sato, H. H. Saxild, E. Scanlan, W. Schumann, J. F. M. L. Seegers, J. Sekiguchi, A. Sekowska, S. J. Séror, M. Simon, P. Stragier, R. Studer, H. Takamatsu, T. Tanaka, M. Takeuchi, H. B. Thomaides, V. Vagner, J. M. van Dijl, K. Watabe, A. Wipat, H. Yamamoto, M. Yamamoto, Y. Yamamoto, K. Yamane, K. Yata, K. Yoshida, H. Yoshikawa, U. Zuber, and N. Ogasawara. Essential *Bacillus subtilis* genes. *Proc Natl Acad Sci U S A*, 100(8):4678–4683, Apr 2003.

[123] P. Kodgire and K. K. Rao. *Hag* expression in *Bacillus subtilis* is both negatively and positively regulated by ScoC. *Microbiology*, 155(Pt 1):142–149, Jan 2009.

[124] S. Kommineni, S. K. Garg, C. M. Chan, and P. Zuber. YjbH-enhanced proteolysis of Spx by ClpXP in *Bacillus subtilis* is inhibited by the small protein YirB (YuzO). *J Bacteriol*, 193(9):2133–2140, May 2011.

[125] W. Kress, Z. Maglica, and E. Weber-Ban. Clp chaperone-proteases: structure and function. *Res Microbiol*, 160(9):618–628, Nov 2009.

[126] E. Krüger and M. Hecker. The first gene of the *Bacillus subtilis clpC* operon, *ctsR*, encodes a negative regulator of its own operon and other class III heat shock genes. *J Bacteriol*, 180(24):6681–6688, Dec 1998.

[127] E. Krüger, U. Völker, and M. Hecker. Stress induction of *clpC* in *Bacillus subtilis* and its involvement in stress tolerance. *J Bacteriol*, 176(11):3360–3367, Jun 1994.

[128] E. Krüger, E. Witt, S. Ohlmeier, R. Hanschke, and M. Hecker. The *clp* proteases of *Bacillus subtilis* are directly involved in degradation of misfolded proteins. *J Bacteriol*, 182(11):3259–3265, Jun 2000.

[129] E. Krüger, D. Zühlke, E. Witt, H. Ludwig, and M. Hecker. Clp-mediated prote-
olysis in Gram-positive bacteria is autoregulated by the stability of a repressor.
EMBO J, 20(4):852–863, Feb 2001.

[130] F. Kunst, N. Ogasawara, I. Moszer, A. M. Albertini, G. Alloni, V. Azevedo, M. G.
Bertero, P. Bessières, A. Bolotin, S. Borchert, R. Borriss, L. Boursier, A. Brans,
M. Braun, S. C. Brignell, S. Bron, S. Brouillet, C. V. Bruschi, B. Caldwell,
V. Capuano, N. M. Carter, S. K. Choi, J. J. Codani, I. F. Connerton, and
A. Danchin. The complete genome sequence of the gram-positive bacterium
Bacillus subtilis. *Nature*, 390(6657):249–256, Nov 1997.

[131] F. Kunst and G. Rapoport. Salt stress is an environmental signal affecting
degradative enzyme synthesis in *Bacillus subtilis*. *J Bacteriol*, 177(9):2403–2407,
May 1995.

[132] K. Kutsukake. Excretion of the anti-sigma factor through a flagellar substruc-
ture couples flagellar gene expression with flagellar assembly in *Salmonella ty-
phimurium*. *Mol Gen Genet*, 243(6):605–612, Jun 1994.

[133] J. Kwak, J. L. Workman, and D. Lee. The proteasome and its regulatory roles
in gene expression. *Biochim Biophys Acta*, 1809(2):88–96, Feb 2011.

[134] U. K. Laemmli. Cleavage of structural proteins during the assembly of the head
of bacteriophage T4. *Nature*, 227(5259):680–685, Aug 1970.

[135] V. Lamour, L. F. Westblade, E. A. Campbell, and S. A. Darst. Crystal structure
of the *in vivo*-assembled *Bacillus subtilis* Spx/RNA polymerase alpha subunit
C-terminal domain complex. *J Struct Biol*, 168(2):352–356, Nov 2009.

[136] J. T. Larsson, A. Rogstam, and C. von Wachenfeldt. YjbH is a novel negative
effector of the disulphide stress regulator, Spx, in *Bacillus subtilis*. *Mol Microbiol*,
66(3):669–684, Nov 2007.

[137] Y. Le Breton, N. P. Mohapatra, and W. G. Haldenwang. *In vivo* random mu-
tagenesis of *Bacillus subtilis* by use of TnYLB-1, a mariner-based transposon.
Appl Environ Microbiol, 72(1):327–333, Jan 2006.

[138] Y. R. Lee, R. T. Nagao, and J. L. Key. A soybean 101-kD heat shock protein complements a yeast HSP104 deletion mutant in acquiring thermotolerance. *Plant Cell*, 6(12):1889–1897, Dec 1994.

[139] M. Leelakriangsak, K. Kobayashi, and P. Zuber. Dual negative control of *spx* transcription initiation from the P3 promoter by repressors PerR and YodB in *Bacillus subtilis*. *J Bacteriol*, 189(5):1736–1744, Mar 2007.

[140] M. Leelakriangsak and P. Zuber. Transcription from the P3 promoter of the *Bacillus subtilis spx* gene is induced in response to disulfide stress. *J Bacteriol*, 189(5):1727–1735, Mar 2007.

[141] I. Levchenko, M. Seidel, R. T. Sauer, and T. A. Baker. A specificity-enhancing factor for the ClpXP degradation machine. *Science*, 289(5488):2354–2356, Sep 2000.

[142] P. J. Lewis and A. L. Marston. GFP vectors for controlled expression and dual labelling of protein fusions in *Bacillus subtilis*. *Gene*, 227(1):101–110, Feb 1999.

[143] M. Li and S. L. Wong. Cloning and characterization of the *groESL* operon from *Bacillus subtilis*. *J Bacteriol*, 174(12):3981–3992, Jun 1992.

[144] A. A. Lin and P. Zuber. Evidence that a single monomer of Spx can productively interact with RNA polymerase in *Bacillus subtilis*. *J Bacteriol*, 194(7):1697–1707, Apr 2012.

[145] A. B. Lindner, R. Madden, A. Demarez, E. J. Stewart, and F. Taddei. Asymmetric segregation of protein aggregates is associated with cellular aging and rejuvenation. *Proc Natl Acad Sci U S A*, 105(8):3076–3081, Feb 2008.

[146] J. Liu, W. M. Cosby, and P. Zuber. Role of *lon* and *clpX* in the post-translational regulation of a sigma subunit of *RNA* polymerase required for cellular differentiation in *Bacillus subtilis*. *Mol Microbiol*, 33(2):415–428, Jul 1999.

[147] J. Liu and P. Zuber. A molecular switch controlling competence and motility: competence regulatory factors ComS, MecA, and ComK control σ^D-dependent gene expression in *Bacillus subtilis*. *J Bacteriol*, 180(16):4243–4251, Aug 1998.

[148] X. Liu and P. Matsumura. The FlhD/FlhC complex, a transcriptional activator of the *Escherichia coli* flagellar class II operons. *J Bacteriol*, 176(23):7345–7351, Dec 1994.

[149] D. Lopez, H. Vlamakis, and R. Kolter. Generation of multiple cell types in *Bacillus subtilis*. *FEMS Microbiol Rev*, 33(1):152–163, Jan 2009.

[150] A. Lupas, P. Zwickl, and W. Baumeister. Proteasome sequences in eubacteria. *Trends Biochem Sci*, 19(12):533–534, Dec 1994.

[151] H. Maamar and D. Dubnau. Bistability in the *Bacillus subtilis* K-state (competence) system requires a positive feedback loop. *Mol Microbiol*, 56(3):615–624, May 2005.

[152] R. M. Macnab. Genetics and biogenesis of bacterial flagella. *Annu Rev Genet*, 26:131–158, 1992.

[153] U. Mäder, L. Zig, J. Kretschmer, G. Homuth, and H. Putzer. mRNA processing by RNases J1 and J2 affects *Bacillus subtilis* gene expression on a global scale. *Mol Microbiol*, 70(1):183–196, Oct 2008.

[154] Z. Maglica, K. Kolygo, and E. Weber-Ban. Optimal efficiency of ClpAP and ClpXP chaperone-proteases is achieved by architectural symmetry. *Structure*, 17(4):508–516, Apr 2009.

[155] S. Makishima, K. Komoriya, S. Yamaguchi, and S. I. Aizawa. Length of the flagellar hook and the capacity of the type III export apparatus. *Science*, 291(5512):2411–2413, Mar 2001.

[156] L. M. Márquez, J. D. Helmann, E. Ferrari, H. M. Parker, G. W. Ordal, and M. J. Chamberlin. Studies of σ^D-dependent functions in *Bacillus subtilis*. *J Bacteriol*, 172(6):3435–3443, Jun 1990.

[157] A. Martin, T. A. Baker, and R. T. Sauer. Distinct static and dynamic interactions control ATPase-peptidase communication in a AAA+ protease. *Mol Cell*, 27(1):41–52, Jul 2007.

[158] J. McLaurin, R. Golomb, A. Jurewicz, J. P. Antel, and P. E. Fraser. Inositol stereoisomers stabilize an oligomeric aggregate of Alzheimer amyloid beta peptide and inhibit abeta -induced toxicity. *J Biol Chem*, 275(24):18495–18502, Jun 2000.

[159] A. L. McLoon, S. B. Guttenplan, D. B. Kearns, R. Kolter, and R. Losick. Tracing the domestication of a biofilm-forming bacterium. *J Bacteriol*, 193(8):2027–2034, Apr 2011.

[160] M. Miethke, M. Hecker, and U. Gerth. Involvement of *Bacillus subtilis* ClpE in CtsR degradation and protein quality control. *J Bacteriol*, 188(13):4610–4619, Jul 2006.

[161] J. Miller. *Experiments in Molecular Genetics.* Cold Spring Harbor Laboratory Press, 1972.

[162] T. Minamino, K. Imada, and K. Namba. Mechanisms of type III protein export for bacterial flagellar assembly. *Mol Biosyst*, 4(11):1105–1115, Nov 2008.

[163] T. Minamino, K. Imada, and K. Namba. Molecular motors of the bacterial flagella. *Curr Opin Struct Biol*, 18(6):693–701, Dec 2008.

[164] T. Minamino and R. M. Macnab. Domain structure of *Salmonella* FlhB, a flagellar export component responsible for substrate specificity switching. *J Bacteriol*, 182(17):4906–4914, Sep 2000.

[165] T. Minamino and K. Namba. Distinct roles of the FliI ATPase and proton motive force in bacterial flagellar protein export. *Nature*, 451(7177):485–488, Jan 2008.

[166] D. B. Mirel and M. J. Chamberlin. The *Bacillus subtilis* flagellin gene (*hag*) is transcribed by the σ^{28} form of RNA polymerase. *J Bacteriol*, 171(6):3095–3101, Jun 1989.

[167] D. B. Mirel, W. F. Estacio, M. Mathieu, E. Olmsted, J. Ramirez, and L. M. Márquez-Magaña. Environmental regulation of *Bacillus subtilis* σ^{D}-dependent gene expression. *J Bacteriol*, 182(11):3055–3062, Jun 2000.

[168] A. Mogk, E. Deuerling, S. Vorderwlbecke, E. Vierling, and B. Bukau. Small heat shock proteins, ClpB and the DnaK system form a functional triade in reversing protein aggregation. *Mol Microbiol*, 50(2):585–595, Oct 2003.

[169] A. Mogk, G. Homuth, C. Scholz, L. Kim, F. X. Schmid, and W. Schumann. The GroE chaperonin machine is a major modulator of the CIRCE heat shock regulon of *Bacillus subtilis*. *EMBO J*, 16(15):4579–4590, Aug 1997.

[170] N. Molière and K. Turgay. Chaperone-protease systems in regulation and protein quality control in *Bacillus subtilis*. *Res Microbiol*, 160(9):637–644, Nov 2009.

[171] T. Morinaga, H. Ashida, and K. I. Yoshida. Identification of two *scyllo*-inositol dehydrogenases in *Bacillus subtilis*. *Microbiology*, 156(Pt 5):1538–1546, May 2010.

[172] N. Moriya, T. Minamino, K. T. Hughes, R. M. Macnab, and K. Namba. The type III flagellar export specificity switch is dependent on FliK ruler and a molecular clock. *J Mol Biol*, 359(2):466–477, Jun 2006.

[173] T. Msadek, V. Dartois, F. Kunst, M. L. Herbaud, F. Denizot, and G. Rapoport. ClpP of *Bacillus subtilis* is required for competence development, motility, degradative enzyme synthesis, growth at high temperature and sporulation. *Mol Microbiol*, 27(5):899–914, Mar 1998.

[174] T. Msadek, F. Kunst, D. Henner, A. Klier, G. Rapoport, and R. Dedonder. Signal transduction pathway controlling synthesis of a class of degradative enzymes in *Bacillus subtilis*: expression of the regulatory genes and analysis of mutations in *degS* and *degU*. *J Bacteriol*, 172(2):824–834, Feb 1990.

[175] J. P. Mueller, G. Bukusoglu, and A. L. Sonenshein. Transcriptional regulation of *Bacillus subtilis* glucose starvation-inducible genes: control of *gsiA* by the ComP-ComA signal transduction system. *J Bacteriol*, 174(13):4361–4373, Jul 1992.

[176] K. Mukai, M. Kawata-Mukai, and T. Tanaka. Stabilization of phosphorylated *Bacillus subtilis* DegU by DegR. *J Bacteriol*, 174(24):7954–7962, Dec 1992.

[177] S. Mukherjee, H. Yakhnin, D. Kysela, J. Sokoloski, P. Babitzke, and D. B. Kearns. CsrA-FliW interaction governs flagellin homeostasis and a checkpoint on flagellar morphogenesis in *Bacillus subtilis*. *Mol Microbiol*, 82(2):447–461, Oct 2011.

[178] E. J. Murray, T. B. Kiley, and N. R. Stanley-Wall. A pivotal role for the response regulator DegU in controlling multicellular behaviour. *Microbiology*, 155(Pt 1):1–8, Jan 2009.

[179] M. M. Nakano, F. Hajarizadeh, Y. Zhu, and P. Zuber. Loss-of-function mutations in *yjbD* result in ClpX- and ClpP-independent competence development of *Bacillus subtilis*. *Mol Microbiol*, 42(2):383–394, Oct 2001.

[180] M. M. Nakano, A. Lin, C. S. Zuber, K. J. Newberry, R. G. Brennan, and P. Zuber. Promoter recognition by a complex of Spx and the C-terminal domain of the RNA polymerase α subunit. *PLoS One*, 5(1):e8664, 2010.

[181] S. Nakano, K. N. Erwin, M. Ralle, and P. Zuber. Redox-sensitive transcriptional control by a thiol/disulphide switch in the global regulator, Spx. *Mol Microbiol*, 55(2):498–510, Jan 2005.

[182] S. Nakano, E. Küster-Schöck, A. D. Grossman, and P. Zuber. Spx-dependent global transcriptional control is induced by thiol-specific oxidative stress in *Bacillus subtilis*. *Proc Natl Acad Sci U S A*, 100(23):13603–13608, Nov 2003.

[183] S. Nakano, M. M. Nakano, Y. Zhang, M. Leelakriangsak, and P. Zuber. A regulatory protein that interferes with activator-stimulated transcription in bacteria. *Proc Natl Acad Sci U S A*, 100(7):4233–4238, Apr 2003.

[184] S. Nakano, G. Zheng, M. M. Nakano, and P. Zuber. Multiple pathways of Spx (YjbD) proteolysis in *Bacillus subtilis*. *J Bacteriol*, 184(13):3664–3670, Jul 2002.

[185] K. J. Newberry, S. Nakano, P. Zuber, and R. G. Brennan. Crystal structure of the *Bacillus subtilis* anti-α, global transcriptional regulator, Spx, in complex with the alpha C-terminal domain of RNA polymerase. *Proc Natl Acad Sci U S A*, 102(44):15839–15844, Nov 2005.

[186] P. Nicolas, U. Mäder, E. Dervyn, T. Rochat, A. Leduc, N. Pigeonneau, E. Bidnenko, E. Marchadier, M. Hoebeke, S. Aymerich, D. Becher, P. Bisicchia, E. Botella, O. Delumeau, G. Doherty, E. L. Denham, M. J. Fogg, V. Fromion, A. Goelzer, A. Hansen, E. Härtig, C. R. Harwood, G. Homuth, H. Jarmer, M. Jules, E. Klipp, L. Le Chat, F. Lecointe, P. Lewis, W. Liebermeister, A. March, R. A. T. Mars, P. Nannapaneni, D. Noone, S. Pohl, B. Rinn, F. Rgheimer, P. K. Sappa, F. Samson, M. Schaffer, B. Schwikowski, L. Steil, J. Stülke, T. Wiegert, K. M. Devine, A. J. Wilkinson, J. M. van Dijl, M. Hecker, U. Völker, P. Bessières, and P. Noirot. Condition-dependent transcriptome reveals high-level regulatory architecture in *Bacillus subtilis*. *Science*, 335(6072):1103–1106, Mar 2012.

[187] M. Ogura, K. Shimane, K. Asai, N. Ogasawara, and T. Tanaka. Binding of response regulator DegU to the *aprE* promoter is inhibited by RapG, which is counteracted by extracellular PhrG in *Bacillus subtilis*. *Mol Microbiol*, 49(6):1685–1697, Sep 2003.

[188] M. Ogura and K. Tsukahara. Autoregulation of the *Bacillus subtilis* response regulator gene *degU* is coupled with the proteolysis of DegU-P by ClpCP. *Mol Microbiol*, 75(5):1244–1259, Mar 2010.

[189] Q. Pan, D. A. Garsin, and R. Losick. Self-reinforcing activation of a cell-specific transcription factor by proteolysis of an anti-sigma factor in *B. subtilis*. *Mol Cell*, 8(4):873–883, Oct 2001.

[190] K. Paul, M. Erhardt, T. Hirano, D. F. Blair, and K. T. Hughes. Energy source of flagellar type III secretion. *Nature*, 451(7177):489–492, Jan 2008.

[191] M. Persuh, I. Mandic-Mulec, and D. Dubnau. A MecA paralog, YpbH, binds ClpC, affecting both competence and sporulation. *J Bacteriol*, 184(8):2310–2313, Apr 2002.

[192] C. Pesavento, G. Becker, N. Sommerfeldt, A. Possling, N. Tschowri, A. Mehlis, and R. Hengge. Inverse regulatory coordination of motility and curli-mediated adhesion in *Escherichia coli*. *Genes Dev*, 22(17):2434–2446, Sep 2008.

[193] S. L. Porter, G. H. Wadhams, and J. P. Armitage. Signal processing in complex chemotaxis pathways. *Nat Rev Microbiol*, 9(3):153–165, Mar 2011.

[194] S. Prakash, T. Inobe, A. J. Hatch, and A. Matouschek. Substrate selection by the proteasome during degradation of protein complexes. *Nat Chem Biol*, 5(1):29–36, Jan 2009.

[195] S. Prakash, L. Tian, K. S. Ratliff, R. E. Lehotzky, and A. Matouschek. An unstructured initiation site is required for efficient proteasome-mediated degradation. *Nat Struct Mol Biol*, 11(9):830–837, Sep 2004.

[196] P. Prepiak and D. Dubnau. A peptide signal for adapter protein-mediated degradation by the AAA+ protease ClpCP. *Mol Cell*, 26(5):639–647, Jun 2007.

[197] F. G. Priest. Extracellular enzyme synthesis in the genus *Bacillus*. *Bacteriol Rev*, 41(3):711–753, Sep 1977.

[198] M. H. Rashid, A. Tamakoshi, and J. Sekiguchi. Effects of *mecA* and *mecB* (*clpC*) mutations on expression of *sigD*, which encodes an alternative sigma factor, and autolysin operons and on flagellin synthesis in *Bacillus subtilis*. *J Bacteriol*, 178(16):4861–4869, Aug 1996.

[199] B. G. Reid, W. A. Fenton, A. L. Horwich, and E. U. Weber-Ban. ClpA mediates directional translocation of substrate proteins into the ClpP protease. *Proc Natl Acad Sci U S A*, 98(7):3768–3772, Mar 2001.

[200] D. Y. Reyes and H. Yoshikawa. DnaK chaperone machine and trigger factor are only partially required for normal growth of *Bacillus subtilis*. *Biosci Biotechnol Biochem*, 66(7):1583–1586, Jul 2002.

[201] D. Y. Reyes and P. Zuber. Activation of transcription initiation by Spx: formation of transcription complex and identification of a Cis-acting element required for transcriptional activation. *Mol Microbiol*, 69(3):765–779, Aug 2008.

[202] S. Riethdorf, U. Vlker, U. Gerth, A. Winkler, S. Engelmann, and M. Hecker. Cloning, nucleotide sequence, and expression of the *Bacillus subtilis lon* gene. *J Bacteriol*, 176(21):6518–6527, Nov 1994.

[203] G. Román-Hernández, J. Y. Hou, R. A. Grant, R. T. Sauer, and T. A. Baker. The ClpS adaptor mediates staged delivery of N-end rule substrates to the AAA+ ClpAP protease. *Mol Cell*, 43(2):217–228, Jul 2011.

[204] Y. Sanchez and S. L. Lindquist. Hsp104 required for induced thermotolerance. *Science*, 248(4959):1112–1115, Jun 1990.

[205] P. Sass, M. Josten, K. Famulla, G. Schiffer, H.-G. Sahl, L. Hamoen, and H. Brötz-Oesterhelt. Antibiotic acyldepsipeptides activate ClpP peptidase to degrade the cell division protein FtsZ. *Proc Natl Acad Sci U S A*, 108(42):17474–17479, Oct 2011.

[206] R. T. Sauer and T. A. Baker. AAA+ proteases: ATP-fueled machines of protein destruction. *Annu Rev Biochem*, 80:587–612, Jun 2011.

[207] H. Schägger. Tricine-SDS-PAGE. *Nat Protoc*, 1(1):16–22, 2006.

[208] E. C. Schirmer, S. Lindquist, and E. Vierling. An arabidopsis heat shock protein complements a thermotolerance defect in yeast. *Plant Cell*, 6(12):1899–1909, Dec 1994.

[209] T. Schlothauer, A. Mogk, D. A. Dougan, B. Bukau, and K. Turgay. MecA, an adaptor protein necessary for ClpC chaperone activity. *Proc Natl Acad Sci U S A*, 100(5):2306–2311, Mar 2003.

[210] R. Schmidt, A. L. Decatur, P. N. Rather, C. Moran, Jr, and R. Losick. *Bacillus subtilis* Lon protease prevents inappropriate transcription of genes under the control of the sporulation transcription factor σ^g. *J Bacteriol*, 176(21):6528–6537, Nov 1994.

[211] R. Schoenheimer, S. Ratner, and D. Rittenberg. The process of continuous deamination and reamination of amino acids in the proteins of normal animals. *Science*, 89(2308):272–273, Mar 1939.

[212] V. J. Schuenemann, S. M. Kralik, R. Albrecht, S. K. Spall, K. N. Truscott, D. A. Dougan, and K. Zeth. Structural basis of N-end rule substrate recognition in

Escherichia coli by the ClpAP adaptor protein ClpS. *EMBO Rep*, 10(5):508–514, May 2009.

[213] A. Schulz, B. Tzschaschel, and W. Schumann. Isolation and analysis of mutants of the *dnaK* operon of *Bacillus subtilis*. *Mol Microbiol*, 15(3):421–429, Feb 1995.

[214] M. Serrano, S. Hövel, C. Moran, Jr, A. O. Henriques, and U. Völker. Forespore-specific transcription of the *lonB* gene during sporulation in *Bacillus subtilis*. *J Bacteriol*, 183(10):2995–3003, May 2001.

[215] J. Shorter and S. Lindquist. Destruction or potentiation of different prions catalyzed by similar Hsp104 remodeling activities. *Mol Cell*, 23(3):425–438, Aug 2006.

[216] L. A. Simmons, A. D. Grossman, and G. C. Walker. Clp and Lon proteases occupy distinct subcellular positions in *Bacillus subtilis*. *J Bacteriol*, 190(20):6758–6768, Oct 2008.

[217] M. V. Simpson. The release of labeled amino acids from the proteins of rat liver slices. *J Biol Chem*, 201(1):143–154, Mar 1953.

[218] W. K. Smits, C. C. Eschevins, K. A. Susanna, S. Bron, O. P. Kuipers, and L. W. Hamoen. Stripping *Bacillus*: ComK auto-stimulation is responsible for the bistable response in competence development. *Mol Microbiol*, 56(3):604–614, May 2005.

[219] J. M. Solomon, R. Magnuson, A. Srivastava, and A. D. Grossman. Convergent sensing pathways mediate response to two extracellular competence factors in *Bacillus subtilis*. *Genes Dev*, 9(5):547–558, Mar 1995.

[220] N. R. Stanley and B. A. Lazazzera. Defining the genetic differences between wild and domestic strains of *Bacillus subtilis* that affect poly-γ-DL-glutamic acid production and biofilm formation. *Mol Microbiol*, 57(4):1143–1158, Aug 2005.

[221] A. Stüdemann, M. Noirclerc-Savoye, E. Klauck, G. Becker, D. Schneider, and R. Hengge. Sequential recognition of two distinct sites in σ^s by the proteolytic targeting factor RssB and ClpX. *EMBO J*, 22(16):4111–4120, Aug 2003.

[222] L. T. Tam, H. Antelmann, C. Eymann, D. Albrecht, J. Bernhardt, and M. Hecker. Proteome signatures for stress and starvation in *Bacillus subtilis* as revealed by a 2-D gel image color coding approach. *Proteomics*, 6(16):4565–4585, Aug 2006.

[223] B. Titz, S. V. Rajagopala, C. Ester, R. Huser, and P. Uetz. Novel conserved assembly factor of the bacterial flagellum. *J Bacteriol*, 188(21):7700–7706, Nov 2006.

[224] R. J. Tomko, Jr and M. Hochstrasser. Order of the proteasomal ATPases and eukaryotic proteasome assembly. *Cell Biochem Biophys*, 60(1-2):13–20, Jun 2011.

[225] K. Tsukahara and M. Ogura. Promoter selectivity of the *Bacillus subtilis* response regulator DegU, a positive regulator of the *fla/che* operon and *sacB*. *BMC Microbiol*, 8:8, 2008.

[226] K. Turgay, J. Hahn, J. Burghoorn, and D. Dubnau. Competence in *Bacillus subtilis* is controlled by regulated proteolysis of a transcription factor. *EMBO J*, 17(22):6730–6738, Nov 1998.

[227] K. Turgay, L. W. Hamoen, G. Venema, and D. Dubnau. Biochemical characterization of a molecular switch involving the heat shock protein ClpC, which controls the activity of ComK, the competence transcription factor of *Bacillus subtilis*. *Genes Dev*, 11(1):119–128, Jan 1997.

[228] K. Turgay, M. Persuh, J. Hahn, and D. Dubnau. Roles of the two ClpC ATP binding sites in the regulation of competence and the stress response. *Mol Microbiol*, 42(3):717–727, Nov 2001.

[229] D. van Sinderen, A. Luttinger, L. Kong, D. Dubnau, G. Venema, and L. Hamoen. ComK encodes the competence transcription factor, the key regulatory protein for competence development in *Bacillus subtilis*. *Mol Microbiol*, 15(3):455–462, Feb 1995.

[230] D. van Sinderen and G. Venema. *comK* acts as an autoregulatory control switch in the signal transduction route to competence in *Bacillus subtilis*. *J Bacteriol*, 176(18):5762–5770, Sep 1994.

[231] J.-W. Veening, O. A. Igoshin, R. T. Eijlander, R. Nijland, L. W. Hamoen, and O. P. Kuipers. Transient heterogeneity in extracellular protease production by *Bacillus subtilis*. *Mol Syst Biol*, 4:184, 2008.

[232] D. T. Verhamme, T. B. Kiley, and N. R. Stanley-Wall. DegU co-ordinates multicellular behaviour exhibited by *Bacillus subtilis*. *Mol Microbiol*, 65(2):554–568, Jul 2007.

[233] D. T. Verhamme, E. J. Murray, and N. R. Stanley-Wall. DegU and Spo0A jointly control transcription of two loci required for complex colony development by *Bacillus subtilis*. *J Bacteriol*, 191(1):100–108, Jan 2009.

[234] S. Versteeg, A. Mogk, and W. Schumann. The *Bacillus subtilis htpG* gene is not involved in thermal stress management. *Mol Gen Genet*, 261(3):582–588, Apr 1999.

[235] H. Vlamakis, C. Aguilar, R. Losick, and R. Kolter. Control of cell fate by the formation of an architecturally complex bacterial community. *Genes Dev*, 22(7):945–953, Apr 2008.

[236] C. L. Ward, S. Omura, and R. R. Kopito. Degradation of CFTR by the ubiquitin-proteasome pathway. *Cell*, 83(1):121–127, Oct 1995.

[237] E. U. Weber-Ban, B. G. Reid, A. D. Miranker, and A. L. Horwich. Global unfolding of a substrate protein by the Hsp100 chaperone ClpA. *Nature*, 401(6748):90–93, Sep 1999.

[238] J. Weibezahn, P. Tessarz, C. Schlieker, R. Zahn, Z. Maglica, S. Lee, H. Zentgraf, E. U. Weber-Ban, D. A. Dougan, F. T. F. Tsai, A. Mogk, and B. Bukau. Thermotolerance requires refolding of aggregated proteins by substrate translocation through the central pore of ClpB. *Cell*, 119(5):653–665, Nov 2004.

[239] Y. Weinrauch, R. Penchev, E. Dubnau, I. Smith, and D. Dubnau. A *Bacillus subtilis* regulatory gene product for genetic competence and sporulation resembles sensor protein members of the bacterial two-component signal-transduction systems. *Genes Dev*, 4(5):860–872, May 1990.

[240] H. Werhane, P. Lopez, M. Mendel, M. Zimmer, G. W. Ordal, and L. M. Márquez-Magaña. The last gene of the *fla/che* operon in *Bacillus subtilis*, *ylxL*, is required for maximal σ^D function. *J Bacteriol*, 186(12):4025–4029, Jun 2004.

[241] S. Wickner, M. R. Maurizi, and S. Gottesman. Posttranslational quality control: folding, refolding, and degrading proteins. *Science*, 286(5446):1888–1893, Dec 1999.

[242] T. Wiegert and W. Schumann. SsrA-mediated tagging in *Bacillus subtilis*. *J Bacteriol*, 183(13):3885–3889, Jul 2001.

[243] J. M. Wood, E. Bremer, L. N. Csonka, R. Kraemer, B. Poolman, T. van der Heide, and L. T. Smith. Osmosensing and osmoregulatory compatible solute accumulation by bacteria. *Comp Biochem Physiol A Mol Integr Physiol*, 130(3):437–460, Oct 2001.

[244] H. Yakhnin, P. Pandit, T. J. Petty, C. S. Baker, T. Romeo, and P. Babitzke. CsrA of *Bacillus subtilis* regulates translation initiation of the gene encoding the flagellin protein (*hag*) by blocking ribosome binding. *Mol Microbiol*, 64(6):1605–1620, Jun 2007.

[245] K. Yonekura, S. Maki-Yonekura, and K. Namba. Complete atomic model of the bacterial flagellar filament by electron cryomicroscopy. *Nature*, 424(6949):643–650, Aug 2003.

[246] K. I. Yoshida, D. Aoyama, I. Ishio, T. Shibayama, and Y. Fujita. Organization and transcription of the myo-inositol operon, *iol*, of *Bacillus subtilis*. *J Bacteriol*, 179(14):4591–4598, Jul 1997.

[247] K. Zeth, R. B. Ravelli, K. Paal, S. Cusack, B. Bukau, and D. A. Dougan. Structural analysis of the adaptor protein ClpS in complex with the N-terminal domain of ClpA. *Nat Struct Biol*, 9(12):906–911, Dec 2002.

[248] Y. Zhang, S. Nakano, S.-Y. Choi, and P. Zuber. Mutational analysis of the *Bacillus subtilis* RNA polymerase alpha C-terminal domain supports the interference model of Spx-dependent repression. *J Bacteriol*, 188(12):4300–4311, Jun 2006.

[249] Y. Zhang and P. Zuber. Requirement of the zinc-binding domain of ClpX for Spx proteolysis in *Bacillus subtilis* and effects of disulfide stress on ClpXP activity. *J Bacteriol*, 189(21):7669–7680, Nov 2007.

[250] J. Zhou, S. A. Lloyd, and D. F. Blair. Electrostatic interactions between rotor and stator in the bacterial flagellar motor. *Proc Natl Acad Sci U S A*, 95(11):6436–6441, May 1998.

[251] P. Zuber. Spx-RNA polymerase interaction and global transcriptional control during oxidative stress. *J Bacteriol*, 186(7):1911–1918, Apr 2004.

[252] P. Zuber, S. Chauhan, P. Pilaka, M. M. Nakano, S. Gurumoorthy, A. A. Lin, S. M. Barendt, B. K. Chi, H. Antelmann, and U. Mäder. Phenotype enhancement screen of a regulatory *spx* mutant unveils a role for the *ytpQ* gene in the control of iron homeostasis. *PLoS One*, 6(9):e25066, 2011.

List of Figures

List of Tables

Lebenslauf

Der Lebenslauf ist in der Online-Version aus Gründen des Datenschutzes nicht enthalten.

Publikationen

Vetsch, M., Erilov, D, Molière, N., Nishiyama, M., Ignatov, O. and Glockshuber, R.

Mechanism of fibre assembly through the chaperone–usher pathway.

EMBO Rep. **7**(7):734-738, 2006.

Kirstein, J., Strahl, H., Molière, N., Hamoen, L.W. and Turgay, K.

Localization of general and regulatory proteolysis in *Bacillus subtilis* cells.

Mol. Microbiol. **70**(3): 682-694, 2008.

Kirstein, J., Molière, N., Dougan, D., Turgay, K.

Adapting the machine: adaptor proteins for Hsp100/Clp and AAA+ proteases.

Nature Rev. Microbiol. **7**(8): 589-599, 2009. Review.

Molière, N., Turgay, K.

Chaperone-protease systems in regulation and protein quality control in *Bacillus sub-tilis.*

Res. Microbiol. **160**(9): 637-644, 2009. Review.